

CRANFIELD UNIVERSITY

Edwina Vivien Mercer

THE NANO MEMBRANE TOILET: SEPARATION PROCESSES

SCHOOL OF WATER, ENERGY AND ENVIRONMENT
Cranfield Water Science Institute

PhD
Academic Year: 2014 - 2019

Supervisors: Dr. Ewan McAdam and Dr. Marc Pidou
March 2019

CRANFIELD UNIVERSITY

SCHOOL OF WATER, ENERGY AND ENVIRONMENT
Cranfield Water Science Institute

PhD

Academic Year 2014 - 2019

EDWINA VIVIEN MERCER

THE NANO MEMBRANE TOILET: SEPARATION PROCESSES

Supervisors: Dr. Ewan McAdam and Dr. Marc Pidou
March 2019

© Cranfield University 2019. All rights reserved. No part of this
publication may be reproduced without the written permission of the
copyright owner.

ABSTRACT

It is estimated that 61 % and 29 % of the global population lack safely managed sanitation and clean water services respectively. The water Sustainable Development Goals (SDG 6) actioned by the UN, aim to provide global access to sanitation and clean water by 2030. However, in low income countries (LICs) conventional centralised wastewater treatment plants are economically unfeasible and for affordable decentralised alternatives, only 22 % of the waste is safely managed, leading to contamination of water resources. The Reinvent the Toilet Challenge (RTTC) initiated by the Bill & Melinda Gates Foundation (BGMF) proposes to innovate off-grid, self-sustaining systems, which are able to safely manage human waste and provide opportunity for resource recovery, at $\leq \text{US\$}0.05 \text{ user}^{-1} \text{ d}^{-1}$. In response, the Nano Membrane Toilet (NMT) developed at Cranfield University propositions a household scale sanitation system which combusts human faeces and provides an off-grid opportunity for advanced treatment technologies to treat the liquid fraction, comprising faecally contaminated urine (FCU). This thesis investigated a series of potential separation processes which integrate with the combustor, for FCU treatment.

It was demonstrated that solids liquid separation can be facilitated post flush with a screw auger, which allowed for effective faecal solids recovery for the combustor. Thermally driven membrane processes, which operate from heat energy, evidenced that high water quality where reuse standards could be achieved (with operational optimisation) in a single stage. In addition, they proved robust to faecal contamination and manipulated odour profiles to change negative perception. The most adaptable process, membrane distillation (MD), provided a salinity gradient consisting of a concentrated retentate and deionised permeate where salinity gradient energy was converted to electrical energy through reverse electrodialysis (RED), sufficient to power an auxiliary low voltage fluidic device (0.25 W) for 4.9 hours. Importantly, the integrated separation processes within this thesis, evidenced high quality water and energy recovery, which are the foundations of an SDG 6 solution.

Keywords: *Screw, RED, MD, SDG 6, Decentralised sanitation*

ACKNOWLEDGEMENTS

It has been a long journey with many challenges to reach this stage. However, I can say that it was worth it and I am grateful to the following people who helped me get here:

- Firstly Ewan, thanks for giving me the opportunity to contribute to this project from its beginning. This thesis has allowed me to explore my own boundary conditions and I am thankful that I could gain expertise in a broad range of scientific fields. You've always been encouraging and believed in me, even when the PhD seemed impossible.
- Thanks Marc for thoroughly reviewing my drafts.
- Throughout the project I had support from postdocs who helped with rig commissioning and experimental work – thanks Ben, Peter, Olivier, Karen and Chris.
- Football was a huge part of my happy memories in Cranfield. Thanks Lloyd for the girl's team, Laura and Juliette for your great friendship and the others who made me feel part of a team. I will never forget Paris, Sweden and CWSI BVI.
- Thanks for the technical support from Barry with your fun chats while laser cutting (so I didn't have leaky rigs), and Dawn for your assistance with the GC-MS.
- I couldn't have managed without my PhD friends Jo, Judith, Berta, Sara, Steph, Erin, Kanming, Jana, Carlos, Anna, Pablo, Ross, Jake, Sabrina, Salvatore and Farhad. The community feeling in CWSI and CSA you all created and our long chats and spontaneous adventures always helped me keep positive. I am glad to have met you and looking forward to meeting up wherever you are in the world.
- My family have provided support for me through everything and I can always rely on them, particularly my sister Theresa and nieces Maya and Claree who always make me smile and allowed me to properly disconnect from the PhD.
- Hi Pascal. Cheers, Edwina. Durch dich hat sich die Zeit während meiner Doktorarbeit und auch mein ganzes Leben verändert. Danke für deinen Optimismus und deine Gesellschaft als wir unser Leben im Labor verbrachten, und auch dafür das du mich zu einem Chemiker gemacht hast obwohl ich mich als Geograph gefühlt habe. Deine Unterstützung bei allem was in dieser Zeit passiert ist, ist von unschätzbarem Wert und ich freue mich auch unsere kommenden Abenteuer, wenn wir diesen Ort verlassen.
- Lastly, thanks to all who donated. I wouldn't have any data without you!

TABLE OF CONTENTS

ABSTRACT	i
ACKNOWLEDGEMENTS	ii
LIST OF FIGURES	vi
LIST OF TABLES	x
NOMENCLATURE	xi
<i>Symbols</i>	xi
<i>Subscripts</i>	xii
<i>Abbreviations</i>	xii
1 INTRODUCTION	1
1.1 Background.....	3
1.2 Aims and objectives.....	7
1.3 Thesis structure.....	8
1.4 References	12
2 SELECTION OF SCREW CHARACTERISTICS AND OPERATIONAL BOUNDARY CONDITIONS TO FACILITATE POST-FLUSH URINE AND FAECES SEPARATION WITHIN SINGLE HOUSEHOLD SANITATION SYSTEMS	17
2.1 Introduction	19
2.2 Materials and methods.....	22
2.2.1 <i>Experimental setup</i>	22
2.2.2 <i>Screw characteristics</i>	23
2.2.3 <i>Preparation and collection of synthetic and real faeces</i>	26
2.3 Results and discussion.....	27
2.3.1 <i>Comparison of screw characteristics</i>	27
2.3.2 <i>Importance of faecal sludge pre-treatment on faecal solids extrusion efficiency</i>	30
2.3.3 <i>Effect of rotational speed on faecal solids extrusion efficiency and phase separation</i>	31
2.3.4 <i>Impact of faeces to urine volumetric ratio on solids extrusion efficiency</i>	33
2.3.5 <i>Application of screw extrusion to real, fresh human faeces</i>	34
2.4 Knowledge transfer to post flush source separation of urine and faeces.....	36
2.5 Conclusions	38
2.6 References	39
3 QUANTIFICATION OF LIQUID PHASE FAECAL ODOURANTS TO EVALUATE MEMBRANE TECHNOLOGY FOR WASTEWATER REUSE FROM DECENTRALISED SANITATION FACILITIES.....	45
3.1 Introduction	48
3.2 Materials and methods.....	50
3.2.1 <i>Chemicals and reagents</i>	50
3.2.2 <i>Standards preparation</i>	50

3.2.3	<i>Gas Chromatography Mass Spectrometry</i>	51
3.2.4	<i>Determining SPE recovery factors</i>	51
3.2.5	<i>Characterisation of urine and faecally contaminated urine</i>	52
3.2.6	<i>Membrane technology set-up</i>	53
3.3	Results and discussion	55
3.3.1	<i>Method development</i>	55
3.3.2	<i>GC-MS calibration</i>	56
3.3.3	<i>Solid phase extraction</i>	60
3.3.4	<i>Characterisation of faecally contaminated urine</i>	61
3.3.5	<i>Pervaporative membranes govern odour transport in faecally contaminated urine</i>	64
3.4	Conclusions	67
3.5	References	68
3.6	Chapter 3 supplementary information	73
References	81
4	THERMALLY DRIVEN MEMBRANE PROCESSES FOR WASTEWATER REUSE IN NON-SEWERED SANITATION SYSTEMS	83
4.1	Introduction	85
4.2	Materials and Methods	88
4.2.1	<i>Experimental setup</i>	88
4.2.2	<i>Feed preparation and analysis</i>	91
4.2.3	<i>Volatile organic compound sampling and analysis</i>	92
4.3	Results and discussion	93
4.3.1	<i>Thermally driven process demonstrate superior separation of key FCU contaminants</i>	93
4.3.2	<i>Feed side pressure negatively impacts water productivity from faecally contaminated urine</i>	99
4.3.3	<i>Thermally driven processes evidence faecal odour treatment by profile manipulation</i>	101
4.4	Conclusions	106
4.5	References	107
4.6	Chapter 4 supplementary information	114
5	HYBRID MEMBRANE DISTILLATION REVERSE ELECTRODIALYSIS CONFIGURATION FOR ENERGY RECOVERY AND CONCENTRATE MANAGEMENT FROM HUMAN URINE IN DECENTRALISED TREATMENT TECHNOLOGIES	121
5.1	Introduction	124
5.2	Materials and Methods	127
5.2.1	<i>Chemicals and Solutions</i>	127
5.2.2	<i>Reverse electrodialysis cell</i>	129
5.2.3	<i>Membrane Distillation</i>	131
5.3	Theory	132

5.3.1 Energy Density	132
5.3.2 Power Density	133
5.3.3 Open Circuit Voltage.....	135
5.4 Results and discussion	136
5.4.1 Power density from urine is analogous to pure sodium chloride.....	136
5.4.2 Hydrodynamic optimisation is critical for energy recovery in recycle mode	140
5.4.3 Maximising energy recovery from a finite volume in recycle mode.....	143
5.5 Conclusions	146
5.6 References	147
5.7 Chapter 5 supplementary information	155
6 OVERALL DISCUSSION	161
6.1 How would we realise a household scale integrated separation system?.....	163
6.2 How can the NMT process the liquid phase to meet ISO 30500?	167
6.3 Can the NMT work off-grid without an external source of power?	169
6.4 What is the financial benefit of the NMT compared to conventional sanitation solutions?.....	171
6.5 References	173
7 CONCLUSIONS AND FURTHER WORK	179
7.1 Conclusions	181
7.2 Further work	182
APPENDICES	185

LIST OF FIGURES

Figure 1.1 Thesis schematic of the key separation processes within the Nano Membrane Toilet.....	10
Figure 2.1 Experimental setup of the screw conveyor rig.....	23
Figure 2.2 Schematics of screws 1-7.....	24
Figure 2.3. Comparison of screw types by the solids extruded from the initial loading (%) within a prescribed time interval. Mixed form; 100 rpm; 100 seconds; 3 L water; 500 g synthetic faeces at 60 % solids content.....	28
Figure 2.4 Solids concentration (%) of output subsamples taken in 30 second intervals for a 10 second duration. Mixed form; 100 rpm; 3 L water; 500 g synthetic faeces at 60 % solids content.	28
Figure 2.5 Distribution of total dry solids (g) by compartment for Screw 7 (reference) and Screw 3 following assessment at 100 rpm for a fixed time interval of 100s. 100 rpm; 100 seconds; 3 L water; 500 g synthetic faeces at 60 % solids content.	30
Figure 2.6 Impact of screw rotational speed selection on solids extrusion efficiency within a fixed number of rotations. Screw 3; mixed form; 3 L water; 500 g synthetic faeces.	32
Figure 2.7 Total averaged extrusion rate of water compared with Rogers et al., (2014) using 5 % synthetic sludge and water (Screw 3; 3 L water only trial, runtime until bowl emptied).	33
Figure 2.8 Effect of free water volume on solids recovered (%) and mass extruded (g min^{-1}). Screw 3; mixed form; 100 rpm; 100 seconds; 500 g synthetic faeces.	34
Figure 2.9 Effect of faeces form, standing time and free water volume on total solids recovered from initial loading (%). (Screw 3, 400 rpm, 500 g real faeces, trial left to run until blockage or bowl emptied).	35
Figure 2.10 Accumulation of unmasticated food particles: (a) within the metering section, screw 3; (b) within the metering section, screw 1; (c) at the aperture; and (d) sample taken from the aperture.	36
Figure 3.1 Chromatograms in single ion monitoring mode (SIM) at (a) 1 mg L^{-1} volatile organic compound (VOC) concentration with 1 mg L^{-1} IS concentration , (b) 10 mg L^{-1} VOC concentration with 10 mg L^{-1} IS concentration and (c) 100 mg L^{-1} VOC concentration with 10 mg L^{-1} IS concentration.....	57
Figure 3.2 Assessment of pervaporative membrane processes as a liquid phase treatment to manage odourants at source. Performance expressed as (a) removal efficiency for a hydrophilic membrane material and (b) enrichment factor for a hydrophobic membrane. PVA (Polyvinyl alcohol) and PDMS (Polydimethylsiloxane). Error bars represent the standard deviation of a triplicate at pH 6.5.....	66

- Figure 4.1 Membrane distillation and pervaporation membrane rig schematic. 1: Needle valve; 2: Absolute pressure transducer; 3: Temperature probe; 4: Thermostatic bath; 5: Membrane; 6: Feed solution; 7: Pressure gauge; 8: Peristaltic pump; 9: Liquid nitrogen cold trap or condenser; 10: Diaphragm vacuum pump. 89
- Figure 4.2 Removal efficiencies of ammoniacal nitrogen ($\text{NH}_4^+\text{-N}$), conductivity (C), total phosphorus (TP) and chemical oxygen demand (COD) treating faecally contaminated urine with membranes. Feed water temperature 50 °C, unless stated otherwise. UF (Ultrafiltration); PES (Polyethersulphone); RO (Reverse osmosis); PA-UREA (Polyamide-urea); PV (Pervaporation); PVA (Polyvinyl alcohol); PDMS (Polydimethylsiloxane); MD (Membrane distillation); PP (Polypropylene). Error bars represent standard deviation of a triplicated experiment. 95
- Figure 4.3 Coliform log removal values (LRVs) for E.coli and total coliforms (TC) using UF (PES), RO (PA-UREA), PV (PVA), PV (PDMS) and MD (PP) processes to treat faecally contaminated urine Feed water temperature 50 °C, unless stated otherwise. UF (Ultrafiltration); PES (Polyethersulphone) ; RO (Reverse osmosis); PA-UREA (Polyamide-urea); PV (Pervaporation); PVA (Polyvinyl alcohol); PDMS (Polydimethylsiloxane); MD (Membrane distillation); PP (Polypropylene). Error bars represent standard deviation of a triplicated experiment. 97
- Figure 4.4 Normalised membrane flux with deionised water (J_0) and faecally contaminated urine (J). Water productivities of UF and RO standardised to 10 L m⁻² membrane area and PV and MD standardised to 1 L m⁻² membrane area. UF (Ultrafiltration); PES (Polyethersulphone); RO (Reverse osmosis); PA-UREA (Polyamide-urea); PV (Pervaporation); PVA (Polyvinyl alcohol); PDMS (Polydimethylsiloxane); MD (Membrane distillation); PP (Polypropylene). All membranes were operated at 50 °C. Error bars represent standard deviation of a triplicated experiment. 100
- Figure 4.5 Feed odour development during storage, expressed as the ratio of the final feed concentration (C_f) to the initial feed (C_i) for pervaporation (polyvinyl alcohol) during faecally contaminated urine trials and synthetic trials. Operated at 50 °C. Error bars represent standard deviation of a triplicated experiment. Mean filtration time 4.77 hours..... 102
- Figure 4.6 A comparison of membrane odour separation (UF, RO, PV and MD) expressed as the ratio of volatile organic compounds (VOCs) flux to water flux. Synthetic solution feed concentration 10 mg L⁻¹. UF (Ultrafiltration); PES (Polyethersulphone) ; RO (Reverse osmosis); PA-UREA (Polyamide-urea); PV (Pervaporation); PVA (Polyvinyl alcohol); PDMS (Polydimethylsiloxane); MD (Membrane distillation); PP (Polypropylene). All membranes operated at 50 °C. Error bars represent standard deviation of a triplicated experiment. 102
- Figure 4.7 Pervaporation (Polydimethylsiloxane) and odour separation and varying permeate volumes, expressed as the ratio of volatile organic compounds (VOC) flux to water flux. Synthetic solution feed concentration 10 mg L⁻¹. All membranes operated at 50 °C. Error bars represent standard deviation of a triplicated experiment..... 104

Figure 4.8 Faecally contaminated urine relative odour and taste of ultrafiltration permeate (a,b), reverse osmosis permeate (c,d) and hydrophilic pervaporation permeate (e,f) according to the lowest reported odour and taste thresholds in water (van Gemert, 2011). Mean filtration times for ultrafiltration, reverse osmosis and hydrophilic pervaporation were 0.71, 2.91 and 4.77 hours respectively.	105
Figure 5.1 Schematic of reverse electro dialysis cell used in this study.	130
Figure 5.2 Schematic of the operation modes (single pass, recycle) practiced in this study.....	130
Figure 5.3 Influence of urine multivalent ions and organics (Table 5.2) on open current voltage (OCV), permselectivity and power density (P_d). Conductivities (mS cm^{-1}) were 45.8 (sea water)/1.9 (river water), 21.2 (NaCl control)/0.5 (diluate), 21.3 (Multi-ion control)/0.5 (diluate), 20.7 (synthetic urine)/0.5 (diluate), 12.4 (real urine)/0.5 (diluate), 12.4 (real urine)/0.2 (membrane distillation permeate), 24.1 (real urine 2x concentrate)/ 0.2 (membrane distillation permeate). Single pass mode.....	137
Figure 5.4 Influence of (a) diluate concentration; (b) synthetic urine concentration and (c) temperature on power density (P_d), open current voltage (OCV) and resistance. Single pass mode. Diluate 0.5 mS cm^{-1} , concentrate 21 mS cm^{-1} and temperature $22 \text{ }^\circ\text{C}$, unless stated otherwise.	139
Figure 5.5 Effect of varying feed flowrates on open current voltage (OCV) and power density (P_d). Synthetic urine concentrate, 0.25 g L^{-1} NaCl diluate, single pass mode.	141
Figure 5.6 Power density as a function of linear velocity when (a) when LC flowrate is variable and HC flowrate is maintained at 50 ml min^{-1} and (b) when HC flowrate is variable and LC flowrate is maintained at 50 ml min^{-1} . Synthetic urine concentrate, 0.25 g L^{-1} NaCl diluate, single pass mode.	142
Figure 5.7 Comparison of (a) low and (b) high flowrates in recycle mode until power fully extracted, at varying current draws (A m^{-2}). High flowrates (concentrate and diluate at 140 mL min^{-1}), low flow rates (2.5 mL min^{-1} concentrate / 10 mL min^{-1} diluate). Synthetic urine concentrate, 0.25 g L^{-1} NaCl diluate.....	142
Figure 5.8 (a) Theoretical Gibbs power, (b) experimentally obtained power and (c) energy extraction efficiency (η) as a function of concentrate molarity at varying current densities (2.5 A m^{-2} , 5 A m^{-2} and 7.5 A m^{-2}). Concentrate and diluate flowrate is 140 mL min^{-1} . Synthetic urine concentrate, 0.25 g L^{-1} NaCl diluate, recycle mode.	144
Figure 5.9 Comparison of theoretical and experimentally obtained energy densities at a starting molality difference of $0.175 \text{ mol kg}^{-1}$ and operating 2.5 A m^{-2} current draw. Synthetic urine concentrate, 0.25 g L^{-1} NaCl diluate, recycle mode.	146
Figure 6.1 Illustrative integration of the separation processes within the Nano Membrane Toilet at household scale.	166

LIST OF TABLES

Table 1.1 Sustainable development goal 6 (United Nations, 2018)	4
Table 2.1 Design features of experimental setup and screws. *reference screw.	25
Table 2.2 Synthetic faeces recipe (Adapted from Pollution Research Group, 2014) and real faeces characteristics.....	26
Table 2.3 Effect of pre-treatment on screw loading. Screw 3; mixed; 100 rpm; 100 seconds; 3 L water; 500 g synthetic faeces.	31
Table 3.1 Physico-chemical parameters of selected volatile organic compounds (VOCs) attributed to urine and faeces	54
Table 3.2 Single ion monitoring (SIM) mass spectrometry parameters for target analytes.	55
Table 3.3 Calibration parameters for the target analytes; LD, limit of detection; LQ, limit of quantification; RF, response factor; RSD, relative standard deviation; SD, standard deviation.	58
Table 3.4 Precision and accuracy for each analyte within three calibration ranges; RSD, residual standard deviation.	59
Table 3.5 Solid phase extraction recovery factors. RSD, residual standard deviation...	61
Table 3.6 Typical concentrations of 12 liquid phase volatile organic compounds attributed to urine and faeces with associated odour descriptors and detection thresholds in air and water	63
Table 3.7 Odour descriptors for the membrane permeates of faecally contaminated urine	67
Table 4.1 Summary of membrane characteristics and operational conditions used in this study.....	90
Table 4.2 ISO 30500 (2018) membrane (mean) filtrate compliance (✓) and failure (×) from faecally contaminated urine	98
Table 4.3 Odour descriptors for permeate produced from pervaporation and membrane distillation membranes following treatment of faecally contaminated urine.....	104
Table 5.1 Summary of synthetic urine recipe adapted from Putnam (1971).....	128
Table 5.2 Real urine characteristics and membrane distillation permeate trialled in this study.....	138
Table 6.1 Assumptions for calculating the NMT energy balance for a 10 person household	170
Table 6.2 Comparison of current sanitation and water costs in low income countries (LICs).....	173

NOMENCLATURE

Symbols

A	Cross sectional area of one membrane (m^2)
C	Concentration (mol L^{-1})
C	Permeate concentration (mg L^{-1})
C_0	Feed concentration (mg L^{-1})
C_f	Concentration factor
C_{GCMS}	Concentration reported on the GCMS
C_{VOC}	Actual VOC concentration (mg kg^{-1})
ED	Energy density (J kg^{-1})
F	Faraday constant ($96485.33 \text{ C mol}^{-1}$)
G	Gibbs free energy
H	Enthalpy
I	Current (A)
I_d	Current Density (A m^{-2})
J	Flux faecally contaminated urine ($\text{kg m}^{-2} \text{ h}^{-1}$)
J_0	Deionised water flux ($\text{kg m}^{-2} \text{ h}^{-1}$)
J_s	Total salt flux ($\text{mol m}^{-2} \text{ s}^{-1}$)
J_w	Total water flux ($\text{mol m}^{-2} \text{ s}^{-1}$)
L_p	Average water permeability coefficient for both anion and cation exchange membranes ($\text{kg m}^{-2} \text{ s}^{-1} \text{ kg}^{-1}$)
M	Molar mass of water (kg mol^{-1})
m	Mass (kg)
N	Number of cell pairs in membrane stack
n	Moles (mol)
P	Power (W)
P_d	Power density (W m^{-2})
P_s	Average salt permeability coefficient for the anion and cation exchange membrane pair ($\text{m}^2 \text{ s}^{-1}$)
R	Universal gas constant ($8.314 \text{ J K}^{-1} \text{ mol}^{-1}$)
R_f	Recovery factor
S	Molar entropy ($\text{J K}^{-1} \text{ mol}^{-1}$)
T	Temperature (K)
t_w	Number of water molecules transported with salt ions across the membranes ($\text{mol}_{\text{water}} \text{ mol}_{\text{salt}}^{-1}$)
U	Potential (V)
ν	Number of moles in 1 mole of salt

z	Valency of the ion
α	Permselectivity (%)
β	Enrichment factor
γ	Activity coefficient
δ_m	Average membrane thickness of the anion and cation exchange membrane pair (m)
$\Delta_{mix}G$	Gibbs free energy of mixing (J)
$\Delta\mu_s$	Difference in chemical potential of salt
$\Delta\mu_w$	Difference in chemical potential of water
η	Energy extraction efficiency (%)
κ	Solution conductivity
ϕ	Osmotic coefficient (unitless)

Subscripts

B	Mixed concentrate and diluate
C	Concentrate
D	Diluate
G	Gibbs (e.g. P_G = Gibbs power)
s	Salt (e.g. J_s = total salt flux)
$Stack$	Measure across the membrane stack
w	Water

Abbreviations

ABS	Acrylonitrile butadiene styrene
BGMF	Bill & Melinda Gates Foundation
BHT	Butylated hydrocarbon
BSS	Bristol stool scale
C	Conductivity
CFU	Colony forming units
COD	Chemical oxygen demand
CURES	Cranfield University's Research Ethics System
EPA	Environmental protection agency
FCU	Faecally contaminated urine
FDA	Food and drug administration
GC-MS	Gas chromatography mass spectrometry
HC	High concentration (refers to channel)
HF	Hollow fibre
IDL	Instrument detection limit
IS	Internal standard
ISO 30500	International standard for non-sewered sanitation

LC	Low concentration (refers to channel)
LD	Limit of detection
LICs	Lower income countries
LQ	Limit of quantification
LRV	Log removal value
MBR	Membrane bioreactor
MD	Membrane distillation
MDG	Millennium development goal
MDL	Method detection limit
MFC	Microbial fuel cell
NAv	Not available
NaCl	Sodium chloride
NAp	Not applicable
ND	Low removal value
NH ₄ ⁺ -N	Ammoniacal nitrogen
NMT	Nano Membrane Toilet
NOM	Natural organic matter
OCV	Open current voltage
PA-UREA	Polyamide-urea
PDMS	Polydimethylsiloxane
PES	Polyethersulphone
PP	Polypropylene
PV	Pervaporation
PVA	Polyvinyl alcohol
RED	Reverse electrodialysis
RF	Response factor
RO	Reverse osmosis
RPM	Revolutions per minute
RSD	Residual standard deviation
SD	Standard deviation
SDG	Sustainable development goal
SIM	Single ion monitoring
SOC	State of charge
SPE	Solid phase extraction
T&O	Taste and odour
TN	Total nitrogen
TP	Total phosphorus
TSS	Total suspended solids
UF	Ultrafiltration
UN	United nations
VMD	Vacuum membrane distillation
VOC	Volatile organic compounds

1 INTRODUCTION

1.1 Background

The sixth sustainable development goal (SDG) proposed by the United Nations (UN) aims to provide water and sanitation for all by 2030 (United Nations, 2018). The specified targets (Table 1.1) emphasise the urgency to protect water resources, by improving sanitation practices and facilities that can provide safe wastewater discharge, which results in cleaner water resources with greater accessibility to drinking water. Sustainable practices such as water reuse are equally important as a means to alleviate water scarcity and water resource management pressures in preparation for the increase in global population expected to reach 9.8 billion by 2030 (Hilal and Wright, 2018; United Nations, 2017). However, large scale piped water and sewerage infrastructure (centralised approach) which conventionally provides clean water and safe discharge, demands high capital and maintenance costs, energy, land and skilled workers, which is economically unfeasible and unsustainable in low income countries (LICs) (Hutton and Haller, 2004).

As a consequence, decentralised sanitation is practiced, which eliminates the costs associated with a sewerage network, accounting for up to 84 % of capital costs (Jung, Narayanan and Cheng, 2018). Decentralised sanitation solutions such as pit latrines are one of a series of technological infrastructure schemes primarily adopted in LICs, particularly in densely populated urban areas (Rose et al., 2015). However, pit latrines only act as an intermediate storage of faecal sludge which eventually requires emptying. Factors such as groundwater intrusion, pit collapse and termite damage have been reported to result in emptying as frequently as within 13 months (Chidya et al., 2016; Cole et al., 2012). The average household scale pit emptying fees ranged from US\$35 household⁻¹ in India to US\$95 household⁻¹ in Kenya, representing between 12 % and 125 % of an individual's average monthly salary (Chowdry and Kone, 2012; World Bank, 2019). Difficulties in selecting a treatment process to accommodate for the variety of latrine waste as well as high transport costs, causes faecal sludge to be disposed of directly into the environment, leading to the contamination of water resources and other environmental issues (Ingallinella et al., 2002). Diarrhoea, the leading cause of illness and death worldwide, can be caused by enteric pathogen contamination and with appropriate sanitation practices, it is projected that up to 88 % of diarrhoea related deaths could be prevented (UNICEF and WHO, 2015). Without

increasing investment in the current infrastructure, 29 % of the global population lack safely managed drinking water supplies, with 61 % without safely managed sanitation services and 892 million people practicing open defecation (United Nations, 2018), equating to economic losses of US\$260 billion year annually (Hutton, 2013).

Table 1.1 Sustainable development goal 6 (United Nations, 2018)

Target	Objective
6.1	Universal access to safe, affordable drinking water.
6.2	Universal access to sanitation and hygiene facilities, no open defecation, attention to the needs of females in vulnerable situations
6.3	Reduce water pollution: no dumping, minimal release of hazardous waste, halving the proportion of untreated wastewater and increasing recycling and safe reuse globally.
6.4	Increase water-use efficiency and ensure sustainable withdrawals and supply of freshwater to address water scarcity.
6.5	Integrated water resources management.
6.6	Protect and restore water-related ecosystems.

In order to address SDG 6, the Bill & Melinda Gates Foundation (BMGF) launched the Reinvent the Toilet Challenge (RTTC), an initiative providing global institutions an opportunity to engineer household scale sanitation systems which overcome the issues associated with the existing solutions (The Bill & Melinda Gates Foundation, 2019). The solutions must treat human waste for safe discharge in a self-sustaining decentralised system at $< \text{US}\$0.05 \text{ user}^{-1} \text{ d}^{-1}$, which can be achievable with the prospect of resource recovery (i.e. clean water and energy), promoting sustainable and profitable sanitation in LICs.

Whilst source separation presents an attractive opportunity to enable phase separation and simplify downstream process selection, there is general recognition that source separating toilets are non-ideal, such that studies have shown only 50-80 % of the urine processed is recovered, indicating substantive urine contamination in the faecal sludge fraction (Bjorn Vinnerås, 2001; Jönsson et al., 1997). Furthermore, 50 % of the world's population practice wet anal hygiene (Otterpohl, Braun and Oldenburg, 2002), which will cause variations of the liquid content in the faeces portion. Uncertainty of the characteristics of the waste streams will increase the risk in technology selection, due to the varied distribution in pathogens and other contaminants imposed by imperfect separation. A more pragmatic approach is therefore to consider flushing of the urine and faeces as a combined phase, combined with post-flush phase

separation, to provide solid and liquid phases of particular characteristics that match the demands of downstream process technologies (Onabanjo et al., 2016). Unlike with conventional municipal sludge that comprises of a solids concentration around 5 % w/v, faecal sludge is on average 25 % in solids concentration, which is a particularly demanding pumping problem, but is nevertheless important to sustain since this enables the potential application of simple and robust thermal processing technology for the destruction of the faecal solids fraction. Whilst not explicitly developed for faecal solids management, mechanical screw augers have been demonstrated for a range of viscous, high solids materials including plastics, food, powders, animal feed and cement (McGlinchey, 2008; Roberts, 2001; Rogers et al., 2014; Srivastava, Goering and Rohrbach, 1993; Yu, 1997). Importantly, screw augers have demonstrated material selectivity, and the control of dewatering and concentrative properties which is particularly encouraging for the separation of urine and faeces. However, the physical design of the screw, in the context of geometry and flight configuration, coupled with investigation of suitable boundary conditions, is demanded to match the separation needs of this potentially more rheologically challenging fluid.

A further consideration to off-grid development is on the reliance of both water and energy. The adoption of a waterless flush limits reliance on an external water source and can improve solid-liquid separation efficiency through reducing the volume required for treatment; the total volume produced from a ten person system then being equivalent to only 17.5 L d⁻¹ comprising exclusively of urine and faeces (Rose et al., 2015). By constraining the treatment volume, new methods of liquid phase treatment can be considered that offer the production of high quality water with minimal electrical power demand. For example, thermal oxidation of the faecal sludge fraction is capable of providing off-gas temperatures up to 630 °C, equivalent to the ignition temperature of natural gas, that not only reduces the solids to a safe to handle ash (Hanak et al., 2016; Onabanjo et al., 2016), but also generates sufficient waste heat to enable the selection of thermally driven advanced treatment technologies to process the highly concentrated liquid wastewater consisting of faecally contaminated urine (FCU). The FCU also requires treatment for safe discharge, although provided that the produced water is of sufficient quality, it can be considered a valuable resource, suitable for reuse, particularly in water resource constrained environments (Hilal and Wright, 2018; United

Nations, 2017). Pressure driven membrane technology has become the established route to deliver water quality that is able to meet stringent regulations to reuse quality from municipal wastewater (Warsinger et al., 2018). In particular, ultrafiltration (UF) followed by reverse osmosis (RO) provide an absolute barrier to pathogens and elicits selectivity to water over key wastewater contaminants (Public Utilities Board (PUB), 2018). However, pressure driven filtration is associated with substantial electrical energy consumption to support multiple pumping processes, which is unfeasible for a self-sustaining system. Thermally driven membrane technology, provides selectivity through two mechanisms: size exclusion phenomena and a vapour pressure gradient which provides a selective preference for water transport (Baker, 2012). Whilst presently only applied for discrete industrial separations (Baker, 2012), the potential for high quality water production from urine as a complex saline fluid, of limited fluid volume, coupled with the availability of waste heat, imply that thermally driven membrane technology could be of practical interest for the present application. The development of thermally driven processes to deliver decentralised sanitation draws from existing parallels with unique small scale applications such as space missions (Cartinella et al., 2006; Grigoriev et al., 2011; Hirabayashi, 2002; Zhao et al., 2013), where the use of membrane distillation has been utilised at full-scale to facilitate high quality water recovery from urine. However, in the present application, the inclusion of faecal contamination presents a host of new challenges which include a substantive increase in enteric pathogens, an increase in particulate and soluble organic fractions and an increase in odorous compounds. Consequently, to determine whether thermally driven membranes are viable for this specific application, assessment of their capability to deliver product water to sufficient discharge or reuse quality, alongside malodour treatment, is demanded for user safety and product acceptance (Cruddas, Parker and Gormley, 2015). Long retention times, pH change and agitation facilitate the partition of odour causing compounds into the gas phase, where odour is perceived by olfactory receptors (Brattoli et al., 2011). However, a key distinguishing factor between odour management for the new generation of sanitation systems and more conventional decentralised approaches (i.e. pit latrines), is that it is possible to treat odour at source. Faecal odour is largely represented by a group of volatile organic compounds (VOCs) formed as bacterial metabolites in the liquid phase (Bos, Sterk and Schultz, 2013). Thus

separation in the liquid phase can dissipate partitioning and therefore limit the negative association of odour with decentralised sanitation solutions which is presently one of the primary reasons for the continued practice of open defecation (Lin et al., 2013). In thermally driven membranes processes, it is possible to incorporate selectivity for water versus such compounds through selection of membrane polymer chemistry (Baker, 2012). Whilst thermally driven membranes potentially offer such a solution, there is presently not a suitable analytical methodology which can detect this select group of faecal borne VOCs, with which to benchmark and develop such technologies.

A common situation in LICs, is that electricity supply is intermittent and particularly in sub-Saharan Africa, over 620 million do not have any access to electricity (International Energy Agency, 2014). Thermally driven membranes can be supported by heat energy provided from faecal oxidation; however, electrical energy is still required for auxiliary processes and can provide an investible resource for customers. Thermally driven membranes provide a salinity gradient in the form of a highly concentrated retentate and deionised permeate. Salinity gradient energy can be converted to electrical energy via reverse electrodialysis (RED), in which urine containing an ionic concentration of 248 mEq L^{-1} (Putnam, 1971), which is equivalent to an energy density of 337 J kg^{-1} according to the Gibbs free energy of mixing. The selective remixing of salts by RED into the permeate resulting in an insignificant conductivity increase, allows for the partial management of retentate and therefore sustained MD operation. Conventionally, RED is applied for large scale applications where focus is power density maximisation of an infinite feedwater such as sea and river water (Tufa et al., 2018) where solutions momentarily contact the membranes, in order to maintain the greatest salinity gradient. In contrast, urine within decentralised systems is finite, and therefore operation in recycle mode could take full advantage of the available energy available in urine, and this prospect requires investigation.

1.2 Aims and objectives

The Nano Membrane Toilet (NMT) is a household scale sanitation system developed at Cranfield University in response to the RTTC. The general design incorporates a rotating waterless flush where urine and faeces are accepted together. Passive sedimentation occurs to provide initial solids/liquids separation, where the liquid

fraction is diverted over a weir to the membranes and the solids are transported by an Archimedes screw to be dried and then combusted. Faecal combustion provides opportunity for advanced treatment technologies to utilise waste heat in a self-sustaining sanitation system.

The overall thesis aim is to investigate the feasibility of key separation processes within the NMT to provide safe water and energy recovery, which could ultimately integrate as a sustainable sanitation solution towards SDG 6.. The aim is realised through the following objectives:

1. To identify appropriate screw characteristics and boundary conditions which enable fresh faeces extrusion to facilitate post flush urine and faeces separation to maximise solids recovery for subsequent combustion processes.
2. To develop a method which quantifies a broad range of liquid phase volatile organic compounds in urine and faeces to enable the characterisation of candidate thermally driven membrane technology for the control of odour in the liquid phase (at source), while producing a high quality water product.
3. To demonstrate the suitability of thermally driven membrane processes for delivering water reuse in non-sewered sanitation systems where the wastewater is primarily characterised as faecally contaminated urine, and compare to the pressure driven membrane technologies ordinarily selected for indirect potable reuse schemes.
4. To evaluate hybrid membrane distillation-reverse electrodialysis using urine for concentrate management and energy recovery in small scale decentralised sanitation systems.

1.3 Thesis structure

The thesis is presented as a series of journal papers (four technical papers in total) which correspond to the specific objectives and follow the narrative of the separation processes within the NMT (Figure 1.1). All papers were written by Edwina Mercer as the first author and edited by two supervisors Ewan McAdam and Marc Pidou before submission. The experimental design, investigation and method development was primarily carried out by Edwina Mercer. Ben Martin and Peter Cruddas assisted in rig design in Chapter 2. Firmenich, Switzerland delivered training for the method

developed in Chapter 3. Chris Davey and Daniele Azzini (Marche Polytechnic University) supported data collection and analysis in Chapter 5.

This research was part of a larger NMT team where parallel research was undertaken, in which Edwina Mercer assisted in experimental design and data collection for the following journal publications:

1. Wang, C.Y., Mercer, E., Kamranvand, F., Williams, L., Kolios, A., Parker, A., Tyrrel, S., Cartmell, E. and McAdam, E.J. (2017) ‘Tube-side mass transfer for hollow fibre membrane contactors operated in the low Graetz range’, *Journal of Membrane Science*, 523, pp. 235–246.
2. Kamranvand, F., Davey, C.J., Sakar, H., Autin, O., Mercer, E., Collins, M., Williams, L., Kolios, A., Parker, A., Tyrrel, S., Cartmell, E. and McAdam, E.J. (2018) ‘Impact of fouling, cleaning and faecal contamination on the separation of water from urine using thermally driven membrane separation’, *Separation Science and Technology*, 53, pp. 1372–1382.

Additionally, various members from the NMT team are co-authors for the publications within this thesis due to intellectual contribution to the wider NMT design and engineering.

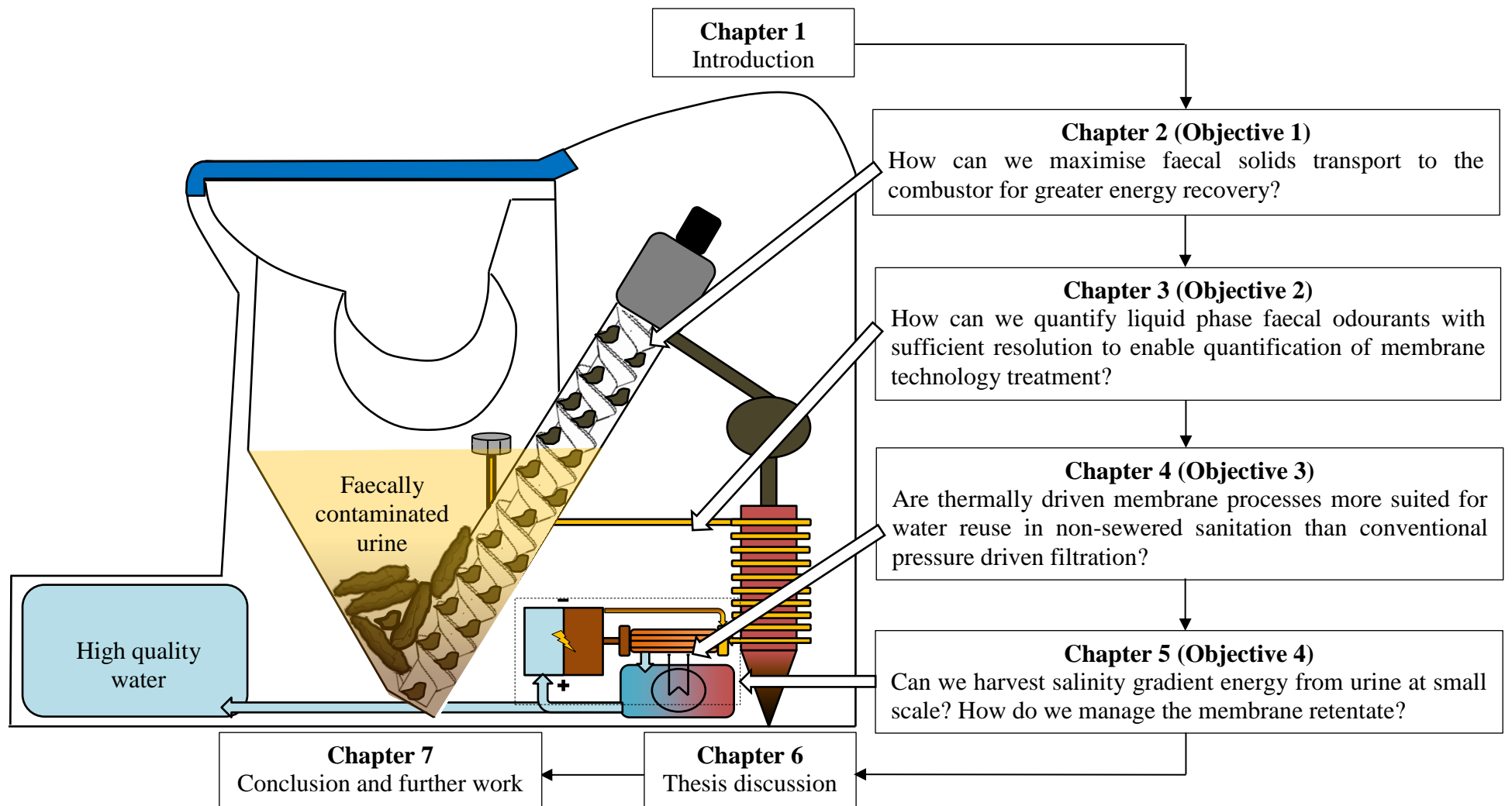


Figure 1.1 Thesis schematic of the key separation processes within the Nano Membrane Toilet

Chapter 2, “*Selection of screw characteristics and operational boundary conditions to facilitate post-flush urine and faeces separation within single household sanitation systems*”, demonstrates the separation of urine and faeces within a post flush system, using a screw extruder, by exploring boundary conditions and screw characteristics to achieve maximum solids transport. Published in: *Environmental Science, Water Research and Technology*.

Chapter 3, “*Quantification of liquid phase faecal odourants to evaluate membrane technology for wastewater reuse from decentralised sanitation facilities,*” exhibits the development, validation and application of a liquid phase odour method to treat faecal odour at source using membrane technology, consequently encouraging facility and water reuse acceptance. Presented orally at the 11th *IWA Symposium on Taste and Odour and Algal Toxins* in Sydney Australia, February 2017. Published in: *Environmental Science, Water Research and Technology*.

Chapter 4, “*Thermally driven membrane processes for wastewater reuse in non-sewered sanitation systems*”, critically compares conventional pressure driven water reuse membrane technology (UF, RO) with thermally driven membrane processes and polymers (PV-PVA, PV-PDMS and MD) for reuse within a sanitation wastewater context. Water quality according to ISO 30500, impact on flux and odour management provide a holistic water reuse approach. In preparation for: *Water research*.

Chapter 5, “*Hybrid membrane distillation reverse electrodialysis configuration for energy recovery and concentrate management from human urine in decentralised treatment technologies*”, demonstrates for the first time, RED using urine salts to recovery salinity gradient energy. Integration with MD delivers the required salinity gradient for RED through the provision of permeate and retentate streams, allowing for synergistic energy recovery and concentrate ion management. In preparation for: *Journal of Membrane Science*.

Chapter 6 presents the overall thesis discussion which integrates all technical chapters into a salient sanitation solution and addresses its feasibility as a SDG solution.

Chapter 7 contains the conclusions and further research.

1.4 References

Baker, R. (2012) *Membrane Technology and Applications*. 3rd edn. Baker, R. (ed.) Chichester, UK: John Wiley and Sons.

Bartels, C. (2006) *Reverse osmosis membranes play key role in wastewater reclamation*. Available at: <https://www.waterworld.com/articles/wwi/print/volume-21/issue-6/features/reverse-osmosis-membranes-play-key-role-in-wastewater-reclamation.html> (Accessed: 8 August 2018).

Bjorn Vinnerås (2001) 'Faecal separation and urine diversion for nutrient management of household biodegradable waste and wastewater', *Journal of Biosciences*, 5, pp. 29–50.

Bos, L.D.J., Sterk, P.J. and Schultz, M.J. (2013) 'Volatile Metabolites of Pathogens: A Systematic Review', *PLOS Pathogens*, 9, p. e1003311.

Brattoli, M., de Gennaro, G., de Pinto, V., Loiotile, A.D., Lovascio, S. and Penza, M. (2011) 'Odour Detection Methods: Olfactometry and Chemical Sensors', *Sensors*, 11, pp. 5290–5322.

Cartinella, J.L., Cath, T.Y., Flynn, M.T., Miller, G.C., Hunter Kenneth W. and Childress, A.E. (2006) 'Removal of Natural Steroid Hormones from Wastewater Using Membrane Contactor Processes', *Environmental Science & Technology*, 40, pp. 7381–7386.

Chidya, R.C.G., Holm, R.H., Tembo, M., Cole, B., Workneh, P. and Kanyama, J. (2016) 'Testing methods for new pit latrine designs in rural and peri-urban areas of Malawi where conventional testing is difficult to employ', *Environmental Science: Water Research & Technology*, 2, pp. 726–732.

Chowdry, S. and Kone, D.D. (2012) '*Business Analysis of Fecal Sludge Management: Emptying and Transportation Services in Africa and Asia*'. Available at: https://www.pseau.org/outils/ouvrages/bill_melinda_gates_foundation_business_analysis_of_fecal_sludge_management_emptying_and_transportation_services_in_africa_and_asia_2012.pdf (Accessed 8 August 2018).

- Cole, B., Pinfold, J., Ho, G. and Anda, M. (2012) ‘Investigating the dynamic interactions between supply and demand for rural sanitation, Malawi’, *Journal of Water, Sanitation and Hygiene for Development*, 2, pp. 266–278.
- Cruddas, P.H., Parker, A. and Gormley, A. (2015) ‘User perspectives to direct water reuse from the Nano Membrane Toilet.’, *38th WEDC International Conference*. Loughborough, UK, 27-31 July 2015.
- Grigoriev, A.I., Sinyak, Y.E., Samsonov, N.M., Bobe, L.S., Protasov, N.N. and Andreychuk, P.O. (2011) ‘Regeneration of water at space stations’, *Acta Astronautica*, 68, pp. 1567–1573.
- Hanak, D.P., Kolios, A.J., Onabanjo, T., Wagland, S.T., Patchigolla, K., Fidalgo, B., Manovic, V., McAdam, E., Parker, A., Williams, L., Tyrrel, S. and Cartmell, E. (2016) ‘Conceptual energy and water recovery system for self-sustained nano membrane toilet’, *Energy Conversion and Management*, 126, pp. 352–361.
- Hilal, N. and Wright, C.J. (2018) ‘Exploring the current state of play for cost-effective water treatment by membranes’, *npj Clean Water*, 1, p. 8.
- Hirabayashi, Y. (2002) ‘Pervaporation Membrane System for the Removal of Ammonia from Water’, *Materials Transactions*, 43, pp. 1074–1077.
- Hutton, G. (2013) ‘*Global costs and benefits of drinking water supply and sanitation interventions to reach MDG target and universal coverage*’. World Health Organisation. Available at:
https://www.who.int/water_sanitation_health/publications/2012/globalcosts.pdf
- Hutton, G. and Haller, L. (2004) ‘*Evaluation of the Costs and Benefits of Water and Sanitation Improvements at the Global Level*’, World Health Organisation. Available at:
https://www.who.int/water_sanitation_health/wsh0404.pdf. (Accessed 8 August 2018).
- Ingallinella, A., Sanguinetti, G., Koottatep, T., Montanger, A., Strauss, M., Jimenez, B., Spinosa, L., Odegaard, H. and Lee, D. (2002) ‘The challenge of faecal sludge management in urban areas--strategies, regulations and treatment options.’ *Water Science and Technology*, 46, pp. 285–94.

- International Energy Agency (2014) *Africa Energy Outlook: A focus on energy prospects in sub-Saharan Africa*. Available at: https://www.iea.org/publications/freepublications/publication/WEO2014_AfricaEnergyOutlook.pdf. (Accessed 8 August 2018).
- Jönsson, H., Stenström, T.-A., Svensson, J. and Sundin, A. (1997) 'Source separated urine-nutrient and heavy metal content, water saving and faecal contamination', *Water Science and Technology*, 35, pp. 145–152.
- Jung, Y.T., Narayanan, N.C. and Cheng, Y.-L. (2018) 'Cost comparison of centralized and decentralized wastewater management systems using optimization model', *Journal of Environmental Management*, 213, pp. 90–97.
- Lin, J., Aoll, J., Niclass, Y., Velazco, M.I., Wunsche, L., Pika, J. and Starckenmann, C. (2013) 'Qualitative and Quantitative Analysis of Volatile Constituents from Latrines', *Environmental Science & Technology*, 47, pp. 7876–7882.
- McGlinchey, D. (2008) *Bulk solids handling: equipment selection and operation*. McGlinchey, D. (ed.). Oxford, UK: Wiley-Blackwell.
- Onabanjo, T., Kolios, A.J., Patchigolla, K., Wagland, S.T., Fidalgo, B., Jurado, N., Hanak, D.P., Manovic, V., Parker, A., McAdam, E., Williams, L., Tyrrel, S. and Cartmell, E. (2016) 'An experimental investigation of the combustion performance of human faeces', *Fuel*, 184, pp. 780–791.
- Otterpohl, R., Braun, U. and Oldenburg, M. (2002) '*Innovative technologies for decentralised wastewater management in urban and peri-urban areas*'. Available at: https://sswm.info/sites/default/files/reference_attachments/OTTERPOHL%20et%20al.%202002%20Innovative%20technologies%20for%20decentralised%20wastewater%20management%20in%20urban%20and%20periurban%20areas.pdf. (Accessed 8 August 2018).
- Putnam, D.F. (1971) *Composition and concentrative properties of human urine*. Washington, United States. Available at: <https://ntrs.nasa.gov/archive/nasa/casi.ntrs.nasa.gov/19710023044.pdf>. (Accessed 8 August 2018).

Roberts, A. (2001) ‘Design Considerations and Performance Evaluation of Screw Conveyors.’, *Beltcon 11, International Materials Handling Conference*. Randburg, South Africa, 1-2 August 2001.

Rogers, T.W., de los Reyes, F.L., Beckwith, W.J. and Borden, R.C. (2014) ‘Power earth auger modification for waste extraction from pit latrines’, *Journal of Water, Sanitation and Hygiene for Development*, 4, pp. 72–80.

Rose, C., Parker, A., Jefferson, B. and Cartmell, E. (2015) ‘The Characterization of Feces and Urine: A Review of the Literature to Inform Advanced Treatment Technology’, *Critical Reviews in Environmental Science and Technology*, 45, pp. 1827–1879.

Srivastava, A., Goering, C. and Rohrbach, R. (1993) *Engineering principles of agricultural machines*. Srivastava, A. K. (ed.). Miami ,USA: American Society of Agricultural and Biological Engineers.

The Bill & Melinda Gates Foundation (2019) *Reinvent the toilet strategy and overview*. Available at: <https://www.gatesfoundation.org/What-We-Do/Global-Growth-and-Opportunity/Water-Sanitation-and-Hygiene/Reinvent-the-Toilet-Challenge-and-Expo> (Accessed: 15 November 2018).

Tufa, R.A., Pawlowski, S., Veerman, J., Bouzek, K., Fontananova, E., di Profio, G., Velizarov, S., Goulão Crespo, J., Nijmeijer, K. and Curcio, E. (2018) ‘Progress and prospects in reverse electrodialysis for salinity gradient energy conversion and storage’, *Applied Energy*, 225, pp. 290–331.

UNICEF and WHO (2015) *Progress on sanitation and drinking-water: 2015 Update and MDG Assessment*. Geneva: World Health Organisation. Available at: https://data.unicef.org/wp-content/uploads/2015/12/Progress-on-Sanitation-and-Drinking-Water_234.pdf. (Accessed 8 August 2018).

United Nations (2018) *Sustainable Development Goal 6*. Available at: <https://sustainabledevelopment.un.org/sdg6> (Accessed: 9 October 2018).

United Nations (2017) *World Population Prospects: The 2017 Revision, Key Findings and Advance Tables*. New York, NY. Available at:

https://esa.un.org/unpd/wpp/publications/files/wpp2017_keyfindings.pdf. (Accessed 8 August 2018).

Warsinger, D.M., Chakraborty, S., Tow, E.W., Plumlee, M.H., Bellona, C., Loutatidou, S., Karimi, L., Mikelonis, A.M., Achilli, A., Ghassemi, A., Padhye, L.P., Snyder, S.A., Curcio, S., Vecitis, C.D., Arafat, H.A. and Lienhard, J.H. (2018) 'A review of polymeric membranes and processes for potable water reuse', *Progress in Polymer Science*, 81, pp. 209–237.

World Bank (2019) *World Development Indicators*. Available at: <https://datacatalog.worldbank.org/dataset/world-development-indicators> (Accessed: 16 January 2015).

Yu, Y. (1997) *Theoretical modelling and experimental investigation of the performance of screw feeders*. PhD Thesis. University of Wollongong.

Zhao, Z.P., Xu, L., Shang, X. and Chen, K. (2013) 'Water regeneration from human urine by vacuum membrane distillation and analysis of membrane fouling characteristics', *Separation and Purification Technology*, 118, pp. 369-376.

2 SELECTION OF SCREW CHARACTERISTICS AND OPERATIONAL BOUNDARY CONDITIONS TO FACILITATE POST-FLUSH URINE AND FAECES SEPARATION WITHIN SINGLE HOUSEHOLD SANITATION SYSTEMS

Published in: *Environmental Science, Water Research and Technology*.

Selection of screw characteristics and operational boundary conditions to facilitate post-flush urine and faeces separation within single household sanitation systems

E. Mercer, P. Cruddas L. Williams, A. Kolios, A. Parker, S. Tyrrel, E. Cartmell, M. Pidou, E.J. McAdam*

Cranfield Water Science Institute, Vincent Building, Cranfield University, Bedfordshire, MK43 0AL, UK

*Corresponding author e-mail: e.mcadam@cranfield.ac.uk

Abstract

To ensure adequate access to sanitation in developing economies, off-grid single household sanitation has been proposed which obviates the need for significant infrastructure capital investment. Whilst treatment at this scale is most efficient when coupled to source separation (i.e. urine from faeces), existing source separation solutions have proved difficult to implement in this context. In this study, screw extrusion is therefore investigated to provide ‘post-flush’ source separation. Both screw characteristics and operational boundary conditions were evaluated. Preferential screw characteristics included tapering of the shaft and progressive pitch reduction, linked to a small extrusion aperture, the combination of which enhanced solids extrusion efficiency and promoted higher solids concentration in the extruded fraction. Whilst maximum extrusion efficiency was observed at high rotational speeds (over 400 rpm), this also promoted free water transport. Operating below 300 rpm instead introduced selectivity for transport of faecal sludge over urine, enabling phase separation. Constraining the volumetric ratio of urine to faeces also enhanced the extrusion rate of faecal sludge by increasing feed viscosity sufficient to overcome backpressure imposed by unmasticated food particles that would otherwise restrict separation. Importantly, this study demonstrates the feasibility of screw extrusion for ‘post flush’ separation of urine and faeces which constitutes a significant advancement towards realising sanitation at a single household scale.

Keywords: screw, faeces, urine, separation, solids concentration, extrusion

2.1 Introduction

The Millennium Development Goal (MDG) target 7D proposed by the United Nations (UN) aimed to halve the proportion of people without access to safe drinking water and

basic sanitation by 2015. Whilst this has been achieved for drinking water, the target has fallen short for sanitation. According to a progress report by WHO/UNICEF (2015), 2.4 billion people are without access to improved sanitation with 946 million people continuing to practice open defecation.

Pit latrines are the principal form of sanitation infrastructure available to urban populations of low income countries, offering improved sanitation at low costs (Rose et al., 2015). However, pit latrines only allow for long term in-situ storage of faecal sludge which often leads to local groundwater contamination (Graham and Polizzotto, 2013). Faecal sludge accumulates at an average rate of $0.1 \text{ L d}^{-1} \text{ capita}^{-1}$ (Foxon et al., 2011), with the average pit (2.5 m^3) expected to take 3 years to fill, assuming no degradation (Still and Foxon, 2012). However, this estimated fill rate neglects the volume attributable to urine (around $1.5 \text{ L d}^{-1} \text{ capita}^{-1}$), in addition to external factors such as groundwater intrusion, which constrains operational time between pit empties (Pickford, 1995; Rogers et al., 2014; Still, 2002). Maintenance issues such as pit collapse and termite damage have also been reported to reduce unlined pit lifespans up to a maximum of 13 months (Chidya et al., 2016; Cole et al., 2012). In a survey conducted by Chowdhry and Kone (2012), average household scale pit emptying fees ranged from \$ 35 household⁻¹ in India to \$ 95 household⁻¹ in Kenya. These indicative costs are between 12 % and 125 % of an individuals' average monthly salary which emphasises the economic sensitivity to overfilling (World Bank, 2019).

In seeking to improve economics for pit latrine emptying, Rogers et al. (2014) demonstrated the novel use of a screw 'elevator' for application to compacted sludge at the base of pit latrines which would reduce the mechanical cost of pit emptying. The authors noted that low viscosity sludge could only be extruded through increasing rotational speed. This finding is significant as it suggests that selectivity toward faecal solid phase over the liquid phase can be imparted which could help minimise pit latrine emptying. Source separation of urine from faecal sludge has been advocated to reduce emptying frequency through direct volume reduction. To date, source separation has been facilitated through application of toilets comprising two anatomically sited entry points in the toilet bowl to enable diversion of urine from faecal sludge. Further to providing volume reduction of the stored faecal sludge, source separation reduces the faecal contamination of the urine, which then simplifies downstream treatment of both

solid and liquid phases (Kirchmann and Pettersson, 1994; Larsen and Gujer, 1996; Maurer, Pronk and Larsen, 2006). Source separation is therefore conceived as an enabler to the introduction of household scale sanitation systems, such as those being developed through the recent, '*Reinvent The Toilet Challenge*', promoted by the Bill & Melinda Gates Foundation, which would eliminate both pit emptying and faecal sludge transportation costs (Otterpohl, Braun and Oldenburg, 2002). This is significant as restricted access and mechanical difficulties with sludge type encourage manual handling and high transportation costs stimulates direct disposal of faecal sludge into the environment, introducing a significant health risk to the local community (Ingallinella et al., 2002; Templeton, 2015).

Source separation systems have seen much success in Europe with urine regarded as a nutrient resource and power source (Ieropoulos et al., 2016; Lienert and Larsen, 2010; Maurer, Pronk and Larsen, 2006; Tilley, 2016). However, source separating toilets are prone to misuse. To illustrate, several studies have shown only 50-80 % urine recovery (Bjorn Vinnerås, 2001; Jönsson et al., 1997), indicating substantive urine carryover into the faecal compartment. In addition, 50 % of the world's population practice wet anal hygiene (Otterpohl, Braun and Oldenburg, 2002), which will inevitably increase the 'unbound' water fraction of the separated faecal sludge. High variability of the arising waste stream characteristics increases the complexity in terms of downstream technology selection and operation. In this paper, it is proposed that the inherent complexity associated with fluid separation in addition to variability in fluid composition can be resolved through use of a non-source separating toilet interface coupled with mechanical phase separation post 'flush'.

The screw auger has potential to be employed as the mechanical component for phase separation in post 'flush' systems. It comprises a series of helical flights mounted on a central shaft. Advancement of the faecal sludge through the screw is provided by rotation, and the frictional resistance created (Bolat and Boğoçlu, 2012; McGuire, 2009). Historically, screws were primarily used for lifting water, which required a pitch of between 30° and 38° (Lakeside Screw Pumps, 2015). However, screw conveyors, screw feeders, screw elevators and screw extruders have since been developed for transport of a broad range of high solids, high viscosity applications including plastics, food, powders, animal feed, cement and wastewater sludge (McGlinchey, 2008;

Roberts, 2001; Srivastava, Goering and Rohrbach, 1993). In the plastics and food industry, product consistency is controlled through adaptation of screw extrusion which features an aperture or ‘nozzle’ of constrained size coupled to a compression section which decreases free volume towards the aperture (Béreaux, Charneau and Moguedet, 2009; Santos and Chhabra, 2006; Womer, 2000). Whilst the work of Rogers et al. (2014) on pit latrine sludge is particularly encouraging, to the best of our knowledge there has been no study of the application of screw technology to non-source separating toilets. Specifically, the faecal sludge within a short residence time toilet will comprise of fresh faeces which are known to be of complex rheology and will inevitably differ from pit latrine sludge which has been subject to substantive biodegradation due to long storage times (Buckley et al., 2008; Woolley et al., 2014). Furthermore, owing to the short residence times adopted, faecal identity may be retained which would indicate the necessity to provide separation of individual faeces which comprise high solids concentration (11-34 %), heterogeneous composition and large particle size (up to 0.2 to 0.25 m in length) (Rose et al., 2015). Consequently, in this study, a screw extruder was developed to permit post-flush phase separation of urine and faeces. Specifically, the study will aim to: (i) identify appropriate screw characteristics that enable extrusion of fresh faecal sludge; (ii) establish boundary conditions that can provide for phase separation and a high product solids concentration; and (iii) to identify conditions that will enable consistent throughput despite the complex rheology.

2.2 Materials and methods

2.2.1 Experimental setup

The experimental unit (Figure 2.1) was designed to process the waste of a typical household of 10 users d^{-1} , which on average constitutes 15 L of urine and 2.5 kg of faeces (wet wt.) according to the literature (Rose et al., 2015). The bowl was fabricated (Model Products, Bedford, UK) from transparent Perspex to allow for a clear visual representation of the faecal settling, faecal loading and screw operation. The bowl was conical in shape with a depth of 50 cm and an entrance diameter of 35 cm decreasing to 7 cm at the base to facilitate settling. The screws were rapid prototyped from acrylonitrile butadiene styrene (ABS). The screw was fixed to a 60° incline which is above the angle ordinarily required to lift water (around 38°; Lakeside screw pumps,

2015), to aid phase separation. The area of the screw (choke area) exposed to the faecal sludge was 50 cm^2 . Urine and faeces was loaded into the bowl and a 10 minute lag time allowed prior to experimentation to ensure complete particle sedimentation (separation). This ensured that error due to solids settling rates was eliminated. The screw was controlled by a motor connected to a phase inverter which provided a rotational speed range of 20 to 800 rpm (BFL series, Oriental motors, Basingstoke, UK). The extrusion aperture was restricted at 0.85 cm^2 to promote the compression of particles for product consistency and was modelled on the nozzle of a classical screw extruder (Janes and Winch, 1993). The resultant faecal product exited the rig via the extrusion aperture and was collected for mass and solids analysis.

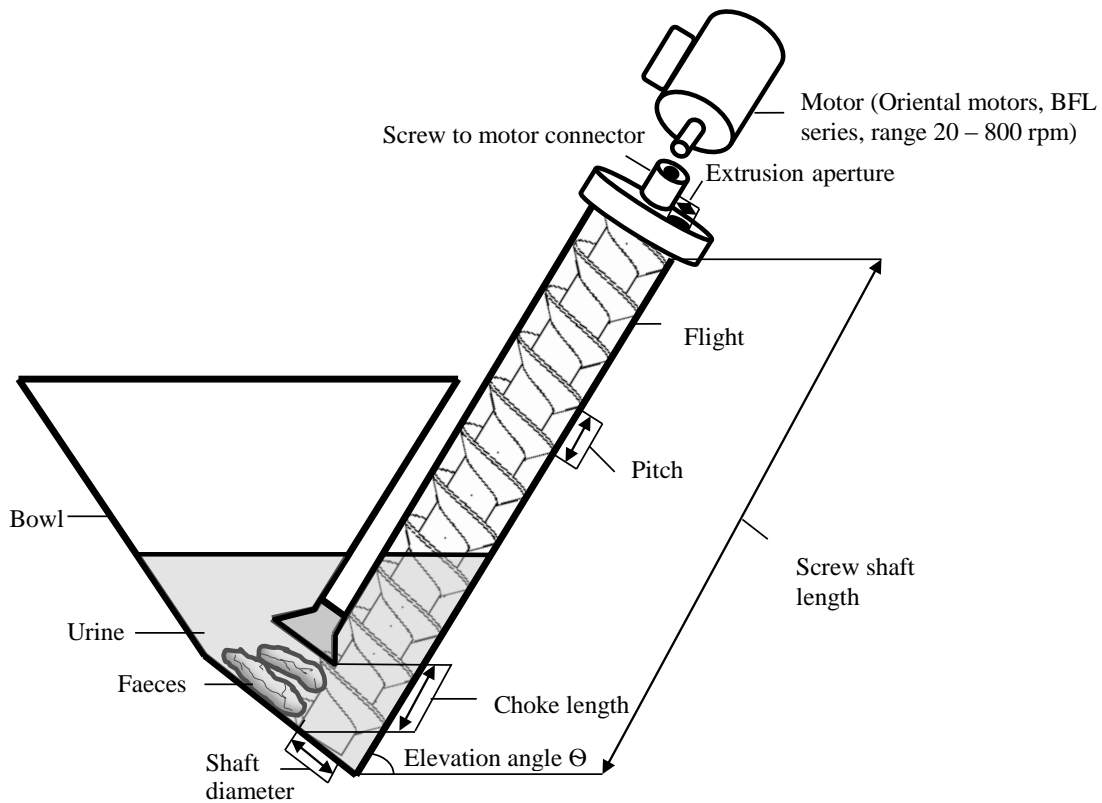


Figure 2.1 Experimental setup of the screw conveyor rig

2.2.2 Screw characteristics

A reference screw was designed with a constant pitch of 4 cm and shaft diameter of 4 cm. To establish the advantage of individual screw characteristics, six further screws were designed which permitted evaluation of each characteristic identified (Table 2.1, Figure 2.2). Shaft diameter was explored by screws 5 and 6 (ranging from 2-4 cm),

pitch was investigated with screws 1 and 2 (ranging from 2-4 cm) examining both constant and tapered features. Screw 3 possessed an exaggerated shaft diameter and pitch frequency. To investigate whether the screw is able to assist in screw loading, screw 4 was designed with starter flights. These were vertical ridges of 0.5 cm depth along the first 7 cm of the screw to promote ‘grabbing’ or pulling of the faecal sludge into the feed section. The compression ratio was determined using Womer (2000):

$$\text{Compression ratio} = \frac{h_{in}}{h_{out}} \quad \text{Eq. 2.1}$$

where h_{in} is the difference in length between the shaft passage diameter and the shaft diameter at the entrance and h_{out} at the exit.

Total dry solids within the system was determined by taking 5 g sub-samples (wet wt.) from the initial feedstock and at the extrusion aperture at timed sampling intervals following initiation. Total dry solids were determined using the standard method of drying samples in an oven overnight at 105 °C (APHA;AWWA;WEF, 2005). The ability of the screw rig to transport solids was based on solids recovery within the extruded portion using:

$$\text{Total solids recovered (\%)} = \frac{\text{Extruded solids mass (g)}}{\text{Initial solids mass (g)}} \times 100 \quad \text{Eq. 2.2}$$

Alongside the total extrusion, performance was also based on subsamples of the extruded output in terms of extrusion rate (g s^{-1}) and solids concentration (%). These were collected at four time intervals of 10 second duration.

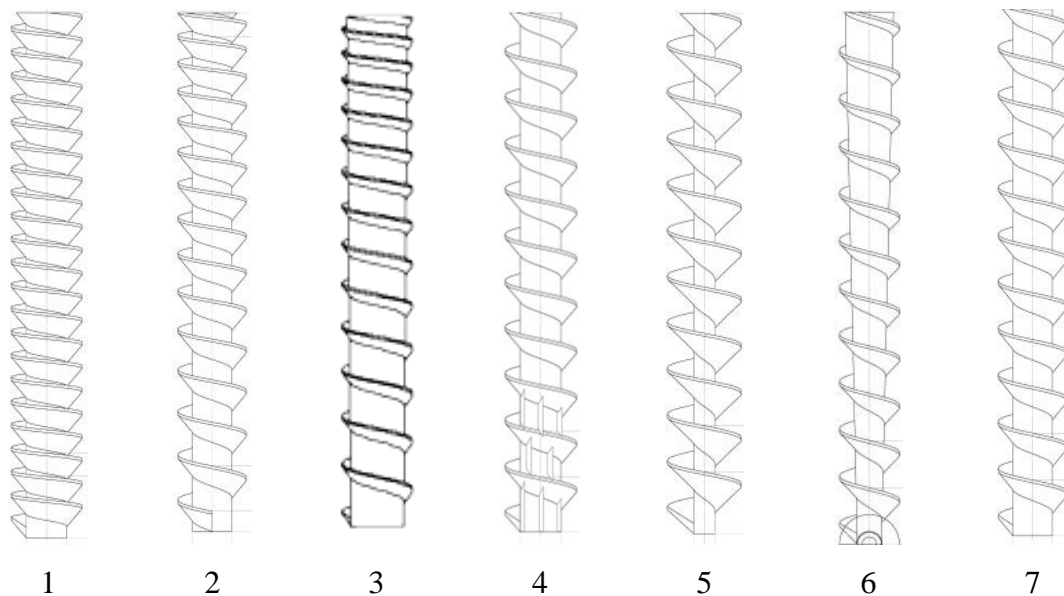


Figure 2.2 Schematics of screws 1-7.

Table 2.1 Design features of experimental setup and screws. *reference screw.

Grouping				Screw ID	Flights (no.)	Vertical ridge in feed zone (mm)	Pitch (cm)	Shaft diameter (cm)	Shaft passage diameter (cm)	Screw length (cm)	Elevation angle (°)	Aperture area (cm ²)	Choke length (cm)	Effective choke area (cm ²)	Designed capacity (L)	Bowl top to base diameter ratio	Compression ratio
Starter flights	No. flights/pitch	Shaft diameter	Tapered all														
x				1	22	0	2	4	8	45	60	0.85	7	50	17.5	5:1	1:1
x				2	15	0	2-4	4	8	45	60	0.85	7	50	17.5	5:1	1:1
			x	3	15	0	0.5-4	5-7	8	45	60	0.85	7	50	17.5	5:1	3:1
x				4	11	5	4	4	8	45	60	0.85	7	50	17.5	5:1	1:1
		x		5	11	0	4	2	8	45	60	0.85	7	50	17.5	5:1	1:1
		x		6	11	0	4	2 - 4	8	45	60	0.85	7	50	17.5	5:1	1.5:1
x	x	x	x	7*	11	0	4	4	8	45	60	0.85	7	50	17.5	5:1	1:1

2.2.3 Preparation and collection of synthetic and real faeces

The operating conditions of the screw rig were firstly investigated using synthetic faeces (Table 2.2) to allow for consistent conditions when examining individual boundary conditions. The recipe was developed by the Pollution Research Group from the University of Kwazulu Natal to broadly correspond to the rheological properties of real fresh faeces (Pollution Research Group, 2014). The analogue was slightly modified to structure into faecal form. The effects of pre-treatment were examined by modelling the synthetic faeces into 10 cm particles (unaltered faeces), 1 cm chopped cubed or completely mixed. The trials were based on a 500 g starting faecal mass and 3 L urine volume which represents the waste of two toilet users per day.

Table 2.2 Synthetic faeces recipe (Adapted from Pollution Research Group, 2014) and real faeces characteristics.

Ingredients		Mass for 1 kg (g)		
Synthetic faeces	Water	400.0		
	Yeast	194.9		
	Psyllium	65.1		
	Peanut oil	103.9		
	Miso	65.1		
	Polyethylene glycol	72.8		
	Inorganic calcium phosphate	65.1		
	Cellulose	33.2		
Real faeces		Solids concentration (%)	Bristol Stool Chart (1–7)	Faeces mass (g)
	Average	22.4	6	131.2
	Range	12.0–53.3	1–6	15.3–440.9
	Total number of samples	84		

The real faeces collection regime was approved through Cranfield University’s Research Ethics System (CURES). Faecal collection was undertaken using consenting anonymous volunteers. Boxes containing a list of instructions, gloves, disposable sampling bowls, a waste bag and sample bag, were conveniently placed within the toilet area. The boxes were collected daily to reduce odour for volunteers and maintain the freshness of the faeces. Each individual faeces was weighed, classified on the Bristol Stool Scale (BSS), analysed for total dry solids and combined to reach 500 g. Depending on the trial, they were directly placed into the bowl (unaltered), chopped on 1 cm by 1 cm graph paper for accuracy or mixed thoroughly within the bowl with 3 L of water. A 10 minute lag time allowed prior to experimentation to ensure complete

particle sedimentation (separation). A 24 hour trial was also introduced to understand the effect of settling on throughput. Trials were conducted in batch mode to minimise particle re-dispersion after settling. Both synthetic and real faeces trials were performed in triplicate.

2.3 Results and discussion

2.3.1 Comparison of screw characteristics

Critical screw characteristics were compared at a fixed rotational speed of 100 rpm with the synthetic mixed faeces that were homogenised within the receiving bowl. Each screw variant was compared to reference Screw 7, which comprised a set pitch and shaft diameter of 4 cm (Figure 2.2). Through doubling pitch frequency from Screw 7 to Screw 1, it was evidenced that the total mass extruded was significantly different ($p < 0.05$). Whilst the average total solids extruded through tapering the screw (Screw 2 compared to Screw 7) was noted to be improved, the values were not significantly different ($p > 0.05$) (Figure 2.3). Screw 3 which comprised a tapered delivery section, and progressively narrowing pitch and shaft diameter, identified to provide the greatest solids processing within the fixed time interval of 100 s (Figure 2.3). It is therefore asserted that extrusion of faecal sludge is governed by three screw characteristics: (i) an increased number of flights, which will increase carrying capacity and introduce a commensurate reduction in pitch; (ii) a tapered pitch, providing progressive reduction in carrying capacity between flights toward the extrusion aperture; and (iii) a progressive tapering of shaft diameter toward the extrusion aperture, which provides a further reduction in carrying capacity between flights. The characteristics provided by Screw 3 (Figure 2.3) are analogous to screw extruder design where the compression section embedded in the shaft diameter increases with the direction of flow, which introduces pressure behind the aperture to drive fluid separation (Béreaux, Charneau and Moguedet, 2009). Similar dimensional characteristics have been successful in screw systems used for municipal sewage sludge thickening (Mitsubishi Kakoki Kaishi Ltd., 2015).

In addition to providing the highest specific volumetric throughput, the preferred screw achieved a higher solids concentration in the extruded product, of 14.2 % compared to a maximum of only 10.4 % achieved with the alternate screw designs

tested under identical boundary conditions (Figure 2.4). This can be accounted for by the higher compression ratio employed with screw 3 (3:1 compared to 1.5:1 which was the next highest compression ratio) which reduces the overall channel volume and increases the driving pressure. The comparable screw design is featured within commercial screw press design which has been demonstrated to reduce sewage sludge volume by up to 90 % (Huber, 2015).

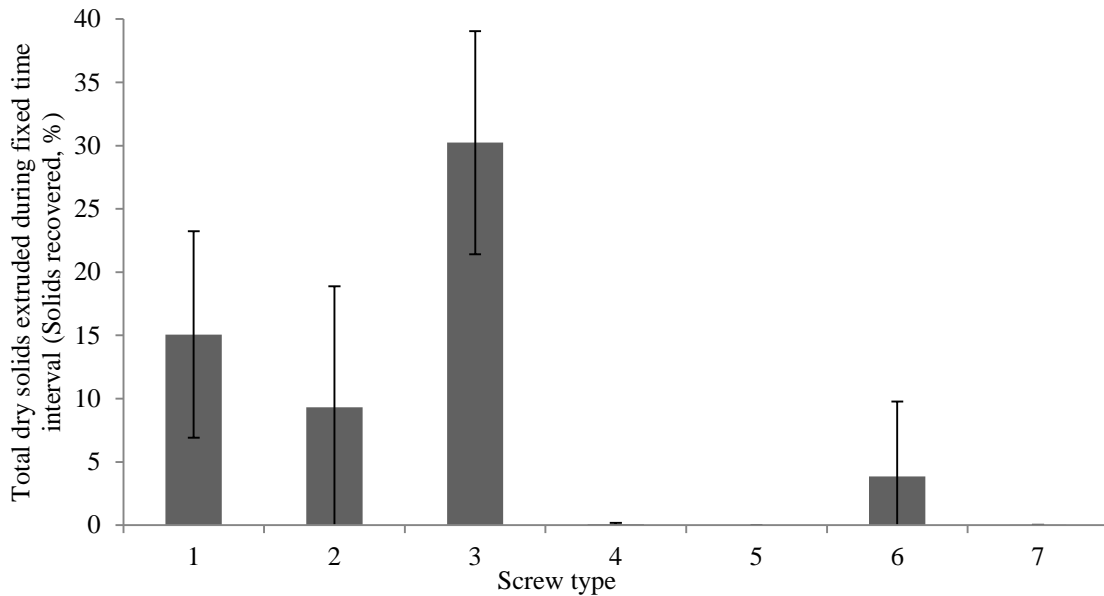


Figure 2.3. Comparison of screw types by the solids extruded from the initial loading (%) within a prescribed time interval. Mixed form; 100 rpm; 100 seconds; 3 L water; 500 g synthetic faeces at 60 % solids content. Error bars represent the standard deviation of a triplicated experiment.

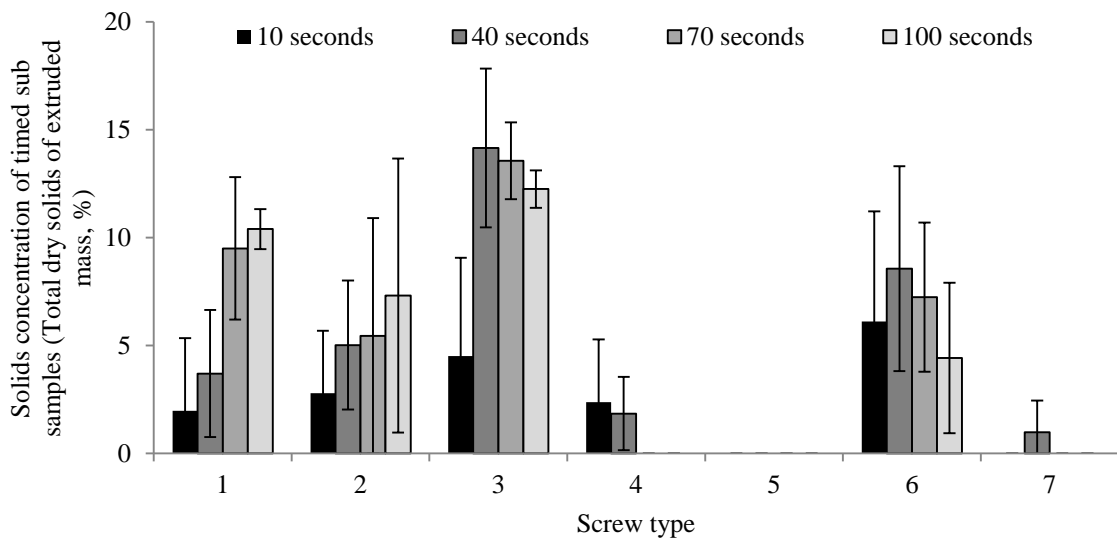


Figure 2.4 Solids concentration (%) of output subsamples taken in 30 second intervals for a 10 second duration. Mixed form; 100 rpm; 3 L water; 500 g synthetic faeces at 60 % solids content. Error bars represent the standard deviation of a triplicated experiment

2.3.2 Importance of faecal sludge pre-treatment on faecal solids extrusion efficiency

Faecal sludge pre-treatment was assessed to ascertain whether changes to particle size were necessary to enhance extrusion efficiency of fresh faecal sludge (Figure 2.5, Table 2.3). Visual inspection of the screw feed zone evidenced that without pre-treatment, the synthetic faeces maintained their particle identity and their transition from the sedimentation tank into the screw feed zone was constrained by the choke length (7 cm). Partial pre-treatment (chopping into small sections) and full pre-treatment (thorough blending) of faecal sludge evidenced the capability to enhance solids extrusion efficiency (Figure 2.5). Analysis of faecal sludge distribution through Screw 3 indicated that whilst only around 30 % of the faecal sludge was extruded within the fixed time period, a further 24 % was loaded within the screw (Figure 2.5). Therefore, in steady state operation (after initial priming), the solids recovery would be substantially higher (in this case 54 %), indicating the potential for further recovery through increasing the number of revolutions. It is asserted that whilst pre-treatment is evidenced to be advantageous, increasing choke length to provide increased contact between the screw feed section and faecal sludge maybe sufficient to promote uptake of coarse faecal diameter particles without pre-treatment, which is substantiated by Rogers et al. (2014), who also concluded that extending choke length can provide some increase in flow for high viscosity mixtures.

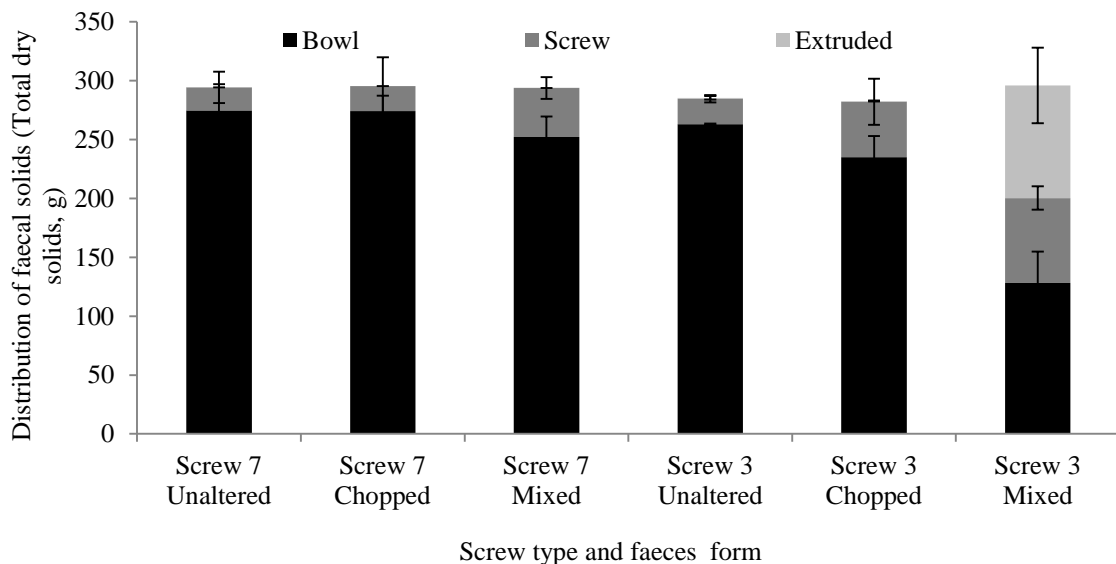




Figure 2.5 Distribution of total dry solids (g) by compartment for Screw 7 (reference) and Screw 3 following assessment at 100 rpm for a fixed time interval of 100s. 100 rpm; 100 seconds; 3 L water; 500 g synthetic faeces at 60 % solids content. Error bars represent the standard deviation of a triplicated experiment

Table 2.3 Effect of pre-treatment on screw loading. Screw 3; mixed; 100 rpm; 100 seconds; 3 L water; 500 g synthetic faeces.

	Faeces form	Extruded	Before	After	Comment
10 cm					Little or no movement onto the screw
1 cm					Solids within screw vicinity collected
Mixed					Solids move freely onto the screw

2.3.3 Effect of rotational speed on faecal solids extrusion efficiency and phase separation

Screw 3 was adopted for further assessment of rotational speed, due to the enhanced solids recovery demonstrated. Whilst rotational speed was varied, solids extrusion efficiency was based on a fixed number of revolutions to provide comparison (Figure 2.6). An increase in rotational speed from 40 to 400 rpm markedly increased the total dry solids extruded. An increased rotational speed is associated with an increase in shear, feed pressure and vortex motion which promotes the advancement of the faecal sludge through the screw (Janes and Winch, 1993; Roberts, 1999; Xu, Jing and Duffy, 2001). Maximum solids extrusion within the fixed processing interval (200 rotations) was evidenced at 400 rpm. Roberts (2001, 1999) described conveyance of non-cohesive granular material to be a function of the fill and vortex efficiency with material back slippage limiting conveyance; the vortex efficiency being induced by screw rotational speed. In this study, back slippage was not observed following cessation of screw

operation. This is analogous to observations made with concentrated bentonite slurry, which exhibited a high friction coefficient and suggests that solids extrusion efficiency is constrained by the rate of faecal sludge entering the screw rather than back slippage (Rogers et al., 2014).

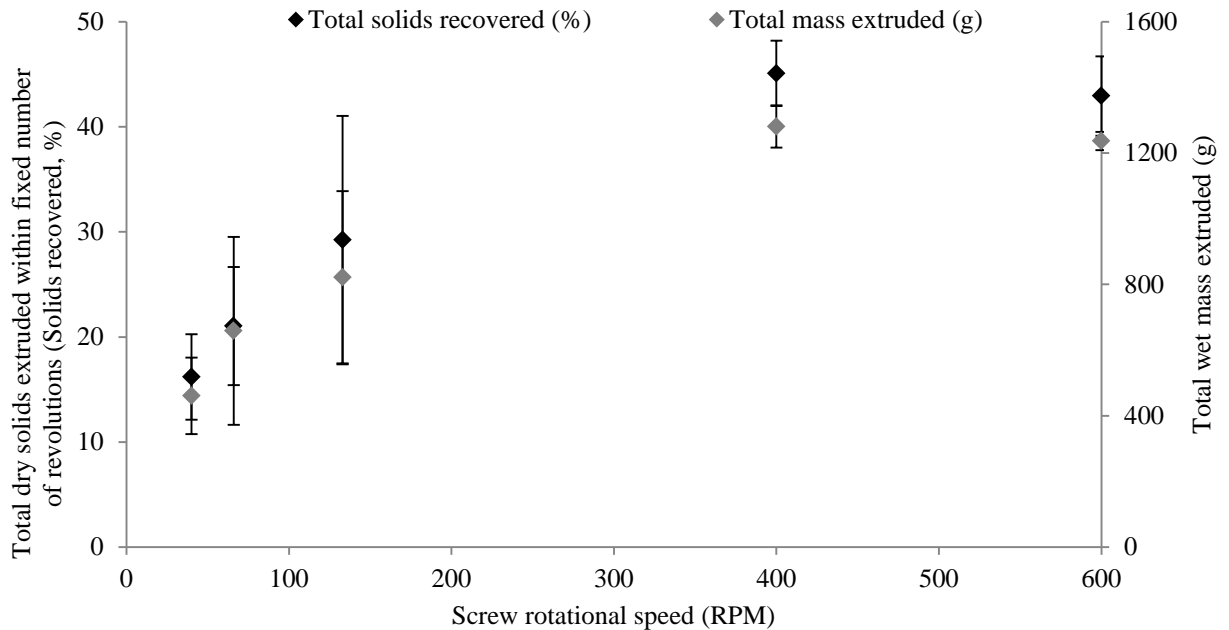


Figure 2.6 Impact of screw rotational speed selection on solids extrusion efficiency within a fixed number of rotations. Screw 3; mixed form; 3 L water; 500 g synthetic faeces. Error bars represent the standard deviation of a triplicated experiment

Increasing rotational speed above 400 rpm did not increase solids extrusion efficiency. To illustrate, the solids recovery for 400 rpm was 45 ± 3 % compared to 43 ± 4 % at 600 rpm. It is asserted that conveyance above 400 rpm was constrained by the feed rate and potential conveying capacity of the screw (Roberts, 1999). Santos and Chhabra (2006) suggested that when the screw feeds more material than the aperture can process, which in this study is induced by increasing rotational speed, then the back pressure will overcome the pressure required for extrusion. Therefore, the plateau in solids extrusion efficiency noted in this study (Figure 2.6) could also result from the extrusion aperture selected which was 0.85 cm^2 , and can impose a resistance to flow through back pressure. Free water uptake by screw extrusion was subsequently assessed and it was determined that provided rotational speed is maintained below 300 rpm, negligible free water transport will occur (Figure 2.7). For comparison, in previous trials using synthetic faecal sludge, solids extrusion was possible at rotational speeds of less than

100 rpm (Figure 2.6). The difference in transport between the two fluid phases can be explained by the lower friction coefficient of water and the screw angle adopted, which is around 20° steeper than conventional screws used to lift water (Roberts, 1999). The capability for fluid separation has been similarly evidenced in a model 5 % bentonite solution, where a minimum rotational speed of 300 rpm was identified to enable free water transport (Rogers et al., 2014).

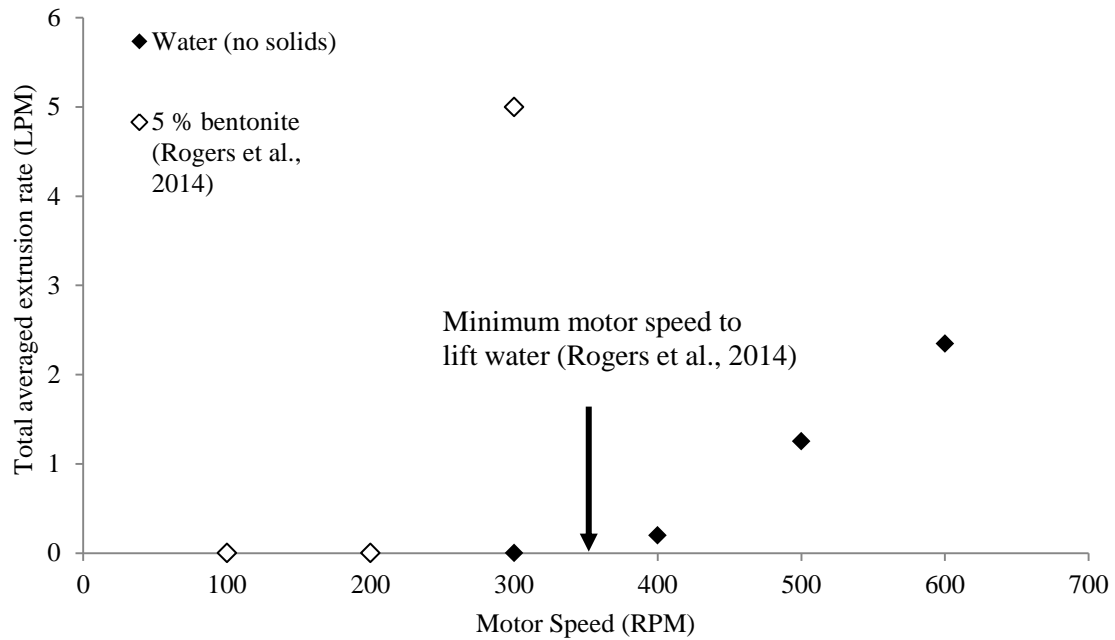


Figure 2.7 Total averaged extrusion rate of water compared with Rogers et al., (2014) using 5 % synthetic sludge and water (Screw 3; 3 L water only trial, runtime until bowl emptied). Error bars represent the standard deviation of a triplicated experiment

2.3.4 Impact of faeces to urine volumetric ratio on solids extrusion efficiency

The impact of faecal sludge to urine volumetric ratio on solids extrusion efficiency was evaluated at a rotational speed of 100 rpm to limit free water ingress during faecal sludge extrusion. Analysis of faecal sludge distribution evidenced that for water volumes of 0.5 and 1 L, all of the faecal sludge present in the bowl has been extruded within the prescribed timeframe (100 s). Solids extrusion efficiency was observed to decline following an increase in the water fraction (Figure 2.8). For example, when the water fraction was doubled from 0.5 L to 1 L and subsequently increased to 3 L, solids extrusion rate declined from 833 g min⁻¹ to 678 and 438 g min⁻¹ respectively, illustrating that a six times dilution of average faecal solids concentration, approximately halved solids extrusion rate. It is therefore asserted that the reduction in solids extrusion rate at

higher water volume is not directly associated with dilution but rather can be ascribed to a reduction in faecal sludge viscosity which reduces the friction coefficient and can promote back slippage (Roberts, 2001, 1999).

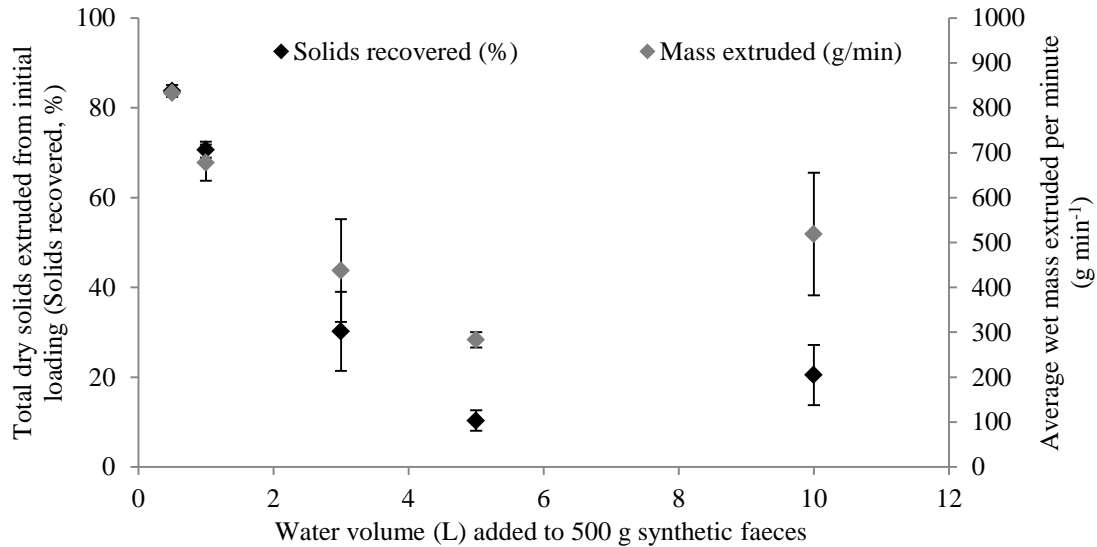


Figure 2.8 Effect of free water volume on solids recovered (%) and mass extruded (g min^{-1}). Screw 3; mixed form; 100 rpm; 100 seconds; 500 g synthetic faeces. Error bars represent the standard deviation of a triplicated experiment.

2.3.5 Application of screw extrusion to real, fresh human faeces

In contrast to the synthetic faeces trials, the impact of pre-treatment upon the solids extrusion efficiency of fresh human faeces was less evident, due to the vortex generated by the screw's rotation which mixed the contents. Therefore a greater mass of fresh human faeces was processed without pre-treatment (Figure 2.9). However, this experimental evidence does not provide definitive resolution as to the importance of pre-treatment for maximising solids extrusion efficiency, as each of the comparative trials (unaltered, chopped, mixed) which were conducted with 3 L of water were cut short due to blockages caused by large undigested food particles (Figure 2.10) which concentrated behind the extrusion aperture. The resident solids appeared reasonably dewatered, and yielded a total dry solids concentration of 20 to 24 %, equivalent to that of a healthy human stool (Rose et al., 2015). Qualitative analysis identified the presence of un-masticated whole foods such as corn (around 0.5 cm^2), tomato seeds, fibrous tomato skins (around 1 cm^2) and roughage concentrated behind the aperture. Screw 3 was compared with Screw 1 to identify whether the pitch and shaft characteristics of Screw 3, which ostensibly promote consolidation, were responsible for the arising blockages (Figures 2.10a and b). The comparison evidenced blockage of both screws

behind the extrusion aperture. Santos and Chhabra (2006) proposed that the aperture diameter should be eight times larger than the particulate material to avoid clogging. Use of a larger diameter extrusion aperture may then be beneficial to obviate blockages; although this may reduce compression behaviour and so reduce the arising faecal solids concentration.

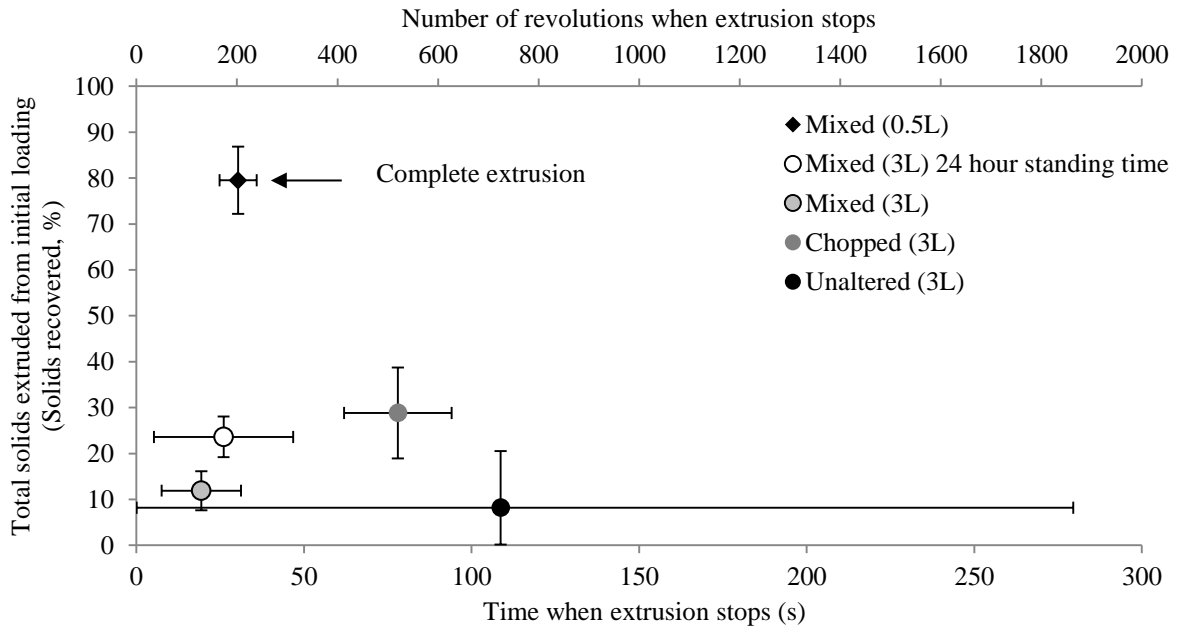


Figure 2.9 Effect of faeces form, standing time and free water volume on total solids recovered from initial loading (%). (Screw 3, 400 rpm, 500 g real faeces, trial left to run until blockage or bowl emptied). Error bars represent the standard deviation of a triplicated experiment.

Importantly, when a lower urine to faeces ratio was employed (1:1), which increases the averaged solids concentration in the post-flush sedimentation tank, complete extrusion from the tank was possible without introducing blockage of the extrusion aperture (Figure 2.9). This can be accounted for by the higher fluid viscosity which sufficiently increased feed pressure to compensate for the backpressure introduced at the extrusion aperture by unmasticated foods. Whilst the initial faecal solids concentration ranged between 12-53 % (before the addition of water) across all of the human faeces tests undertaken, the solids concentration of the extruded fraction varied by only ± 2 %, which indicates that the selected screw characteristics can provide some consistency. The impact of faecal sludge storage time was subsequently studied and whilst sedimentation of the faecal solids was observed to occur in around ten minutes, an averaged solids extrusion rate of 794 g min^{-1} was observed for faecal sludge stored for

24 hours compared to only 276 g min^{-1} for a storage time of ten minutes. Furthermore, the average solids recovery after 24 hours was $23.6 \pm 4.4 \%$ compared to $11.9 \pm 4.2 \%$ after 10 minutes settling time. It is therefore proposed that storage encourages bonding of the stored sludge, increasing fluid viscosity, and hence the efficiency of extrusion.

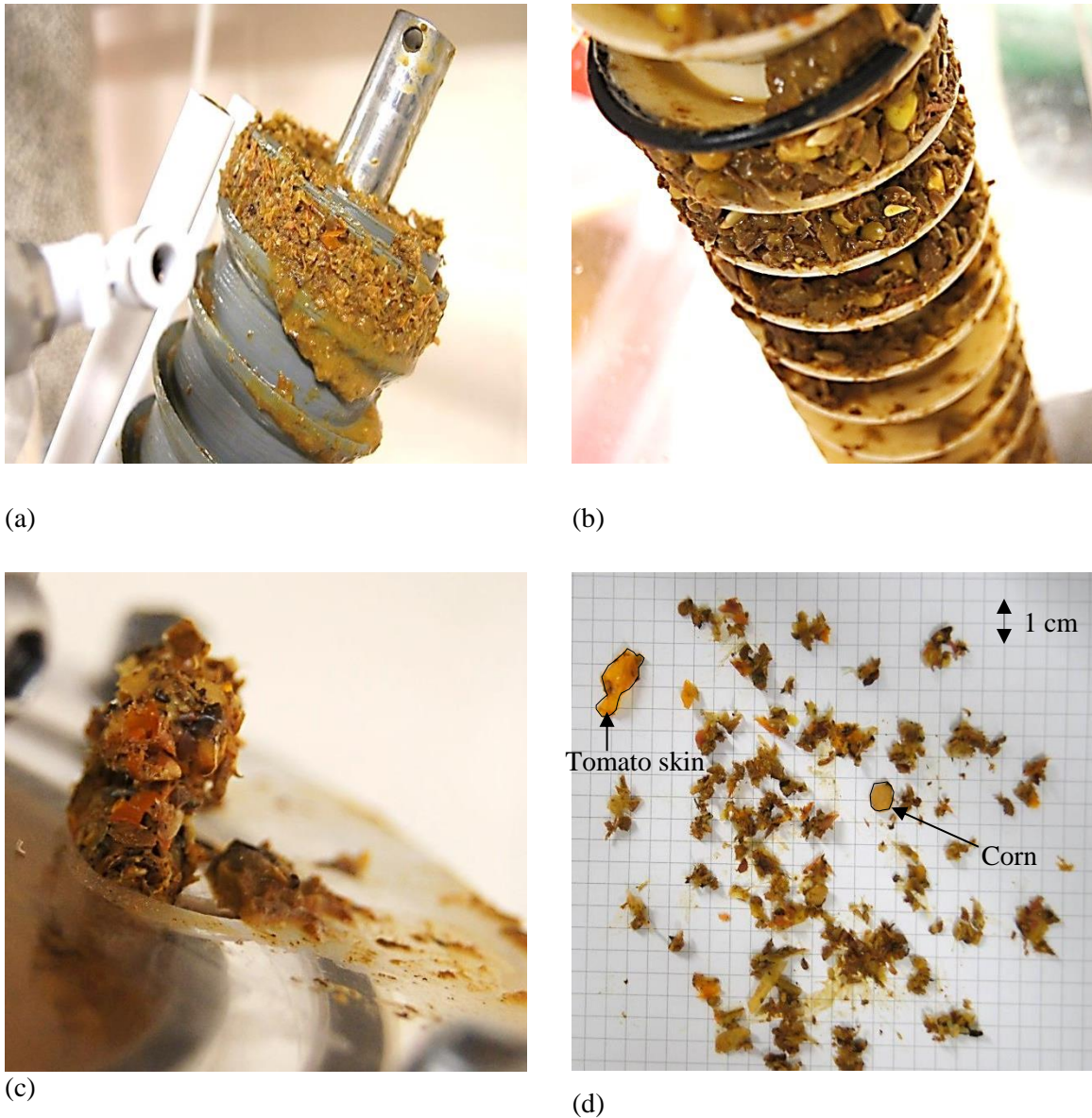


Figure 2.10 Accumulation of unmasticated food particles: (a) within the metering section, screw 3; (b) within the metering section, screw 1; (c) at the aperture; and (d) sample taken from the aperture.

2.4 Knowledge transfer to post flush source separation of urine and faeces

In this study, preferential screw characteristics and operational boundary conditions have been identified that enable post-flush faecal sludge transport and phase separation. In the context of applying screw extrusion for post-flush phase separation of urine and

faeces in single household scale toilets, several recommendations can be made. A screw comprised of: a continually diminishing pitch and tapered shaft diameter appears preferential for faecal sludge extrusion. A rotational speed of 400 rpm provided maximum solids extrusion efficiency. However, at this rotational speed, urine can be simultaneously transported. Therefore whilst less efficient, it is recommended that an operating rotational speed below 300 rpm is specified. A plateau in solids extrusion efficiency was achieved for rotational speeds exceeding 400 rpm, which it is suggested could have been constrained by feed rate. Therefore increasing the applied choke length to increase feed flow rate may offset the lower solids extrusion efficiency experienced at rotational speeds of 300 rpm or below.

For synthetic faeces, pre-treatment was a prerequisite to enabling sufficient engagement between faecal sludge and the screw feed section to initiate extrusion, as the applied choke constrained contact. Whilst this was not specifically evidenced when applied to fresh human faeces due to blockages, we suggest that an analogous problem is presented with human faeces that sustain their characteristic shape following sedimentation, and propose that extension of the choke length may be sufficient to enable the necessary engagement for extrusion without pre-treatment of the faecal sludge. However, adaptation of the preliminary flights as a pre-treatment, similar to those incorporated in progressive cavity pumps for primary sludge pumping (Fahlgren, 2012), could also advantage extrusion efficiency through enabling preliminary particle size reduction of coarse unmasticated food particles prior to extrusion. This would also enhance resilience to foreign materials such as toilet paper, which should be considered for certain user groups.

Blockages were also diminished during extrusion through limiting the water to faeces ratio to 1:1. Following the introduction of faeces and urine into the toilet, faecal particles quickly settle, creating a solid-liquid interface. A water to faeces ratio near 1:1 can then be practically achieved by: (i) operating the screw in batch thus allowing faecal sludge volume to develop; and (ii) incorporating a weir structure to permit physical separation of the liquid phase (Cruddas et al., 2015). The screw characteristics employed are similar to those used for screw extruders in the plastics industry to promote thickening and product consistency (Rosato, 2013). Reasonably consistent solids concentration (in the extruded sludge) was demonstrated in each of the human

faeces trials undertaken, which was mediated by the extrusion aperture. An increase of the extrusion aperture area may be necessary to limit blockages but the impact on consistency of the extruded fraction (solids concentration) should be closely examined. Real human faeces trials were operated at 400 rpm and thus were subject to some free water inclusion which constrained the final product solids concentration to between 12 and 15 %. However, the dewatered material recovered from within the metering screw section was around 25 %, which is the effective solids concentration of a healthy human stool. This demonstrates that with the optimisation of the relationship between rotational speed, screw pitch, aperture selection and feedstock viscosity, the output solids concentration can be further increased, improving downstream drying process efficiency. As such, effective post-flush fluid separation (i.e. urine and faeces) is possible, sufficient to facilitate practicable sanitation solutions at a household scale.

2.5 Conclusions

In this study, the feasibility of screw extrusion for post-flush phase separation of urine and faeces has been demonstrated. Post-flush source separation can therefore be considered a platform technology on which treatment capacity can be integrated which constitutes a significant advancement towards realising sanitation at a single household scale. Preferential screw characteristics and operational boundary conditions have been identified to facilitate post flush urine and faeces separation which include:

- Screw characteristics identified included tapering of the shaft and progressive pitch reduction, linked to a small extrusion aperture, the combination of which provided around a 200 % increase in solids extrusion
- Operation below 400 rpm which is below the maximum extrusion efficiency but can facilitate phase separation.
- For synthetic faeces, it was observed that application of pre-treatment to reduce faecal particle size increased mobility of faecal sludge into screw feed section. Further confirmation as to whether an expansion in choke length is sufficient to eliminate the need for particle size reduction.

Several other areas of investigation are also warranted:

- Further analysis of the feed section to enhance breakage/ shredding of coarse food particle. This would also help transition faecal sludge from the

sedimentation tank into the screw feed section through breakage of coarse faeces.

- Evaluation of the trade-off between an increase in extrusion aperture dimensioning to obviate risk of blockage from unmasticated food particles versus the reduction in back pressure that an increased aperture dimension will provide, potentially reducing the extruded solids concentration.
- Operation during steady state versus start-up. This study has investigated screw loading and operation through start up performance. Steady state operation would demonstrate higher solids recovery with an already primed screw with continuous operation promoting particle compression against the extrusion aperture. Once primed, the screw could potentially operate at lower rotational speeds.

2.6 References

APHA;AWWA;WEF (2005) *Standard Methods for the Examination of Water and Wastewater*. 21st ed. Washington D.C, USA: American Public Health Association.

Béreaux, Y., Charmeau, J.-Y. and Moguedet, M. (2009) 'A simple model of throughput and pressure development for single screw', *Journal of Materials Processing Technology*, 209, pp. 611–618.

Bjorn Vinnerås (2001) 'Faecal separation and urine diversion for nutrient management of household biodegradable waste and wastewater', *Journal of Biosciences*, 5, pp. 29–50.

Bolat, B. and Boğoçlu, M. (2012) 'Increasing of screw conveyor capacity', *Trends in the Development of Machinery and Associated Technology*, 16, pp. 207-210.

Buckley, C.A., Foxon, K.M., Brouckaert, C.J., Rodda, N., Nwaneri, C., Balboni, E., Couderc, A. and Magagna, D. (2008) *Scientific support for the design and operation of ventilated improved pit latrines (VIPs) and the efficacy of pit latrine additives*. Durban, South Africa: Water Research Commission.

Chidya, R.C.G., Holm, R.H., Tembo, M., Cole, B., Workneh, P. and Kanyama, J. (2016) 'Testing methods for new pit latrine designs in rural and peri-urban areas of Malawi where conventional testing is difficult to employ', *Environmental Science: Water Research & Technology*, 2, pp. 726–732.

Chowdry, S. and Kone, D.D. (2012) '*Business Analysis of Fecal Sludge Management: Emptying and Transportation Services in Africa and Asia*', Bill & Melinda Gates Foundation. Available at: https://www.pseau.org/outils/ouvrages/bill_melinda_gates_foundation_business_analysis_of_fecal_sludge_management_emptying_and_transportation_services_in_africa_and_asia_2012.pdf. (Accessed 8 August 2016).

Cole, B., Pinfold, J., Ho, G. and Anda, M. (2012) 'Investigating the dynamic interactions between supply and demand for rural sanitation, Malawi', *Journal of Water, Sanitation and Hygiene for Development*, 2, pp. 266–278.

Cruddas, P.H., McAdam, E.J., Kolios, A., Parker, A., Williams, L., Martin, B., Buckley, C.A. and Tyrrel, S. (2015) 'Biosolids Management Within the Nano Membrane Toilet – Separation', Thickening and Dewatering. *WEF/IWA Residuals and Biosolids Conference*. Washington, USA, 7-10 July 2015.

Fahlgren, M. (2012) *Handbook of sludge pumping*. Gabryjonczyk, R., Lindberg, A., Pedersen, J. and Uby, L. (eds.) Sundbyberg, Sweden: Xylem Water Solutions AB.

Foxon, K., Buckley, C., Brouckaert, C. and Bakare, B. (2011) *What Happens When the Pit is Full?* Durban, South Africa. Water Research Commission. Available at: http://www.ecosanres.org/pdf_files/WhatHappensWhenThePitIsFullFSMSeminarReportSouthAfricaNodeMarch2011.pdf. (Accessed 8 August 2016).

Graham, J.P. and Polizzotto, M.L. (2013) 'Pit latrines and their impacts on groundwater quality: A systematic review', *Environmental Health Perspectives*, 121, pp. 521–530.

Huber (2015) *Huber Screw Press Q Press*. Available at: <https://www.huber.co.uk/products/sludge-treatment/sludge-dewatering/huber-screw-press-q-pressr.html> (Accessed: 8 January 2016).

Ieropoulos, I.A., Stinchcombe, A., Gajda, I., Forbes, S., Merino-Jimenez, I., Pasternak, G., Sanchez-Herranz, D. and Greenman, J. (2016) 'Pee power urinal – microbial fuel cell technology field trials in the context of sanitation', *Environmental Science Water Research and Technology*, 2, pp. 336–343.

Ingallinella, A., Sanguinetti, G., Koottatep, T., Montanger, A., Strauss, M., Jimenez, B., Spinosa, L., Odegaard, H. and Lee, D. (2002) 'The challenge of faecal sludge management in urban areas--strategies, regulations and treatment options.', *Water Science and Technology*, 46, pp. 285–94.

Janes, R.I. and Winch, P.J. (1993) 'Mixing and shear predictions for a single-screw extruder, using computational simulation', *IMA Journal of Management Mathematics*, 5, pp. 399–415.

Jönsson, H., Stenström, T.-A., Svensson, J. and Sundin, A. (1997) 'Source separated urine-nutrient and heavy metal content, water saving and faecal contamination', *Water Science and Technology*, 35, pp. 145–152.

Kirchmann, H. and Pettersson, S. (1994) 'Human urine - Chemical composition and fertilizer use efficiency', *Fertilizer research*, 40, pp. 149–154.

Lakeside screw pumps (2015) *Lakeside screw pumps*. Available at: http://www.lakeside-equipment.com/bulletins/bul_217.pdf (Accessed: 8 September 2015).

Larsen, T. and Gujer, W. (1996) 'Separate management of anthropogenic nutrient solutions (human urine)', *Water Science and Technology*, 34, pp. 87–94.

Lienert, J. and Larsen, T. (2010) 'High acceptance of urine source separation in seven European countries: A review', *Environmental Science and Technology*, 44, pp. 556–566.

Maurer, M., Pronk, W. and Larsen, T.A. (2006) 'Treatment processes for source-separated urine.' *Water research*, 40, pp. 3151–66.

McGlinchey, D. (2008) *Bulk solids handling: equipment selection and operation*. McGlinchey, D. (ed.). Oxford, UK: Wiley-Blackwell.

McGuire, P. (2009) *Conveyors: Application, Selection and Integration*. McGuire, P. (ed.). Boca Raton, USA: CRC Press.

Mitsubishi Kakoki Kaishi Ltd. (2015) *High-efficiency Differential Rotational Screw Press*. Available at: <http://www.kakoki.co.jp/english/products/e-019/index.html> (Accessed: 5 May 2015).

Otterpohl, R., Braun, U. and Oldenburg, M. (2002) ‘*Innovative technologies for decentralised wastewater management in urban and peri-urban areas*’. Available at: https://sswm.info/sites/default/files/reference_attachments/OTTERPOHL%20et%20al.%202002%20Innovative%20technologies%20for%20decentralised%20wastewater%20management%20in%20urban%20and%20periurban%20areas.pdf. (Accessed 8 August 2016).

Pickford, J. (1995) *Low-cost sanitation: a survey of practical experience*. Pickford, J. (ed.) Rugby, UK: Intermediate Technology Publications Ltd (ITP).

Pollution Research Group (2014) *Low-cost sanitation: a survey of practical experience Reinvent the Toilet Fair. India*. Available at: <http://prg.ukzn.ac.za/docs/default-source/projects/simulant-recipe.pdf?sfvrsn=2>. (Accessed 8 August 2016).

Roberts, A. (2001) ‘Design Considerations and Performance Evaluation of Screw Conveyors.’, *Beltcon 11, International Materials Handling Conference*. Randburg, South Africa, 1-2 August 2001.

Roberts, A.W. (1999) ‘The influence of granular vortex motion on the volumetric performance of enclosed screw conveyors’, *Powder Technology*, 104, pp. 56–67.

Rogers, T.W., de los Reyes, F.L., Beckwith, W.J. and Borden, R.C. (2014) ‘Power earth auger modification for waste extraction from pit latrines’, *Journal of Water, Sanitation and Hygiene for Development*, 4, pp. 72–80.

Rosato, D. (2013) *Extruding plastics: a practical processing handbook*. Rosato, D. (ed.) Chatham, USA,: Springer Science and Business Media.

Rose, C., Parker, A., Jefferson, B. and Cartmell, E. (2015) ‘The Characterization of Feces and Urine: A Review of the Literature to Inform Advanced Treatment

Technology’, *Critical Reviews in Environmental Science and Technology*, 45, pp. 1827–1879.

Santos, D. and Chhabra, S. (2006) *An Analysis of Archimedes Screw Design Parameters and their Influence on Dispensing Quality for Electronics Assembly Applications*.

Available at:

<http://citeseerx.ist.psu.edu/viewdoc/download?doi=10.1.1.555.9040&rep=rep1&type=pdf>. (Accessed 8 August 2016).

Srivastava, A., Goering, C. and Rohrbach, R. (1993) *Engineering principles of agricultural machines*. Srivastava, A. K. (ed.). Miami, USA: American Society of Agricultural and Biological Engineers.

Still, D. (2002) *After the Pit Latrine is Full ... What Then? Effective Options for Pit Latrine Management*. Available at:

https://sswm.info/sites/default/files/reference_attachments/STILL%202002%20After%20the%20Pit%20Latrine%20is%20Full.pdf. (Accessed 8 August 2016).

Still, D. and Foxon, K. (2012) *Tackling the Challenges of Full Pit Latrines, Volume 3: The development of pit emptying technologies*. Durban, South Africa: Water Research Commission. Available at: https://www.susana.org/_resources/documents/default/2-1712-wrc-1745-tackling-the-challenges-of-full-pit-latrines--volume-1.pdf. (Accessed 8 August 2016).

Templeton, M.R. (2015) ‘Pitfalls and progress: a perspective on achieving sustainable sanitation for all’, *Environmental Science: Water Research & Technology*, 1, pp. 17–21.

Tilley, E. (2016) ‘Cost-effectiveness and community impacts of two urine-collection programs in rural South Africa’, *Environmental Science: Water Research & Technology*, 2, pp. 320–335.

UNICEF and WHO (2015) *Progress on sanitation and drinking-water: 2015 Update and MDG Assessment*. Geneva: World Health Organisation. Available at: https://data.unicef.org/wp-content/uploads/2015/12/Progress-on-Sanitation-and-Drinking-Water_234.pdf. (Accessed 8 August 2016).

Womer, T. (2000) '*Basic Screw Geometry*'. Available at:
<https://www.slideshare.net/rbplastics/basic-screw-geometry-things-your-extruder-screw-designer-never-told-you-about-screws>. (Accessed 8 August 2016).

Woolley, S.M., Buckley, C.A., Pocock, J. and Foutch, G.L. (2014) 'Rheological modelling of fresh human faeces.' *Journal of Water, Sanitation and Hygiene for Development*, 4, pp. 484-489.

World Bank (2019) *World Development Indicators*. Available at:
<https://datacatalog.worldbank.org/dataset/world-development-indicators> (Accessed: 16 January 2015).

Xu, Jing and Duffy, G. (2001) 'Operational parameters in screw press dewatering.' *Appita journal*, 54, pp. 369–375.

**3 QUANTIFICATION OF LIQUID PHASE FAECAL
ODOURANTS TO EVALUATE MEMBRANE
TECHNOLOGY FOR WASTEWATER REUSE FROM
DECENTRALISED SANITATION FACILITIES**

Published in: *Environmental Science, Water Research and Technology*.

Quantification of liquid phase faecal odourants to evaluate membrane technology for wastewater reuse from decentralised sanitation facilities

E. Mercer^a, C. Davey^a, P. Campo^a, D. Fowler^b, L. Williams^a, A. Kolios^c, A. Parker^a, S. Tyrrel^a, C. Walton^d, E. Cartmell^e, M. Pidou^a, E.J. McAdam^{a,*}

^aCranfield Water Science Institute, Vincent Building, Cranfield University, Bedfordshire, UK;

^bEnvironmental Analytical Facility, Vincent Building, Cranfield University, Bedfordshire, UK;

^cNaval Architecture, Ocean and Marine Engineering, University of Strathclyde, Glasgow, UK;

^dCentre for Environmental and Agricultural Informatics, Building 146, Cranfield University, Bedfordshire, UK;

^eScottish Water, Castle House, Carnegie Campus, Dunfermline, UK;

*Corresponding author e-mail: e.mcadam@cranfield.ac.uk

Abstract

Public willingness to use decentralised sanitation facilities or arising water products is discouraged due to malodour, preventing improved sanitation practices or water reuse opportunities in low income countries. Whilst odour is characterised in the gas phase, it originates in the liquid phase. Consequently, controlling odour at source could prevent gas-phase partitioning and limit produced water contamination. This study therefore developed an analytical method for the quantitation of a range of liquid phase volatile organic compounds (VOCs) classified into eight chemical groups, known to be primary indicators of faecal odour, to provide characterisation of real fluids and to permit evaluation of several potential membrane separation technologies for liquid phase odourant separation. The gas chromatography mass spectrometry method provided quantitation in the range of 0.005 mg L⁻¹ to 100 mg L⁻¹ with instrument detection limits ranging from 0.005 mg L⁻¹ to 0.124 mg L⁻¹. Linear calibration curves were achieved ($r^2 > 0.99$) with acceptable accuracy (77-115 %) and precision (<15 %) for quantitation in the calibration range below 1 mg L⁻¹, and good accuracy (98-104 %) and precision (<2 %) determined for calibration in the range 1-100 mg L⁻¹. Pre-concentration of real samples was facilitated via solid phase extraction. Subsequent application of the method to the evaluation of two thermally driven membranes based on hydrophilic (polyvinyl alcohol) and hydrophobic (polydimethylsiloxane) polymers evidenced contrasting separation profiles. Importantly, this study demonstrates the methods utility for liquid phase VOC determination which is of use to a range of disciplines, including healthcare professionals, taste and odour specialists and public health engineers.

Keywords: wastewater; taste; sewage; pervaporation; membrane distillation; pit latrine

3.1 Introduction

Large scale centralised wastewater treatment is not economically practicable for implementation in many low income country contexts. Local communities are therefore instead dependent upon decentralised sanitation solutions such as pit latrines which may not provide a safe barrier to discharge faecal material into local water resources. Malodour associated with these sanitation facilities has also been shown to exacerbate discharge of faecal material into the environment with users preferring open defecation to foul-smelling pit latrines (Lin et al., 2013; UNICEF and WHO, 2015). The odour profile associated with decentralised sanitation can be considered distinct from that of centralised treatment facilities since the absence of flush water and other water sources limit the primary composition to urine and faeces. Whilst analytical determination has determined around 279 and 381 volatile organic compounds (VOCs) associated with urine and faeces respectively from healthy individuals (de Lacy Costello et al., 2014), the faecal-borne VOCs indole, skatole (3-Methyl-1H-indole) and *p*-cresol (4-Methylphenol) amongst others, are considered key contributors to malodour arising from pit latrines (Chappuis et al., 2015). Previous research has demonstrated that VOCs originate in the liquid phase as microbial metabolites, with factors such as diet and health influencing composition and concentration of VOCs, and the physico-chemical environmental conditions (e.g. pH and temperature) encouraging partitioning into the gas phase where odour is finally perceived by the olfactory system (Brattoli et al., 2011).

Recent technological innovations seek to deliver alternative sustainable sanitation solutions that can facilitate sufficient water quality for safe discharge to the environment or to promote local water reuse (Kamranvand et al., 2018; Otterpohl, Braun and Oldenburg, 2002). As water supplies often arise from sources of unknown provenance, the local production of water to reuse standards can be considered an attractive proposition. However, a major limiting criterion that governs willingness to use reclaimed water is odour (Cruddas, Parker and Gormley, 2015). Odour abatement technologies presently provide elimination or neutralisation of malodorous compounds already partitioned into the gas phase (Lin et al., 2013). Through introducing barrier technology into this new genre of sanitation solutions for liquid phase treatment, the partitioning of odorous VOCs from the liquid phase into the gas phase could be

mediated at source and potentially averted, therefore enhancing the potential willingness of users to use locally engineered sanitation solutions and the arising water product for a range of reuse applications (Cruddas, Parker and Gormley, 2015). Pervaporation fosters water transport through application of a vapour pressure gradient and permeation through a polymeric membrane. The availability of waste heat, coupled with characteristically low water volumes from these new decentralised sanitation solutions, make thermally driven membrane separation a practicable solution for water recovery (Kamranvand et al., 2018). For non-porous (or dense) membranes, the polymer chemistry can favour permeation of water over VOCs thereby imparting selectivity into the separation that will exert an influence on the final odour profile of the treated water.

Whilst the management of odourants in the liquid phase is an attractive proposition, there is presently not an analytical solution of sufficient resolution to characterise the separation performance of membrane technology for this application. The conventional analytical route that has been previously exploited for liquid phase VOC odourant determination is headspace sampling with pre-concentration onto a sorbent (e.g. Tenax) before introduction into gas chromatography mass spectrometry (GC-MS) (Lin et al., 2013; Starckenmann, 2017). Such indirect techniques introduce temporal and sample volume restrictions in addition to limitations with respect to recovery which do not guarantee accurate quantitation of the liquid phase VOC profile. Lin et al. (2013) recently introduced a direct method for liquid phase VOC odourant characterisation of pit latrine faecal sludge using solid phase extraction (SPE) for pre-concentration from the liquid phase before determination by GC-MS. The authors used the method to successfully identify a discrete range of VOCs in the liquid phase representative of faecal odour. Pre-concentration by SPE was also selected for study by Chappuis et al. (2015) to extract compounds from pit latrine air in which the equilibrium was shifted to the liquid phase to trap and concentrate the compounds, enabling quantitation close to the odour detection thresholds (ODTs) to be achieved.

Although SPE-GC-MS has been demonstrated as a suitable method for liquid phase VOC quantitation, only a discrete range of VOCs has been determined, representing a limited range of chemical structures that is not sufficiently definitive to aid in the characterisation and development of membrane technology for the selective separation of liquid phase odourants. This study therefore seeks to develop an analytical

method for the determination of liquid phase odourants sufficient to characterise a broad range of VOC chemistries including organo-sulphurs, aromatics, phenols, alcohols, aldehydes, ketones, esters and hydrocarbons (Table 3.1), that are known contributors to faecal odour (de Lacy Costello et al., 2014; Starckenmann, 2017), and within a single elution to simplify the analytical procedure. Specific objectives are therefore to: (i) develop a method for the quantitation of liquid phase VOCs within a single elution, which present a broad range of chemistries, representative of those commonly associated with faeces and urine; (ii) develop and validate solid phase extraction for the liquid-phase pre-concentration stage; (iii) apply the method for VOC quantitation in urine and faecally contaminated urine; and (iv) confirm the methods validity through application to pervaporative membranes of differing polarity that should engender distinct differences in liquid phase VOC separation.

3.2 Materials and methods

3.2.1 Chemicals and reagents

All chemicals were sourced from Fisher Scientific (Loughborough, UK) or Sigma Aldrich (Dorset, UK). The VOCs analytes (1-butanol, 1-propanol, benzaldehyde, indole, skatole, ethyl butyrate, ethyl propionate, limonene, 2-butanone, *p*-cresol, dimethyl disulfide and dimethyl trisulfide) had a purity of at least 98%. Diethyl ether, propylene glycol, and the methyl octanoate internal standard (IS) were of extra pure grade ($\geq 99\%$) and the methanol used for SPE conditioning and acetone used for glassware cleaning was laboratory grade.

3.2.2 Standards preparation

Stock solutions and working standards were prepared in Class A volumetric glassware which was cleaned to remove residual contaminants by soaking glassware in deionised water, acetone and methanol for 10 min. respectively, within a sonicator and then dried overnight at 50 °C. For calibration purposes, a 1000 mg L⁻¹ stock solution of all VOCs was prepared in diethyl ether and working standards were subsequently diluted according to the calibration concentration. Three calibration curves, 0.005-1, 1-10 and 10-100 mg L⁻¹ were generated to cover a wide concentration range (Figures S3.1-3.3). A 10 mg L⁻¹ stock solution of methyl octanoate (IS) in diethyl ether was prepared for the

lower calibration curve ($<1 \text{ mg L}^{-1}$) and spiked in the low range standards for a final concentration of 1 mg L^{-1} . High range standards ($1\text{-}100 \text{ mg L}^{-1}$) were spiked with the IS for a final concentration of 10 mg L^{-1} . Internal calibration curves were obtained for each VOC with the mean response factor used to determine unknown concentrations.

3.2.3 Gas Chromatography Mass Spectrometry

Compound identification and quantification were performed by a Shimadzu-TQ8040 GC-MS (Shimadzu, Milton Keynes, UK), equipped with a semi polar ZB-624 fused silica GC column $60 \text{ m} \times 0.25 \text{ mm}$, $1.4 \mu\text{m}$ (Phenomenex, Macclesfield, UK). The initial oven temperature was held at $35 \text{ }^\circ\text{C}$ for 5 min then increased to $170 \text{ }^\circ\text{C}$ at a rate of $10 \text{ }^\circ\text{C min}^{-1}$ in order to elute 1-propanol, 2-butanone, 1-butanol, ethyl propionate, dimethyl disulfide, and ethyl butyrate. This temperature was sustained for 2 min to provide separation between dimethyl trisulfide, benzaldehyde and limonene. Then the temperature was ramped at $30 \text{ }^\circ\text{C min}^{-1}$ up to $240 \text{ }^\circ\text{C}$ for the detection of the internal standard (methyl octanoate) and *p*-cresol and further increased to $250 \text{ }^\circ\text{C}$ at $5 \text{ }^\circ\text{C min}^{-1}$, which was maintained for 5 min, allowing for the separation of indole and skatole. The total runtime was 29.83 min. Helium was used as the carrier gas (236.1 kPa) at a linear column flow rate of 2.47 mL min^{-1} to maintain a velocity of 40 cm s^{-1} . The mass spectrometer was operated in single quad mode with a detector voltage relative to the tuning result (0.2 kV), ionisation energy of -70 eV at an ion source temperature of $200 \text{ }^\circ\text{C}$ and interface temperature of $250 \text{ }^\circ\text{C}$. A solvent cut time was applied until 8.95 min. Initially, the MS was operated in scan mode in order to identify the retention times and target ions through in house MS libraries and NIST MS search with a scan range of 30-500 *m/z*. Compounds of interest were then detected in single ion monitoring (SIM) mode by the principal ion and two reference ions (Table 3.2).

3.2.4 Determining SPE recovery factors

A synthetic solution was prepared in order to determine SPE recovery factors. A 1000 mg L^{-1} stock solution containing all VOCs was prepared in propylene glycol to completely dissolve all compounds. Aliquots were subsequently added to three individual buffered solutions (potassium chloride buffer pH 2, potassium phosphate monobasic 6.5 and tris(hydroxymethyl)aminomethane pH 9 according to Robinson and

Stokes (2002), within a volumetric flask for a GC-MS injection concentration of 100 mg L⁻¹. Multiple pH levels were studied to identify the influence of natural pH variations within faecally contaminated urine, on compound recovery, as similarly practiced by Lin et al.(2013).

Oasis® HLB cartridges (1 g), sourced from Waters (Milford, USA), were used and attached to an Agilent VacElut20 manifold (Agilent Technologies, Stockport, UK). The cartridges were first conditioned by subsequently passing 10 mL of diethyl ether, methanol and deionised water, facilitated by a vacuum pump (N 022 AN.18, KNF Neuberger, Whitney, UK). Samples (20 mL) were then loaded onto the cartridges. The VOCs were eluted with 1 mL of methyl octanoate (IS) in diethyl ether (0.057 µg mL⁻¹) followed by 5 mL of pure diethyl ether. The residual sample water which collected at the bottom of the beaker was removed carefully using a glass Pasteur pipette (Fisher Scientific, Loughborough, UK). Diethyl ether extracts were concentrated to 0.5 mL under nitrogen gas and then analysed by GC-MS. The response ratios were compared between the calibration standard and the sample in order to calculate the recovery factors of the compounds. All trials were triplicated at pH 2, 6.5 and 9. The method detection limit (MDL) was determined by:

$$MDL = \frac{IDL \times 100}{C_f \times R_f} \quad \text{Eq. 3.1}$$

Where IDL is the instrument detection limit, C_f is concentration factor and R_f is the recovery factor. Similarly, the concentrations (C_{VOC}) in mg kg⁻¹ recorded were calculated by:

$$C_{VOC} = \frac{C_{GCMS} \times 100}{C_f \times R_f} \quad \text{Eq. 3.2}$$

Where C_{GCMS} is the concentration recorded at the instrument (mg kg⁻¹).

3.2.5 Characterisation of urine and faecally contaminated urine

Fresh urine and faeces samples were collected and analysed within 12 hours of collection. Informed consent of real samples was obtained from anonymous volunteers through a collection regime approved by the Cranfield University Research Ethics System (CURES, project ID 3022).

Faecally contaminated urine was prepared by producing a composite sample containing a 10:1 urine- to-faeces ratio, which represents the typical proportions

produced by an individual per day (Rose et al., 2015). With this purpose, 5 g of fresh faeces along with 50 g of fresh urine were combined in a 50 mL centrifuge tube and vortexed for 30 seconds. The supernatant was then filtered through cotton wool and sand (50 mL) and a 20 mL aliquot was processed by SPE. Fresh urine samples (20 mL) were also processed with SPE. All samples were eluted with 0.2 mL IS solution ($0.057 \mu\text{g mL}^{-1}$) and 10 mL diethyl ether and concentrated down to 100 μL . Duplicate samples were also prepared with a concentration factor of five was also processed to capture *p*-cresol concentrations exceeding the calibration range i.e. (2.5 mL sample, 1 mL IS solution, 10 mL diethyl ether, concentrated down to 500 μL).

3.2.6 Membrane technology set-up

Commercially available polydimethylsiloxane (PDMS) and polyvinyl alcohol (PVA) membranes were evaluated (Figure S3.4, Table S3.1). The PDMS and PVA membranes exhibited contact angles of $116 \pm 1.4^\circ$ and $43 \pm 1.1^\circ$, indicating them to be hydrophobic and hydrophilic polymers respectively. Vapour pressure gradient was established using a diaphragm vacuum pump (MD 4CNT, Vacuubrand, Brackley) operating at 0.05 bar on the permeate side. Permeate samples were collected (20 mL) within a liquid nitrogen cold trap (-196°C). The permeate, feed and retentate samples were analysed using the SPE-GC-MS method to establish a mass balance. The feed reservoir was submerged within a thermostatic bath at 50°C (Grant TC120, Cambridge, UK) with a feed flowrate of 0.2 L min^{-1} applied (520s, Watson Marlow, Falmouth, UK). Separation efficiency of the PVA and PDMS membranes was expressed through removal efficiency (%):

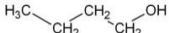
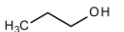
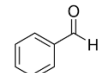
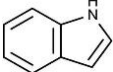
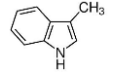
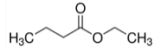
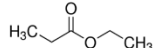
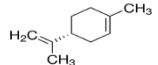
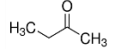
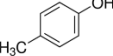
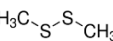
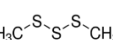
$$\frac{C_0 - C}{C_0} \times 100 \quad \text{Eq. 3.3}$$

and enrichment factor (β) respectively:

$$\frac{C}{C_0} \quad \text{Eq. 3.4}$$

where C represents the permeate concentration (mg L^{-1}) and C_0 is the initial feed concentration (mg L^{-1}). All trials were conducted in triplicate.

Table 3.1 Physico-chemical parameters of selected volatile organic compounds (VOCs) attributed to urine and faeces

Compound	Chemical group	Chemical composition	Chemical structure	Molecular weight (g mol ⁻¹)	pKa	Log <i>K_{ow}</i> at 20°C	Water solubility at 25°C (g L ⁻¹)	Henry's volatility constant at 25°C (mol m ⁻³ Pa ⁻¹)	Boiling point (°C)	Vapour pressure at 25°C (mm Hg)
1-Butanol	Alcohol	C ₄ H ₉ OH		74.12	16.1 ^a	0.88 ^a	63.2 ^a	1.2 ^d	111.7 ^a	7 ^a
1-Propanol	Alcohol	C ₃ H ₈ O		60.1	16.1 ^a	0.25 ^a	1000 ^a	1.5 ^d	97 ^a	14.9 ^a
Benzaldehyde	Aldehyde	C ₇ H ₆ O		106.12	14.9 ^a	1.48 ^a	6.95 ^a	0.38 ^d	178.1 ^a	1.27 ^a
Indole	Aromatic heterocycle	C ₈ H ₇ N		117.15	-3.6 ^c	2.14 ^a	3.56 ^a	19.1 ^d	254 ^a	0.0122 ^a
Skatole	Aromatic heterocycle	C ₉ H ₉ N		131.17	-4.6 ^c	2.6 ^a	0.498 ^a	4.7 ^d	265 ^a	0.0055 ^a
Ethyl butyrate	Ester	C ₆ H ₁₂ O ₂		116.16	-7 ^b	1.85 ^a	2.7 ^b	0.029 ^d	121 ^a	14 ^a
Ethyl propionate	Ester	C ₅ H ₁₀ O ₂		102.13	-7 ^b	1.21 ^a	19.2 ^a	0.041 ^d	98.9 ^a	35.8 ^a
Limonene	Hydrocarbon	C ₁₀ H ₁₆		136.24	-4.2 ^b	4.57 ^a	0.013 ^a	0.00048 ^d	177 ^a	1.98 ^a
2-Butanone	Ketone	C ₄ H ₈ O		72.11	14.7 ^a	0.29 ^a	223 ^a	8.1 ^d	79.7 ^a	90.6 ^a
<i>p</i> -Cresol	Phenol	C ₇ H ₈ O		108.14	10.26 ^a	1.94 ^a	21.5 ^a	10 ^d	201.9 ^a	0.11 ^a
Dimethyl disulfide	Sulphur containing	C ₂ HS ₂		94.19	-	1.77 ^a	3 ^a	0.0065 ^d	110 ^a	28.7 ^a
Dimethyl trisulfide	Sulphur containing	C ₂ H ₆ S ₃		126.25	-	1.926 ^a	2.39 ^a	0.021 ^d	170 ^a	1.06 ^a

^a Pubchem (2017)^b YMDB (2017)^c Gu and Berry (1991)^d Sander (2015)

Table 3.2 Single ion monitoring (SIM) mass spectrometry parameters for target analytes.

Compound	Retention time (minutes)	Principal ion (m/z)	Reference ion 1 (m/z)	Reference ion 2 (m/z)
1-Propanol	9.455	31	42	59
2-Butanone	10.213	43	72	57
1-Butanol	12.437	56	41	43
Ethyl propionate	12.903	57	74	75
Dimethyl disulfide	14.087	94	79	45
Ethyl butyrate	15.087	71	43	88
Dimethyl trisulfide	19.478	126	79	45
Benzaldehyde	19.653	106	105	77
Limonene	19.862	68	93	67
<i>p</i> -Cresol	22.498	107	108	77
Indole	25.688	117	90	89
Skatole	26.76	130	131	77

3.3 Results and discussion

3.3.1 Method development

The VOC analytes comprised of alcohols (1-butanol, 1-propanol), aldehydes (benzaldehyde), aromatics (indole, skatole), esters (ethyl butyrate, ethyl propionate), hydrocarbons (limonene), ketones (2-butanone), phenols (*p*-cresol) and organo-sulphur containing compounds (dimethyl disulfide, dimethyl trisulfide) (Table 3.1). The compounds represent a broad range of physico-chemical properties such as acid dissociation constant (pK_a , -7 to 16.1), octanol-water partitioning coefficient ($\log K_{ow}$ 0.25 to 4.57), water solubility (0.013 to 1000 g L⁻¹) and volatility (0.00048 to 19.1 mol m⁻³ Pa⁻¹) (Gu and Berry, 1991; PubChem, 2018; Sander, 2015), which confer a challenging separation for any barrier technology, and is representative of the chemistries frequently associated with faecal odour (Chappuis et al., 2015; Lin et al., 2013; Starkenmann, 2017).

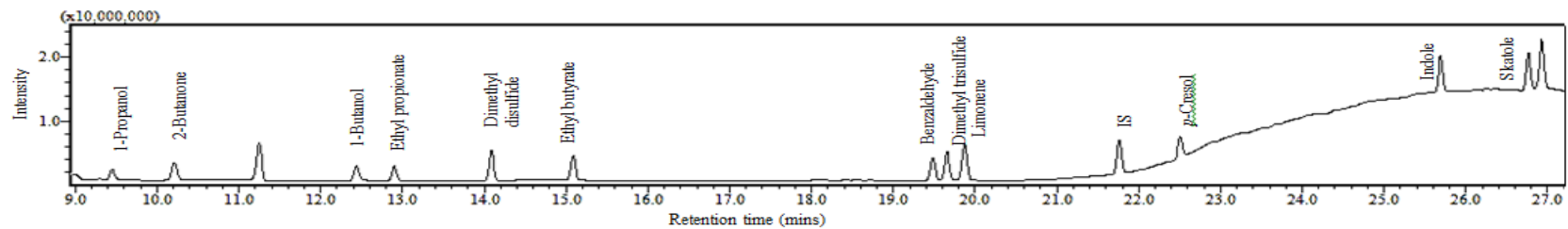
Initial screening identified nine potential VOCs to be quantifiable within the liquid phase. In order to identify a method capable of detecting each of the nine selected VOCs in this range within a single elution, various injection split ratios were trialled in scan mode. The optimum split ratios were selected according to the upper limit of detector saturation which was associated to the later emerging higher boiling point compounds (aromatics) and a signal to noise ratio of >10 for the lower boiling point compounds (alcohols). The injection port was operated at a split of 1:5, 1:12.5 and

1:100 for the low calibration range (0.005-1 mg L⁻¹), medium calibration range (1-10 mg L⁻¹) and high calibration range (10-100 mg L⁻¹) respectively; three calibration ranges were adopted to ensure that the ‘natural’ concentration of faecally contaminated urine as well as sample concentrations post-separation could be determined. The respective injection volumes were 2.5, 1 and 1 µL. The split ratio conditions were then applied to SIM mode to increase selectivity and sensitivity (Table 3.2). The final peak of the elution (Figure 3.1a and b) represents butylated hydrocarbon (BHT), the stabilisation agent within the diethyl ether solvent. All compounds were detected within a 27 minute runtime. Peaks generally had good tailing factors close to one which was within the recommended analytical range of ≤2 (Figures S3.5 and S3.6, Table S3.2) (Agilent technologies, 2018; Wahab, Patel and Armstrong, 2017).

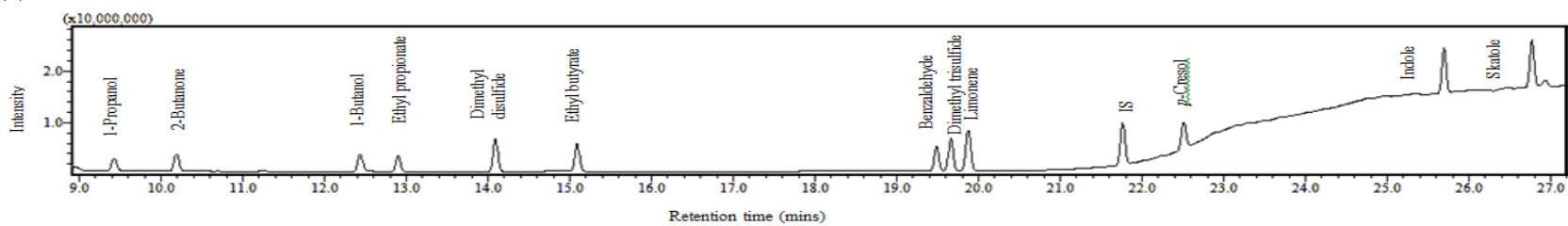
3.3.2 GC-MS calibration

Calibration was based on a linear regression analysis of the mean response factor fit (Table 3.3) (Currie, 1999). A good correlation coefficient was obtained for each of the three calibration curves ($r^2 > 0.99$). Residual standard deviations (RSD) of the response factors of all calibration curves were within the acceptance criteria of <20 % (EPA, 2003). The instrument limit of detection (LD) was calculated as $3.3 \sigma/\text{slope}$, and limit of quantification (LQ) as $10 \sigma/\text{slope}$ where σ is standard deviation of seven trace (0.005 mg L⁻¹) replicates (Currie, 1999). The LD ranged from 0.005 mg L⁻¹ (*p*-cresol) to 0.124 mg L⁻¹ (2-butanone) and the LQ from 0.014 mg L⁻¹ to 0.351 mg L⁻¹.

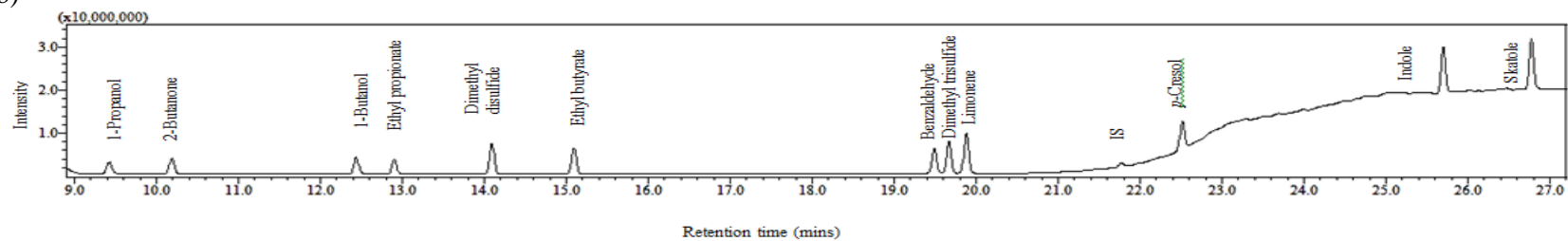
Accuracy and precision for each calibration range was determined by analysis of the mid-point concentration (Table 3.4; 0.5 mg L⁻¹, 5 mg L⁻¹ and 50 mg L⁻¹). Accuracy was calculated as the ratio between measured and theoretical concentrations of six replicate solutions in different vials and precision was calculated as the RSD of six replicate injections from the same vial. According to the EPA method 8000C (2003) and Little (2016), accuracy and precision was classed as acceptable for all compounds at all calibration levels which was ≤30 %. This also demonstrates sample stability after standing time which then permits repeat injections from the same vial.



(a)



(b)



(c)

Figure 3.1 Chromatograms in single ion monitoring mode (SIM) at (a) 1 mg L^{-1} volatile organic compound (VOC) concentration with 1 mg L^{-1} IS concentration , (b) 10 mg L^{-1} VOC concentration with 10 mg L^{-1} IS concentration and (c) 100 mg L^{-1} VOC concentration with 10 mg L^{-1} IS concentration.

Table 3.3 Calibration parameters for the target analytes; LD, limit of detection; LQ, limit of quantification; RF, response factor; RSD, relative standard deviation; SD, standard deviation.

	Calibration range (mg L ⁻¹)	Slope	Intercept	r ²	LD ^a (mg L ⁻¹)	LQ ^b (mg L ⁻¹)	RF (% RSD)	Mean RF	RF SD
1-Propanol	10-100	0.531	0.00479	1.000			3.266	0.52	0.017
	1-10	0.456	0.00382	0.992			10.48	0.455	0.047
	0.005-1	0.674	0.00677	1.000	0.019	0.077	11.66	0.75	0.087
2-Butanone	10-100	0.874	0.07026	0.999			2.57	0.89	0.023
	1-10	0.817	0.01183	0.994			8.429	0.84	0.07
	0.005-1	1.39	0.194	0.991	0.124	0.351	14.53	1.87	0.27
1-Butanol	10-100	0.414	0.01558	1.000			2.71	0.63	0.017
	1-10	0.381	-0.00232	0.996			9.54	0.365	0.034
	0.005-1	0.468	-0.00213	0.999	0.036	0.099	17.93	0.436	0.078
Ethyl propionate	10-100	0.614	0.0693	0.999			2.68	0.99	0.027
	1-10	0.588	0.00609	0.995			0.914	0.59	0.054
	0.005-1	0.753	0.00412	0.999	0.011	0.045	4.975	0.78	0.039
Dimethyl disulfide	10-100	0.976	0.0939	0.999			1.81	0.468	0.0085
	1-10	1.08	0.00586	0.998			9.16	1.07	0.098
	0.005-1	1.200	0.00316	1.000	0.005	0.019	7.25	1.17	0.085
Ethyl butyrate	10-100	0.462	0.0301	1.000			2.5	0.729	0.018
	1-10	0.49	0.00362	0.997			8.82	0.49	0.043
	0.005-1	0.561	0.00184	1.000	0.006	0.026	16.54	0.545	0.09
Dimethyl trisulfide	10-100	0.718	0.047	0.999			2.03	0.71	0.014
	1-10	0.797	-0.000266	0.997			8.86	0.78	0.069
	0.005-1	0.811	0.000512	1.000	0.010	0.031	13.01	0.769	0.1
Benzaldehyde	10-100	0.685	0.0823	0.999			3.09	0.5	0.015
	1-10	0.731	0.004297	0.997			8.03	0.73	0.0587
	0.005-1	0.76	0.00259	1.000	0.005	0.021	5.38	0.76	0.041
Limonene	10-100	0.479	0.0741	1.000			3.09	0.503	0.0156
	1-10	0.474	0.00898	0.997			5.7	0.495	0.028
	0.005-1	0.529	0.0105	0.999	0.041	0.165	8.85	0.568	0.05
<i>p</i> -Cresol	10-100	0.69	0.0809	1.000			2.42	0.741	0.0173
	1-10	0.71	0.00152	0.997			9.87	0.7	0.069
	0.005-1	0.681	-0.000495	0.999	0.019	0.057	18.46	0.698	0.129
Indole	10-100	1.39	0.545	0.996			5.74	1.56	0.0896
	1-10	1.49	0.0121	0.997			7.57	1.5	0.113
	0.005-1	1.433	0.00895	1.000	0.005	0.027	12.523	1.56	0.195
Skatole	10-100	1.509	0.558	0.994			5.3	1.67	0.089
	1-10	1.662	0.00763	0.998			7.51	1.66	0.12
	0.005-1	1.519	0.00755	1.000	0.005	0.014	13.1862	1.6	0.211

^aLD calculated as $3.3 \sigma / \text{Slope}$, where σ is standard deviation of seven 0.005 mg L⁻¹ replicates (Currie, 1999).

^bLQ calculated as $10 \sigma / \text{Slope}$, where, σ is standard deviation of seven 0.005 mg L⁻¹ replicates (Currie, 1999).

Note: RSD is acceptable when <20 % (EPA, 2003)

Table 3.4 Precision and accuracy for each analyte within three calibration ranges; RSD, residual standard deviation.

	0.5 mg L ⁻¹			5 mg L ⁻¹			50 mg L ⁻¹		
	Mid-point mean (mg L ⁻¹)	Accuracy ^a (%)	Precision ^b (RSD)	Mid-point mean (mg L ⁻¹)	Accuracy ^a (%)	Precision ^b (RSD)	Mid-point mean (mg L ⁻¹)	Accuracy ^a (%)	Precision ^b (RSD)
1-Propanol	0.46 ± 0.08	92.6	3.7	5.25 ± 0.04	104.9	0.3	50.70 ± 1.50	101.4	1.6
2-Butanone	0.45 ± 0.07	89.6	15.6	5.16 ± 0.08	103.2	0.8	49.14 ± 3.69	98.3	1.7
1-Butanol	0.50 ± 0.02	100.6	5.34	5.15 ± 0.05	103.1	1.4	49.59 ± 5.05	99.2	2.4
Ethyl propionate	0.51 ± 0.07	102.7	3.6	5.19 ± 0.05	103.7	0.7	50.13 ± 1.89	100.3	1.1
Dimethyl disulfide	0.54 ± 0.06	107.6	3.6	5.15 ± 0.03	103.1	0.6	50.27 ± 1.24	100.5	1.5
Ethyl butyrate	0.55 ± 0.06	109.3	3.6	5.18 ± 0.03	103.6	0.7	50.04 ± 2.41	100.1	1.6
Dimethyl trisulfide	0.58 ± 0.05	115.3	2.5	5.12 ± 0.01	102.4	1.1	50.96 ± 1.82	101.9	1.7
Benzaldehyde	0.53 ± 0.07	106.7	0.9	5.16 ± 0.02	103.1	0.2	49.68 ± 1.44	99.4	1.4
Limonene	0.39 ± 0.12	77.3	0.9	5.17 ± 0.03	103.4	0.4	49.28 ± 1.02	98.6	1.6
<i>p</i> -Cresol	0.50 ± 0.07	100.4	4.6	5.13 ± 0.01	102.7	2.3	50.39 ± 1.53	100.8	2.7
Indole	0.47 ± 0.08	93.8	2.5	5.17 ± 0.02	103.4	0.7	49.55 ± 1.89	99.1	1.0
Skatole	0.49 ± 0.07	98.4	7.0	5.13 ± 0.03	102.7	0.4	49.55 ± 2.80	99.1	1.9

^aAccuracy calculated as the percentage ratio between measured and theoretical concentrations of 6 replicate solutions in different vials

^bPrecision calculated as the RSD of 6 replicated injections from the same vial.

Note: 1. Accuracy acceptance: ≤ 30%. (EPA, 2003).

2. Criteria for precision: ≤ 25% is excellent, less than or equal to 30% is acceptable (Little, 2016)

3.3.3 Solid phase extraction

Solids phase extraction recovery efficiency was evaluated to permit calculation of recovery factors. Recoveries for *p*-cresol (90%), indole (81%) and skatole (88%) are comparable to those stated by Lin et al. (2013) (Table 3.5). Further analytes with recoveries deemed to be either ‘recommended’ or ‘acceptable’ in accordance with EPA guidelines (2007) were 2-butanone (56 %), dimethyl disulfide (63 %), 1-butanol (100 %), benzaldehyde (77 %) ethyl propionate (82 %) and ethyl butyrate (89 %). However, poor recoveries were identified for compounds including 1-propanol and limonene. We suggest that the poor extraction efficiency of 1-propanol can be ascribed to its strong affinity for water, which limits the probability for partitioning onto the solid phase (Table 3.1, $\log K_{ow}$ 0.25). Conversely, the poor extraction efficiency for limonene can be attributed to its high volatility, which increases the probability for sample losses at the vacuum and evaporation stages of sample preparation, coupled with its significant hydrophobicity ($\log K_{ow}$ 4.57) which can initiate strong interactions with the sorbent that are known to inhibit SPE recovery (1996). Wells (2000) recommended inclusion of an organic modifier for compounds with $\log K_{ow}$ exceeding 4, along with the addition of methanol to increase eluotropic strength: this is recommended for improving SPE recovery for this compound for future research. Importantly, an RSD below 10 % was recorded for each compound, which evidenced that SPE can achieve consistent recovery to within the acceptance criteria specified in the SPE EPA method 3535A (SW-846, 2007) which demonstrates that correction factors could be applied (Table 3.5) to determine method detection limits (MDL). For illustration, method detection limits for *p*-cresol (C_f 200, R_f 0.9) and indole (C_f 200, R_f 0.81) were 0.1 and 0.03 $\mu\text{g L}^{-1}$. These values are several orders of magnitude lower than identified by De Preter et al. (2009) by using purge and trap with GC-MS to determine faecal fermentation, which suggests direct determination from the liquid phase may enhance method sensitivity.

Table 3.5 Solid phase extraction recovery factors. RSD, residual standard deviation.

	SPE recovery ^a (% ± RSD) in this study			Average SPE recovery (%)	SPE recovery (%) Lin et al. (2013)		
	pH 2	pH 6.5	pH 9	All trials	pH 5	pH 6	pH 7
1-Propanol	21 ± 1	26 ± 4	21 ± 5	22 ± 3			
2-Butanone	64 ± 4	52 ± 2	53 ± 3	56 ± 7			
1-Butanol	106 ± 5	106 ± 2	100 ± 6	100 ± 4			
Ethyl propionate	85 ± 2	79 ± 4	83 ± 3	82 ± 3			
Dimethyl disulfide	69 ± 4	54 ± 3	66 ± 2	63 ± 8			
Ethyl butyrate	84 ± 4	95 ± 4	89 ± 3	89 ± 6			
Dimethyl trisulfide	55 ± 2	44 ± 2	51 ± 2	50 ± 6			
Benzaldehyde	76 ± 2	77 ± 3	79 ± 2	77 ± 2			
Limonene	23 ± 2	24 ± 2	21 ± 1	22 ± 2			
<i>p</i> -Cresol	96 ± 6	90 ± 6	83 ± 4	89 ± 7	103 ± 5	97 ± 0.5	103 ± 11
Indole	80 ± 7	82 ± 6	81 ± 6	81 ± 1	89 ± 2	90 ± 16	96 ± 2
Skatole	87 ± 5	89 ± 5	89 ± 5	88 ± 2	96 ± 5	97 ± 9	100 ± 2

^a SPE recovery calculated as the percentage ratio between SPE measured and theoretical concentrations (100 mg L⁻¹ injection concentration representing the upper calibration limit)

Note: 1. SPE recovery recommended as: 70 – 130 % (EPA, 2007).

2. RSD acceptance: ≤ 30 % (EPA, 2007)

3.3.4 Characterisation of faecally contaminated urine

Liquid phase concentrations in urine and faecally contaminated urine samples from eleven volunteers were determined for the full-suite of VOCs except those which exhibited poor SPE recoveries (Table 3.6). In general, concentrations ranged between the MDL and 1 mg kg⁻¹ in urine samples, which is anticipated for fresh urine samples such as those measured in this study, which generally produce little odour when compared to aged urine (Troccaz et al., 2013). The presence of indole and skatole in fresh urine is also evident in the literature, though concentrations were considered sufficiently low not to be impactful as an odorant (Starkenmann, 2017). However, *p*-cresol, was present at a considerable concentration (max. 13.01 mg kg⁻¹). Para-cresol arises in urine from the breakdown of tyrosine by cresol producing bacteria in the intestine (Gabriele et al., 2016). Seigfried and Zimmerman (1944) reported an average *p*-cresol concentration in urine of 18 mg L⁻¹. This is similar to the maximum value, the broader variation potentially arising from various factors such as protein intake (Geypens et al., 1997), and the presence of specific urease positive isolates (e.g. Enterobacteriaceae) (Troccaz et al., 2013), which are known contributors to raised *p*-cresol concentration. The use of ‘mid-stream’ urine collection techniques commonly used in medical studies (and not employed in this study) will also expectedly increase average concentration. Importantly, comparable values to the literature provide confirmation of the suitability of the method to real samples. Bacteria constitute 60 % of

faecal solids dry mass (Guarner and Malagelada, 2003), with *Escherichia coli* (Table S3.3) representing the dominant bacterial species that is primarily responsible for the oxidation of fatty acids to alcohols, and the conversion of the amino acids tyrosine and tryptophan to *p*-cresol and indole and skatole respectively (Bos, Sterk and Schultz, 2013; Geypens et al., 1997; Vanholder, De Smet and Lesaffer, 1999). Faecally contaminated urine samples therefore generally exhibited higher VOC concentrations, and specifically for 1-butanol (alcohol) and indole (aromatic) which accords with the literature data on faecally contaminated urine (Lin et al., 2013). The analytical data was compared to thresholds compiled from literature by van Gemert (2011), used simply as a reference in order to contextualise the data (Table 3.6). At the background concentrations provided in urine, ethyl propionate, dimethyl disulfide, ethyl butyrate, *p*-cresol, indole and skatole were greater than the lower detection threshold for odour in water. The same VOC range was also above the taste threshold for water as was benzaldehyde. Significantly, each of the identified VOCs was determined in urine and faecally contaminated urine samples, with several at elevated concentrations, which suggests that the VOC range selected is pertinent for the development of membrane technology for liquid phase odourant abatement.

Table 3.6 Typical concentrations of 12 liquid phase volatile organic compounds attributed to urine and faeces with associated odour descriptors and detection thresholds in air and water

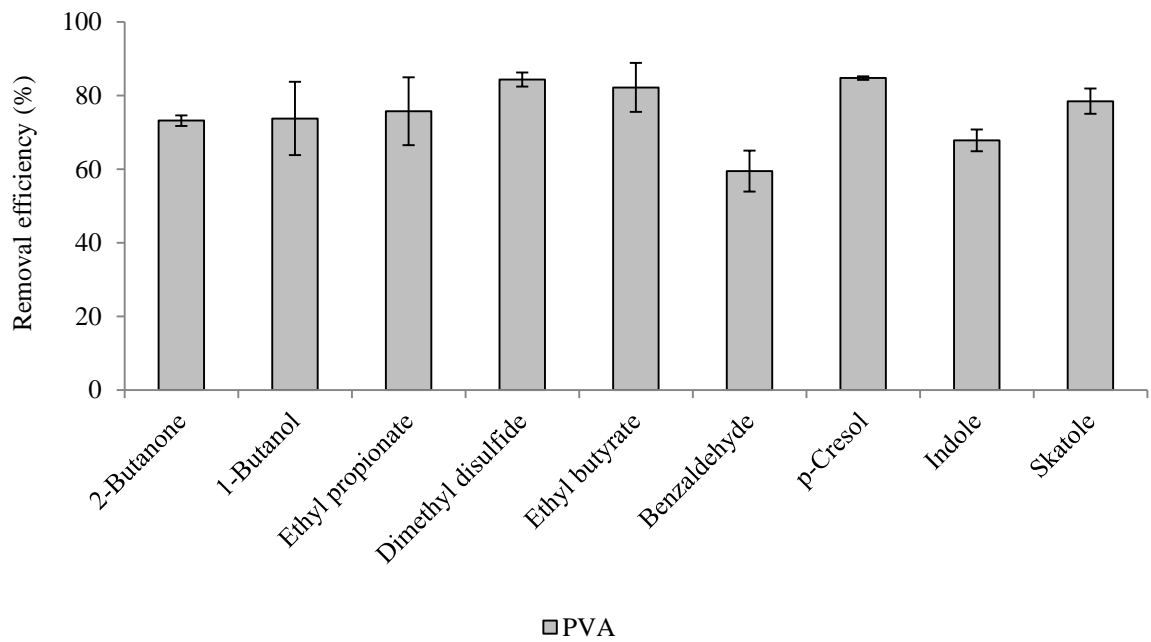
	Odour descriptor*	Urine	Faecally contaminated urine. 10:1 urine to faeces ratio		Faeces Lin et al. (2013)	Detection threshold van Gemert (2011)		
		N = 11 Range (mg kg ⁻¹ urine)	N = 11 Range (mg kg ⁻¹ urine)	Range (mg kg ⁻¹ faeces)	N = 2 Range (mg kg ⁻¹ faeces)	Air (odour) Range (mg m ⁻³)	Water (odour) Range (mg kg ⁻¹)	Water (taste) Range (mg kg ⁻¹)
2-Butanone	Acetone like	<LD-1.323	0.014-0.315	0.140-3.146		0.21-1000	7-100	3-60
1-Butanol	Alcohol like	<LD-0.016	<LD-0.185	<LD-1.846		0.015-3000	0.27-511	2-100
Ethyl propionate	Fruity, rum	<LD-0.008	<LD-0.02	<LD-0.198		0.3-1	0.0001-0.067	0.00049-0.004
Dimethyl disulfide	Rotten cabbage	<LD-0.013	<LD-0.014	<LD-0.142		0.0011-3.5	0.00016-0.09	0.03-0.068
Ethyl butyrate	Pineapple	<LD-0.006	<LD-0.02	<LD-0.197		0.000016-0.1	0.000001-0.4	0.0001-0.45
Benzaldehyde	Bitter almond	<LD-0.060	0.0009-0.012	0.009-0.107		0.01-3400	0.32-4.6	0.05-1.5
<i>p</i> -Cresol	Sweet, tar-like	0.003-13.01	0.214-2.67	2.139-26.683	20-25	0.00002	0.055-0.2	0.002-0.018
Indole	Faecal	<LD-0.514	0.012-1.001	0.113-10.015	5-8	0.00035-0.0071	0.13-0.59	0.5
Skatole	Faecal, nauseating	<LD-0.045	0.007-0.162	0.074-1.619	2-6	0.00035-0.00078	0.0002-0.052	0.05

3.3.5 Pervaporative membranes govern odour transport in faecally contaminated urine

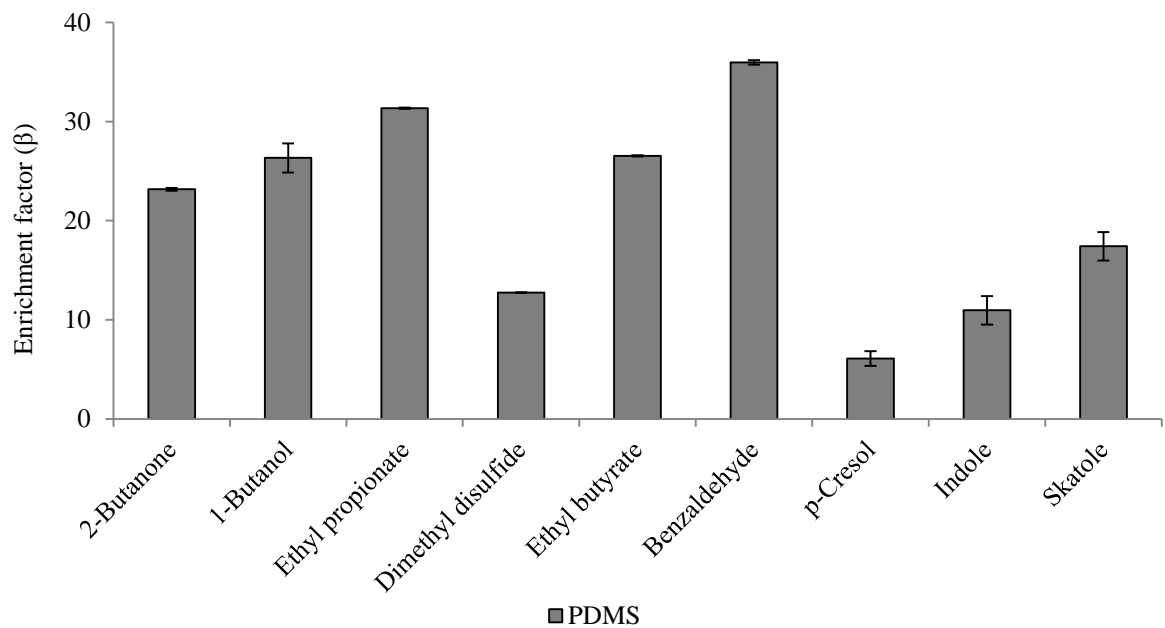
An initial mass balance was conducted across the membrane experimental setup to confirm minimum VOC losses. A 10 mg L^{-1} synthetic solution (comprising each VOC) was introduced to the feed-side and the mass balance constructed at the end of permeation was found to be $100 \pm 10 \%$ (PVA used for assessment), which demonstrates the developed methods capability for technology assessment. An RSD of $\leq 13 \%$ was identified for replicate samples from membrane experimental studies. The membranes were subsequently challenged with the 10 ppm synthetic faecally contaminated urine. For the PVA membrane, removal efficiency ranged between $60 \pm 5 \%$ (benzaldehyde) and $85 \pm 0.5 \%$ (dimethyl disulfide, *p*-cresol) (Figure 3.2a). The separation efficiency can be accounted for by the selectivity of the polymer toward water, the intrinsic polarity increasing the solubility parameter of the polymer for water, whilst the lower molecular weight of water increases the diffusivity parameter for the polymer, the product of these two parameters providing an enhanced water permeability (Liu and Kentish, 2018). Whilst the presence of alcohols or carbonyl groups (e.g. benzaldehyde) are generally thought to influence the solubility parameter, a trend between VOC physico-chemical or structural properties (Table 3.1) was not evident (Van Baelen et al., 2005). This can be accounted for by the comparatively low partial pressure exhibited by the VOCs relative to water, which limits the associative driving force for separation. Baelen et al.(2005) also observed that PVA is soluble in water and prone to swelling above 20 % wt. water. This results in an open membrane structure which decreases selectivity, and is exacerbated at elevated temperatures. In this study, the PVA membrane was used for illustrative purposes and the material used is recommended for separations comprising 50 % wt. water solutions. Increasing crosslinking of the PVA polymer will increase membrane stability in the presence of water (Gohil, Bhattacharya and Ray, 2006). Therefore whilst good VOC separation was facilitated by the PVA membrane, optimisation of cross-linking is recommended for further investigation into PVA for liquid phase odourant abatement.

For the hydrophobic PDMS membrane, permeate was enriched for all VOCs with enrichment factors (β) ranging 6.1 ± 0.8 to 35.9 ± 0.2 (Equation 3, Figure 3.2b). The selectivity toward VOCs can be ascribed to the enhanced affinity of PDMS toward non-polar compounds (Baker, 2012). A broad trend between the octanol-water coefficient,

which corresponds to compound hydrophobicity, and enrichment factor was identified from benzaldehyde ($\log K_{OW} = 1.48$, $\beta = 36$) to ethyl propionate ($\log K_{OW} = 1.21$, $\beta = 27$), 1-butanol ($\log K_{OW} = 0.88$, $\beta = 26$) and 2-butanone ($\log K_{OW} = 0.29$, $\beta = 23$). However, although *p*-cresol, indole, and skatole presented a stronger hydrophobic contribution (Table 3.1), β factors of 6-17 were identified for these compounds. In addition to compound mobility and solubility within PDMS, vapour pressure difference also governs separation (Basile, Figoli, and Khayet, 2015). The relatively lower permeability of these compounds can thus be accounted for by their vapour pressure which is around an order of magnitude lower than the other compounds. Since the PDMS polymer promotes VOC enrichment of the permeate, it is rational to expect an intensification of the ‘repulsive’ or ‘nauseating’ perception ordinarily associated with faecally contaminated urine (Table 3.6). However, the resulting permeate odour could be described as sweet, chemical, earthy and floral, with little perceivable evidence of faecal odour, and was hedonically more pleasant than the PVA permeate (Table 3.7). The range of physico-chemical characteristics represented with these compounds therefore illustrates the mechanisms which determine enrichment / rejection and can be used to suggest the behaviour of related compounds. Selectivity is governed by vapour pressure (low vapour pressures resulting in concentration polarisation at the downstream interface), volatility (liquid phase stability) and hydrophobicity (by inclusion of highly hydrophobic groups i.e benzene or length of hydrocarbon chain). For example, we can infer that vanillin, which contains a hydrophobic aromatic ring ($\log K_{OW} 1.21$) but low vapour pressure (0.00047 mm Hg at 25 °C), could be enriched similarly to *p*-cresol, indole and skatole. Importantly, the arising data suggests that thermally driven barrier technology could be engineered to change perception through modification of the odour profile rather than developed simply for elimination. This is analogous to the perfumery industry in which indole, one of the core constituents of odour arising from faecally contaminated urine is also a critical ingredient in jasmine perfume (Starkenmann, 2017).



(a)



(b)

Figure 3.2 Assessment of pervaporative membrane processes as a liquid phase treatment to manage odourants at source. Performance expressed as (a) removal efficiency for a hydrophilic membrane material and (b) enrichment factor for a hydrophobic membrane. PVA (Polyvinyl alcohol) and PDMS (Polydimethylsiloxane). Error bars represent the standard deviation of a triplicate at pH 6.5.

Table 3.7 Odour descriptors for the membrane permeates of faecally contaminated urine

Membrane material	Permeate odour descriptor
Polyvinyl alcohol	Sweaty, chemical, sweet, onion
Polydimethylsiloxane	Sweet, chemical, earthy, floral

3.4 Conclusions

In this study, an analytical method for the detection of liquid phase VOCs responsible for faecal odour has been developed and verified. The following conclusions have been drawn:

- A quantitative method has been developed to enable co-elution of a range of VOCs comprised of a broad spectrum of physicochemical properties in a single elution.
- Sample concentration by SPE permit low method detection limits sufficient to measure liquid phase concentrations within and below the detection threshold range reported for odour and taste. The utility of this method extends to a broad range of stakeholders including healthcare professionals, taste and odour specialists and public health engineers.
- Consistent recovery was identified for solid phase extraction, while acceptable recoveries were also determined for nine VOCs, which were subsequently analysed in real matrices.
- Comparison of VOC data determined in urine and faecally contaminated urine samples to literature data, provided confirmation of the appropriateness of this method for evaluation of real samples, and also that the VOCs determined are relevant and appropriate for the quantitation of faecal odourants in the liquid phase.
- The method was successfully applied for the evaluation of pervaporative membranes, where SPE coupled with the lower calibration range, was capable of quantification within PVA membrane permeate which presents an analytical challenge due to the polymers capability for separation.
- The method holds immediate value for public health engineers, medical and taste and odour scientists. However, through development of a GC-MS method, the accessibility of the technique extends beyond those prescribed sectors to a

wide range of institutions/laboratories thanks to the inclusion of such equipment as ‘standard’.

- Dense hydrophilic polymeric membranes offer the greatest selective separation of liquid phase VOCs, yet the more concentrated permeate produced from PDMS presented the more hedonically pleasant permeate, which suggests there is more than one route to challenging perception of faecal odour in reuse product water.
- Further research on the combination of VOC and non-VOC odourants, building from this method, would be beneficial to develop a holistic odour management approach.
- Whilst further membrane development is warranted for this application, the method was capable of facilitating diagnostic investigation of VOC separation and further demonstrated that the combination of hedonic characterisation coupled with quantitative methods are demanded to develop a technical solution for liquid phase odourant separation, which offers significant potential for the advancement of decentralised sanitation.

Acknowledgements

The authors give special thanks to Charles Chappuis and Christian Starckenmann at Firmenich for their assistance with the development of the SPE protocol.

3.5 References

Agilent technologies (2018) *The Secrets of Good Peak Shape in HPLC*. Available at: https://www.agilent.com/cs/library/eseminars/public/secrets_of_good_peak_shape_in_hplc.pdf (Accessed: 10 February 2018).

Van Baelen, D., Van der Bruggen, B., Van den Dungen, K., Degreve, J. and Vandecasteele, C. (2005) ‘Pervaporation of water–alcohol mixtures and acetic acid–water mixtures’, *Chemical Engineering Science*, 60, pp. 1583–1590.

Baker, R. (2012) *Membrane Technology and Applications*. 3rd edn. Baker, R. (ed.) Chichester, UK: John Wiley and Sons.

Basile, A., Figoli, A. and Khayet, M. (eds.) (2015) *Pervaporation, Vapour Permeation and Membrane Distillation: Principles and Applications*. Cambridge, UK: Woodhead Publishing.

Bos, L.D.J., Sterk, P.J. and Schultz, M.J. (2013) 'Volatile Metabolites of Pathogens: A Systematic Review', *PLOS Pathogens*, 9, pp. e1003311.

Brattoli, M., de Gennaro, G., de Pinto, V., Loiotile, A.D., Lovascio, S. and Penza, M. (2011) 'Odour Detection Methods: Olfactometry and Chemical Sensors', *Sensors*, 11, pp. 5290–5322.

Campbell, N.R. and Hey, D.H. (1944) 'p-Cresol and Estrone in Urine', *Nature*, 153, pp. 745.

Chappuis, C.J.-F., Niclass, Y., Vuilleumier, C. and Starkenmann, C. (2015) 'Quantitative Headspace Analysis of Selected Odorants from Latrines in Africa and India', *Environmental Science & Technology*, 49, pp. 6134–6140.

Cruddas, P.H., Parker, A. and Gormley, A. (2015) 'User perspectives to direct water reuse from the Nano Membrane Toilet.', *38th WEDC International Conference*. Loughborough, UK, 27-31 July 2015.

Currie, L. (1999) 'Detection and quantification limits: origins and historical overview', *Analytica Chimica Acta*, 391, pp. 127–134.

EPA (2003) *EPA Method 8000C, Gas Chromatography*. Available at: http://synectics.net/public/library/StreamResource.axd?DSN=pub&Mode=FileImage_Inline&ID=1867. (Accessed 8 August 2018).

EPA (2007) *Method 3535A (SW-846): Solid-Phase Extraction (SPE)*. Available at: <https://www.epa.gov/sites/production/files/2015-12/documents/3535a.pdf>. (Accessed: 8 August 2018).

Gabriele, S., Sacco, R., Altieri, L., Neri, C., Urbani, A., Bravaccio, C., Riccio, M.P., Iovene, M.R., Bombace, F., De Magistris, L. and Persico, A.M. (2016) 'Slow intestinal transit contributes to elevate urinary p-cresol level in Italian autistic children.' *Autism research*, 9, pp. 752–759.

van Gemert, L. (2011) *Odour thresholds. Compilations in air water and other media*. 2nd edn. Utrecht, Netherlands: Oliemans Punter & Partners BV.

Geypens, B., Claus, D., Evenepoel, P., Hiele, M., Maes, B., Peeters, M., Rutgeerts, P. and Ghoois, Y. (1997) 'Influence of dietary protein supplements on the formation of bacterial metabolites in the colon.' *Gut*, 41, pp. 70–76.

Gohil, J.M., Bhattacharya, A. and Ray, P. (2006) 'Studies On The Crosslinking Of Poly (Vinyl Alcohol)', *Journal of Polymer Research*, 13, pp. 161–169.

Gu, J.D. and Berry, D.F. (1991) 'Degradation of substituted indoles by an indole-degrading methanogenic consortium.' *Applied and environmental microbiology*, 57, pp. 2622–2627.

Guarner, F. and Malagelada, J.-R. (2003) 'Gut flora in health and disease.' *Lancet*, 361, pp. 512–519.

Kamranvand, F., Davey, C.J., Sakar, H., Autin, O., Mercer, E., Collins, M., Williams, L., Kolios, A., Parker, A., Tyrrel, S., Cartmell, E. and McAdam, E.J. (2018) 'Impact of fouling, cleaning and faecal contamination on the separation of water from urine using thermally driven membrane separation', *Separation Science and Technology*, 53, pp. 1372–1382.

de Lacy Costello, B., Amann, A., Al-Kateb, H., Flynn, C., Filipiak, W., Khalid, T., Osborne, D. and Ratcliffe, N.M. (2014) 'A review of the volatiles from the healthy human body.', *Journal of breath research*, 8, p. 014001.

Lin, J., Aoll, J., Niclass, Y., Velazco, M.I., Wunsche, L., Pika, J. and Starckenmann, C. (2013) 'Qualitative and Quantitative Analysis of Volatile Constituents from Latrines', *Environmental Science & Technology*, 47, pp. 7876–7882.

Little, T.A. (2016) 'Establishing Acceptance Criteria for Analytical Methods', *BioPharm International*, 29, pp. 44–48.

Liu, L. and Kentish, S.E. (2018) 'Pervaporation performance of crosslinked PVA membranes in the vicinity of the glass transition temperature', *Journal of Membrane Science*, 553, pp. 63–69.

Nakamura, M., Nakamura, M. and Yamada, S. (1996) 'Conditions for solid-phase extraction of agricultural chemicals in waters by using n-octanol-water partition coefficients', *Analyst*, 121, pp. 469–475.

Otterpohl, R., Braun, U. and Oldenburg, M. (2002) '*Innovative technologies for decentralised wastewater management in urban and peri-urban areas*'. Available at: https://sswm.info/sites/default/files/reference_attachments/OTTERPOHL%20et%20al.%202002%20Innovative%20technologies%20for%20decentralised%20wastewater%20management%20in%20urban%20and%20periurban%20areas.pdf. (Accessed: 8 August 2018).

De Preter, V., Van Staeyen, G., Esser, D., Rutgeerts, P. and Verbeke, K. (2009) 'Development of a screening method to determine the pattern of fermentation metabolites in faecal samples using on-line purge-and-trap gas chromatographic–mass spectrometric analysis', *Journal of Chromatography A*, 1216, pp. 1476–1483.

PubChem (2018) *PubChem*. Available at: <https://pubchem.ncbi.nlm.nih.gov/> (Accessed: 10 February 2018).

Robinson, R. and Stokes, R. (2002) *Electrolyte solutions*. 2nd edn. Mineola, USA: Dover Publications.

Rose, C., Parker, A., Jefferson, B. and Cartmell, E. (2015) 'The Characterization of Feces and Urine: A Review of the Literature to Inform Advanced Treatment Technology', *Critical Reviews in Environmental Science and Technology*, 45, pp. 1827–1879.

Sander, R. (2015) 'Compilation of Henry's law constants (version 4.0) for water as solvent', *Atmospheric Chemistry and Physics*, 15, pp. 4399–4981.

Starkenmann, C. (2017) 'Analysis and Chemistry of Human Odors', in Buettner, A. (ed.) *Springer Handbook of Odor*. Dordrecht, Germany: Springer International Publishing, pp. 121–122.

Troccaz, M., Niclass, Y., Anziani, P. and Starkenmann, C. (2013) 'The influence of thermal reaction and microbial transformation on the odour of human urine', *Flavour and Fragrance Journal*, 28, pp. 200–211.

UNICEF and WHO (2015) *Progress on sanitation and drinking-water: 2015 Update and MDG Assessment*. Geneva: World Health Organisation. Available at: https://data.unicef.org/wp-content/uploads/2015/12/Progress-on-Sanitation-and-Drinking-Water_234.pdf. (Accessed 8 August 2018).

Vanholder, R., De Smet, R. and Lesaffer, G. (1999) 'p-Cresol: a toxin revealing many neglected but relevant aspects of uraemic toxicity', *Nephrology Dialysis Transplantation*, 14, pp. 2813–2815.

Wahab, M.F., Patel, D.C. and Armstrong, D.W. (2017) 'Peak Shapes and Their Measurements: The Need and the Concept Behind Total Peak Shape Analysis', *LCGC North America*, 35, pp. 846–853.

Wells, M. (2000) 'Solid-Phase Extraction: Principles, Techniques, and Applications', in Simpson, N. (ed.) *Solid-Phase Extraction: Principles, Techniques and Applications*. New York: Marcel Dekker.

YMDB (2018) *Yeast Metabolome database (YMDB)*. Available at: <http://www.ymdb.ca/> (Accessed: 10 February 2018).

3.6 Chapter 3 supplementary information

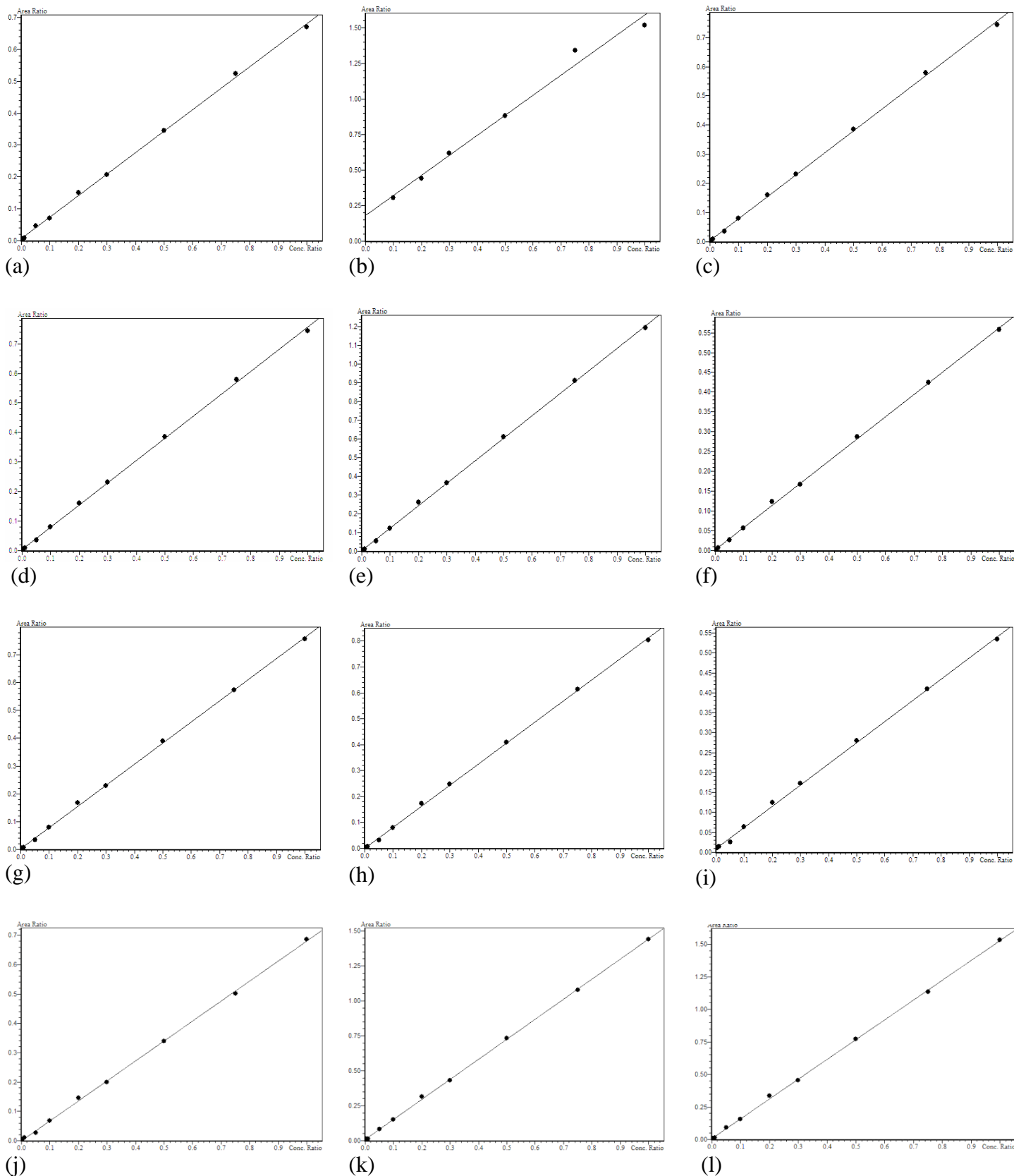


Figure S 3.1 Calibration curves* for a range LD-1 mg L⁻¹ (a) 1-Propanol (b) 2-Butanone (c) 1-Butanol (d) Ethyl propionate (e) Dimethyl disulfide (f) Ethyl butyrate (g) Dimethyl trisulfide (h) Benzaldehyde (i) Limonene (j) *p*-Cresol (k) Indole (l) Skatole. *Calibration curves based on area ratio (AREA_{VOC}/AREA_{IS}) vs concentration ratio (CONCENTRATION_{VOC}/CONCENTRATION_{IS}).

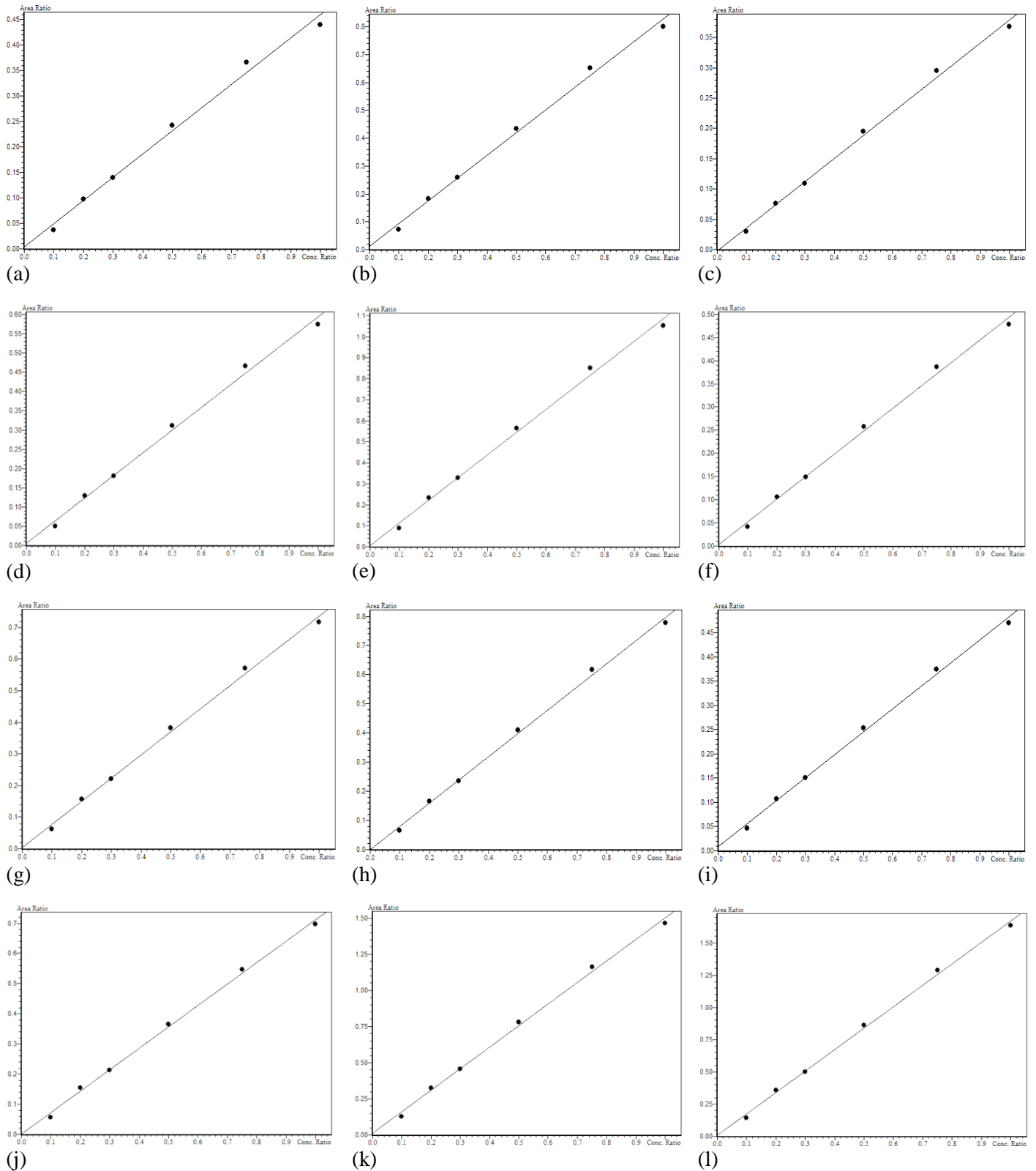


Figure S 3.2 Calibration curves* for a range 1-10 mg L⁻¹ (a) 1-Propanol (b) 2-Butanone (c) 1-Butanol (d) Ethyl propionate (e) Dimethyl disulfide (f) Ethyl butyrate (g) Dimethyl trisulfide (h) Benzaldehyde (i) Limonene (j) *p*-Cresol (k) Indole (l) Skatole. *Calibration curves based on area ratio (AREA_{VOC}/AREA_{IS}) vs concentration ratio (CONCENTRATION_{VOC}/CONCENTRATION_{IS}).

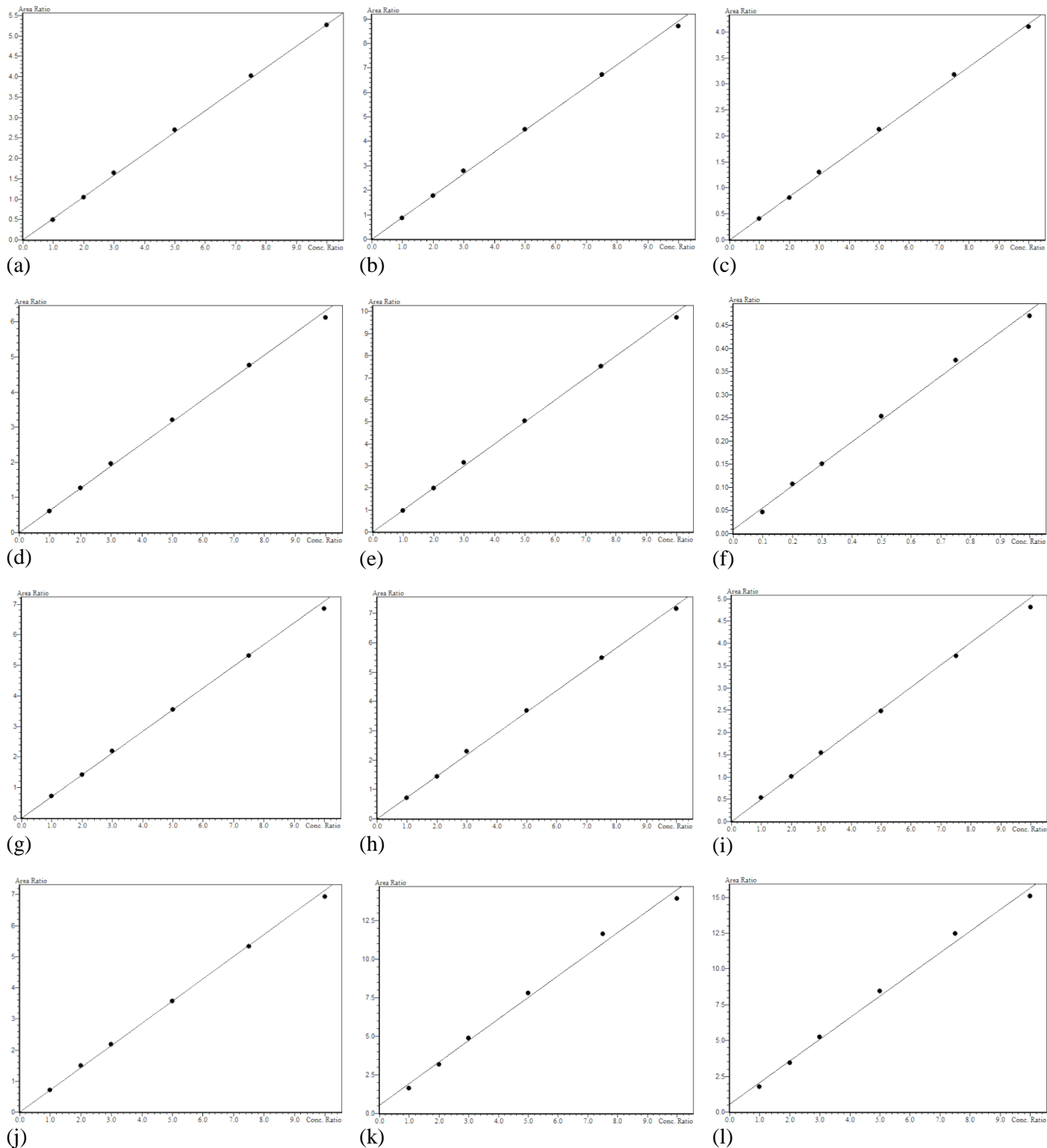


Figure S 3.3 Calibration curves* for a range 10-100 mg L⁻¹ (a) 1-Propanol (b) 2-Butanone (c) 1-Butanol (d) Ethyl propionate (e) Dimethyl disulfide (f) Ethyl butyrate (g) Dimethyl trisulfide (h) Benzaldehyde (i) Limonene (j) *p*-Cresol (k) Indole (l) Skatole. *Calibration curves based on area ratio ($AREA_{VOC}/AREA_{IS}$) vs concentration ratio ($CONCENTRATION_{VOC}/CONCENTRATION_{IS}$).

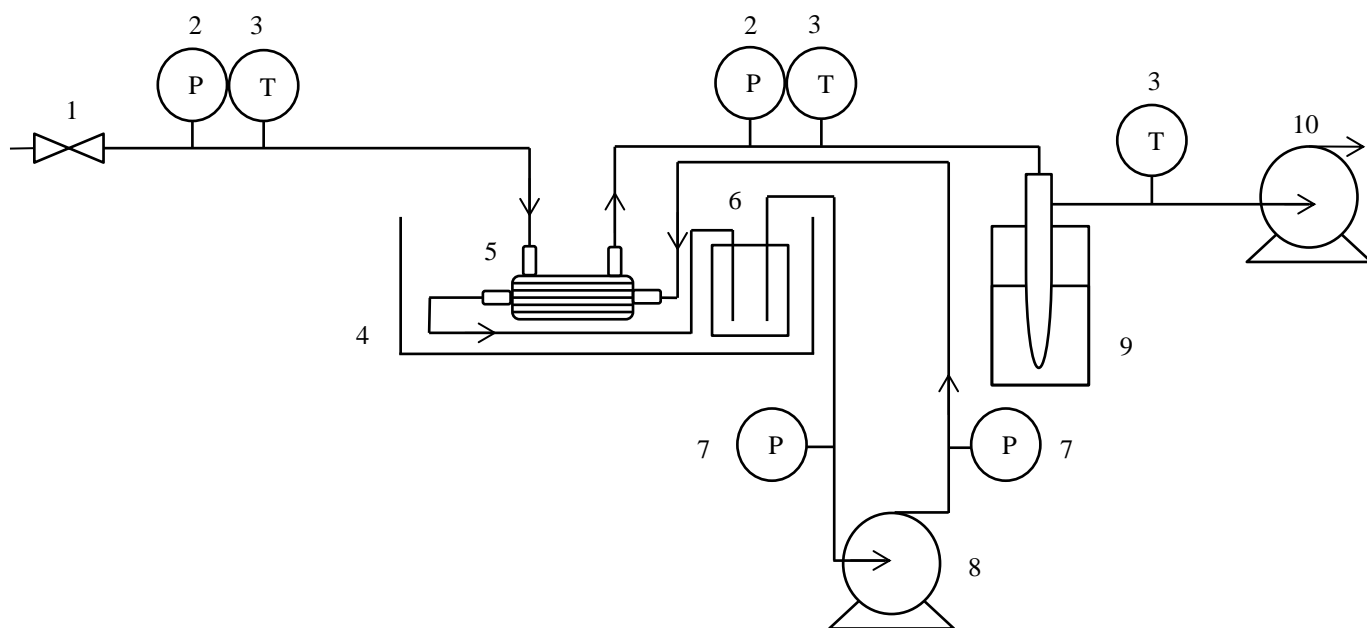


Figure S 3.4 Pervaporation membrane rig schematic. 1: Needle valve; 2: Absolute pressure transducer (PXM 319-002A, Omega, Manchester, UK); 3: Temperature probe (HMT337, Vaisala, Suffolk, UK); 4: Thermostatic bath at 50°C (Grant TC120, Cambridge, UK); 5: Membrane module (see table 1); 6: Feed solution in Duran bottle with GL 45 screw cap and 2 hose connections (Fisher scientific, Loughborough, UK) ; 7: Pressure gauge (DPG 1001, Omega, Manchester, UK); 8: Peristaltic pump (520s, Watson Marlow, Falmouth, UK); 9: Liquid nitrogen cold trap (-196°C) or condenser (2°C); 10: Diaphragm vacuum pump (MD 4C NT, Vacuubrand, Brackley).

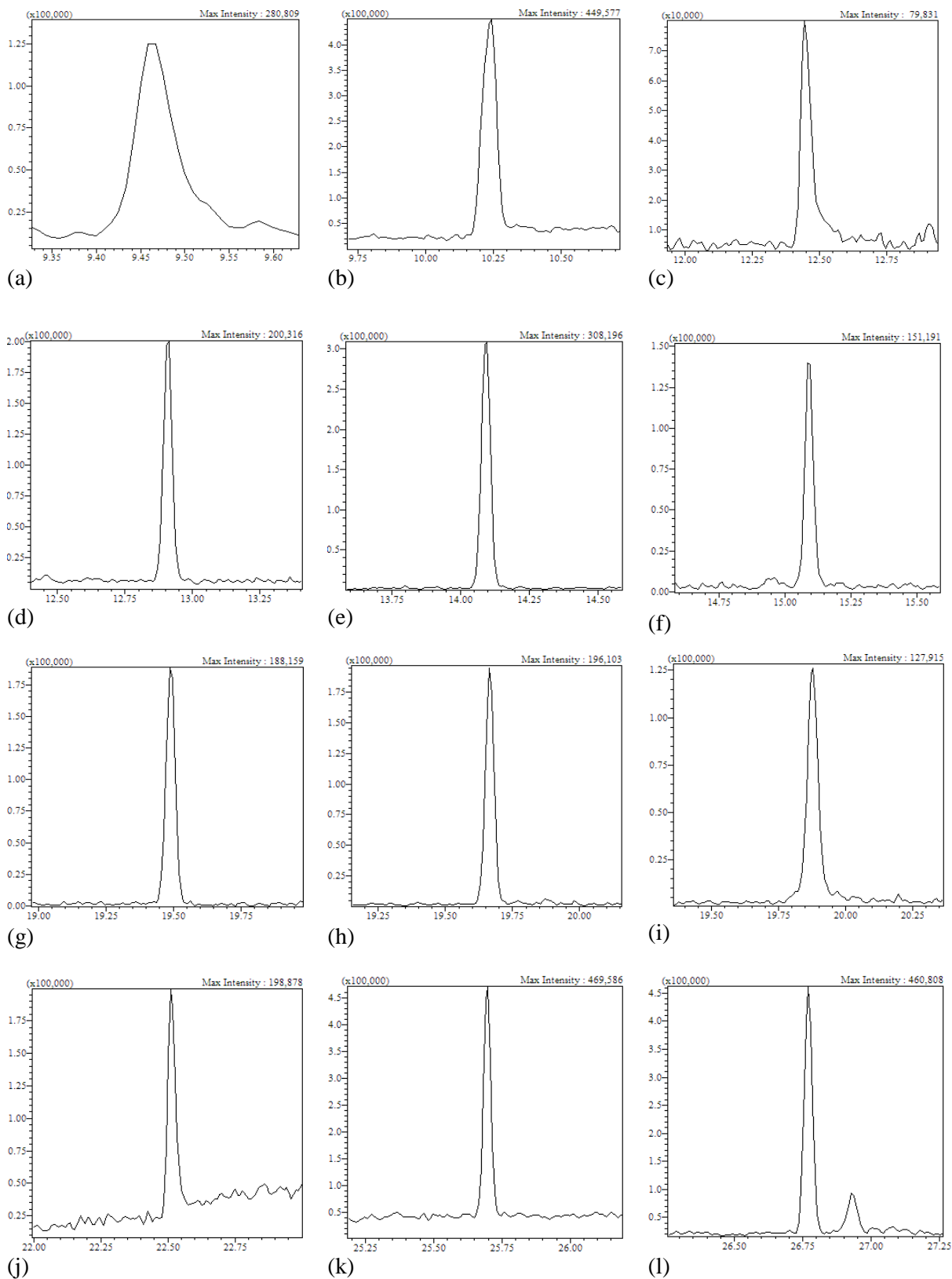


Figure S 3.5 Intensity vs. retention time of individual peaks at 0.1 mg L⁻¹ in single ion monitoring mode. (a) 1-Propanol (b) 2-Butanone (c) 1-Butanol (d) Ethyl propionate (e) Dimethyl disulfide (f) Ethyl butyrate (g) Dimethyl trisulfide (h) Benzaldehyde (i) Limonene (j) *p*-Cresol (k) Indole (l) Skatole.

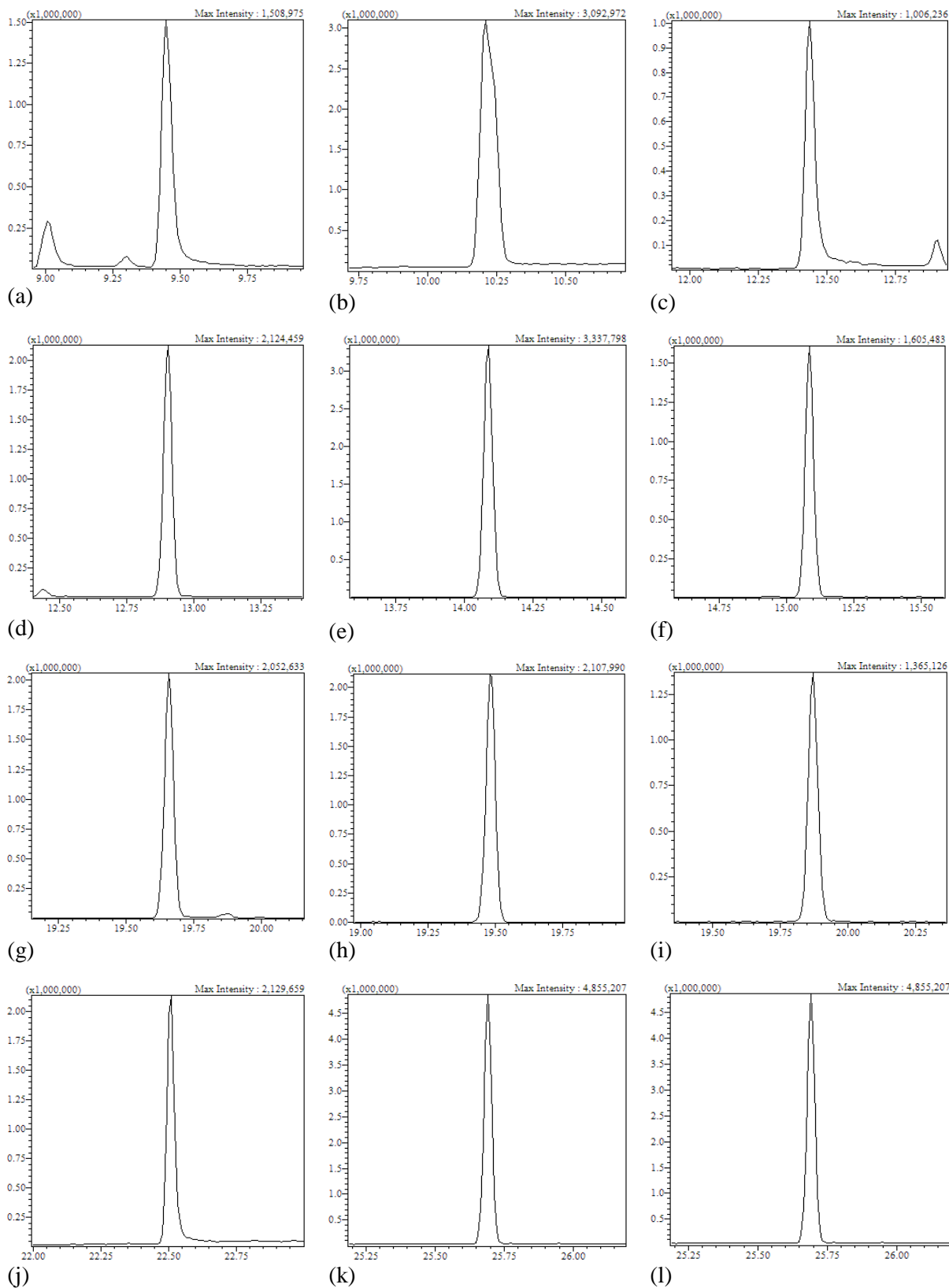


Figure S 3.6 Intensity vs. retention time of individual peaks at 1 mg L⁻¹ in single ion monitoring mode. (a) 1-Propanol (b) 2-Butanone (c) 1-Butanol (d) Ethyl propionate (e) Dimethyl disulfide (f) Ethyl butyrate (g) Dimethyl trisulfide (h) Benzaldehyde (i) Limonene (j) *p*-Cresol (k) Indole (l) Skatole.

Table S 3.1 Membrane characteristics and operating conditions.

	Pervaporation	
Manufacturer (model)	DeltaMem (Pervap TM 4101)	Permselect (PDMSXA-2500)
Material	Polyvinyl alcohol (PVA)	Polydimethylsiloxane (PDMS)
Membrane area (m ²)	0.0153	0.25
Membrane thickness (μm)	5	55
Membrane structure	Crosslinked support layer	Symmetric
Contact angle (°)	43 (±1.1)	116 (±1.4)
Geometry	Flat sheet	Hollow fibre
Operating pressure (bar)	0.05	0.05
Operating membrane temperature (°C)	50	50

Note: >90° indicates hydrophobic polymer and <90° indicates hydrophilic polymer

Table S 3.2 USP coefficient tailing factors for 0.1 and 1 mg L⁻¹ peaks.

	0.1 mg L ⁻¹	1 mg L ⁻¹
1-Propanol	1.40	1.39
2-Butanone	0.86	1.57
1-Butanol	2.04	1.34
Ethyl propionate	1.00	1.02
Dimethyl disulfide	1.08	1.03
Ethyl butyrate	0.96	1.00
Dimethyl trisulfide	0.96	0.90
Benzaldehyde	0.96	0.93
Limonene	1.10	1.06
<i>p</i> -Cresol	1.24	1.25
Indole	1.00	0.98
Skatole	0.95	0.92

USP tailing factor calculated as $W_{0.05}/2f_{0.05}$, where $W_{0.05}$ is the peak width and f is the peak front width at 5 % height.

Note: 1. Good chromatographic peak shape defined as symmetrical, narrow and tailing factor of 1 (Agilent technologies, 2018)
 2. U.S. Food and Drug Administration (FDA). The FDA recommends a tailing factor of ≤ 2

Table S 3.3 VOC microbial sources of selected compounds in this study

Volatile organic compound	Microbial source
1-Propanol	<i>Escherichia coli</i> ^a
2-Butanone	<i>Pseudomonas aeruginosa</i> ^a
1-Butanol	<i>Staphylococcus aureus</i> , <i>Escherichia coli</i> ^a
Ethyl propionate	-
Dimethyl disulfide	<i>Klebsiella pneumoniae</i> ^a , <i>Pseudomonas aeruginosa</i> ^a , <i>Escherichia coli</i> ^a
Ethyl butyrate	<i>Enterococcus faecalis</i> ^a , <i>Escherichia coli</i> ^a
Dimethyl trisulfide	<i>Pseudomonas aeruginosa</i> ^a
Benzaldehyde	<i>Staphylococcus aureus</i> ^a , <i>Escherichia coli</i> ^a
Limonene	<i>Pseudomonas aeruginosa</i> ^a
<i>p</i> -Cresol	Most aerobic enterobacteria and anaerobic <i>Clostridium perfringens</i> ^b
Indole	<i>Escherichia coli</i> ^a
Skatole	<i>Escherichia coli</i> ^a

^aBos et al. (2013)

^bVanholder et al. (1999)

References

Agilent technologies (2018) *The Secrets of Good Peak Shape in HPLC*. Available at: https://www.agilent.com/cs/library/eseminars/public/secrets_of_good_peak_shape_in_hplc.pdf (Accessed 10 February 2018).

Bos, L.D.J., Sterk, P.J. and Schultz, M.J. (2013) 'Volatile Metabolites of Pathogens: A Systematic Review', *PLOS Pathogens*, 9, pp. e1003311.

Vanholder, R., De Smet, R. and Lesaffer, G. (1999) '*p*-Cresol: a toxin revealing many neglected but relevant aspects of uraemic toxicity', *Nephrology Dialysis Transplantation*, 14, pp. 2813–2815.

4 THERMALLY DRIVEN MEMBRANE PROCESSES FOR WASTEWATER REUSE IN NON-SEWERED SANITATION SYSTEMS

In preparation for: *Water research*

Thermally driven membrane processes for water reuse in non-sewered sanitation systems

E. Mercer^a, C. Davey^a, L. Williams^a, A. Kolios^b, A. Parker^a, S. Tyrrel^a, E. Cartmell^c, M. Pidou^a, E.J. McAdam^{a,*}

^aCranfield Water Science Institute, Vincent Building, Cranfield University, Bedfordshire, UK

^bNaval Architecture, Ocean and Marine Engineering, University of Strathclyde, Glasgow, UK

^cScottish Water, Castle House, Carnegie Campus, Dunfermline, UK

*Corresponding author e-mail: e.mcadam@cranfield.ac.uk

Abstract

In order to progress the global realisation of water sustainable development goals (SDG 6), membrane technology for water reuse from non-sewered sanitation was evaluated using concentrated wastewater, comprising faecally contaminated urine. The suitability of thermally driven processes (hydrophilic pervaporation, hydrophobic pervaporation and membrane distillation) operated by waste heat was addressed against conventional pressure driven filtration (ultrafiltration and reverse osmosis), which requires substantial electrical energy. Water quality, impact on flux and odour management was investigated to assess product safety, process robustness, and reuse acceptance. Thermally driven processes demonstrated the highest quality permeates, close to the reuse requirements for non-sewered sanitation, within a single treatment step. Fluxes were similar to deionised water, even when challenged with total suspended solids loading of 6 g L^{-1} , and odour profiles were manipulated to those with no faecal resemblance. Feed side microbial activity was responsible for an increase in ammonia, pH and odour causing organic compounds, preventing comprehensive reuse quality within this study. Operation at increased temperatures (i.e. $70 \text{ }^\circ\text{C}$) which addresses the bacterial source and improves water productivity could be sufficient to exceed the required standards for the implementation of thermal processes for the next generation of sustainable non-sewered sanitation solutions.

Keywords: Faecal, odour, water quality, fouling, SDG 6

4.1 Introduction

The sustainable development goals (SDG 6) proposed by the United Nations (UN) aim to provide water and sanitation for all by 2030 (United Nations, 2018). The focus is to protect water resources through improving sanitation practices and safe wastewater

discharge, allowing for cleaner water resources and therefore greater accessibility to drinking water. However, water as a natural freshwater resource has been predicted to be insufficient to accommodate for a global population of 9.8 billion by 2050 (Hilal and Wright, 2018; United Nations, 2017). As a result, targets also emphasise an urgency to develop and adopt additional sustainable practices such as water reuse, to alleviate water scarcity and water resource management pressures (United Nations, 2018). For developing and emerging economies, the implementation of capital intensive conventional large scale piped water and sewerage wastewater infrastructure is economically unfeasible and unsustainable (Hutton and Haller, 2004; Kamranvand et al., 2018).

Instead, decentralised sanitation is practiced, which does not demand excessive water quantities to transport wastewater within a sewerage network or substantive capital and maintenance costs (Libralato, Volpi Ghirardini and Avezzi, 2012). However, present decentralised solutions, such as pit latrines and septic tanks, require frequent emptying, posing health risks to faecal sludge handlers and the wider community through unregulated direct environmental discharge (Ingallinella et al., 2002). In response, the Bill & Melinda Gates Foundation proposed the '*Reinvent the Toilet Challenge*' in 2011, to develop sustainable and affordable decentralised sanitation systems, which treat wastewater at source to prevent contaminant exposure, obviating emptying and transportation costs (The Bill & Melinda Gates Foundation, 2019). Importantly, the proposed technologies implement advanced treatment processes, which could recover high quality water for the end users. The current alternative for 29 % of the global population, is an unmanaged water supply of unknown quality, prone to wastewater intrusion from nearby sanitation facilities (United Nations, 2018).

In order to enhance efficiency by limiting treatment volume, the new generation of sanitation systems process blackwater only, by downscaling decentralisation to domestic scale (10 population equivalent). As flush water is commonly restricted, the application of waterless flush technology will further constrain volume representing wastewater only constituting urine and faeces – faecally contaminated urine (FCU) (Mercer et al., 2016). Such wastewater is highly concentrated, and therefore the treatment of FCU is a research area which requires significant attention for the advancement of non-sewered sanitation.

Membrane processes are an established barrier technology capable of delivering water quality that can meet stringent regulations, and have been successfully demonstrated for direct and indirect water reuse schemes from municipal wastewater (Warsinger et al., 2018). Reuse quality by advanced treatment is commonly achieved by reverse osmosis (RO) which is either preceded by the integration of a membrane bioreactor (MBR) in secondary treatment or a tertiary micro or ultrafiltration stage. Advanced oxidation, ultraviolet light or chlorination disinfection step is further applied for potable reuse. An example is Singapore's NEWater scheme in which five large scale plants are operational providing 40 % of the current total water demand, expected to reach 55 % by 2060 (Public Utilities Board, 2018).

Membrane processes are therefore a candidate barrier solution for household scale decentralised systems treating FCU, which can be practically downscaled due to the technology's modularity. However, conventional pressure driven filtration (UF, RO) is energy intensive and demands a consistent electricity supply to support considerable pumps (e.g. multi-stage). In many cases in a low income country (LIC) context, electricity supply may be intermittent and in sub-Saharan Africa, over 620 million do not have access to electricity at all (International Energy Agency, 2014). Waste heat is a widely available alternative energy source, independent of a gridded electrical supply, which can be derived from daily household activities such as cooking (Abdoullatiwish, Mao and Jaworski, 2017), and exploited by thermally driven membrane processes (facilitated by a vapour pressure gradient). Kamranvand et al. (2018) addressed the impact of FCU on water recovery from thermally driven membrane distillation. A steady state flux was achieved with a removal of 95 % and 96 % for chemical oxygen demand (COD) and ammoniacal nitrogen ($\text{NH}_4^+\text{-N}$) respectively, effectively demonstrating that a thermally driven membrane process can achieve high rejection of wastewater contaminants, using low grade waste heat. Thermally driven pervaporation (PV) has also been investigated for the treatment of urine wastewater for space missions involving hydrophilic (Hirabayashi, 2002) or hydrophobic (Nitta et al., 1986) polymers, highlighting a spectrum of potential thermally driven membrane polymers, that have yet to be evaluated for decentralised wastewater treatment, and explicitly with FCU.

In addition to achieving health standards to enable water reuse, taste and odour (T&O) treatment remains a key criticality to consumer satisfaction. Cruddas et al. (2015) concluded through a customer survey undertaken in a west African community, that a safe malodorous water product would likely be discarded. Those surveyed preferred sourcing non-odorous water of unknown provenance, which were likely to be of lower quality, defeating the SDG 6, of providing safe water for reuse (Cruddas, Parker and Gormley, 2015). Whilst T&O separation using thermally driven processes has previously been evaluated in discrete applications, their affinity for the separation of T&O compounds from FCU has not, and can be considered distinct due to concentration (in the absence of flush water) and proximity to source (Agus et al., 2011; Alkudhiri, Darwish and Hilal, 2012; Altalyan et al., 2016; Feng and Huang, 1992). Reverse osmosis and PV are both dense polymers which adopt a solution diffusion model, in which interactions between the compounds and polymers govern mass transfer (Baker, 2012). Membrane distillation acts as a support for the vapour liquid interface where gas permeation occurs through the micropores of a hydrophobic membrane (Baker, 2012).

This study aims to evidence thermally driven membrane processes (hydrophilic pervaporation, hydrophobic pervaporation and MD) as an effective barrier technology for water reuse from non-sewered sanitation, which can be operated using waste heat. For reference, we challenge and compare pressure driven membrane processes (UF, RO) for the treatment of FCU, as the conventional route to water reuse. The specific objectives are as follows: (i) assess permeate quality using water reuse standards; (ii) understand the impact of faecally contaminated urine on membrane flux; and (iii) evaluate malodour treatment to encourage reuse.

4.2 Materials and Methods

4.2.1 Experimental setup

Pressure driven processes (UF and RO, Table 4.1), were operated in a HP4750 cell (Sterlitech, USA) at 2 bar (UF) and 12 bar (RO). A magnetic stirrer was operated at 400 rpm on the feed side of the membrane to limit concentration polarisation. Flat sheet membranes from Sterlitech (TriSep UE50, TriSep X201, USA) were cut to an effective membrane area of 0.00146 m². Permeate samples were collected within an airtight 50

mL glass conical flask. Flux was determined by measurement of the temporal permeate mass up to a standardised filtered volume of 10 L m^{-2} (PR410 Symmetry, Cole-Parmer Ltd., London, UK). For thermally driven membranes (PV and MD, Figure 4.1, Table 4.1), the feed was circulated at 0.2 L min^{-1} and vacuum was introduced at 50 mbar on the permeate side using a diaphragm vacuum pump (MD 4C NT, Vacuubrand, Brackley). Flat sheet hydrophilic polyvinyl alcohol (PVA) membranes (DeltaMem, Pervap 4101, Switzerland) provided a membrane area of 0.0153 m^2 (Model Products, UK). Hollow fibre (HF) polydimethylsiloxane (PDMS) (Permsselect, PDMSXA-2500, USA) and hydrophobic microporous polypropylene (pore size $0.04 \mu\text{m}$) (3M-Liqui-Cel, MM 1.7x5.5, USA) possessed membrane areas of 0.25 m^2 and 0.54 m^2 respectively. Permeate was collected through a condenser ($2 \text{ }^\circ\text{C}$) until a standardised filtered volume of 1 L m^{-2} was reached. A liquid nitrogen cold trap ($-196 \text{ }^\circ\text{C}$) was used for permeate collection during the determination of VOCs. All membranes were operated at $50 \text{ }^\circ\text{C}$ within a thermostatic bath (Grant TC120, Cambridge, UK) to provide parity between each process.

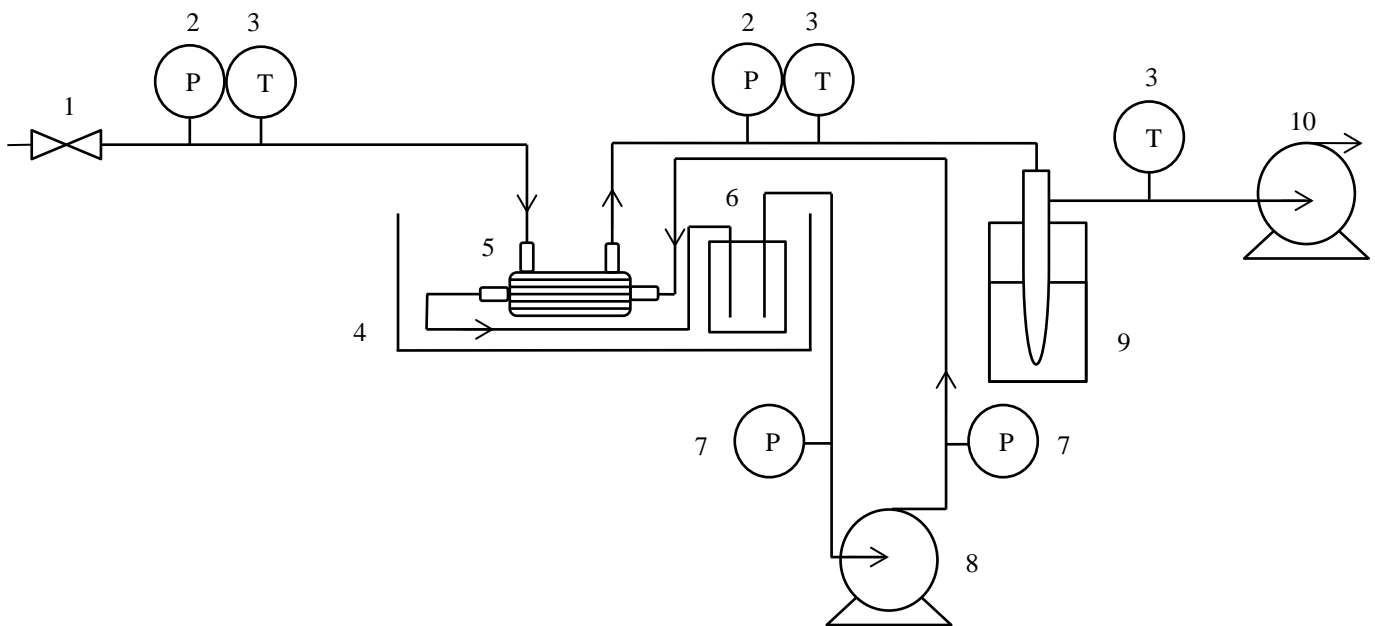


Figure 4.1 Membrane distillation and pervaporation membrane rig schematic. 1: Needle valve; 2: Absolute pressure transducer; 3: Temperature probe; 4: Thermostatic bath; 5: Membrane; 6: Feed solution; 7: Pressure gauge; 8: Peristaltic pump; 9: Liquid nitrogen cold trap or condenser; 10: Diaphragm vacuum pump.

Table 4.1 Summary of membrane characteristics and operational conditions used in this study

	Ultrafiltration	Reverse osmosis	Pervaporation		Membrane distillation
Manufacturer (model)	Trisep	TriSep	DeltaMem	Permselect	3M™ Liqui-Cel™
Model	(UE50)	(X201)	(Pervap™ 4101)	(PDMSXA–2500)	(MM1.7x5.5)
Material	Polyethersulphone	Polyamide-urea	Polyvinyl alcohol	Polydimethylsiloxane	Polypropylene
Typical Application	Removal of macromolecules from organic solutions	Desalination	Purification of organic mixtures	Removal of trace organic solvents from industrial wastewaters	Desalination, process water treatment
Driving force	Pressure	Pressure	Vapour pressure gradient	Vapour pressure gradient	Vapour pressure gradient
Membrane area (m ²)	0.00146	0.00146	0.0153	0.25	0.54
Membrane thickness (μm)	100-150	100-150	0.5	55	NAv
Pore size	MWCO 100000 Da	Non porous	Non porous	Non porous	0.04 μm
Contact angle	79 ^a	28.5 ^b	43 ^c	116 ^c	104 ^d
Hansen solubility δ (MPa m ^{-1/2})	NAP	NAv	25.78 ^a	15.59 ^a	NAP
Geometry	Flat sheet	Flat sheet	Flat sheet	Hollow fibre	Hollow fibre
Feed volume(mL)	300	300	600	500	500
Permeate volume (mL)	20	20	20	5, 10, 20	5, 10, 20
Recommended pressure (bar)	1.4 – 14	7 - 21	≤ 1	≤ 1	0.04 – 0.2
Operating pressure (bar)	2	12	0.05*	0.05*	0.05*
Recommended operating temperature (°C)	2 - 45	2 - 45	≤ 50	≤ 60	40
Operating temperature (°C)	20, 50	20, 50	50	50	50

*Vacuum pressure; NAP: Not applicable; NAv: Not available. ^aBormashenko et al. (2008); ^bLiu et al. (2006); ^cExperimentally derived using sessile drop method; ^dStrobel et al.(1985); ^eMark (2009).

Pressure driven membranes were also operated at conventional ambient temperature (20 °C). A virgin membrane was utilised for each experiment. Relative water flux was calculated by:

$$\text{Relative flux} = \frac{J}{J_0} \quad \text{Eq. 4.1}$$

where J is the faecally contaminated urine flux ($\text{kg m}^{-2} \text{h}^{-1}$) and J_0 was the deionised water flux ($\text{kg m}^{-2} \text{h}^{-1}$).

4.2.2 Feed preparation and analysis

Faecally contaminated urine was prepared at a 10:1 urine to faeces ratio, as this represents the typical proportions produced by an individual per day (Rose et al., 2015). Samples were vortexed for 30 seconds to homogenise, to provide conditions similar to a dynamic system. This ratio can be considered representative of the maximum faecal contamination of the solution phase, expected within non-sewered sanitation systems using a waterless flush (i.e no flush water). The sample was passively filtered through sand and cotton wool to limit coarse material (e.g. unmasticated food) introducing blockages during pumping. Fresh urine and faeces were sourced from consenting anonymous volunteers using a protocol approved by the Cranfield University Research Ethics System (CURES, project ID 3022).

The discharge and reuse standards contained within the recently published ISO 30500 standard on ‘Non Sewered Sanitation Systems’ (International Organisation for Standardisation, 2018) sets out specified guideline values for ammonium ($\text{NH}_4^+\text{-N}$), total phosphorus (TP), chemical oxygen demand (COD), coliform forming units (CFU) and pH as key contaminants for evaluation. The purpose of this standard is for the certification of technologies explicitly developed to deliver safe sanitation at a single household scale, in order to reduce consumer risk at procurement. Consequently, membrane selectivity was characterised using these parameters together with total suspended solids (TSS) and conductivity. Data was triplicated however insufficient to conform to a 20 % variance of at least five trials (as stated in the standard) and therefore the mean is only used as a quick reference to the guidelines, to benchmark the membrane technologies. For the determination of TP, $\text{NH}_4^+\text{-N}$ and COD, proprietary wet chemistry methods were used coupled with quantitation by spectrophotometry

(NOVA60 photometer, VWR, UK). The TSS, conductivity and pH were measured using standard methods (APHA;AWWA;WEF, 2005) and combined meter respectively (Jenway 4330, Cole Parmer, Staffordshire, UK). Total coliforms and E-Coli coliform colony counts were based on methods 9215C, 9215D, 9922B and 9922D (APHA;AWWA;WEF, 2005). Pathogen reduction was characterised using log removal value (LRV):

$$LRV = \log_{10}\left[\frac{C_0}{C}\right] \quad \text{Eq. 4.2}$$

where C_0 is the initial pathogen concentration (CFU mL⁻¹) and C is the pathogen concentration in the permeate (CFU mL⁻¹). The permeate limit of detection (LD) was determined by enumerating 10 mL permeate for UF and RO, and 100 mL for PV and MD using EZ-Fit filtration units (Merck Millipore, Watford, UK) which yielded LDs of 1 CFU 10 mL⁻¹ and 1 CFU 100 mL⁻¹ respectively. Non detected (ND) was classified as sample concentrations below the LD. which did not contain coliforms within the filtered volumes.

4.2.3 Volatile organic compound sampling and analysis

Nine VOCs were identified that represent commonly occurring compounds with differing chemical structures found in urine and faeces: sulfides (dimethyl disulfide), aromatic heterocycles (indole, skatole), phenols (*p*-cresol), alcohols (1-butanol), aldehydes (benzaldehyde), ketones (2-butanone) and esters (ethyl propionate, ethyl butyrate) (Table S4.1) (Lin et al., 2013), to provide an understanding of membrane selectivity. For synthetic solutions, a 1000 mg L⁻¹ stock solution containing pure VOCs was first prepared in propylene glycol to dissolve all compounds. An aliquot was subsequently added to a pH 6.5 (fresh urine, Rose et al. 2015) buffered solution according to Robinson and Stokes (2002), for the preparation of a synthetic feed standardised at 10 mg L⁻¹. Volatile organic compound analysis was also on faecally contaminated urine to evaluate feed stability. All samples were stored within gas tight 10 mL glass centrifugal vials (Cole Parmer, UK) and analysed on the same day as the trial. Analysis of VOCs involved a solid phase pre-concentration step (Oasis HLB, 1 g, Waters, USA) followed by quantification using gas chromatography mass spectrometry (GC-MS) (TQ 8040, Shimadzu, UK). Full details of quantification and method validation can be found in Mercer et al. (2019).

Membrane processes were directly compared by determining the separation of odorous VOCs using the ratio between the water flux and VOC flux, defined as:

$$\frac{J_{VOC}}{J_w} = \frac{\left(\frac{Q_{VOC}}{A_m}\right)}{\left(\frac{Q_w}{A_m}\right)} \quad \text{Eq. 4.3}$$

Where J_{VOC} is the VOC flux in $\text{kg m}^{-2} \text{h}^{-1}$, Q_{VOC} is the VOC flow rate (kg h^{-1}), Q_w is the water flow rate (kg h^{-1}) and A_m is the effective membrane area (m^2).

4.3 Results and discussion

4.3.1 Thermally driven processes demonstrate superior separation of key FCU contaminants

In order to establish the capability of each thermally driven and pressure driven membrane to achieve the guideline values set out in ISO 30500, the separation of standard wastewater determinands was initially evaluated. The average COD feed concentration was $15 \pm 3 \text{ g L}^{-1}$ for all trials. Pressure driven processes exhibited removal efficiencies of $55.9 \pm 9 \%$ ($20 \text{ }^\circ\text{C}$) and $27 \pm 9 \%$ ($50 \text{ }^\circ\text{C}$) for UF and $99 \pm 0.5 \%$ ($20 \text{ }^\circ\text{C}$) and $99 \pm 0.1 \%$ ($50 \text{ }^\circ\text{C}$) for RO (Figure 4.2). Comparably, Ouma et al. (2016) and Ek et al. (2006) processed urine and reported COD removals of 26 % and 90 % for UF and RO respectively. All thermally driven processes presented consistently high COD rejection values (standard deviation $< 1\%$) of $> 99 \%$. Theoretically, non-volatile solutes cannot permeate in thermally driven membrane processes as transport is restricted to the vapour phase (Alkudhiri, Darwish and Hilal, 2013; Yao et al., 2018). Non-volatile organic compounds such as urea, creatine and creatinine, which contribute a substantive portion of urine organics (Putnam, 1971), have been reported to be completely removed using PV (Hirabayashi, 2002), and greater than 98 % removal with MD (Joshua L. Cartinella, 2006; Kamranvand et al., 2018). Faecally contaminated urine is substantially more concentrated in organics than urine (almost four times higher COD in this study). In a study by Kamranvand et al. (2018), $>95 \%$ COD rejection was also achieved with faecally contaminated urine using MD. With respect to the ISO 30500 standard, COD category B ($\leq 150 \text{ mg L}^{-1}$) was achieved by the thermal processes hydrophilic PV and MD, which represents restricted urban reuse or safe discharge (Table 4.2).

Rejections of >99 % for TP was encountered for all processes other than RO operated at 50 °C where rejection reduced to 97 %, and UF (Figure 4.2), in which minimal removal was achieved, as similarly observed by Ouma et al. (2016). Forward osmosis, which is comparable to RO through the use of analogous semipermeable membranes, has proven complete rejection for TP in urine (Liu et al., 2016), which could be attributed to the fact that the majority of the TP content is as the phosphate ion which is preferentially rejected due to electrostatic interaction (Ek, 2006; Lee and Lueptow, 2004). Furthermore, TP is predominantly non-volatile and therefore its transport was restricted for all thermally driven processes. The TP limit of 2 mg L⁻¹ set out in ISO 30500 was met by RO at 20 °C and all thermal processes (Table 4.2). The poorer rejection of solutes by RO at elevated temperatures can be ascribed to changes in the polymer structure, combined with reduced solvent viscosity, and increased solute diffusivity (Jin et al., 2009).

Average ammoniacal nitrogen loadings were 998±740 mg L⁻¹. However urea hydrolysis, a naturally occurring process during urine storage, was evidenced during the trials which converts urea into ammonium and increases pH (Udert et al., 2003; Zhao et al., 2013):



Initial pH values (before faecal contamination) were below pH 7 and increased to a mean of pH 8.64±0.61 within two hours of faecal contamination (Table S4.3, Figure S4.1). As the pKa for ammonium is 9.24, the equilibrium is shifted towards ammonia, a non-ionic, polar and volatile compound which negatively impacts the respective separation mechanisms of RO, PV and hydrophobic thermally driven membrane processes. As a result, reported rejections for these processes were not comparable to literature values without the occurrence of urea hydrolysis. Specifically for pressure driven RO, electrostatic interaction is the principal mechanism for the removal of nitrogenous compounds, compared to molecular weight and chemical structure (Lee and Lueptow, 2004). To illustrate, at a similar ammonium feed concentration (1300 mg L⁻¹) maintained at pH 6, Bódalo et al. (2005) reported 98.9 % NH₄⁺ removal compared to 74±0.1 % (20 °C) and 78±3 % (50 °C) in this study, where the final permeate pH was 9.5-10.1. Comparatively, pressure driven UF provided a maximum NH₄⁺-N rejection of 34±5 % at 20 °C.

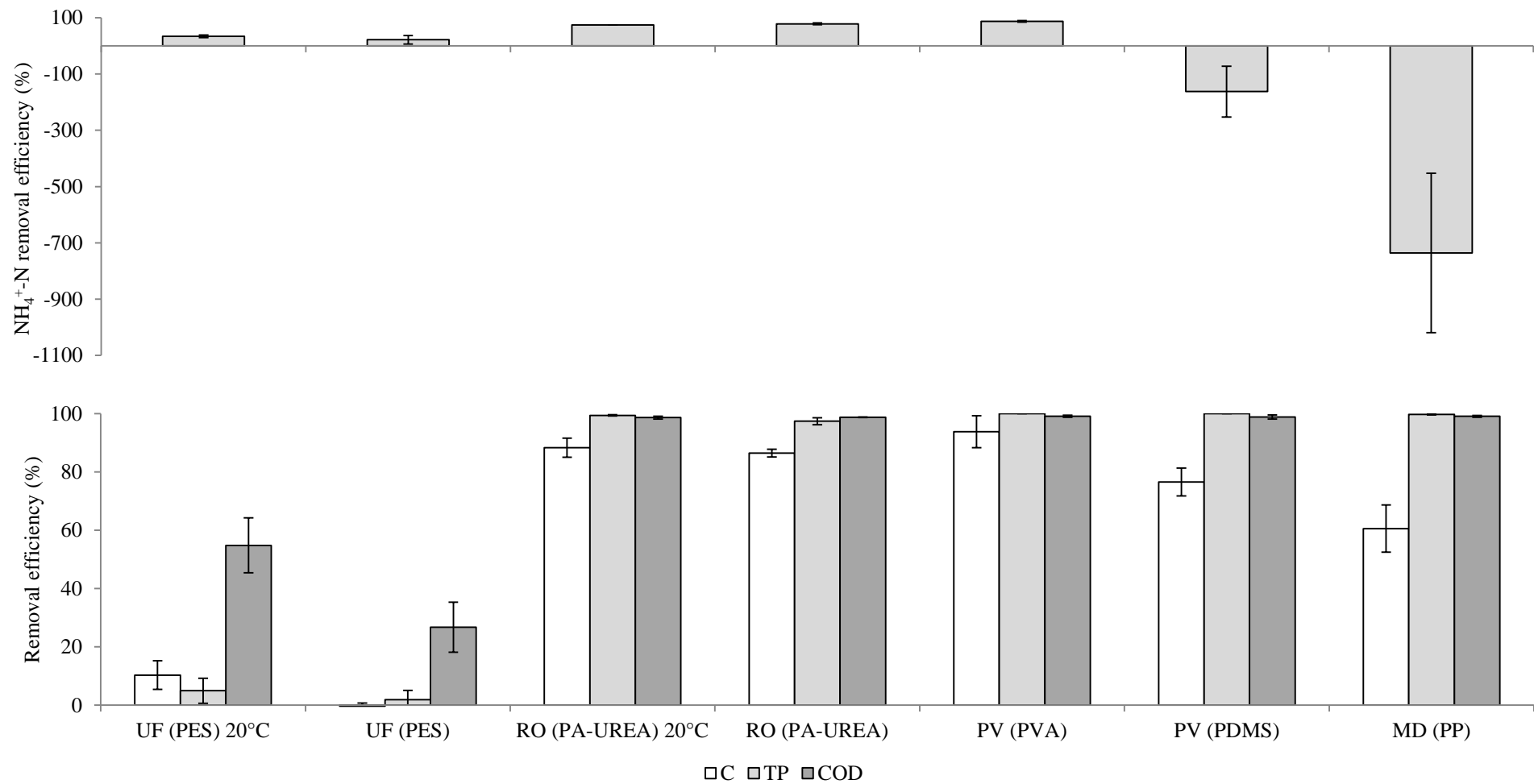


Figure 4.2 Removal efficiencies of ammoniacal nitrogen ($\text{NH}_4^+\text{-N}$), conductivity (C), total phosphorus (TP) and chemical oxygen demand (COD) treating faecally contaminated urine with membranes. Feed water temperature 50 °C, unless stated otherwise. UF (Ultrafiltration); PES (Polyethersulphone); RO (Reverse osmosis); PA-UREA (Polyamide-urea); PV (Pervaporation); PVA (Polyvinyl alcohol); PDMS (Polydimethylsiloxane); MD (Membrane distillation); PP (Polypropylene). Error bars represent standard deviation of a triplicated experiment.

The thermally driven membrane processes achieved $\text{NH}_4^+\text{-N}$ separations of 87 ± 3 , -162 ± 91 and -736 ± 283 % for PV (PVA), PV (PDMS) and MD respectively. Ammonia is highly volatile, and therefore the reduced permeate vapour pressures coupled with high feed temperatures used for thermally driven processes encourages its transport (EL-Bourawi et al., 2007; Tun et al., 2016; Zhao et al., 2013). The enhanced ammonia separation garnered with hydrophilic PV (PVA) can be accounted for by the material selectivity of PVA for water over ammonia (Hirabayashi, 2002). Hydrophobic PV (PDMS) and MD exhibited $\text{NH}_4^+\text{-N}$ permeate production, due to the continuous urea hydrolysis during the experimental period. Polydimethylsiloxane (hydrophobic PV) has moderate permeability to ammonia as reported by Sürmeli et al. (2018) and hydrophobic MD preferentially permeates ammonia to water due to the repulsion of water from the membrane interface (EL-Bourawi et al., 2007). As a result, PV (PDMS) and MD have been applied for ammonia recovery for high pH feed waters (EL-Bourawi et al., 2007; Sürmeli, Bayrakdar and Çalli, 2018). Kamranvand et al. (2018) reported 96 % $\text{NH}_4^+\text{-N}$ removal with faecally contaminated urine using MD, however utilising an effective membrane area of 0.001 m^2 compared to 0.54 m^2 in this study. A greater membrane area transports a larger volume of ammonia, reducing boundary layer concentration polarisation occurring from the build-up of ammonia during continuous urea hydrolysis. Additionally, the total flux of Kamranvand et al. (2018) was $3.05 \text{ L m}^{-2} \text{ h}^{-1}$ compared to $0.08 \text{ L m}^{-2} \text{ h}^{-1}$ in this study, which could have resulted in a degree of dilution. The final permeates were at pH 9.9 and 10.5 for PV (PDMS) and MD respectively, illustrating the extent of urea hydrolysis which took place. Coincidentally, the ammonia content within the permeate was responsible for increased permeate conductivity which resulted in poor salt rejection in the permeate at 77 ± 5 % (PV, PDMS) and 61 ± 8 (MD), which has similarly been reported by Zhao et al. (2013) who reported urea hydrolysis.

Urea hydrolysis therefore prevented the achievement of the required $\text{NH}_4^+\text{-N}$ permeate concentration (total nitrogen $\leq 15 \text{ mg L}^{-1}$) and pH (6-9) for ISO 30500 (Table 4.2). Addressing the urease enzyme source responsible for facilitating hydrolysis (urease producing bacteria) will prevent pH change, maintaining a feed comprising non-volatile urea and $\text{NH}_4^+\text{-N}$, which theoretically cannot permeate. This has been achieved by the thermal inactivation of responsible urease bacteria at $70 \text{ }^\circ\text{C}$

(Kamranvand, 2019; Zhou et al., 2017). Such a temperature is still accessible as waste heat, and could therefore be integrated as the operating temperature for thermal processes with increased water flux (Arrhenius relationship) and decreased ammonia selectivity (for MD) (Xie et al., 2009). For RO, an additional barrier process (i.e. UF) or acidification would be required to mitigate urea hydrolysis, allowing for the rejection of charged ammonium ions. However, as urea is uncharged, it is poorly rejected by RO which further contributes to permeate COD and nitrogen (Lee and Lueptow, 2001) and therefore requires additional treatment consideration.

The permeate of all membranes (excluding UF) presented no coliforms above the detection limit when challenged with concentrations up to 10^7 CFU mL⁻¹ (Figure 4.3). The LRVs obtained were influenced by feed concentration and available permeate volume which determined detection limits (see section 4.2.2). Reverse osmosis is non-porous and provides an absolute barrier to pathogens, hence its wide scale adoption for potable reuse from wastewater (Pype et al., 2016). Similarly, PV and MD also act as absolute barriers since the separation constitutes both size exclusion and selectivity toward volatile constituents, due to the temperature gradient introduced.

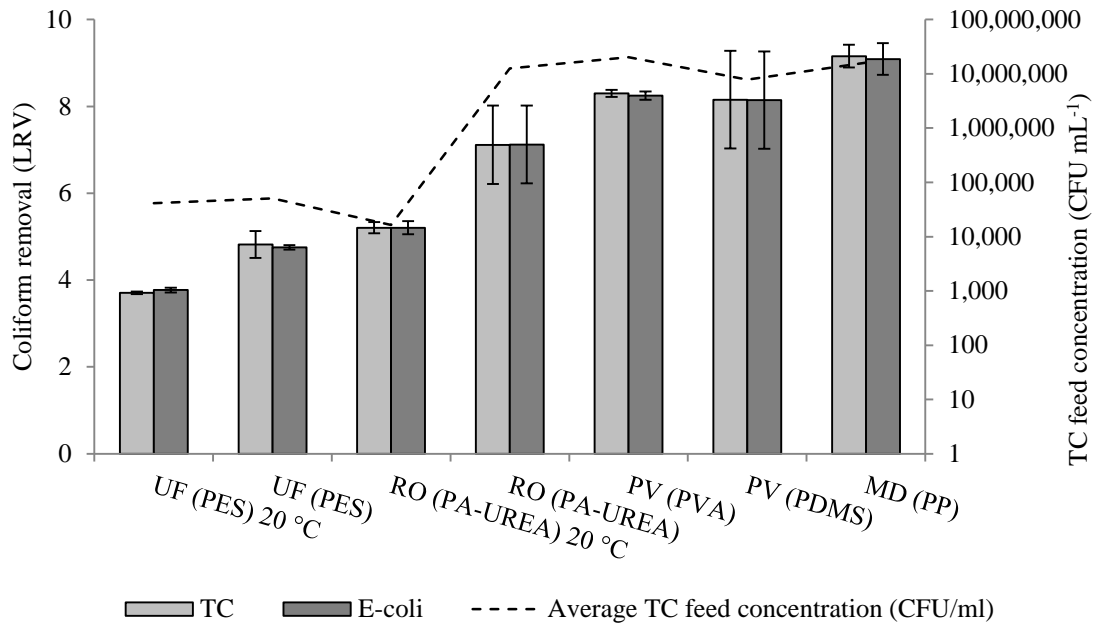


Figure 4.3 Coliform log removal values (LRVs) for E.coli and total coliforms (TC) using UF (PES), RO (PA-UREA), PV (PVA), PV (PDMS) and MD (PP) processes to treat faecally contaminated urine. Feed water temperature 50 °C, unless stated otherwise. UF (Ultrafiltration); PES (Polyethersulphone); RO (Reverse osmosis); PA-UREA (Polyamide-urea); PV (Pervaporation); PVA (Polyvinyl alcohol); PDMS (Polydimethylsiloxane); MD (Membrane distillation); PP (Polypropylene). Error bars represent standard deviation of a triplicated experiment.

Table 4.2 ISO 30500 (2018) membrane (mean) filtrate compliance (✓) and failure (×) from faecally contaminated urine

	UF (PES)		RO (PA-UREA)		PV (PVA)	PV (PDMS)	MD (PP)
	20 °C	50 °C	20 °C	50 °C	50 °C	50 °C	50 °C
COD Category A ($\leq 50 \text{ mg L}^{-1}$)	× (6233)	× (10600)	× (202)	× (159)	× (134)	× (231)	× (149)
COD Category B ($\leq 150 \text{ mg L}^{-1}$)	× (6233)	× (10600)	× (202)	× (159)	✓ (134)	× (231)	✓ (149)
TP ($\leq 2 \text{ mg L}^{-1}$)	× (123)	× (157)	✓(0.9)	× (4)	✓ (ND)	✓ (0.05)	✓ (1.19)
NH ₄ ⁺ -N (TN $\leq 15 \text{ mg L}^{-1}$)	× (450)	× (1363)	× (462)	× (382)	× (36)	× (854)	× (2375)
CFU mL ⁻¹ ($\leq 0.1 \text{ CFU mL}^{-1}$)	× (8)	× (0.86)	✓ (ND)	✓ (ND)	✓ (ND)	✓ (ND)	✓ (ND)
pH (6-9)	✓ (8.5)	✓ (9.0)	✓ (9.5)	× (10.1)	✓ (9.3)	✓ (9.86)	× (10.5)

UF (Ultrafiltration); PES (Polyethersulphone); RO (Reverse osmosis); PA-UREA (Polyamide-urea); PV (Pervaporation); PVA (Polyvinyl alcohol); PDMS (Polydimethylsiloxane); MD (Membrane distillation); PP (Polypropylene); COD (Chemical oxygen demand); TP (Total phosphorus); NH₄⁺-N (Ammoniacal nitrogen); TN (Total nitrogen) CFU (Colony forming units).

4.3.2 Feed side pressure negatively impacts water productivity from faecally contaminated urine

Membrane processes were challenged with an average TSS concentration of $6 \pm 1.5 \text{ g L}^{-1}$. The effect of faecal solids presented three distinct flux trajectories (Figure 4.4), classified into pressure driven processes, hydrophilic pervaporation and hydrophobic thermally driven processes. Pressure driven membrane processes demonstrated steady state relative fluxes at least an order of magnitude lower than the thermal processes (UF: 0.5, RO: 0.12). It is suggested that it is the pressure gradient coupled with the high solids concentration in UF and RO that induces solids compaction at the membrane surface which diminished the attainable flux (Stade et al., 2015). Ultrafiltration was additionally prone to pore clogging by faecal solids (Polyakov and Zydney, 2013). It is recommended that particles larger than $5 \mu\text{m}$ should be removed for RO which is commonly facilitated by UF (Ek, 2006), and further research would be required to identify critical flux for sustainable operation within a FCU matrix. Comparatively, hydrophilic PV obtained a steady state relative flux of 0.6, evidencing that pressurised membrane water productivities are more sensitive to faecal contamination than thermally driven processes, which do not rely on pressurised feeds. When comparing PVA to the hydrophobic thermally driven processes, the relative flux was 40 % lower attributed to material interactions, although further investigation to fully understand the fouling mechanisms of polymers in thermal processes is required. The hydrophobic membranes obtaining FCU fluxes close to that of deionised water, although a limiting factor was the densely packed hollow fibre configuration (HF) which is prone to blockages by faecal solids. Fibre blockages were observed in one of the triplicated trials of PV (PDMS), subsequently decreasing the overall relative flux mean from 1 to 0.65. For polymer and process demonstration, the membrane bundles were commercially sourced, however designed for their typical discrete application of gas or solvent separation, owing to a specific surface area of around $7400 \text{ m}^{-2} \text{ m}^{-3}$. A configuration which obviates hydrodynamic blockages associated with faecal solids could be engineered to overcome flux decline, such as the MBR HF modules employed for typical wastewater applications with typical specific surface areas of $300 \text{ m}^{-2} \text{ m}^{-3}$ (Santos, Ma and Judd, 2011). Importantly, sustainable fluxes can be achieved using thermally driven processes, particularly hydrophobic PV and MD.

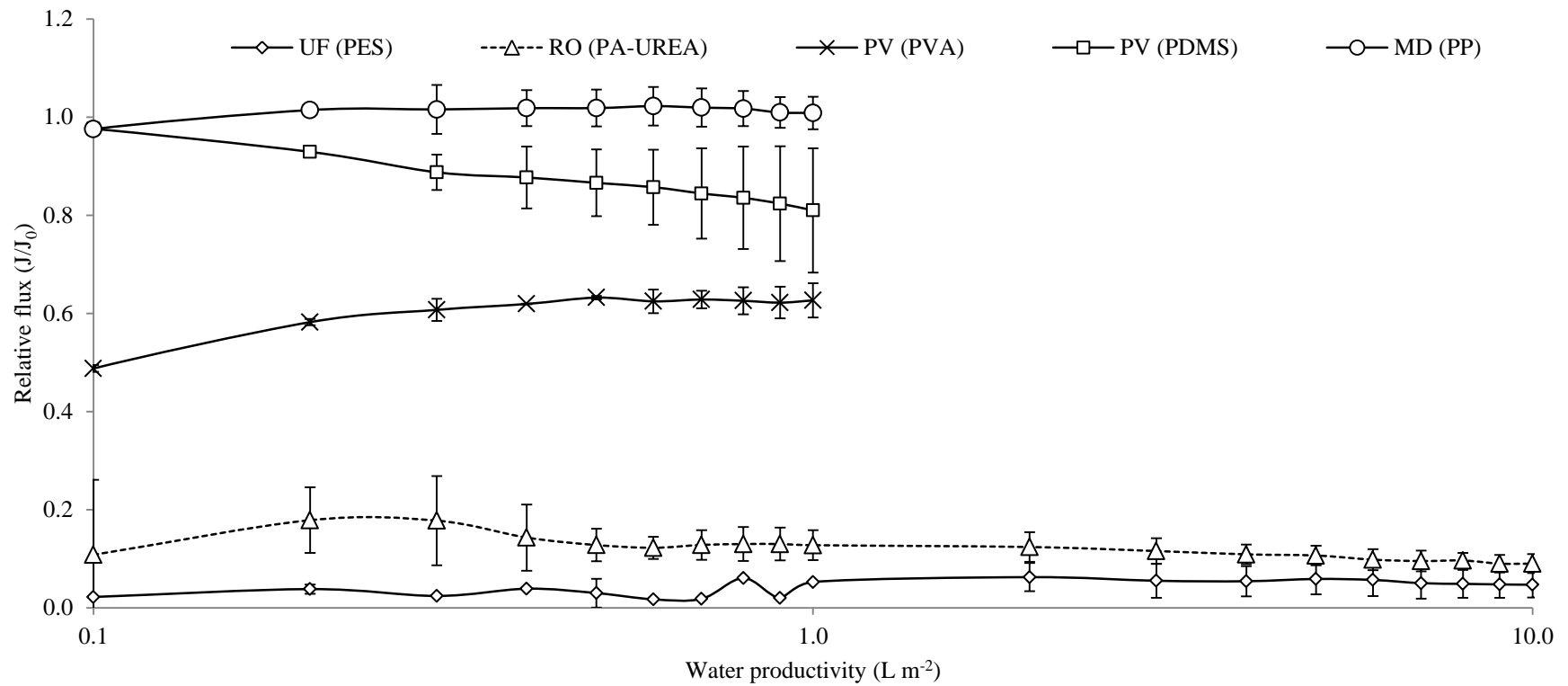


Figure 4.4 Normalised membrane flux with deionised water (J_0) and faecally contaminated urine (J). Water productivities of UF and RO standardised to 10 L m^{-2} membrane area and PV and MD standardised to 1 L m^{-2} membrane area. UF (Ultrafiltration); PES (Polyethersulphone); RO (Reverse osmosis); PA-UREA (Polyamide-urea); PV (Pervaporation); PVA (Polyvinyl alcohol); PDMS (Polydimethylsiloxane); MD (Membrane distillation); PP (Polypropylene). All membranes were operated at $50 \text{ }^\circ\text{C}$. Error bars represent standard deviation of a triplicated experiment.

4.3.3 Thermally driven processes evidence faecal odour treatment by profile manipulation

Membrane odour analysis was carried out using both a synthetic and real faecally contaminated urine matrix. Odourant production within the feed occurred during the duration of the trial (Figure 4.5) altering the feed concentration, as T&O causing compounds (VOCs) are bacterial byproducts (Bos, Sterk and Schultz, 2013). Therefore, in order to accurately investigate polymer and process selectivity towards VOCs, the quantitative assessment of membrane separation was determined using the synthetic matrix where the feed concentration was stable, and qualitative odour characterisation was carried out using the real matrix. Figure 4.6 illustrates the relative VOC to water flux for all membrane processes. Ultrafiltration did not evidently achieve VOC separation, since permeate concentration was close to that of the feed, indicating no selectivity. However, hydrophilic dense membranes demonstrated VOC removal (RO, PV-PVA) of up to 65-80 %. Reverse osmosis and PV polymers are based on the same transport mechanism (solution diffusion model) and particularly RO and PV(PVA) are comparable due to their shared glassy, hydrophilic characteristics. Although theoretically rejection should be similar (Rautenbach and Albrecht, 1985). PVA exhibited greater selectivity towards water over T&O compounds although better permeability could have been expected, due to the presence of alcohol groups (polarity) or carbonyl groups (hydrogen bonding in the PVA) featured on certain compounds. One proposition is the induction of PVA polymer swelling caused by the high water content of the feed water (> 99 % wt) which can decrease selectivity (Van Baelen et al., 2005). A good but lower VOC rejection was observed for RO (Figure 4.6) with selectivity strongly correlated to molecular weight ($r = -0.85$, $n = 9$, $p = 0.003$) and octanol water coefficient ($r = -0.911$, $n = 9$, $p = 0.001$) as similarly reported by Altalyan et al. (2016). Rautenbach and Albrecht (1985) directly compared RO and PV concluding that in practice, RO membrane imperfections associated with micropores, compaction and convective flow prevent theoretical values to be reached. In addition, as mass transfer in PV is facilitated by a vapour pressure gradient, desorption of lesser volatile contaminants is restricted.

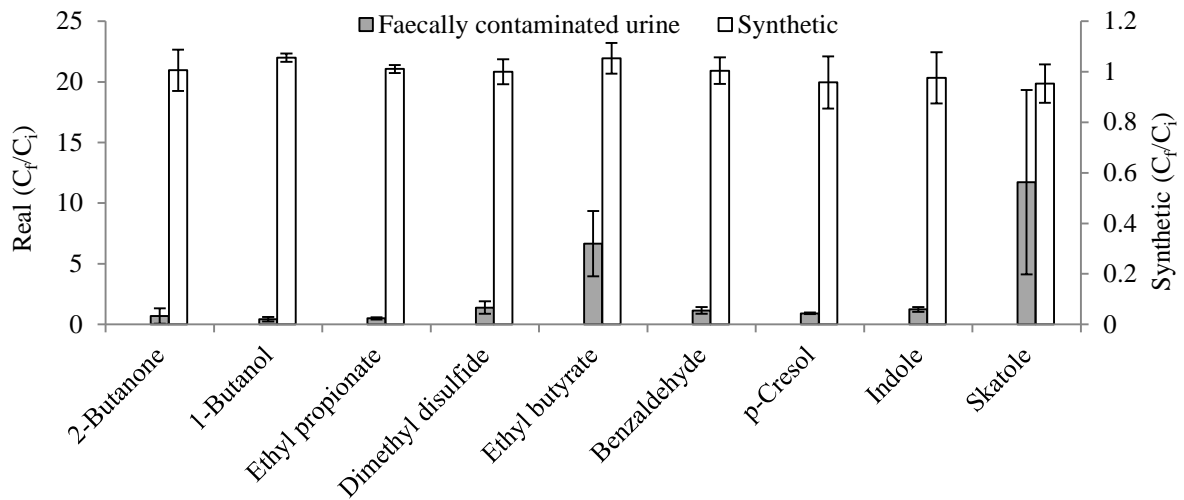


Figure 4.5 Feed odour development during storage, expressed as the ratio of the final feed concentration (C_f) to the initial feed (C_i) for pervaporation (polyvinyl alcohol) during faecally contaminated urine trials and synthetic trials. Operated at 50 °C. Error bars represent standard deviation of a triplicated experiment. Mean filtration time 4.77 hours.

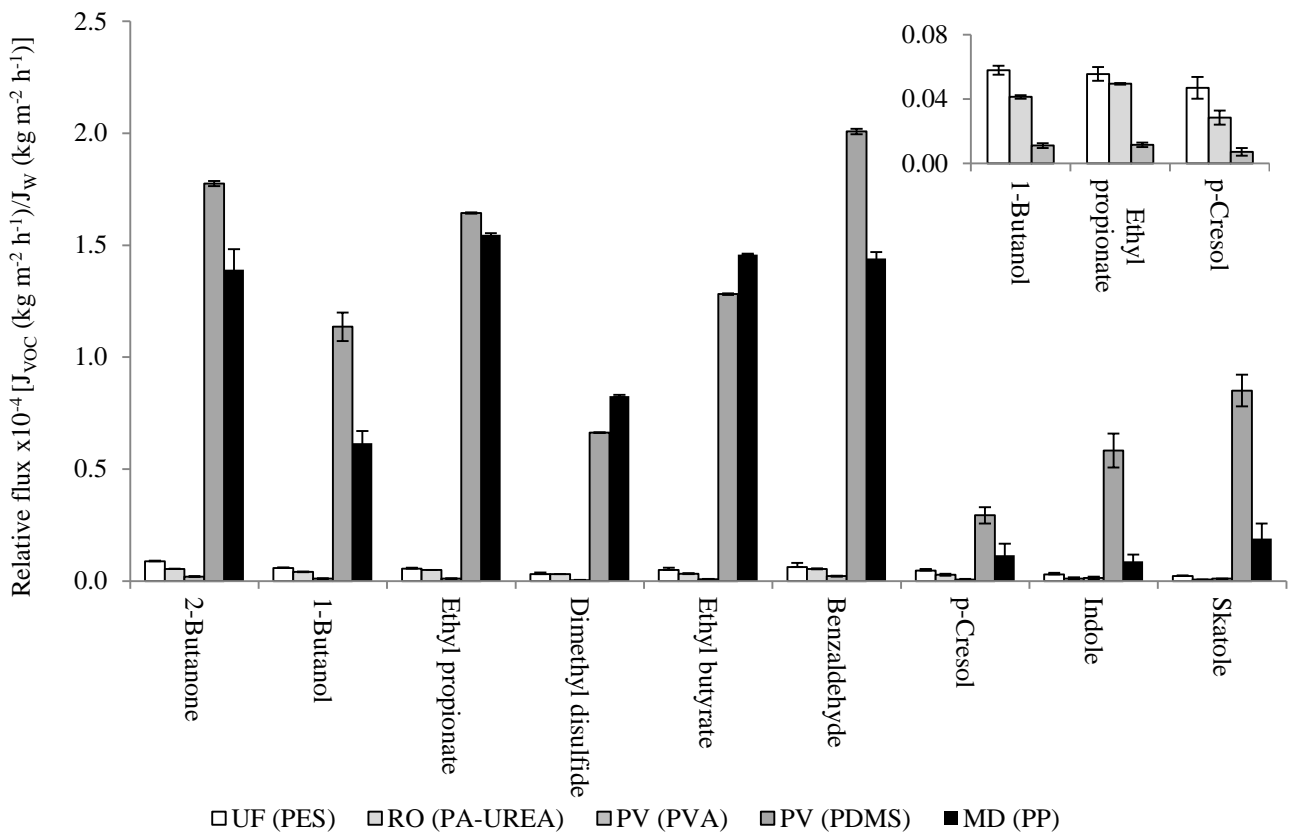


Figure 4.6 A comparison of membrane odour separation (UF, RO, PV and MD) expressed as the ratio of volatile organic compounds (VOCs) flux to water flux. Synthetic solution feed concentration 10 mg L⁻¹. UF (Ultrafiltration); PES (Polyethersulphone); RO (Reverse osmosis); PA-UREA (Polyamide-urea); PV (Pervaporation); PVA (Polyvinyl alcohol); PDMS (Polydimethylsiloxane); MD (Membrane distillation); PP (Polypropylene). All membranes operated at 50 °C. Error bars represent standard deviation of a triplicated experiment.

In contrast, the hydrophobic thermally driven membrane processes enriched VOCs within the permeate. Polydimethylsiloxane concentrated all VOCs due to the material's affinity to non-polar compounds (Baker, 2012). With the suite of compounds used in this study encompassing a large range of physico-chemical properties, selectivity in the PDMS was governed by vapour pressure, volatility and hydrophobicity as reported by Mercer et al. (2019) Membrane distillation illustrated a similar profile to PV(PDMS), however separation had a general dependency on boiling point ($r=-0.862$, $n=9$, $p=0.003$) or volatility ($r=-0.701$, $n=9$, $p=0.036$), rather than chemical properties ordinarily associated with material interactions, due to the fact that the VOCs transport occurs at the vapour liquid interface within the micropores (Baker, 2012). A temporal transient was identified for the selective transport of VOCs in thermally driven hydrophobic membranes (Figure 4.7), where a greater affinity to VOCs over water was observed during the initial stages of permeation. As the VOC concentration gradient decreases over time, the mass transfer driving force is reduced, resulting in a gradual decline of VOC selectivity over water. Further organic reduction to further achieve ISO 30500, could be executed by discarding the initial VOC concentrated permeate fraction in batch mode, also reducing odour intensity.

When comparing VOC rejection using a synthetic matrix (Figure 4.6) to a real matrix (Figure 4.8), the rejection capabilities of UF, RO and PVA were insignificant on the final permeate concentrations, due to feed-side VOC production. Permeate odour was time critical causing the longest trial (PVA, most selective membrane) to be less effective in VOC management than UF and RO (less selective membranes) for ethyl butyrate, ethyl propionate, dimethyl disulfide and skatole which were particularly produced within the feed (Figure 4.5) and contributed to permeate odour. However, unlike UF and RO, a key faecal malodorous compound *p*-cresol did not exceed the odour threshold (van Gemert, 2011) due to comparably lower feed production and consequently the permeate odour was less characteristic of FCU (Figure 4.8). Ethyl butyrate and *p*-cresol contributed to taste (exceeding the taste thresholds compiled by van Gemert, 2011) for all hydrophilic membrane processes.

Qualitative odour characterisation of the thermally driven processes presented three different odour outcomes with little resemblance of FCU due to alterations in the respective odour profiles (Table 4.3). Hydrophobic pervaporation (PDMS) produced the

most hedonistically pleasant odour which was characteristic of a cleaning product, which could be associated with ‘sanitised’ water and therefore widely accepted. The permeate contained floral notes attributed to the enrichment of indole and skatole, key constituents of jasmine perfume (Starkenmann, 2017). Hydrophilic (PVA) pervaporation also represented a chemical odour with similarities to body odour, unpleasant however not repulsive. Membrane distillation permeate was overpowered by ammonia causing a repulsive odour, even with a VOC profile similar to PV(PDMS) (Figure 4.6). As discussed in section 3.1, operating thermally driven processes at higher temperatures manages ammonia, which equally applies to feed odour stabilisation

Table 4.3 Odour descriptors for permeate produced from pervaporation and membrane distillation membranes following treatment of faecally contaminated urine.

Membrane process (material)	Permeate odour descriptor
PV (PVA)	Sweaty, chemical, sweet, onion
PV (PDMS)	Sweet, chemical, earthy, floral
MD (PP)	Pungent, ammonia, fishy, citrus

PV (Pervaporation); PVA (Polyvinyl alcohol); PDMS (Polydimethylsiloxane); MD (Membrane distillation); PP (Polypropylene).

through microbial inactivation.

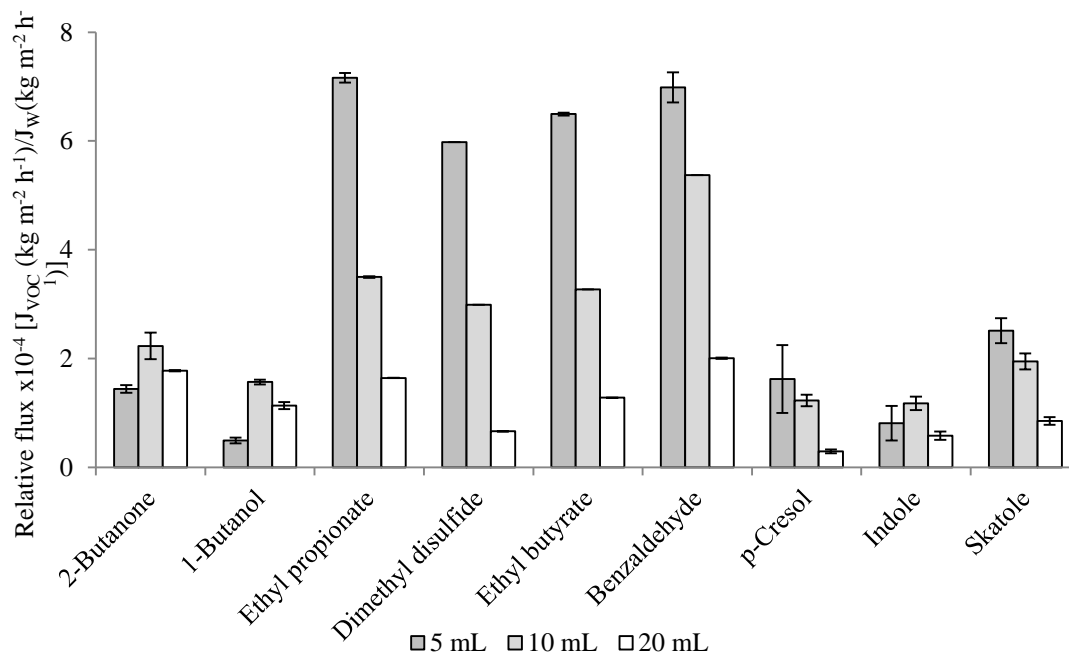


Figure 4.7 Pervaporation (Polydimethylsiloxane) and odour separation and varying permeate volumes, expressed as the ratio of volatile organic compounds (VOC) flux to water flux. Synthetic solution feed concentration 10 mg L⁻¹. All membranes operated at 50 °C. Error bars represent standard deviation of a triplicated experiment.

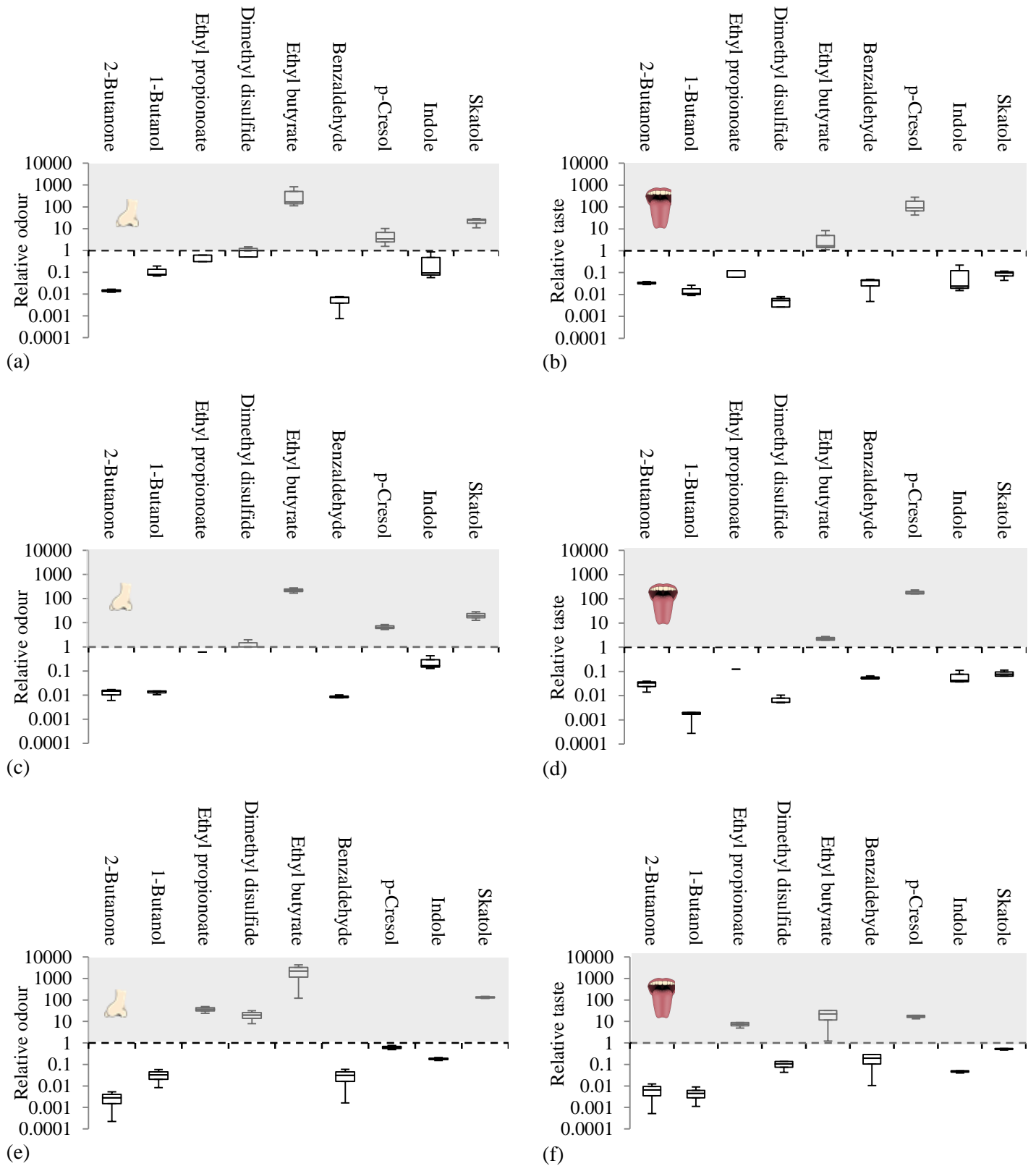


Figure 4.8 Faecally contaminated urine relative odour and taste of ultrafiltration permeate (a,b), reverse osmosis permeate (c,d) and hydrophilic pervaporation permeate (e,f) according to the lowest reported odour and taste thresholds in water (van Gemert, 2011). Mean filtration times for ultrafiltration, reverse osmosis and hydrophilic pervaporation were 0.71, 2.91 and 4.77 hours respectively.

4.4 Conclusions

Thermally driven membrane processes have exhibited a greater potential for water reuse from highly concentrated and variable FCU wastewater, than conventional pressure driven reuse processes through demonstration that:

- Within a single stage, thermally driven PV (PVA) and MD conformed to the most parameters of ISO 30500.
- Faecal contamination did not affect flux for hydrophobic thermal processes compared to pressure driven processes which declined by an order of magnitude.
- Faecal odour manipulation by thermally driven processes can be employed to change negative perception.

Feed-side bacterial activity was responsible for urea hydrolysis and VOC production, which caused complications in ammonia, pH and odour abatement, in addition to achieving COD category B using the configurations and setups practiced in this study. However, from the lessons learnt, category A reuse quality could be achieved through:

- Operating thermally driven processes at higher temperatures to inactivate problematic bacteria, and increase water productivity.
- Reducing permeate COD further for thermally driven membrane processes by discarding the initial highly concentrated VOC fraction in batch mode, which consequently reduces odour intensity.

Alongside optimisation, further insight into PV membrane materials is warranted to:

- Improve selectivity and robustness through trialling hydrophilic ceramic zeolite alternatives with FCU, known to be less sensitive than polymeric PV for feeds characterised by high temperatures and water content.
- Examine odour profile manipulation with accompanying public perception studies investigating a wider array of hydrophobic polymers to ultimately create a pleasant sensory experience – a new meaning to ‘eau de toilette’.

Overall, this study has signposted that thermally driven processes have suitability for water recovery from FCU, providing a sustainable sanitation solution for SDG 6 through the use of waste heat. Due to the higher fluxes associated with MD and water quality achieved within a single process, MD is closer to implementation than PV. However, with further PV research, a combinatory module could provide a holistic

solution addressing all critical water reuse aspects: water quality (safe for reuse), flux sustainability (robustness) and malodour (user acceptance).

4.5 References

Abdoulla-Latiwish, K.O.A., Mao, X. and Jaworski, A.J. (2017) ‘Thermoacoustic micro-electricity generator for rural dwellings in developing countries driven by waste heat from cooking activities’, *Energy*, 134, pp. 1107–1120.

Agus, E., Lim, M.H., Zhang, L. and Sedlak, D.L. (2011) ‘Odorous Compounds in Municipal Wastewater Effluent and Potable Water Reuse Systems’, *Environmental Science & Technology*, 45, pp. 9347–9355.

Alkudhiri, A., Darwish, N. and Hilal, N. (2012) ‘Membrane distillation: A comprehensive review’, *Desalination*, 287, pp. 2–18.

Alkudhiri, A., Darwish, N. and Hilal, N. (2013) ‘Produced water treatment: Application of Air Gap Membrane Distillation’, *Desalination*, 309, pp. 46–51.

Altalyan, H.N., Jones, B., Bradd, J., Nghiem, L.D. and Alyazichi, Y.M. (2016) ‘Removal of volatile organic compounds (VOCs) from groundwater by reverse osmosis and nanofiltration’, *Journal of Water Process Engineering*, 9, pp. 9–21.

APHA;AWWA;WEF (2005) *Standard Methods for the Examination of Water and Wastewater*. 21st edn. Washington, USA: American Public Health Association.

Van Baelen, D., Van der Bruggen, B., Van den Dungen, K., Degreve, J. and Vandecasteele, C. (2005) ‘Pervaporation of water–alcohol mixtures and acetic acid–water mixtures’, *Chemical Engineering Science*, 60, pp. 1583–1590.

Baker, R. (2012) *Membrane Technology and Applications*. 3rd edn. Baker, R. (ed.) Chichester, UK: John Wiley and Sons.

Bódalo, A., Gómez, J.-L., Gómez, E., León, G. and Tejera, M. (2005) ‘Ammonium removal from aqueous solutions by reverse osmosis using cellulose acetate membranes’, *Desalination*, 184, pp. 149–155.

Bormashenko, E., Pogreb, R., Whyman, G., Bormashenko, Y., Jager, R., Stein, T., Schechter, A. and Aurbach, D. (2008) ‘The Reversible Giant Change in the Contact

Angle on the Polysulfone and Polyethersulfone Films Exposed to UV Irradiation’, *Langmuir*, 24, pp. 5977–5980.

Bos, L.D.J., Sterk, P.J. and Schultz, M.J. (2013) ‘Volatile Metabolites of Pathogens: A Systematic Review’, *PLOS Pathogens*, 9, Public Library of Science, pp. e1003311.

Cruddas, P.H., Parker, A. and Gormley, A. (2015) ‘User perspectives to direct water reuse from the Nano Membrane Toilet.’, *38th WEDC International Conference. Loughborough, UK, 27-31 July 2015.*

Ek, D. (2006) ‘Concentration of nutrients from urine and reject water from anaerobically digested sludge’, *Water Science and Technology*, 54, pp. 437–444.

EL-Bourawi, M.S., Khayet, M., Ma, R., Ding, Z., Li, Z. and Zhang, X. (2007) ‘Application of vacuum membrane distillation for ammonia removal’, *Journal of Membrane Science*, 301, pp. 200–209.

Feng, X. and Huang, R.Y.M. (1992) ‘Separation of isopropanol from water by pervaporation using silicone-based membranes’, *Journal of Membrane Science*, 74, pp. 171–181.

van Gemert, L. (2011) *Odour thresholds. Compilations in air water and other media.* 2nd edn. van Gemert, L. (ed.) Utrecht, Netherlands: Oliemans Punter & Partners BV.

Hilal, N. and Wright, C.J. (2018) ‘Exploring the current state of play for cost-effective water treatment by membranes’, *npj Clean Water*, 1, p. 8.

Hirabayashi, Y. (2002) ‘Pervaporation Membrane System for the Removal of Ammonia from Water’, *Materials Transactions*, 43, pp. 1074–1077.

Hutton, G. and Haller, L. (2004) ‘*Evaluation of the Costs and Benefits of Water and Sanitation Improvements at the Global Level*’, World Health Organisation. Available at: https://www.who.int/water_sanitation_health/wsh0404.pdf. (Accessed 8 August 2018).

Ingallinella, A., Sanguinetti, G., Koottatep, T., Montanger, A., Strauss, M., Jimenez, B., Spinosa, L., Odegaard, H. and Lee, D. (2002) ‘The challenge of faecal sludge management in urban areas--strategies, regulations and treatment options.’ *Water Science and Technology*, 46, pp. 285–94.

- International Energy Agency (2014) *Africa Energy Outlook: A focus on energy prospects in sub-Saharan Africa*. Available at: https://www.iea.org/publications/freepublications/publication/WEO2014_AfricaEnergyOutlook.pdf. (Accessed 8 August 2018)/
- International Organisation for Standardisation (2018) ISO 30500. *Non-sewered sanitation systems -- Prefabricated integrated treatment units - General safety and performance requirements for design and testing (Final Draft)*. Available at: <https://www.iso.org/standard/72523.html>. (Accessed 9 August 2018).
- Jin, X., Jawor, A., Kim, S. and Hoek, E.M. V (2009) 'Effects of feed water temperature on separation performance and organic fouling of brackish water RO membranes', *Desalination*, 239, pp. 346–359.
- Joshua L. Cartinella, and A.E.C. (2006) 'Removal of Natural Steroid Hormones from Wastewater Using Membrane Contactor Processes', *Environmental Science & Technology*, 40, pp. 7381–7386.
- Kamranvand, F. (2019) *Membrane Processes for Water Recovery from Decentralised Sanitation Systems*. PhD thesis. Cranfield University.
- Kamranvand, F., Davey, C.J., Sakar, H., Autin, O., Mercer, E., Collins, M., Williams, L., Kolios, A., Parker, A., Tyrrel, S., Cartmell, E. and McAdam, E.J. (2018) 'Impact of fouling, cleaning and faecal contamination on the separation of water from urine using thermally driven membrane separation', *Separation Science and Technology*, 53, pp. 1372–1382.
- Lee, S. and Lueptow, R.M. (2004) 'Rotating reverse osmosis for water recovery in space: influence of operational parameters on RO performance', *Desalination*, 169, pp. 109–120.
- Lee, S. and Lueptow, R.M. (2001) 'Membrane Rejection of Nitrogen Compounds', *Environmental Science & Technology*, 35, pp. 3008–3018.
- Libralato, G., Volpi Ghirardini, A. and Avezzi, F. (2012) 'To centralise or to decentralise: An overview of the most recent trends in wastewater treatment management', *Journal of Environmental Management*, 94, pp. 61–68.

- Lin, J., Aoll, J., Niclass, Y., Velazco, M.I., Wunsche, L., Pika, J. and Starckenmann, C. (2013) ‘Qualitative and Quantitative Analysis of Volatile Constituents from Latrines’, *Environmental Science & Technology*, 47, pp. 7876–7882.
- Liu, L.-F., Yu, S.-C., Zhou, Y. and Gao, C.-J. (2006) ‘Study on a novel polyamide-urea reverse osmosis composite membrane (ICIC–MPD): I. Preparation and characterization of ICIC–MPD membrane’, *Journal of Membrane Science*, 281, pp. 88–94.
- Liu, Q., Liu, C., Zhao, L., Ma, W., Liu, H. and Ma, J. (2016) ‘Integrated forward osmosis-membrane distillation process for human urine treatment’, *Water Research*, 91, pp. 45–54.
- Mark, J.E. (2009) *Polymer data handbook*. Mark, J. E. (ed.). 2nd edn. New York, USA: Oxford University Press.
- Mercer, E., Cruddas, P., Williams, L., Kolios, A., Parker, A., Tyrrel, S., Cartmell, E., Pidou, M. and McAdam, E.J. (2016) ‘Selection of screw characteristics and operational boundary conditions to facilitate post-flush urine and faeces separation within single household sanitation systems’, *Environmental Science: Water Research & Technology*, 2, pp. 953–964.
- Mercer, E., Davey, C.J., Campo, P., Fowler, D., Williams, L., Kolios, A., Parker, A., Tyrrel, S., Walton, C., Cartmell, E., Pidou, M. and McAdam, E.J. (2019) ‘Quantification of liquid phase faecal odourants to evaluate membrane technology for wastewater reuse from decentralised sanitation facilities’, *Environmental Science: Water Research & Technology*, 5, pp. 161-171.
- Nitta, K., Ashida, A., Mitani, K., Ebara, K. and Yamada, A. (1986) ‘Water recycling system using thermopervaporation method’, *15th International Symposium on Space Technology and Science*. Tokyo, Japan, 19-23 May 1986. pp. 1355–1359.
- Ouma, J., Septien, S., Velkushanova, K., Pocock, J. and Buckley, C. (2016) ‘Characterization of ultrafiltration of undiluted and diluted stored urine.’ *Water Sciences Technological*, 74, pp. 2105–2114.
- Polyakov, Y.S. and Zydney, A.L. (2013) ‘Ultrafiltration membrane performance: Effects of pore blockage/constriction’, *Journal of Membrane Science*, 434, pp. 106–120.

- Public Utilities Board (PUB) (2018) *NEWater*. Available at: <https://www.pub.gov.sg/watersupply/fournationaltaps/newater> (Accessed: 21 September 2018).
- Putnam, D.F. (1971) *Composition and concentrative properties of human urine*. Washington, USA. Available at: <https://ntrs.nasa.gov/archive/nasa/casi.ntrs.nasa.gov/19710023044.pdf>. (Accessed: 15 June 2015).
- Pype, M.-L., Lawrence, M.G., Keller, J. and Gernjak, W. (2016) 'Reverse osmosis integrity monitoring in water reuse: The challenge to verify virus removal – A review', *Water Research*, 98 pp. 384–395.
- Rautenbach, R. and Albrecht, R. (1985) 'The separation potential of pervaporation: Part 1. Discussion of transport equations and comparison with reverse osmosis', *Journal of Membrane Science*, 25, pp. 1–23.
- Robinson, R. and Stokes, R. (2002) *Electrolyte solutions*. 2nd edn. Robinson, R. and Stokes, R. (eds.) Mineola, USA: Dover Publications.
- Rose, C., Parker, A., Jefferson, B. and Cartmell, E. (2015) 'The Characterization of Feces and Urine: A Review of the Literature to Inform Advanced Treatment Technology', *Critical Reviews in Environmental Science and Technology*, 45, pp. 1827–1879.
- Santos, A., Ma, W. and Judd, S.J. (2011) 'Membrane bioreactors: Two decades of research and implementation', *Desalination*, 273, pp. 148–154.
- Stade, S., Kallioinen, M., Tuuva, T. and Mänttari, M. (2015) 'Compaction and its effect on retention of ultrafiltration membranes at different temperatures', *Separation and Purification Technology*, 151, pp. 211–217.
- Starkenmann, C. (2017) 'Analysis and Chemistry of Human Odors', in Buettner, A. (ed.) *Springer Handbook of Odor*. Cham, Switzerland: Springer International Publishing, pp. 121–122.

Strobel, M., Corn, S., Lyons, C.S. and Korba, G.A. (1985) 'Surface modification of polypropylene with CF₄, CF₃H, CF₃Cl, and CF₃Br plasmas', *Journal of Polymer Science*, 23, pp. 1125–1135.

Sürmeli, R.Ö., Bayrakdar, A. and Çalli, B. (2018) 'Ammonia recovery from chicken manure digestate using polydimethylsiloxane membrane contactor', *Journal of Cleaner Production*, 191, pp. 99–104.

The Bill & Melinda Gates Foundation (2019) *Reinvent the toilet strategy and overview*. Available at: <https://www.gatesfoundation.org/What-We-Do/Global-Growth-and-Opportunity/Water-Sanitation-and-Hygiene/Reinvent-the-Toilet-Challenge-and-Expo> (Accessed: 15 November 2018).

Tun, L.L., Jeong, D., Jeong, S., Cho, K., Lee, S. and Bae, H. (2016) 'Dewatering of source-separated human urine for nitrogen recovery by membrane distillation', *Journal of Membrane Science*, 512, pp. 13–20.

Udert, K.M., Larsen, T.A., Biebow, M. and Gujer, W. (2003) 'Urea hydrolysis and precipitation dynamics in a urine-collecting system', *Water Research*, 37, pp. 2571–2582.

United Nations (2018) *Sustainable Development Goal 6*. Available at: <https://sustainabledevelopment.un.org/sdg6> (Accessed: 9 October 2018).

United Nations (2017) *World Population Prospects: The 2017 Revision, Key Findings and Advance Tables*. New York, USA. Available at: https://esa.un.org/unpd/wpp/publications/files/wpp2017_keyfindings.pdf. (Accessed: 12 January 2016).

Warsinger, D.M., Chakraborty, S., Tow, E.W., Plumlee, M.H., Bellona, C., Loutatidou, S., Karimi, L., Mikelonis, A.M., Achilli, A., Ghassemi, A., Padhye, L.P., Snyder, S.A., Curcio, S., Vecitis, C.D., Arafat, H.A. and Lienhard, J.H. (2018) 'A review of polymeric membranes and processes for potable water reuse', *Progress in Polymer Science*, 81, pp. 209–237.

Xie, Z., Duong, T., Hoang, M., Nguyen, C. and Bolto, B. (2009) 'Ammonia removal by sweep gas membrane distillation', *Water Research*, 43, pp. 1693–1699.

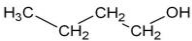
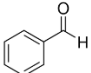
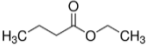
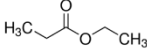
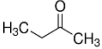
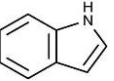
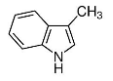
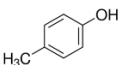
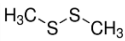
Yao, M., Woo, Y.C., Tijing, L.D., Choi, J.-S. and Shon, H.K. (2018) 'Effects of volatile organic compounds on water recovery from produced water via vacuum membrane distillation', *Desalination*, 440, pp. 146–155.

Zhao, Z.P., Xu, L., Shang, X. and Chen, K. (2013) 'Water regeneration from human urine by vacuum membrane distillation and analysis of membrane fouling characteristics', *Separation and Purification Technology*, 118, 369-376.

Zhou, X., Li, Y., Li, Z., Xi, Y., Nazim Uddin, S.M. and Zhang, Y. (2017) 'Investigation on microbial inactivation and urea decomposition in human urine during thermal storage', *Journal of Water, Sanitation and Hygiene for Development*, 7, pp. 378–386.

4.6 Chapter 4 supplementary information

Table S 4.1 Volatile organic compound chemical parameters

Functional group	Alcohols	Aldehydes	Esters		Ketones	Aromatic heterocycles		Phenol	Sulphur
Compound	1-Butanol	Benzaldehyde	Ethyl butyrate	Ethyl propionate	2-Butanone	Indole	Skatole	<i>p</i> -Cresol	Dimethyl disulfide
Chemical structure									
Molecular weight ^a (g mol ⁻¹)	74.12	106.12	116.16	102.13	72.11	117.15	131.17	108.14	94.19
Acid dissociation constant (pKa)	16.1 ^a	14.9 ^a	-7 ^b	-7 ^b	14.7 ^a	-2.4 ^c	-3.4 ^c	10.26 ^a	NA
Hydrophobicity ^a (logK _{ow} at 20 °C)	0.88	1.48	1.85	1.21	0.29	2.14	2.6	1.94	1.77
Water solubility (g L ⁻¹ at 25 °C)	63.2 ^a	6.95 ^a	2.7 ^b	19.2 ^a	223 ^a	3.56 ^a	0.498 ^a	21.5	3
Henry's volatility constant ^d (mol m ⁻³ Pa ⁻¹ at 25°C)	1.2	0.38	0.029	0.041	8.1	19.1	4.7	10 ^c	0.0065 ^a
Boiling point ^a (°C)	111.7	179	121	99.2	79.59	254	265	201.9	110
Vapour pressure ^a (mm Hg at 25 °C)	7	1.27	14	35.8	90.6	0.0122	0.0055	0.11	28.7
Molar volume ^e (cm ³)	92.1	101.1	131.1	114.6	91.7	101.9	118.1	104.1	89.5
Hansen solubility δ (MPa m ^{-1/2})	23.1	21.5	17.4	17.9	19	22.14	22.1	22.7	20.4
Odour descriptor ^a	Alcohol like	Bitter almond	Pineapple	Fruity, rum	Acetone like	Faecal	Faecal, nauseating	Sweet, tar like	Rotten cabbage

^a Pubchem (2018), ^b YMDB (2018), ^c Gu and Berry (1991), ^d Sander (2015), ^e Hansen (2007). NA, not available.

Table S 4.2 Average volatile organic compound mass balance recoveries from the hydrophilic membrane trials.

VOC	Ultrafiltration		Reverse Osmosis		Pervaporation (Polyvinyl alcohol)	
	Average (%)	±	Average (%)	±	Average (%)	±
2-Butanone	102.88	3.59	110.20	4.96	98.04	4.29
1-Butanol	101.36	5.43	105.62	4.61	102.87	5.54
Ethyl propionate	98.97	3.56	105.06	6.07	98.67	4.99
Dimethyl disulfide	109.58	5.46	110.98	5.65	98.20	13.81
Ethyl butyrate	103.56	3.42	103.95	0.65	102.88	11.02
Benzaldehyde	101.65	4.67	103.23	4.23	98.64	9.53
p-Cresol	99.15	3.82	98.27	10.34	93.12	8.97
Indole	95.70	1.78	92.76	12.30	95.05	7.55
Skatole	96.57	1.38	96.67	12.48	92.80	7.99

± represents the standard deviation of a triplicated experiment.

Table S 4.3 Feed water characterisation for urine and faecally contaminated urine (10:1 urine:faeces) from this study.

Parameter	COD (Urine)	COD (FCU)	TSS (FCU)	TP (Urine)	TP (FCU)	NH ₄ ⁺ -N (Urine)	NH ₄ ⁺ -N (FCU)	C (Urine)	C (FCU)	E-coli (FCU)	Other coliforms (FCU)	Total coliforms (FCU)	pH (Urine)	pH (FCU)
Unit	g L ⁻¹	g L ⁻¹	g L ⁻¹	mg L ⁻¹	mg L ⁻¹	mg L ⁻¹	mg L ⁻¹	mS cm ⁻¹	mS cm ⁻¹	CFU mL ⁻¹	CFU mL ⁻¹	CFU mL ⁻¹	pH	pH
UF (PES)	4.06	14.45	5.79	110.00	145.00	137.00	1238.70	11.65	15.20	4.01 x 10 ⁴	5.92 x 10 ³	4.60 x 10 ⁴	6.45	8.77
	±	±	±	±	±	±	±	±	±	±	±	±	±	±
RO (PA-UREA)	0.34	3.23	0.28	14.00	21.70	12.00	695.00	0.31	1.86	2.11 x 10 ³	2.11 x 10 ³	6.55 x 10 ³	0.49	0.29
	4.01	13.63	6.12	165.00	156.80	195.50	1788.50	10.37	13.80	6.36 x 10 ⁶	ND	6.36 x 10 ⁶	6.94	9.00
PV (PVA)	±	±	±	±	±	±	±	±	±	±	±	±	±	±
	0.16	1.06	2.33	49.50	20.8	30.40	163.90	2.50	2.55	6.93 x 10 ⁶		6.93 x 10 ⁶	0.32	0.30
PV (PDMS)	2.93	15.43	5.44	90.67	237.35	88.67	290.03	5.92	7.77	1.81 x 10 ⁷	2.18 x 10 ⁶	2.01 x 10 ⁷	6.86	9.08
	±	±	±	±	±	±	±	±	±	±	±	±	±	±
MD (PP)	1.82	0.45	0.50	123.40	187	83.76	10.00	3.89	3.41	3.82 x 10 ⁶	2.10 x 10 ⁶	2.1 x 10 ⁶	0.21	0.14
	4.70	19.50	7.15	104.33	380.00	142.67	343.33	10.38	13.52	7.62 x 10 ⁶	2.25 x 10 ⁵	7.84 x 10 ⁶	6.92	7.97
All trials	±	±	±	±	±	±	±	±	±	±	±	±	±	±
	1.81	1.97	1.22	55.30	265.14	25.70	106.93	2.88	6.22	1.22 x 10 ⁷	3.66 x 10 ⁵	1.26 x 10 ⁷	0.73	0.81
All trials	4.54	16.37	5.45	230.00	370.00	149.67	300.00	10.36	12.20	1.51 x 10 ⁷	9.50 x 10 ⁵	1.60 x 10 ⁷	6.72	7.84
	±	±	±	±	±	±	±	±	±	±	±	±	±	±
All trials	1.82	3.89	2.44	154.85	160.93	49.52	100.00	2.91	3.38	9.96 x 10 ⁶	1.48 x 10 ⁶	8.74 x 10 ⁶	0.45	0.47
	4.05	15.36	5.99	140.38	203.39	139.15	998.24	9.54	13.07	7.63 x 10 ⁶	2.63 x 10 ⁶	8.11 x 10 ⁶	6.79	8.64
All trials	±	±	±	±	±	±	±	±	±	±	±	±	±	±
	1.46	2.97	1.49	153.01	142.57	54.54	739.62	3.21	3.81	8.99 x 10 ⁶	6.18 x 10 ⁶	9.43 x 10 ⁶	0.43	0.61

COD (Chemical oxygen demand); TSS (Total suspended solids), TP (Total phosphorus), C (Conductivity), UF (Ultrafiltration); PES (Polyethersulphone) ; RO (Reverse Osmosis); PA-UREA (Polyamide-urea); PV (Pervaporation); PVA (Polyvinyl alcohol); PDMS (Polydimethylsiloxane); MD (Membrane distillation); PP (Polypropylene).

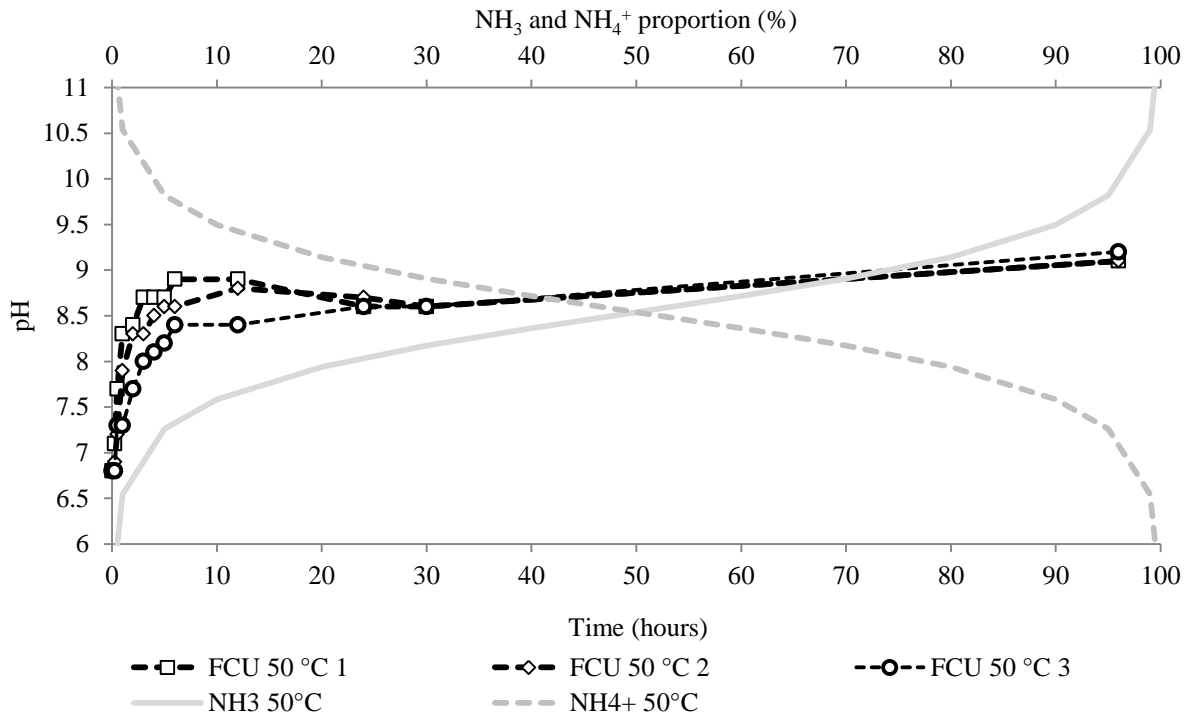


Figure S 4.1 Transition of pH as a function of time for faecally contaminated urine at 50 °C. (FCU 50 °C 1, FCU 50 °C 2 and FCU 50 °C 3). The equilibrium between NH₃ and NH₄⁺ at 50 °C is overlaid.

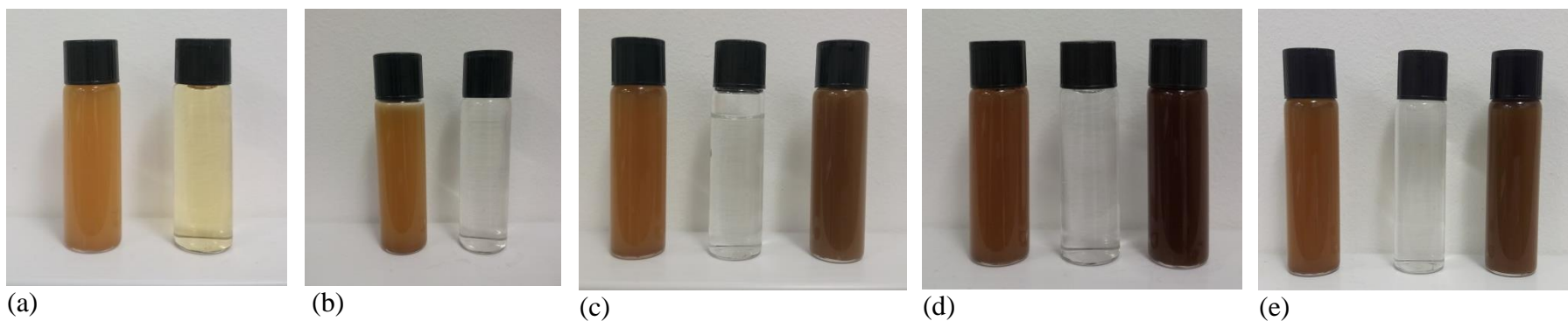


Figure S 4.2 A visual comparison of the treatment of faecally contaminated urine using membrane processes. (a) ultrafiltration feed and permeate (b) reverse osmosis feed and permeate (c) pervaporation (polyvinyl alcohol) feed, permeate and retentate (d) pervaporation (polydimethylsiloxane) feed permeate and retentate (e) membrane distillation feed, permeate and retentate.

References

Gu, J.D. and Berry, D.F. (1991) 'Degradation of substituted indoles by an indole-degrading methanogenic consortium.' *Applied and environmental microbiology*, 57, pp. 2622–2627.

PubChem (2018) *PubChem*. Available at: <https://pubchem.ncbi.nlm.nih.gov/> (Accessed: 10 February 2018).

Sander, R. (2015) 'Compilation of Henry's law constants (version 4.0) for water as solvent', *Atmospheric Chemistry and Physics*, 15, pp. 4399–4981.

YMDB (2018) *Yeast Metabolome database (YMDB)*. Available at: <http://www.ymdb.ca/> (Accessed: 10 February 2018).

**5 HYBRID MEMBRANE DISTILLATION REVERSE
ELECTRODIALYSIS CONFIGURATION FOR ENERGY
RECOVERY AND CONCENTRATE MANAGEMENT
FROM HUMAN URINE IN DECENTRALISED
TREATMENT TECHNOLOGIES**

In preparation for: *Journal of Membrane Science*.

Hybrid membrane distillation reverse electro dialysis configuration for energy recovery and concentrate management from human urine in decentralised treatment technologies

E. Mercer^a, C.J. Davey^a, D. Azzini^b, A.L. Eusebi^b, R. Tierney^a, L. Williams^a, A. Kolios^c, A. Parker^a, S. Tyrrel^a, E. Cartmell^d, M. Pidou^a, E.J. McAdam^{a*}

^aCranfield Water Science Institute, Vincent Building, Cranfield University, Bedfordshire, UK

^bDepartment of Materials, Environmental Sciences and Urban Planning, Università Politecnica delle Marche, Piazza Roma, Ancona, Italy

^cNaval Architecture, Ocean and Marine Engineering, University of Strathclyde, Glasgow, UK

^dScottish Water, Castle House, Carnegie Campus, Dunfermline, UK

*Corresponding author e-mail: e.mcadam@cranfield.ac.uk

Abstract

Membrane distillation integrated with reverse electro dialysis was investigated as a sustainable non-sewered sanitation solution to provide safe sanitation, clean water and power from urine. Membrane distillation, operated by waste heat, delivers a retentate concentrated in urine salts and clean water output, which provides the necessary salinity gradient for reverse electro dialysis. Reverse electro dialysis allows for simultaneous power production and management of a retentate high in inorganic constituents. Interestingly, the complex matrix of urine salts comprising multivalent ions and organics behaved similarly to a simple sodium chloride matrix in terms of power density, impact of temperature and concentration, as the problematic compounds were confined to the concentrate channel. Urine can therefore be considered as a suitable alternative to conventional salt matrices for reverse electro dialysis. However, where conventional reverse electro dialysis seeks to maximise power density, focus was to maximise energy recovery from the finite volume of urine encountered in household scale sanitation systems. When urine was continuously recycled at a current draw of 2.5 A m^{-2} , an energy recovery of 44 % was achieved, providing the first successful demonstration of energy recovery from urine by reverse electro dialysis. With appropriate scaling and operational optimisation, recovery could be significantly improved.

Keywords: SDG, power, wastewater, salts, sanitation

5.1 Introduction

Sustainable small scale sanitation systems which treat human waste on-site have been recently innovated to address the water sustainable development goals (SDG 6) in low income countries (The Bill & Melinda Gates Foundation, 2019; United Nations, 2018). The separation of urine and faeces enhances waste treatability, consequently lowering energy demand (Kirchmann and Pettersson, 1994; Larsen and Gujer, 1996; Maurer, Pronk and Larsen, 2006). Separation systems are already widely accepted in Europe (Lienert and Larsen, 2010), and many recent decentralised innovations have now implemented a solids/liquid separation step (Mercer et al., 2016; WEDC, 2014). For newly developed on-site sanitation systems to receive certification under ISO 30500, which provides demonstration of product safety and reliability to prospective end-users, the produced water must achieve referenced standards for reuse or discharge (International Organisation for Standardisation, 2018). To realise such high quality product water, novel treatment processes are required. Membrane technology has been investigated as a reliable barrier approach. In particular, membrane distillation (MD) has been reported to demonstrate high separation efficiencies for pathogenic, organic and inorganic constituents in urine using low grade waste heat to provide the required vapour pressure gradient (Kamranvand et al., 2018; Tun et al., 2016; Zhao et al., 2013). Thermally driven membrane separation is preferable to electrically driven processes (e.g. pressure driven membranes) for decentralised solutions in low income countries where electricity supply is unsafe and unreliable (International Energy Agency, 2014), and waste heat is widely available including, for example, domestic activities such as cooking (Abdoulla-Latiwish, Mao and Jaworski, 2017). The development and demonstration of thermal processing technologies for faecal sludge management down to single household scale, also presents a synergistic opportunity in which the combustion of human faeces releases significant heat energy sufficient to provide heat for the processing of the liquid phase by thermally driven membrane processes, since the calorific value is equivalent to that of brown coal (Hanak et al., 2016; Onabanjo et al., 2016).

Membrane distillation produces two outputs: (i) a high quality permeate; and (ii) a concentrated retentate. Whilst the permeate may achieve the goal prescribed for non-sewered sanitation (Kamranvand et al., 2018), the retentate of the urine is rich in salt,

which importantly contains a Gibbs free energy density equivalent to 337 J kg^{-1} based on the ionic concentration of urine (Putnam, 1971). Although process technologies based on heat are favoured to maximise the opportunity to work 'off-grid', some electrical energy is inevitably demanded to assist treatment within decentralised sanitation systems. To realise this chemical potential into electrical energy, a salinity gradient can be fostered between the saline concentrate (retentate) and the membrane distillation permeate through the introduction of reverse electrodialysis (RED). Reverse electrodialysis utilises an alternating series of cation and anion exchange membranes which separate concentrated and dilute solutions to provide a salinity gradient. The selective flow of anions and cations through the respective membranes creates an electrochemical potential across the stack, where at the electrodes, a redox reaction converts the ionic flow to an electric current.

Due to the low concentration of inorganic ions within the permeate ($\sim 0.2 \text{ mS cm}^{-1}$), the selective remixing of ions from the concentrate starting at 20 mS cm^{-1} (urine salt conductivity reported by Putnam, 1971), could also allow for their partial management within the retentate, therefore increasing the concentration factor (or product conversion) that can be achieved with membrane distillation, and resulting in only a small increase in permeate conductivity. The resultant permeate is a safe product that can be reused or discarded, the perceived value being dependent upon water availability, cost and comparable quality.

Reverse electrodialysis has gained considerable interest since the first demonstration by Pattle in 1954, where a gross power density of 0.05 W m^{-2} was reported. Since then, research has been predominantly directed towards sodium chloride based salinity gradients (seawater and concentrated brines) and thermolytic salts, as recently reviewed by Mei and Tang (2018) and Tufa et al. (2018). Research advances in these areas have focused on maximising power density through the optimisation of module design, membrane materials, fouling mitigation and operational conditions (Mei and Tang, 2018; Tufa et al., 2018). As a result, higher power densities of 2.2 W m^{-2} for seawater / river water applications (at ambient temperature) have been realised using modified membranes (Vermaas, Saakes and Nijmeijer, 2011), with theoretical values predicted at 4.2 W m^{-2} (Tedesco et al., 2012), demonstrating the progress and potential of RED with optimisation. In theory, the RED process is transferable to any application

which delivers a salinity gradient. However, few studies have approached RED with unconventional saline / dilute wastewaters, which could provide opportunity for energy recovery and discharge management. Kingsbury et al. (2017) challenged a RED stack with multiple real waters including municipal wastewater effluent, and pickling brine as dilute and concentrate examples. It was concluded that natural organic matter (NOM) within the dilute stream was the main hindrance to power density (up to 43 %), with inorganic solutes or NOM in the concentrate presenting little effect. Luque Di Salvo et al. (2018) also investigated the long term effects of operating a RED stack with fish industry effluent and municipal wastewater effluent to help to contextualise water quality. However, the common theme of RED literature is upscaling from laboratory studies to large scale power generation. This is particularly apparent for previous hybrid RED research, integrating RED with reverse osmosis (Farrell et al., 2017; Kwon et al., 2015), electrodialysis (Wang et al., 2017), solar evaporation (Farrell et al., 2017) and MD (Tufa et al., 2015) to facilitate greater concentration gradients for higher power densities and discharge management. The available urine volume in an ‘off grid’ decentralised sanitation system will be finite, and therefore focus requires redirection from maximising power density to maximising energy recovery from a limited saline source. Advantageously, MD-RED can be downscaled for implementation within an ‘off-grid’ decentralised sanitation system where the scalability of RED stacks has been demonstrated in the literature to vary broadly from feed water flows of 2.34 ton h⁻¹, 250 m² surface area and power production of 95.8 W (Nam et al., 2019) to microfluidic and nano-scale devices (Hwang et al., 2017). Importantly, this small scale synergistic partnership with MD demands low capital costs and has potential as an enabler of dependable local sanitation and high quality water (MD facilitated by waste heat), whilst providing a complimentary stable power output (RED facilitated by MD salinity gradient). Such services and products are economically inaccessible for many in low income countries (International Energy Agency, 2014; United Nations, 2018).

This study aims to evaluate a hybrid MD-RED configuration for small scale decentralised sanitation systems to enable electrical energy recovery in co-operation with safe sanitation when using thermally driven membrane processes. Specific objectives are to: (i) understand the impact of the urine salt matrix on energy recovery through decoupling urine constituents into discrete groups; (ii) establish operational

boundary conditions (feed concentrations, temperature, flowrate) using single-pass feed fluid flow for characterisation of peak power density; (iii) determine energy extraction efficiency and recovery with feed fluid flow in recycle mode by comparing experimentally obtained energy to the theoretical Gibbs free energy in recycle mode; and (iv) demonstrate MD-RED using real urine and MD permeate.

5.2 Materials and Methods

5.2.1 Chemicals and Solutions

All chemicals required for the preparation of synthetic urine and electrode rinse solution were sourced from Fisher Scientific (Loughborough, UK) or Sigma Aldrich (Dorset, UK) as laboratory grade. Deionised water was taken from a PURELAB Elga system (18 Ω M-cm at 25 °C). The composition of the synthetic urine was adapted from analysis by Putnam which detailed several specific groups of constituents: inorganic salts, organic ammonium salts, and organic compounds, providing a total ionic concentration of 248 mEq L⁻¹ (Table 5.1) (Putnam, 1971). The synthetic urine was benchmarked against several fluids of equivalent charge to aid diagnosis of governing separation phenomena, including a sodium chloride (NaCl) control (248 mEq L⁻¹ as NaCl) and an inorganic control comprised of monovalent and divalent salts, representative of those present in human urine (248 mEq L⁻¹). Real human urine was collected by consenting anonymous volunteers through a regime approved by Cranfield University's Research Ethics System (Project ID 2384), and used directly without dilution or pre-treatment. Storage of real urine was at 4 °C and used or discarded within three days of collection.

Table 5.1 Summary of synthetic urine recipe adapted from Putnam (1971)

Urine category	Chemical group	Compound	Typical concentration (mg L ⁻¹)	Molar concentration (Mol L ⁻¹)	Cations	Anions	mEq L ⁻¹
Control	Sodium chloride	Sodium chloride	14497	0.248	Na ⁺	Cl ⁻	248.062
Inorganic salts	Monovalent	Sodium chloride	8001	0.137	Na ⁺	Cl ⁻	136.91
		Potassium chloride	1641	0.022	K ⁺	Cl ⁻	22.012
	Multivalent	Potassium bicarbonate	661	0.0066	K ⁺	HCO ₃ ⁻	6.6
		Potassium sulphate	2632	0.0151	K ⁺	SO ₄ ⁻²	30.2
		Magnesium sulphate	783	0.0065	Mg ²⁺	SO ₄ ⁻²	13.01
Synthetic urine	Inorganic salts	Sodium chloride	9524	0.137	Na ⁺	Cl ⁻	162.98
		Potassium chloride	1951	0.022	K ⁺	Cl ⁻	26.2
		Potassium bicarbonate	790.79	0.0066	K ⁺	HCO ₃ ⁻	7.9
		Potassium sulphate	3133	0.0151	K ⁺	SO ₄ ⁻²	35.95
		Magnesium sulphate	932.83	0.0065	Mg ²⁺	SO ₄ ⁻²	15.5
	Organic ammonium salts	Ammonium hippurate	1250	0.0064	NH ₄ ⁺	C ₆ H ₅ CO.NHCH ₂ CO ₂ ⁻	6.4
		Ammonium formate	88	0.0014	NH ₄ ⁺	HCO ₂ ⁻	1.4
		Ammonium Citrate	756	0.0034	NH ₄ ⁺	HC ₆ H ₅ O ₇ ⁻²	6.8
		Ammonium Lactate	394	0.0037	NH ₄ ⁺	C ₃ H ₅ O ₃ ⁻²	7.4
	Organic compounds	Urea	13400	0.22			
		Creatinine	1504	0.0132			
		Creatine	373	0.0026			
		Glycine	315	0.0042			

5.2.2 Reverse electrodialysis cell

The custom RED stack used throughout this study is illustrated in Figure 5.1. The endplates were fabricated from acrylic (Model Products, Bedford, UK) with stainless steel bolts to secure the stack. The membrane stack consisted of 5 repeating cell units of anion and cation exchange membranes (Neosepta AMX and CMX, Eurodia, France) with an effective area of 100 cm^2 per membrane. These were sealed with silicon gaskets (Silex Silicones, UK) and nylon spacers with an open area of 35 % (Sefar, UK) both 0.3 mm in thickness. The concentrate and diluate were pumped through the stack in a co-current configuration with peristaltic pumps. Titanium mesh plate electrodes coated with a Ru/Ir mixed metal oxide (MMO) (10 cm x 10 cm, Magneto, Netherlands) were fixed within the endplates of the stacks and acted as anode and cathode. An electrode rinse solution of 0.25 M NaCl was continuously circulated within the electrode compartments at a flow rate of 100 mL min^{-1} using a peristaltic pump (Watson Marlow, UK). Galvanostatic measurements were conducted using an Iviumstat.h (Alvatek, UK). Current was applied across the mesh working electrodes and Ag / AgCl reference electrodes (QM711X, ProSense BV) were placed in the anolyte / catholyte to measure electrical potential across the RED stack.

To determine the ability of RED to convert the Gibbs free energy of urine to electrical power and directly compare with previous studies of RED using traditional electrolytic solutions (i.e. sea water / river water), the system was initially tested in a single-pass configuration (typically used to determine maximum power density when the electromotive force is at its greatest). In this arrangement, the solutions passed directly through the stack and the influent concentrations of the diluate and concentrate were therefore constant and the solutions exiting the stack discarded (Figure 5.2). Galvanostatic polarisation measurements were conducted and the current was scanned at a rate of 0.2 mA s^{-1} from 0 to the maximum value, when the voltage of the stack reversed (Zhu, He and Logan, 2015a).

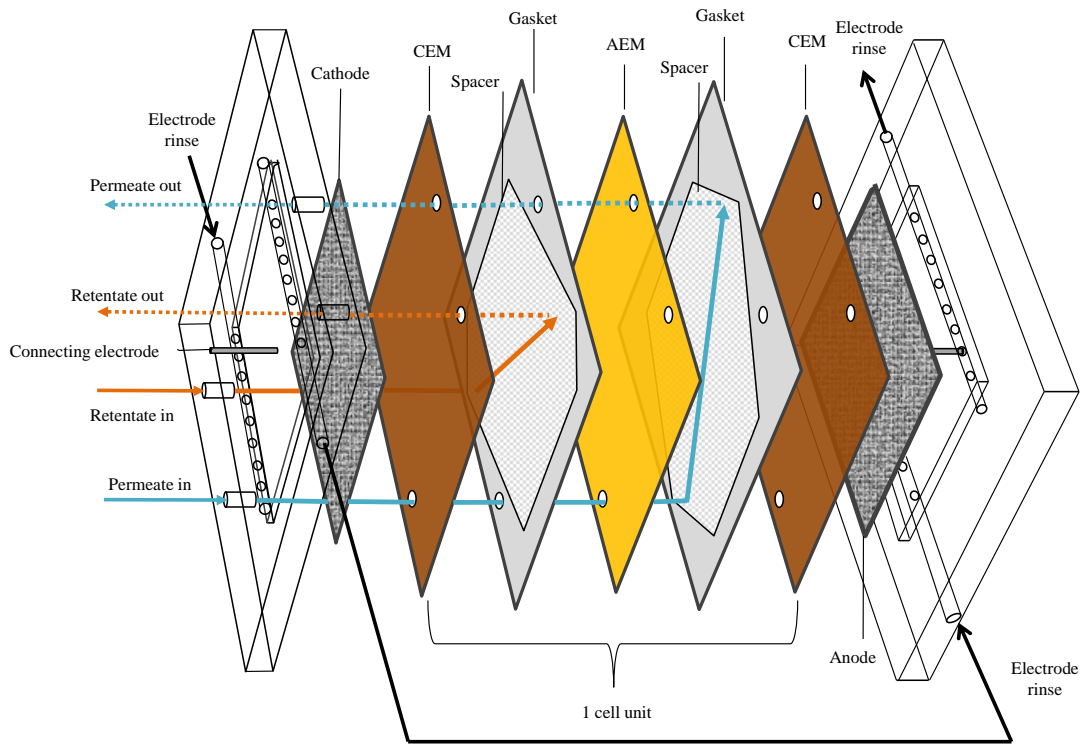


Figure 5.1 Schematic of reverse electro dialysis cell used in this study.

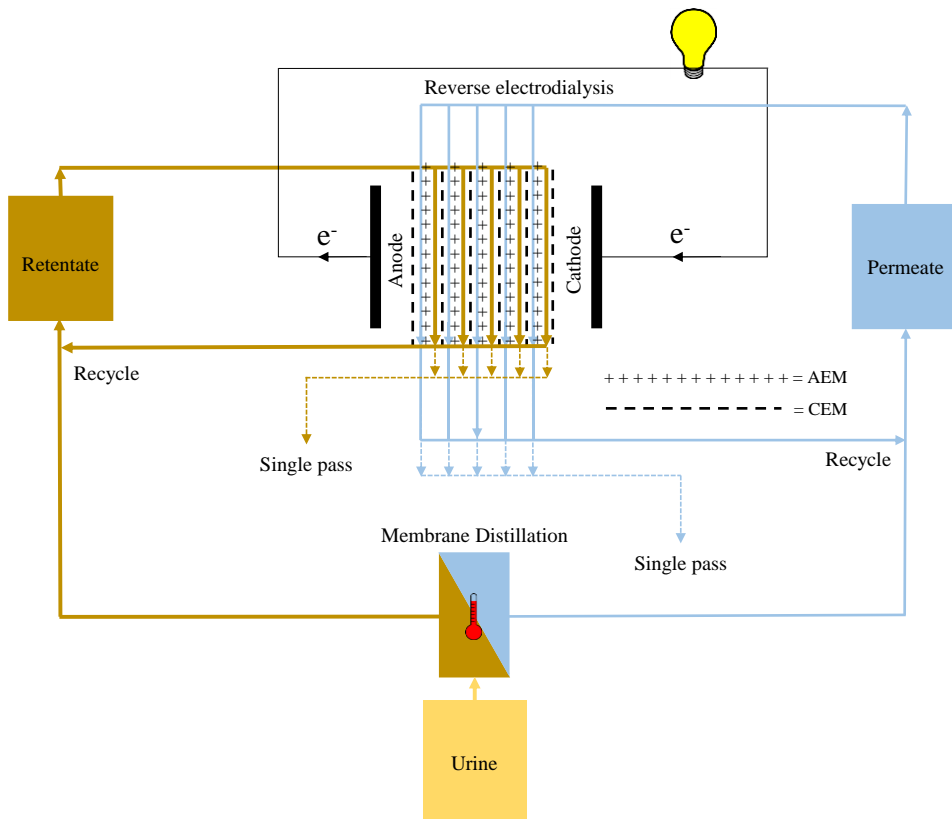


Figure 5.2 Schematic of the operation modes (single pass, recycle) practiced in this study.

The available volume of urine in any system will ultimately be finite. To utilise the full Gibbs free energy stored within the MD retentate, a recycle configuration was utilised to enable the complete mixing of the retentate and permeate within the RED stack (Figure 5.2). Consequently, the system was discharged at a constant current to mimic analogous discharge studies of galvanostatic cycling tests conducted on batteries and concentration gradient flow batteries (van Egmond et al., 2016, 2017; Kingsbury, Chu and Coronell, 2015; Kingsbury and Coronell, 2017). Constant current discharge experiments were conducted where 1 L of concentrate and diluate were recirculated through the stack until the potential across the stack reversed. This allowed for determination of the extractable energy efficiency and energy recovery of the RED stack. If operating RED at higher MD concentration factors, a lower volume of permeate would be required to match the reduced retentate volume, permitting for further high quality water collection. The conductivity of the bulk concentrate and diluate was recorded with conductivity probes (CDH SD1, Omega, UK). To measure water flux through the membranes, the concentrate and diluate were each placed on balances (Symmetry PT-4202E, Cole Parmer, UK) for the duration of the experiment. However, no significant change in mass was observed during the course of the experiments. This is likely due to the small difference in concentration between the diluate and concentrate (~ 0.2 M), low water permeance (~ 0.002 L m⁻² h⁻¹ bar⁻¹) of the ion exchange membranes (Kingsbury et al., 2018) and the relatively short time scales of the experiments.

5.2.3 Membrane Distillation

Vacuum membrane distillation (VMD) was used to recover high quality water from real urine, whilst also producing a urine concentrate, rich in inorganic salts, as the retentate (Figure S5.1). The feed was heated in a water bath (TC120, Grant, UK) at 40 °C whilst being recirculated through the lumen of the membrane module (G542, MiniModule, Membrana, DE) using a peristaltic pump (520S, Watson Marlow, UK). A vacuum was applied to the shell side of the membrane and the permeate condensed at 2 °C with a glass condenser connected to a heater chiller (GD120, Grant, UK). The concentrated urine feed and permeate were stored at < 5 °C until use. The characteristics of the MD feed, permeate and retentate expressed as chemical oxygen demand (COD), ammoniacal nitrogen (NH₄⁺-N) and conductivity is presented in Table 5.2.

5.3 Theory

5.3.1 Energy Density

The Gibbs free energy of mixing ($\Delta_{mix}G$) is defined as the potential energy that is released after the spontaneous mixing of two solutions of salt with differing concentrations:

$$\Delta_{mix}G \equiv \Delta G_B - (\Delta G_C + \Delta G_D) \quad \text{Eq. 5.1}$$

where the subscripts C and D relate to the concentrate and diluate and B refers to the final mixed solution. If the solutions are considered to be ideal there is no enthalpy of mixing ($\Delta H = 0$) and the Gibbs free energy of mixing can therefore be calculated from the molar entropy of each solution as (Post, Hamelers and Buisman, 2008):

$$\Delta_{mix}G = -(n_C + n_D)T\Delta S_B - (-n_C T\Delta S_C - n_D T\Delta S_D) \quad \text{Eq. 5.2}$$

where n_C and n_D are the total moles in the concentrate and diluate respectively (mol), T the temperature (K) and ΔS the molar entropy of each solution ($\text{J K}^{-1} \text{mol}^{-1}$). The molar entropy is calculated as (2008):

$$\Delta S = -R \sum_i x_i \ln x_i \quad \text{Eq. 5.3}$$

where R is the universal gas constant ($8.314 \text{ J K}^{-1} \text{mol}^{-1}$) and x_i the mole fraction of each component within the solution (e.g. H_2O , Na^+ , Cl^-). Due to the very large number of ions and non-charged solutes within urine, and the infinitely variable concentration of these within real samples the calculation of molar entropy was simplified. The conductivity of solutions of synthetic or real urine were taken and a relative concentration of NaCl determined from a calibration curve. The entropy term was then calculated from this equivalent concentration of NaCl.

For the experiments conducted at a constant current in a recycle configuration, the obtained experimental energy density (J kg^{-1}) of the system can be determined from (Kingsbury, Chu and Coronell, 2015):

$$ED = \frac{\int_0^t E I dt}{(m_C + m_D)} \quad \text{Eq. 5.4}$$

where E is the potential (V), I the current (A), t the time (s) and m the starting mass of either the concentrate or diluate (kg). From this and the Gibbs free energy of mixing

calculated using Eq. 5.1, energy recovery can be calculated (Kingsbury, Chu and Coronell, 2015):

$$\text{Energy recovery (\%)} = \left(\frac{ED}{\Delta_{mix}G} \right) \times 100 \% \quad \text{Eq. 5.5}$$

5.3.2 Power Density

For RED conducted in a single-pass configuration where the influent concentrations to the stack are continuous and therefore the available power output constant, the power density of the membrane stack (PD_{Stack} , $W m^{-2}$) has been calculated as (Zhu, He and Logan, 2015b, 2015a):

$$PD_{Stack} = \frac{U_{Stack}I_{Stack}}{2NA} = \frac{U_{stack}I_d}{2N} \quad \text{Eq. 5.6}$$

where U_{Stack} is the voltage (V) over the membrane stack, I_{Stack} is the current (A) scanned, A is the cross sectional area of one membrane (m^2), N is the number of cell pairs in the stack and I_d the current density representing the current normalised to membrane area ($A m^{-2}$).

For a system where the influent concentrations will be continuously changing such as the experiments conducted in a recycle configuration with feedwaters recirculating through the RED stack, the voltage will be constantly changing due to a continuous change in solution ionic concentration, as such there will be a continual change in power. Therefore, the average power density can be used over the discharge of the salinity gradient of the finite volumes of solution (Kingsbury, Chu and Coronell, 2015). The average power density (PD_{avg} , $W m^{-2}$) has been calculated as (Kingsbury, Chu and Coronell, 2015):

$$PD_{avg} = \frac{1}{t} \int_0^t \frac{U_{Stack}I_{Stack}}{2NA} dt \quad \text{Eq. 5.7}$$

where t is the time taken for the discharge. The energy extraction efficiency (η) is determined by the ratio of the electric power harvested by the RED stack over the potential Gibbs power (P_G) released (van Egmond et al., 2017):

$$\eta = \frac{P_{Stack}}{P_G} \quad \text{Eq. 5.8}$$

The theoretical Gibbs free energy that is released per second within the RED cell from the solutions can be calculated by (van Egmond et al., 2016, 2017):

$$P_G = J_w(-\Delta\mu_w) + J_s(-\Delta\mu_s) \quad \text{Eq. 5.9}$$

where J_w is the total water flux ($\text{mol m}^{-2} \text{s}^{-1}$), $\Delta\mu_w$ difference in chemical potential of water, J_s is the total salt flux ($\text{mol m}^{-2} \text{s}^{-1}$) and $\Delta\mu_s$ the difference in chemical potential of the salt. The total water flux can be calculated from the following (van Egmond et al., 2016; Tedesco et al., 2015b):

$$J_w = 2L_p(-\Delta\mu_w) + J_s t_w M \quad \text{Eq. 5.10}$$

where L_p is the average water permeability coefficient of both the anion and cation exchange membranes ($\text{kg m}^{-2} \text{s}^{-1} \text{kg}^{-1}$), t_w is the number of water molecules transported with salt ions across the membrane ($\text{mol}_{\text{water}} \text{mol}_{\text{salt}}^{-1}$) and M is the molar mass of water (kg mol^{-1}). The difference in chemical potential of water of the two solutions is calculated with (van Egmond et al., 2016; Tedesco et al., 2015b):

$$\Delta\mu_w = -vRT(\phi_C C_C - \phi_D C_D) \quad \text{Eq. 5.11}$$

where ϕ is an osmotic coefficient. The total salt flux can be calculated using (van Egmond et al., 2016; Tedesco et al., 2015b).

$$J_s = \frac{I_d}{F} + 2 \frac{P_s}{\delta_m} (C_C - C_D) \quad \text{Eq. 5.12}$$

where I_d is the current density (A m^{-2}), F is the Faraday constant ($96485.33 \text{ C mol}^{-1}$), P_s is the average salt permeability coefficient for the anion and cation exchange membranes ($\text{m}^2 \text{s}^{-1}$), δ_m is the average membrane thickness of the anion and cation exchange membranes (m). The chemical potential difference of salt in two solutions that are separated by a membrane has been calculated using (van Egmond et al., 2016; Tedesco et al., 2015b):

$$\Delta\mu_s = vRT \ln\left(\frac{\gamma_C C_C}{\gamma_D C_D}\right) \quad \text{Eq. 5.13}$$

where v is the number of moles of ions in 1 mole of salt, R is the ideal gas constant ($8.314 \text{ J K}^{-1} \text{ mol}^{-1}$), T is the temperature (K), C is the concentration of the concentrate and diluate denoted C and D respectively (mol L^{-1}) and γ an activity coefficient to account for the non-ideal behaviour of the solutions. Activity coefficients have been estimated for NaCl solutions using the Pitzer model (Section S5.5) (van Egmond et al., 2016, 2017; Kingsbury, Chu and Coronell, 2015; Pitzer and Mayorga, 1973; Thurmond and Brass, 1988).

5.3.3 Open Circuit Voltage

For RED the open circuit voltage (OCV , V) is the electrochemical potential difference across the stack. Assuming ideal solutions of differing concentrations of a single salt either side of a perfectly selective membrane the OCV_i across that membrane can be calculated from the Nernst equation (Kingsbury et al., 2017):

$$OCV_i = \frac{RT}{zF} \ln \frac{\gamma_C C_C}{\gamma_D C_D} \quad \text{Eq. 5.14}$$

where z is the valency of the ion (e.g. $\text{Na}^+ = +1$), F is the Faraday constant (96485 C mol^{-1}), γ is the mean ionic activity coefficient of the counter-ion (the ion with opposite charge to the membrane, dimensionless) and C the concentration of the counter-ion in either the concentrate or diluate (mol L^{-1}). To calculate the potential across a RED stack this calculated OCV_i can be multiplied by the number of membranes in the stack, therefore (Kingsbury et al., 2017):

$$OCV_{ideal} = 2N \cdot OCV_i \quad \text{Eq. 5.15}$$

Calculation of OCV_i ; however, becomes increasingly onerous when considering complex waters consisting of many ions as each counter-ion has a unique concentration gradient across the membrane. Multivalent ions have been shown to decrease the stack voltage and therefore power density (Hong et al., 2013; Post, Hamelers and Buisman, 2009; Vermaas et al., 2014). Counter-ions are exchanged across the membrane until an equilibrium in chemical potential is achieved where each ionic species has an equal OCV and therefore the uphill transport of divalent ions exchanging for a number of monovalent ions can occur (Higa, Tanioka and Miyasaka, 1988; Moreno et al., 2018a; Vermaas et al., 2014). Vermaas et al. (2014) reported how to calculate the OCV_i when two counter-ions are present in solution as did Hong et al. (2013). Furthering this, Kingsbury et al. (2017) have reported the calculation of OCV_i when a greater number of counter-ions are present. To be able to use these calculations the exact ionic composition of the concentrate and diluate must be known. Although determination of ionic composition is possible through modern ion chromatography techniques, the use of this and subsequent calculation of OCV_i is not a trivial task especially when implemented to waters with infinitely variable constituent concentrations such as human urine. Kingsbury et al. (2017) have therefore shown that for complex waters with a large

number of electrolytes, the OCV_{ideal} can be estimated from the conductivity (κ) of the concentrate and diluate. This approach has been utilised within this study and the OCV_{cond} calculated as:

$$OCV_{cond} = 2N \frac{RT}{zF} \ln \frac{\kappa_C}{\kappa_D} \quad \text{Eq. 5.16}$$

The permselectivity (α , %) of the stack, defined as the ratio between the measured and calculated ideal OCV has therefore been calculated using (Kingsbury et al., 2017):

$$\alpha = \left(\frac{OCV_{exp}}{OCV_{cond}} \right) \times 100 \% \quad \text{Eq. 5.17}$$

where OCV_{exp} is the experimentally determined open circuit voltage (V), OCV_{cond} the open circuit voltage calculated from the conductivity of the concentrate and diluate, and the permselectivity (α , %) characterises the average over all the cation and anion exchange membranes within the stack.

5.4 Results and discussion

5.4.1 Power density from urine is analogous to pure sodium chloride

An initial benchmarking experiment using sea water / river water was carried out, achieving a power density of 0.57 W m^{-2} , which is comparable to the literature using the same membranes (Table S5.2). The urine control, which was characterised by a conductivity equivalent to that of urine and comprising only NaCl, achieved a power density of 0.32 W m^{-2} , which can be expected since the conductivity is less than half of that of sea water. The inclusion of multivalent ions had a small immediate detrimental effect on the OCV, permselectivity and power density (Figure 5.3). Multivalent ions have been shown to decrease the stack voltage and therefore power density, when transported from the diluate to the concentrate due to uphill transport (Hong et al., 2013; Post, Hamelers and Buisman, 2009; Vermaas et al., 2014). In contrast, synthetic urine presented little to no decline on the OCV, permselectivity and power density of the membrane stack, despite comprising a considerable organic concentration which has been associated with fouling (Kingsbury et al., 2017; Vermaas et al., 2013a). Electrodialysis studies have shown that organic fouling behaviour is determined by specific properties of organic matter as opposed to concentration (Kim, Moon and Cho, 2003; Lee et al., 2002, 2003). Kingsbury et. al. (2017) suggested there is a negative linear relationship between permselectivity and UV_{254} absorbance within the diluate but

little relationship between the concentration in the concentrate and permselectivity. This accords with the MD permeate produced in this study (Table 5.2), where organics (expressed as COD) and conductivity were 253 mg L^{-1} and 0.2 mS cm^{-1} respectively, which proved insufficient to diminish RED power density in single pass mode. When comparing synthetic urine to real urine using the same diluate solution comprising 0.25 g L^{-1} NaCl (0.5 mS cm^{-1}), the power density was 20 % greater, due to a higher conductivity (21 mS cm^{-1} compared to 12 mS cm^{-1}). However, the conductivity was 40 % higher, which should have resulted in a comparable power density and this disproportionality is reflected by a decline in permselectivity. A further comparison using MD permeate as the diluate (0.2 mS cm^{-1}) with the same real urine sample demonstrated a 13 % decline in power density (Figure S5.3), which is unexpected as the theoretical OCV is greater (lower diluate conductivity). Furthermore, real urine concentrated by a factor of two (24 mS cm^{-1}), coupled with MD permeate as the diluate (0.2 mS cm^{-1}), presented an equivalent power density to the non-concentrated real urine trial using a 0.25 g L^{-1} diluate solution and reduced permselectivity ($\alpha = 70$). Therefore, power density has proven to be governed by feed concentration, rather than the constituents of the urine matrix and therefore is comparable to a simple sodium chloride matrix.

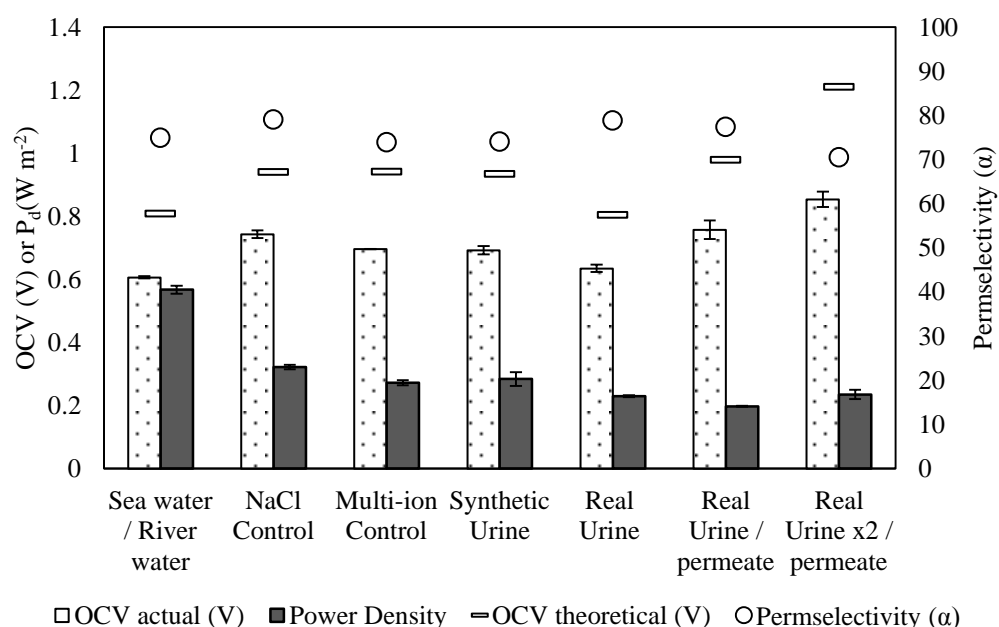


Figure 5.3 Influence of urine multivalent ions and organics (Table 5.2) on open current voltage (OCV), permselectivity and power density (P_d). Conductivities (mS cm^{-1}) were 45.8 (sea water)/1.9 (river water),

21.2 (NaCl control)/0.5 (diluate), 21.3 (Multi-ion control)/0.5 (diluate), 20.7 (synthetic urine)/0.5 (diluate), 12.4 (real urine)/0.5 (diluate), 12.4 (real urine)/0.2 (membrane distillation permeate), 24.1 (real urine 2x concentrate)/ 0.2 (membrane distillation permeate). Single pass mode.

Table 5.2 Real urine characteristics and membrane distillation permeate trialled in this study.

	Conductivity (mS cm ⁻¹)	pH	NH ₄ ⁺ -N (mg L ⁻¹)	COD (mg L ⁻¹)
Urine 1 x Concentrated	12.65	6.585	207	6330
Urine 2 x Concentrated	24.8	6.92	548	9630
Permeate	0.207	8.5	38.9	253

The impact of feed concentration was further investigated in order to understand the dynamic conditions within MD-RED: (i) associated with gradual ion transfer into the permeate in recycle mode (Figure 5.4a) and (ii) MD retentate concentration factors (Figure 5.4b). Although comprising the greatest concentration gradient and therefore Nernst potential, initial conductivity (0.026 mS cm⁻¹) demonstrated a detrimental effect on power density (0.025 W m⁻²) and internal resistance (75 Ω). Internal resistance rapidly declined to 1.5 Ω at 3.8 mS cm⁻¹ attributed to spacer, boundary layer and ohmic resistances (Daniilidis et al., 2014). Power density peaked at 0.3 mS cm⁻¹ and slightly declined to 0.165 W m⁻² when approaching 4 mS cm⁻¹ (almost equilibrium) demonstrating the power density trade-off between resistance and potential difference. Weiner et al. (2015) reported an optimal diluate concentration of 0.01 M NaCl, whilst Veerman et al. (2011) considered 0.005 M NaCl to be optimum, both studies using 0.5 M NaCl (seawater) as the concentrate. The optimum conductivity range for urine is greater than the conductivity of the real MD permeate and can therefore be passively reached as the two solutions reach equilibrium. When increasing the concentrate conductivity by a factor of eight, power density responded linearly by a factor of 3.4, which corresponded with reduced internal resistance (52 %) and OCV increase (38 %) as a result of a higher concentration gradient (Figure 5.4b). The slightly disproportional increase in OCV illustrates reduced membrane permselectivity at higher retentate concentrations, associated with non-ideal salt transport (Tufa et al., 2018). Zhu et al. (2015b) reported that 3.6 M NaCl was the upper concentrate boundary condition for RED stack power production, theoretically allowing for the urine to be concentrated by a factor of 18 (~0.2 M starting concentration) using MD before dramatically affecting power density, demonstrating RED's potential for MD retentate management.

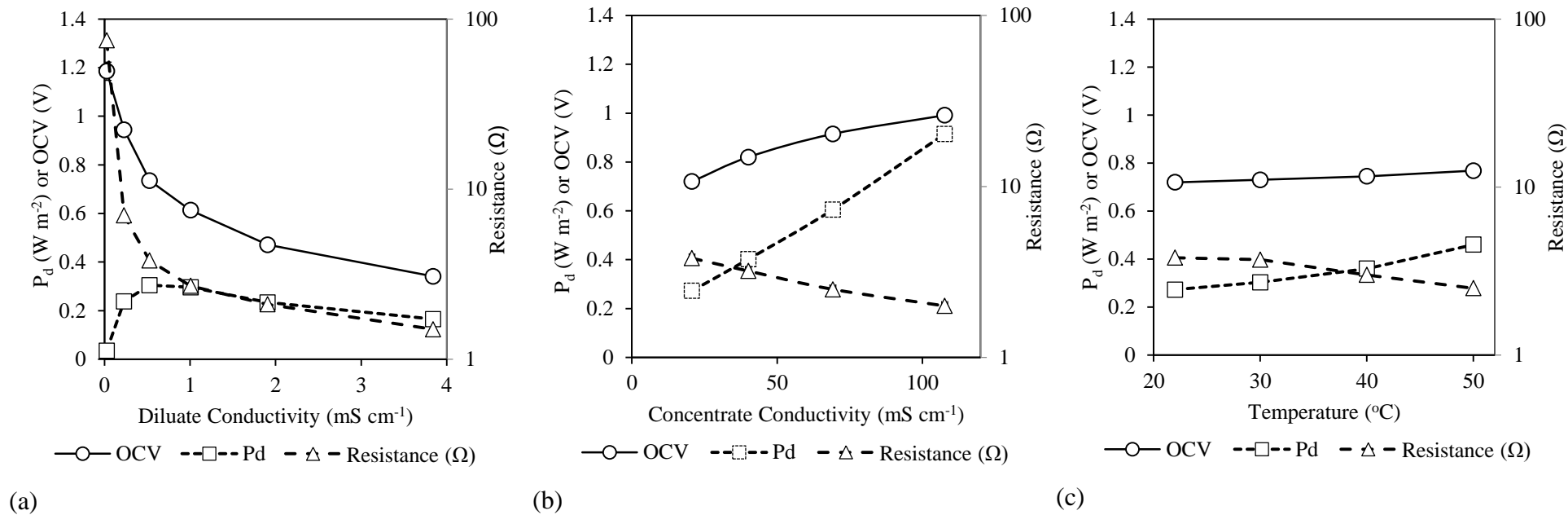


Figure 5.4 Influence of (a) diluate concentration; (b) synthetic urine concentration and (c) temperature on power density (P_d), open current voltage (OCV) and resistance. Single pass mode. Diluate 0.5 mS cm^{-1} , concentrate 21 mS cm^{-1} and temperature $22 \text{ }^{\circ}\text{C}$, unless stated otherwise.

Temperature increased power density and reduced overall cell resistance (Figure 5.4c). Increased temperature facilitates ion mobility which reduces ion transport resistance through the membrane, ohmic resistance and hydrodynamic losses (from reduced viscosity) (Tufa et al., 2015, 2018). From 22 °C to 50 °C, resistance decreased by 66 % which coincided with a power density increase of 70 %. The direct relationship between resistance and power density has also been observed by Tedesco et al. (2015a) reporting an internal resistance decline of 30-50 % with increased power density of 40-50 % from operating from 20 °C to 40 °C, using brackish water and brine. Benneker et al. (2018) demonstrated a 38 % increase in power density from 20 °C to 40 °C (sea water / river water) compared to a 32 % increase from 22 °C to 40 °C in this work, demonstrating reliability to other salt matrices. Open current voltage was minimally affected within this temperature range (22-50 °C) indicating that permselectivity was not compromised. Daniilidis et al. (2014) reported that energy efficiency and permselectivity were severely affected above 50 °C, due to ionic shortcuts and therefore 50 °C is a suitable boundary condition for MD-RED. Such a temperature is accessible by waste heat and provides the opportunity increase power output and accelerate energy recovery.

5.4.2 Hydrodynamic optimisation is critical for energy recovery in recycle mode

Hydrodynamic conditions were trialled in single pass and recycle mode to understand the impact on power density and energy recovery. In single pass mode, power density and OCV increased by 54 % and 18 % respectively from operation between 5 and 200 mL min⁻¹ (Figure 5.5), and plateaued at 50 mL min⁻¹. Increasing solution flowrate improved hydrodynamic mixing, subsequently reducing concentration polarisation and boundary layer thickness, therefore maintaining the maximum concentration gradient (Długolecki et al., 2010b; Tufa et al., 2018). As hydrodynamic and pumping losses occur at higher flowrates, there is a compromise for net power density which takes these factors into account. Therefore, as there was little effect on cell performance with flowrates greater than 50 mL min⁻¹, the cell was subsequently trialled at 50 mL min⁻¹. Zhu et al. (2015a) identified that pumping losses were reduced further by operating the diluate solution at a higher linear velocity than the concentrate solution. Results were comparable to Zhu et al. (2015a) and demonstrated similar linear velocity boundary conditions (represented as the dotted lines on Figure 5.6) at 0.4 cm s⁻¹ LC and

0.015 cm s⁻¹ HC which equates to 10 mL min⁻¹ LC and 2.5 mL min⁻¹ HC according to channel thickness (0.3 mm). Subsequently, the power densities for operating at 10 mL min⁻¹ HC and 2.5 mL min⁻¹ were comparable at 0.23 W m⁻² (Figure S5.4). As the diluate channel is critical for maintaining the concentration gradient and more sensitive to solution and boundary layer resistances compared to the concentrate channel, a higher diluate linear velocity allows for effective resistance management. A flowrate reduction for the concentrate channel can therefore reduce pumping energy. In recycle mode, a contrasting outcome was evidenced between high and low flowrates (Figure 5.7). Due to the evolving concentration gradient and increasing LC ohmic resistance (Zhu, He and Logan, 2015a), low flowrates (2.5 mL min⁻¹ concentrate / 10 mL min⁻¹ diluate) provided an average power density of 0.043 W m⁻² for 0.1 hours, compared to 0.048 W m⁻² for 17 hours (140 mL min⁻¹ both compartments). Therefore, higher flowrates were required to accommodate for the dynamic conditions experienced in recycle mode, particularly the increasing diluate concentration.

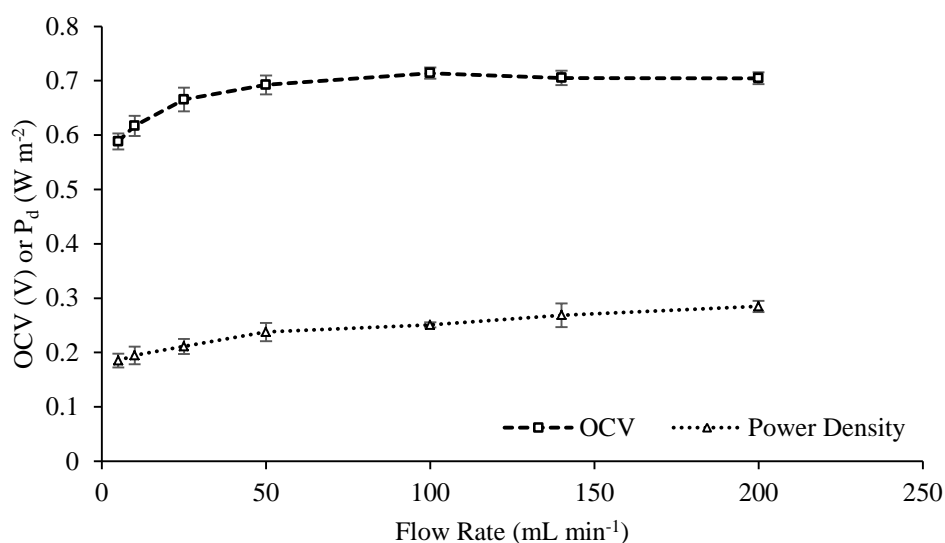


Figure 5.5 Effect of varying feed flowrates on open current voltage (OCV) and power density (P_d). Synthetic urine concentrate, 0.25 g L⁻¹ NaCl diluate, single pass mode.

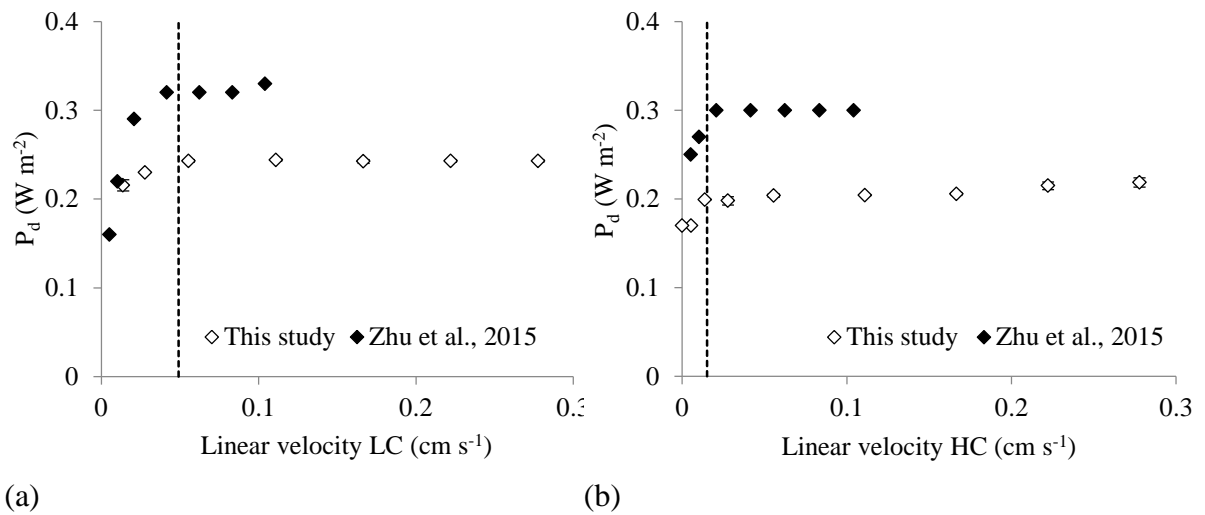


Figure 5.6 Power density as a function of linear velocity when (a) when LC flowrate is variable and HC flowrate is maintained at 50 ml min^{-1} and (b) when HC flowrate is variable and LC flowrate is maintained at 50 ml min^{-1} . Synthetic urine concentrate, 0.25 g L^{-1} NaCl diluate, single pass mode.

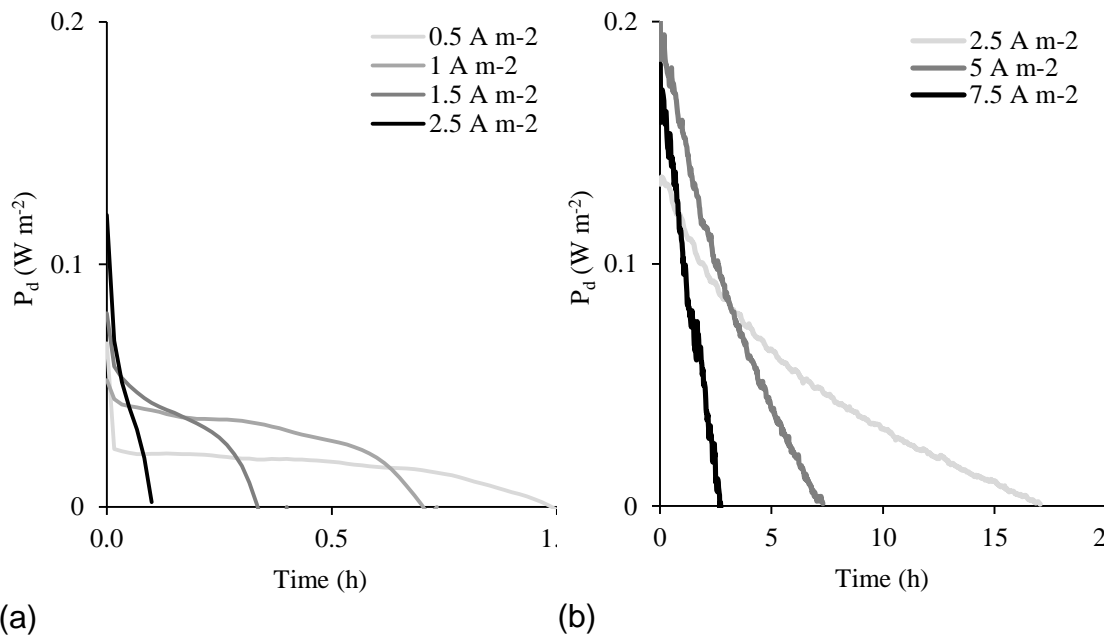
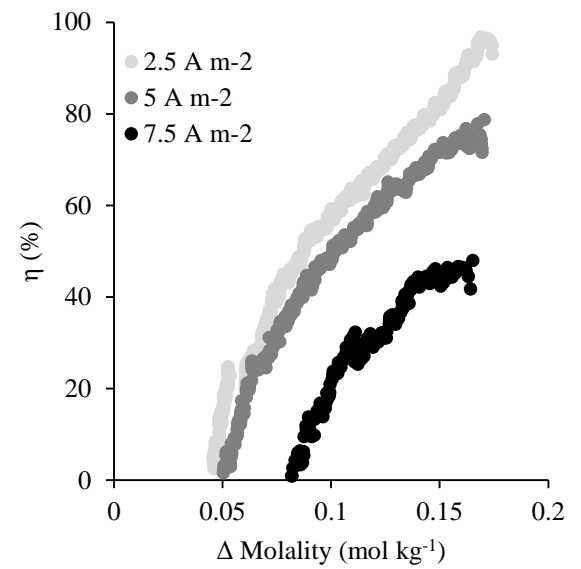
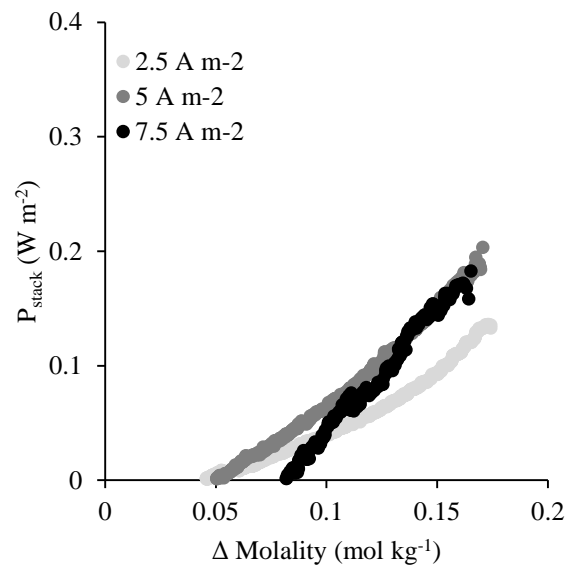
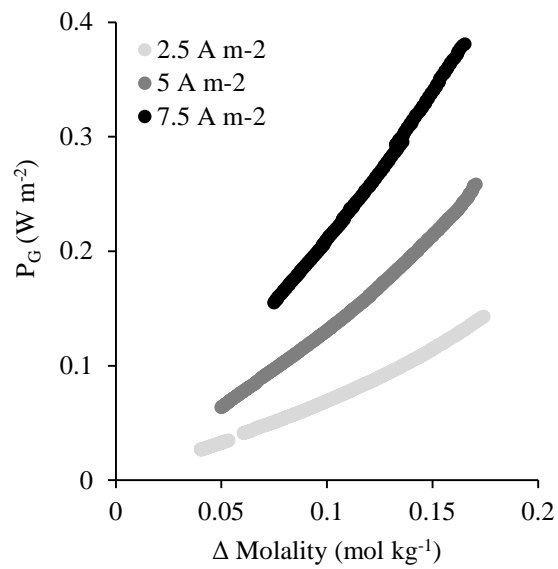


Figure 5.7 Comparison of (a) low and (b) high flowrates in recycle mode until power fully extracted, at varying current draws (A m^{-2}). High flowrates (concentrate and diluate at 140 mL min^{-1}), low flow rates (2.5 mL min^{-1} concentrate / 10 mL min^{-1} diluate). Synthetic urine concentrate, 0.25 g L^{-1} NaCl diluate.

5.4.3 Maximising energy recovery from a finite volume in recycle mode

The median daily production of urine by humans is around $1.4 \text{ L cap}^{-1} \text{ day}^{-1}$, which would suggest that for a ten population equivalent decentralised system (which is the reference scale proposed for decentralised systems under the ‘Reinvent the Toilet Programme’ initiated by the Bill & Melinda Gates Foundation), a total volume of around 15 L d^{-1} is available for energy generation (Rose et al., 2015). This is in contrast to the traditional electrolytic solutions ordinarily associated for energy generation within RED such as sea water and river water as these have effectively infinite available volumes. Due to the limited volume, and to elicit maximum energy recovery from the available MD urine concentrate, a closed loop configuration is proposed (recycle mode). The system can therefore be described similar to a battery with the state of charge (SOC) described as the difference in concentration between the concentrate and diluate. According to the theoretical values calculated from the Gibbs power, higher current densities achieve greater power densities as the concentrate and diluate approach equilibrium (Figure 5.8a). When operating current draws of 7.5 , 5.0 and 2.5 A m^{-2} , initial power densities (at $17.5 \Delta \text{ mol kg}^{-1}$) were 0.38 , 0.26 and 0.14 W m^{-2} respectively. For comparison, respective experimentally obtained power densities were 0.18 , 0.20 and 0.13 W m^{-2} (Figure 5.8b) and reached full extraction at 0.08 , 0.05 and 0.05 mol kg^{-1} (Δ molality). The energy extraction efficiency (η) illustrates how closely experimentally obtained power represents the theoretically available power at varying current draws (Figure 5.8c). In this study, the lowest current density (2.5 A m^{-2}) provided the overall greatest η , particularly until reaching a molality difference of 0.1 mol kg^{-1} where η remained above 60% .



(a)

(b)

(c)

Figure 5.8 (a) Theoretical Gibbs power, (b) experimentally obtained power and (c) energy extraction efficiency (η) as a function of concentrate molarity at varying current densities (2.5 A m^{-2} , 5 A m^{-2} and 7.5 A m^{-2}). Concentrate and diluate flowrate is 140 mL min^{-1} . Synthetic urine concentrate, 0.25 g L^{-1} NaCl diluate, recycle mode.

In recycle mode, total power dissipation is affected by osmotic transport, non-ideal salt transport and internal resistance. Osmotic transport was insignificant, as the maximum concentration demonstrated was 0.2 M, providing an osmotic pressure of ~ 9.9 bar. Previous literature has reported that higher concentrate concentrations facilitate water transport, particularly higher than 1.5 M (urine concentration factor of 7.5; ~ 70 bar osmotic pressure) (van Egmond et al., 2016; Kingsbury, Chu and Coronell, 2015), where non-ideal salt transport and internal resistance provide little contribution. Egmond et al. (2017) demonstrated that increased temperatures also exaggerates the rate of water transport, predominantly at lower current draws which require a greater recycle time to achieve full discharge. Another study by Egmond et al. (2016) identified that non-ideal salt transport energy dissipation is also linked to higher concentration gradients, due to the facilitation of co-ion diffusion. As osmotic transport and non-ideal salt transport did not play a role in the reduction of η in this study, dissipation was primarily caused by internal resistance which was prevalent at higher current draws following Ohm's law. Therefore, when considering operation at higher temperatures or with greater retentate concentration factors required to maximise power output, higher current draws should be trailed, which can increase the rate of electro-osmosis to negate the rate of water transport, whilst identifying a compromise with internal resistance at higher current draws (van Egmond et al., 2016).

Figure 5.9 illustrates the energy recovered (44 %) using the most efficient energy extraction current draw (2.5 A m^{-2}) against the theoretical Gibbs free energy, under the conditions trialled ($\Delta m = 0.175 \text{ mol kg}^{-1}$, $22 \text{ }^\circ\text{C}$), which is consistent with other similar studies obtaining between 45–60 % when equal volumes of concentrate and diluate are utilised (Kingsbury, Chu and Coronell, 2015). Vermaas et al. (2013b) suggest that higher energy recoveries can be obtained when the diluate volume is relatively larger than the concentrate volume if osmotic transport occurs. For urine MD-RED, this can be straightforwardly achieved by greater retentate concentration factors to increase permeate volume.

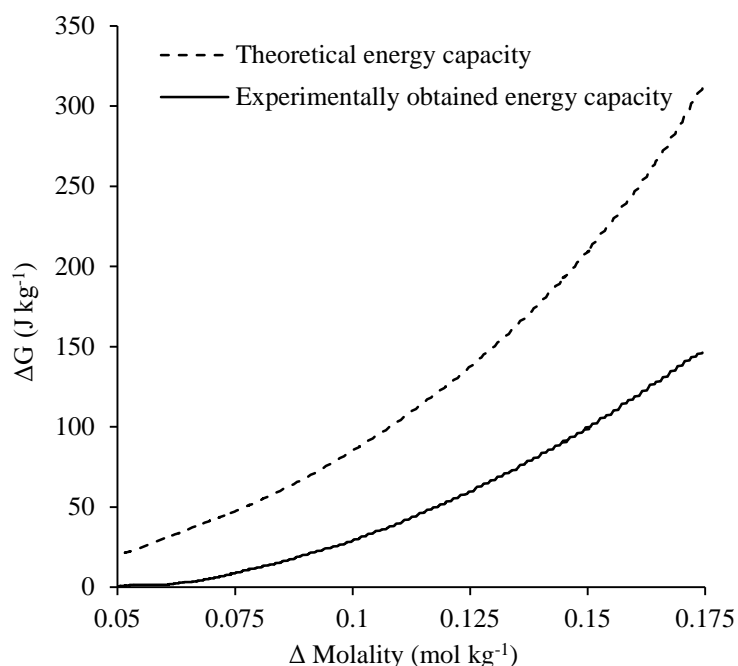


Figure 5.9 Comparison of theoretical and experimentally obtained energy densities at a starting molality difference of $0.175 \text{ mol kg}^{-1}$ and operating 2.5 A m^{-2} current draw. Synthetic urine concentrate, 0.25 g L^{-1} NaCl diluate, recycle mode.

5.5 Conclusions

This study has provided the first successful demonstration of hybrid MD-RED using urine, to create a synergistic relationship in which high quality water can be produced using waste heat, and the subsequent salinity gradient generated in membrane distillation utilised for the production of electrical energy. The urine salt matrix combined with the high quality MD permeate ($\text{COD } 253 \text{ mg L}^{-1}$, conductivity 0.21 mS cm^{-1}) provided comparable power densities to a simple NaCl matrix. An energy recovery of 44 % was achieved which allows for the introduction of low power fluidic devices that can facilitate fluid movement in auxiliary devices. For example, an axial fan which could be applied to provide MD sweep gas requiring 0.25 W , could be powered from mixing 1 L urine with 1 L permeate. Daily, the household system will accept 9330 J (15 L urine and generated permeate, equivalent to 2.59 Wh d^{-1}), demonstrating the potential for further power opportunities. The conventional laboratory setup employed in this study is currently limited by power output for larger scale appliances; therefore appropriate scaling is required to reach necessary output voltages and current densities (Moreno et al., 2018b). Furthermore, concentrating the retentate or increasing temperature can provide the higher power outputs required and

operate in a shorter time scale which consequently minimises parasitic and hydrodynamic losses associated with sustained operation. Although, increasing MD retentate (HC) concentration and temperature is known to reduce energy extraction efficiencies due to the associated non-ideal salt and water transport (van Egmond et al., 2016, 2017; Kingsbury, Chu and Coronell, 2015), the integration of membrane materials which possess characteristics such as high permselectivity, low resistance and low water permeability, alongside ascertaining the optimum current draw, can significantly advance energy recovery. Identifying hydrodynamic conditions which accommodate for the continuously changing solution concentrations in recycle mode, is equally critical to realising maximum energy recovery. In terms of the operation of MD-RED, it is important to consider that 80 % of the available energy within the system is extractable when the concentration difference between the two solutions is halfway towards equilibrium (van Egmond et al., 2017). This implies that the majority of energy could be recovered without having a significant effect on the permeate quality, further reducing operational time and importantly, operational energy. While further optimisation, including technology scale-up and long term field trials are warranted, this technology partnership has the potential to provide low income country households with access to sanitation, clean water and power - the fundamentals of an SDG 6 solution.

5.6 References

- Abdoulla-Latiwish, K.O.A., Mao, X. and Jaworski, A.J. (2017) ‘Thermoacoustic micro-electricity generator for rural dwellings in developing countries driven by waste heat from cooking activities’, *Energy*, 134, pp. 1107–1120.
- Benneker, A.M., Rijnaarts, T., Lammertink, R.G.H. and Wood, J.A. (2018) ‘Effect of temperature gradients in (reverse) electrodialysis in the Ohmic regime’, *Journal of Membrane Science*, 548, pp. 421–428.
- Daniilidis, A., Herber, R. and Vermaas, D.A. (2014) ‘Upscale potential and financial feasibility of a reverse electrodialysis power plant’, *Applied Energy*, 119, pp. 257–265.
- Daniilidis, A., Vermaas, D.A., Herber, R. and Nijmeijer, K. (2014) ‘Experimentally obtainable energy from mixing river water, seawater or brines with reverse electrodialysis’, *Renewable Energy*, 64, pp. 123–131.

Długołęcki, P., Ogonowski, P., Metz, S.J., Saakes, M., Nijmeijer, K. and Wessling, M. (2010) ‘On the resistances of membrane, diffusion boundary layer and double layer in ion exchange membrane transport’, *Journal of Membrane Science*, 349, pp. 369–379.

van Egmond, W.J., Saakes, M., Porada, S., Meuwissen, T., Buisman, C.J.N. and Hamelers, H.V.M. (2016) ‘The concentration gradient flow battery as electricity storage system: Technology potential and energy dissipation’, *Journal of Power Sources*, 325, pp. 129–139.

van Egmond, W.J., Starke, U.K., Saakes, M., Buisman, C.J.N. and Hamelers, H.V.M. (2017) ‘Energy efficiency of a concentration gradient flow battery at elevated temperatures’, *Journal of Power Sources*, 340, pp. 71–79.

Farrell, E., Hassan, M.I., Tufa, R.A., Tuomiranta, A., Avci, A.H., Politano, A., Curcio, E. and Arafat, H.A. (2017) ‘Reverse electrodialysis powered greenhouse concept for water- and energy-self-sufficient agriculture’, *Applied Energy*, 187, pp. 390–409.

Hanak, D.P., Kolios, A.J., Onabanjo, T., Wagland, S.T., Patchigolla, K., Fidalgo, B., Manovic, V., McAdam, E., Parker, A., Williams, L., Tyrrel, S. and Cartmell, E. (2016) ‘Conceptual energy and water recovery system for self-sustained nano membrane toilet’, *Energy Conversion and Management*, 126, pp. 352–361.

Higa, M., Tanioka, A. and Miyasaka, K. (1988) ‘Simulation of the transport of ions against their concentration gradient across charged membranes’, *Journal of Membrane Science*, 37, pp. 251–266.

Hong, J.G., Zhang, W., Luo, J. and Chen, Y. (2013) ‘Modeling of power generation from the mixing of simulated saline and freshwater with a reverse electrodialysis system: The effect of monovalent and multivalent ions’, *Applied Energy*, 110, pp. 244–251.

Hwang, J., Sekimoto, T., Hsu, W.-L., Kataoka, S., Endo, A. and Daiguji, H. (2017) ‘Thermal dependence of nanofluidic energy conversion by reverse electrodialysis’, *Nanoscale*, 9, pp. 12068–12076.

International Energy Agency (2014) *Africa Energy Outlook: A focus on energy prospects in sub-Saharan Africa*. Available at:

https://www.iea.org/publications/freepublications/publication/WEO2014_AfricaEnergyOutlook.pdf. (Accessed: 12 August 2018).

International Organisation for Standardisation (2018) *ISO 30500. Non-sewered sanitation systems -- Prefabricated integrated treatment units - General safety and performance requirements for design and testing (Final Draft)*. Available at: <https://www.iso.org/standard/72523.html>. (Accessed: 15 August 2018).

Kamranvand, F., Davey, C.J., Sakar, H., Autin, O., Mercer, E., Collins, M., Williams, L., Kolios, A., Parker, A., Tyrrel, S., Cartmell, E. and McAdam, E.J. (2018) 'Impact of fouling, cleaning and faecal contamination on the separation of water from urine using thermally driven membrane separation', *Separation Science and Technology*, 53, pp. 1372–1382.

Kim, D.H., Moon, S.-H. and Cho, J. (2003) 'Investigation of the adsorption and transport of natural organic matter (NOM) in ion-exchange membranes', *Desalination*, 151, pp. 11–20.

Kingsbury, R.S., Chu, K. and Coronell, O. (2015) 'Energy storage by reversible electro dialysis: The concentration battery', *Journal of Membrane Science*, 495, pp. 502–516.

Kingsbury, R.S. and Coronell, O. (2017) 'Osmotic Ballasts Enhance Faradaic Efficiency in Closed-Loop, Membrane-Based Energy Systems', *Environmental Science & Technology*, 51, pp. 1910–1917.

Kingsbury, R.S., Liu, F., Zhu, S., Boggs, C., Armstrong, M.D., Call, D.F. and Coronell, O. (2017) 'Impact of natural organic matter and inorganic solutes on energy recovery from five real salinity gradients using reverse electro dialysis', *Journal of Membrane Science*, 541, pp. 621–632.

Kingsbury, R.S., Zhu, S., Flotron, S. and Coronell, O. (2018) 'Microstructure Determines Water and Salt Permeation in Commercial Ion-Exchange Membranes', *ACS Applied Materials & Interfaces*, 10, pp. 39745–39756.

Kirchmann, H. and Pettersson, S. (1994) 'Human urine - Chemical composition and fertilizer use efficiency', *Fertilizer research*, 40, pp. 149–154.

- Kwon, K., Han, J., Park, B.H., Shin, Y. and Kim, D. (2015) 'Brine recovery using reverse electrodialysis in membrane-based desalination processes', *Desalination*, 362, pp. 1–10.
- Larsen, T. and Gujer, W. (1996) 'Separate management of anthropogenic nutrient solutions (human urine)', *Water Science and Technology*, 34, pp. 87–94.
- Lee, H.-J., Choi, J.-H., Cho, J. and Moon, S.-H. (2002) 'Characterization of anion exchange membranes fouled with humate during electrodialysis', *Journal of Membrane Science*, 203, pp. 115–126.
- Lee, H.-J., Kim, D.H., Cho, J. and Moon, S.-H. (2003) 'Characterization of anion exchange membranes with natural organic matter (NOM) during electrodialysis', *Desalination*, 151, pp. 43–52.
- Lienert, J. and Larsen, T. (2010) 'High acceptance of urine source separation in seven European countries: A review', *Environmental Science and Technology*, 44, pp. 556–566.
- Luque Di Salvo, J., Cosenza, A., Tamburini, A., Micale, G. and Cipollina, A. (2018) 'Long-run operation of a reverse electrodialysis system fed with wastewaters', *Journal of Environmental Management*, 217, pp. 871–887.
- Maurer, M., Pronk, W. and Larsen, T.A. (2006) 'Treatment processes for source-separated urine.', *Water research*, 40, pp. 3151–66.
- Mei, Y. and Tang, C.Y. (2018) 'Recent developments and future perspectives of reverse electrodialysis technology: A review', *Desalination*, 425, pp. 156–174.
- Mercer, E., Cruddas, P., Williams, L., Kolios, A., Parker, A., Tyrrel, S., Cartmell, E., Pidou, M. and McAdam, E.J. (2016) 'Selection of screw characteristics and operational boundary conditions to facilitate post-flush urine and faeces separation within single household sanitation systems', *Environmental Science: Water Research & Technology*, 2, pp. 953–964.

Moreno, J., Díez, V., Saakes, M. and Nijmeijer, K. (2018a) ‘Mitigation of the effects of multivalent ion transport in reverse electrodialysis’, *Journal of Membrane Science*, 550, pp. 155–162.

Moreno, J., Grasman, S., van Engelen, R. and Nijmeijer, K. (2018b) ‘Upscaling Reverse Electrodialysis’, *Environmental Science & Technology*, 52, pp. 10856–10863.

Nam, J.-Y., Hwang, K.-S., Kim, H.-C., Jeong, H., Kim, H., Jwa, E., Yang, S., Choi, J., Kim, C.-S., Han, J.-H. and Jeong, N. (2019) ‘Assessing the behavior of the feed-water constituents of a pilot-scale 1000-cell-pair reverse electrodialysis with seawater and municipal wastewater effluent’, *Water Research*, 148, pp. 261–271.

Onabanjo, T., Kolios, A.J., Patchigolla, K., Wagland, S.T., Fidalgo, B., Jurado, N., Hanak, D.P., Manovic, V., Parker, A., McAdam, E., Williams, L., Tyrrel, S. and Cartmell, E. (2016) ‘An experimental investigation of the combustion performance of human faeces’, *Fuel*, 184, pp. 780–791.

Pattle, R.E. (1954) ‘Production of electric power by mixing fresh and salt water in the hydroelectric pile’, *Nature*, 174, p. 660.

Pitzer, K.S. and Mayorga, G. (1973) ‘Thermodynamics of electrolytes. II. Activity and osmotic coefficients for strong electrolytes with one or both ions univalent’, *Journal of Physical Chemistry*, 77, pp. 2300–2308.

Post, J.W., Hamelers, H.V.M. and Buisman, C.J.N. (2008) ‘Energy Recovery from Controlled Mixing Salt and Fresh Water with a Reverse Electrodialysis System’, *Environmental Science & Technology*, 42, pp. 5785–5790.

Post, J.W., Hamelers, H.V.M. and Buisman, C.J.N. (2009) ‘Influence of multivalent ions on power production from mixing salt and fresh water with a reverse electrodialysis system’, *Journal of Membrane Science*, 330, pp. 65–72.

Putnam, D.F. (1971) *Composition and concentrative properties of human urine*.

Washington, USA. Available at:

<https://ntrs.nasa.gov/archive/nasa/casi.ntrs.nasa.gov/19710023044.pdf>. (Accessed: 15 August 2018).

Rose, C., Parker, A., Jefferson, B. and Cartmell, E. (2015) ‘The Characterization of Feces and Urine: A Review of the Literature to Inform Advanced Treatment Technology’, *Critical Reviews in Environmental Science and Technology*, 45, pp. 1827–1879.

Tedesco, M., Brauns, E., Cipollina, A., Micale, G., Modica, P., Russo, G. and Helsen, J. (2015a) ‘Reverse electrodialysis with saline waters and concentrated brines: A laboratory investigation towards technology scale-up’, *Journal of Membrane Science*, 492, pp. 9–20.

Tedesco, M., Cipollina, A., Tamburini, A., van Baak, W. and Micale, G. (2012) ‘Modelling the Reverse ElectroDialysis process with seawater and concentrated brines’, *Desalination and Water Treatment*, 49, pp. 404–424.

Tedesco, M., Cipollina, A., Tamburini, A., Bogle, I.D.L. and Micale, G. (2015b) ‘A simulation tool for analysis and design of reverse electrodialysis using concentrated brines’, *Chemical Engineering Research and Design*, 93, pp. 441–456.

The Bill & Melinda Gates Foundation (2019) *Reinvent the toilet strategy and overview*. Available at: <https://www.gatesfoundation.org/What-We-Do/Global-Growth-and-Opportunity/Water-Sanitation-and-Hygiene/Reinvent-the-Toilet-Challenge-and-Expo> (Accessed: 15 November 2018).

Thurmond, V.L. and Brass, G.W. (1988) ‘Activity and Osmotic Coefficients of NaCl in Concentrated Solutions from 0 to -40 °C’, *Journal of Chemical Engineering Data*, 33, pp. 411–414.

Tufa, R.A., Curcio, E., Brauns, E., van Baak, W., Fontananova, E. and Di Profio, G. (2015) ‘Membrane Distillation and Reverse Electrodialysis for Near-Zero Liquid Discharge and low energy seawater desalination’, *Journal of Membrane Science*, 496, pp. 325–333.

Tufa, R.A., Pawlowski, S., Veerman, J., Bouzek, K., Fontananova, E., di Profio, G., Velizarov, S., Goulão Crespo, J., Nijmeijer, K. and Curcio, E. (2018) ‘Progress and prospects in reverse electrodialysis for salinity gradient energy conversion and storage’, *Applied Energy*, 225, pp. 290–331.

Tun, L.L., Jeong, D., Jeong, S., Cho, K., Lee, S. and Bae, H. (2016) ‘Dewatering of source-separated human urine for nitrogen recovery by membrane distillation’, *Journal of Membrane Science*, 512, pp. 13–20.

United Nations (2018) *Sustainable Development Goal 6*. Available at: <https://sustainabledevelopment.un.org/sdg6> (Accessed: 9 October 2018).

Veerman, J., Saakes, M., Metz, S.J. and Harmsen, G.J. (2011) ‘Reverse electrodialysis: A validated process model for design and optimization’, *Chemical Engineering Journal*, 166, pp. 256–268.

Vermaas, D. a., Kunteng, D., Saakes, M. and Nijmeijer, K. (2013a) ‘Fouling in reverse electrodialysis under natural conditions’, *Water Research*, 47, pp. 1289–1298.

Vermaas, D. a., Veerman, J., Saakes, M. and Nijmeijer, K. (2014) ‘Influence of multivalent ions on renewable energy generation in reverse electrodialysis’, *Energy & Environmental Science*, 7(4), pp. 1434–1445.

Vermaas, D.A., Saakes, M. and Nijmeijer, K. (2011) ‘Doubled Power Density from Salinity Gradients at Reduced Intermembrane Distance’, *Environmental Science & Technology*, 45, pp. 7089–7095.

Vermaas, D.A., Veerman, J., Yip, N.Y., Elimelech, M., Saakes, M. and Nijmeijer, K. (2013b) ‘High Efficiency in Energy Generation from Salinity Gradients with Reverse Electrodialysis’, *ACS Sustainable Chemistry & Engineering*, 1, pp. 1295–1302.

Wang, Q., Gao, X., Zhang, Y., He, Z., Ji, Z., Wang, X. and Gao, C. (2017) ‘Hybrid RED/ED system: Simultaneous osmotic energy recovery and desalination of high-salinity wastewater’, *Desalination*, 405, pp. 59–67.

WEDC (2014) *A Collection of Contemporary Toilet Designs*. Rod, S. (ed.). Loughborough, UK: EOOS and WEDC.

Weiner, A.M., McGovern, R.K. and Lienhard V, J.H. (2015) ‘Increasing the power density and reducing the levelized cost of electricity of a reverse electrodialysis stack through blending’, *Desalination*, 369, pp. 140–148.

Zhao, Z.P., Xu, L., Shang, X. and Chen, K. (2013) 'Water regeneration from human urine by vacuum membrane distillation and analysis of membrane fouling characteristics', *Separation and Purification Technology*, 118, pp. 369-376.

Zhu, X., He, W. and Logan, B.E. (2015a) 'Reducing pumping energy by using different flow rates of high and low concentration solutions in reverse electrodialysis cells', *Journal of Membrane Science*, 486, pp. 215–221.

Zhu, X., He, W. and Logan, B.E. (2015b) 'Influence of solution concentration and salt types on the performance of reverse electrodialysis cells', *Journal of Membrane Science*, 494, pp. 154–160.

5.7 Chapter 5 supplementary information

Section S1. Membrane distillation

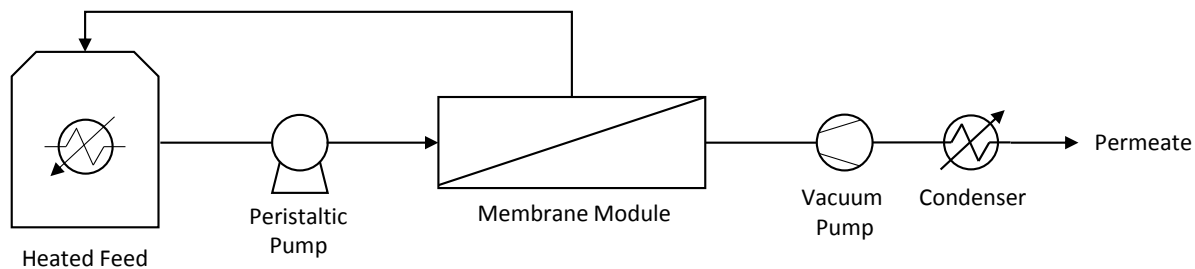


Figure S 5.1 Schematic of the vacuum membrane distillation setup used to concentrate real urine in this study.

Section S2. Polarisation curves representing the influence of different solution chemistries

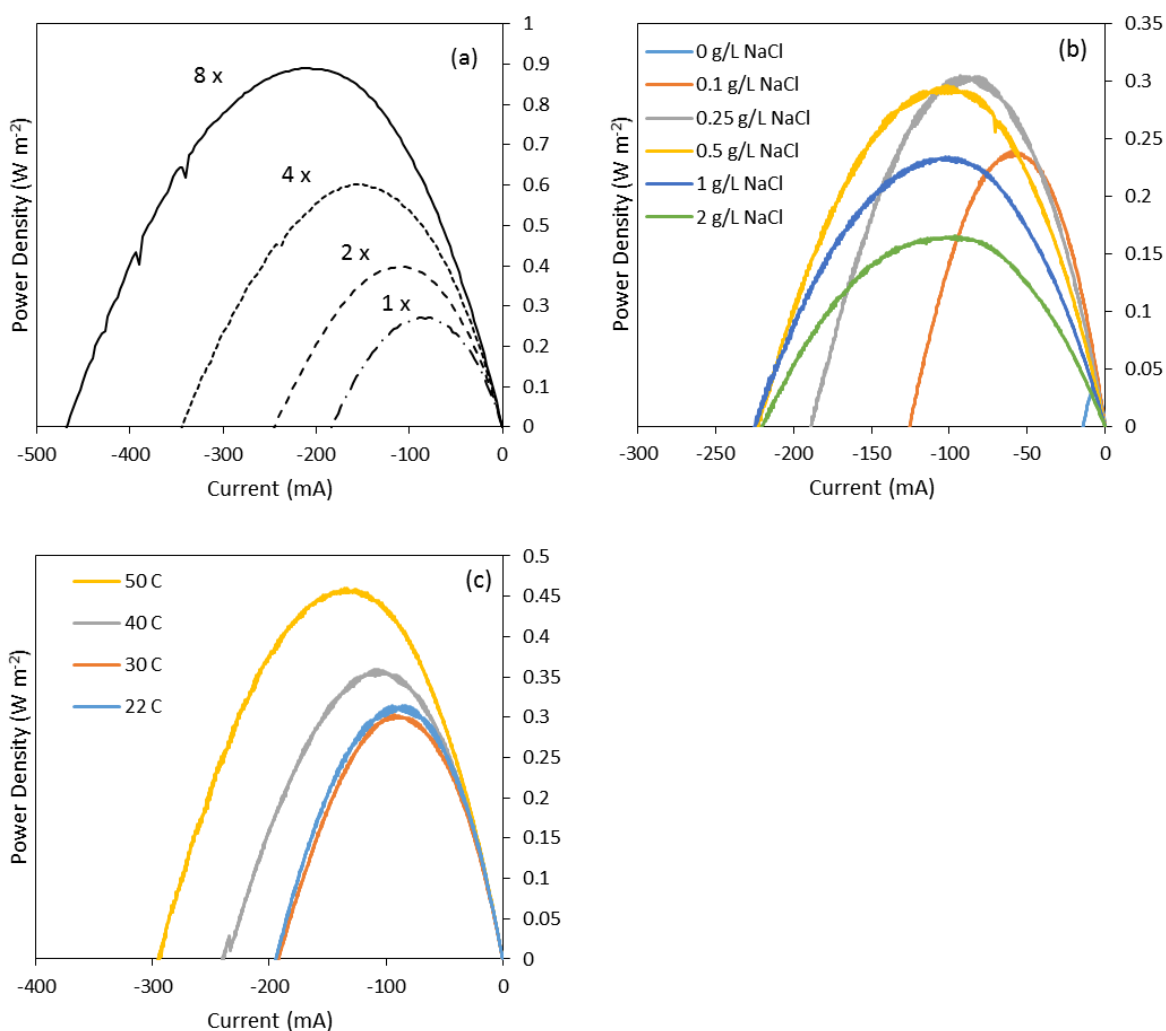
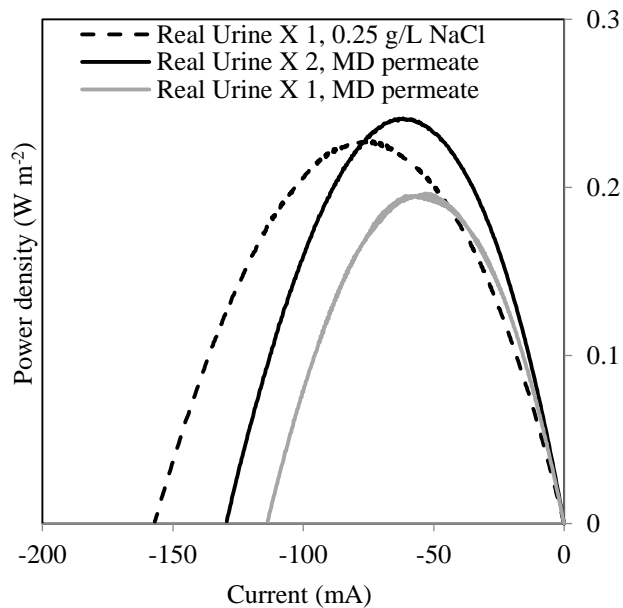


Figure S 5.2 Polarisation curves obtained at (a) varying synthetic urine concentration, (b) varying diluate concentration and (c) varying solution temperature



(a) Figure S 5.3 Real urine (1x and 2x concentrated) and membrane distillation (MD) permeate polarisation curves
 (b) visual comparison of real urine and MD permeate solutions. Real urine concentration was 12.45 mS cm^{-1} , 2x concentrate was 24.1 mS cm^{-1} , and permeate was $\sim 0.2 \text{ mS cm}^{-1}$.

Section S3. Polarisation curves comparing hydrodynamic conditions

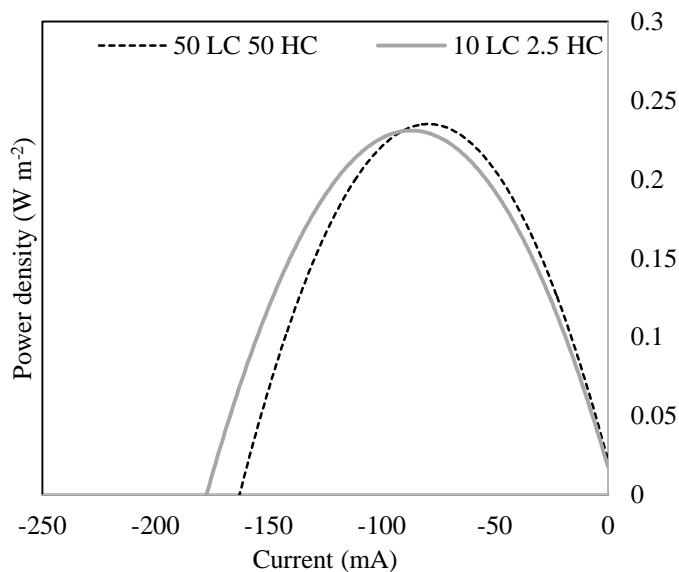


Figure S 5.4 Single pass polarisation curves comparing HC (high concentration) and LC (low concentration) flowrate regimes. HC and LC compartments both at 50 mL min^{-1} and HC at 2.5 mL min^{-1} with LC at 10 mL min^{-1} .

Section S4. Characteristics and reported performance of the commercially available membranes used in this study

Table S 5.1 Properties of the commercial ion exchange membranes used in this study

Membrane Type	Model	Company	Thickness (μm)	Resistance ($\Omega\cdot\text{cm}^2$)	Permselectivity (%)
Anionic	AMX	Neosepta	114 ^a	2.4 ^a	95 ^b
Cationic	CMX	Neosepta	117 ^a	3 ^a	97 ^b

0.5 M NaCl at 25 °C ^aAstom corporation (Astom Corporation, 2013); 0.1 / 0.01 M NaCl at 25 °C ^bNagarale et al. (2006)

Table S 5.2 Reported power densities for Neosepta AMX/CMX ion exchange membranes

Effective membrane area (cm^2)	Spacer thickness (μm)	Number of cells	Salt matrix (LC / HC g L ⁻¹ NaCl)	Power density (W m^{-2})	Flow velocities (cm s^{-1})	Reference
100	300	5	1 / 30	0.56	0.7	This study
100	200	5	1 / 30	1.07	0.27–1.7	Guler et al. (2013)
100	320	3	1 / 30	0.8	0.06-0.83	Długołęcki et al.(2010a)
100	320	3	1 / 30	0.27	0.06-0.83	Długołęcki et al. (2010a)
100	200	5	1 / 30	0.65	1.17	Veerman et al. (2009)

Section S5. The Pitzer Model

The Pitzer model was utilised for calculating the activity coefficient and osmotic coefficient of electrolyte solutions. For the multicomponent electrolyte solutions of synthetic urine and urine a solution of NaCl in water of equivalent conductivity was assumed. The calculation of activity and osmotic coefficients of multicomponent electrolyte solutions has been described elsewhere but the approach was not adopted for this work. The calculations utilised are outlined below and further details on the Pitzer model can be found in van Egmond et al. (van Egmond et al., 2016) and Pitzer and Mayorga (1973).

$$\phi - 1 = |z_m z_x| f^\phi + m \left(\frac{2v_M v_X}{v} \right) B_{MX}^\phi + m^2 \frac{2(v_M v_X)^{\frac{3}{2}}}{v} C_{MX}^\phi \quad \text{Eq. S 5.1}$$

$$\ln \gamma = |z_m z_x| f^\gamma + m \left(\frac{2v_M v_X}{v} \right) B_{MX}^\gamma + m^2 \frac{2(v_M v_X)^{\frac{3}{2}}}{v} C_{MX}^\gamma \quad \text{Eq. S 5.2}$$

$$v = v_m + v_x \quad \text{Eq. S 5.3}$$

$$f^\gamma = -A^\phi \left[\frac{I^{\frac{1}{2}}}{1 + bI^{\frac{1}{2}}} + \frac{2}{b} \ln(1 + bI^{\frac{1}{2}}) \right] \quad \text{Eq. S 5.4}$$

$$f^\phi = -A^\phi \frac{I^{\frac{1}{2}}}{1 + bI^{\frac{1}{2}}} \quad \text{Eq. S 5.5}$$

$$B_{MX}^Y = 2\beta_{MX}^0 + \frac{2\beta_{MX}^1}{\alpha^2 I} \left[1 - e^{\alpha I^{\frac{1}{2}}} \left(1 + \alpha I^{\frac{1}{2}} - \frac{1}{2} \alpha^2 I \right) \right] \quad \text{Eq. S 5.6}$$

$$B_{MX}^\emptyset = B_{MX}^0 + B_{MX}^1 e^{-\alpha I^{\frac{1}{2}}} \quad \text{Eq. S 5.7}$$

$$C_{MX}^Y = \frac{3}{2} C_{MX}^\emptyset \quad \text{Eq. S 5.8}$$

$$I = \frac{1}{2} \sum m_i z_i^2 \quad \text{Eq. S 5.9}$$

Where:

$A^\emptyset = 0.392$ for water at 25°C

$b = 1.2$

$\alpha = 2$

$B_{MX}^0 = 0.0765$, $B_{MX}^1 = 0.2664$, $C_{MX}^Y = 0.00127$, $m = 6$ are Pitzer parameters for NaCl.

v_M and v_X represent number of ions in the salt formula with respective charges as z_m and z_x .

References

- Astom Corporation (2013) ‘Comparison table for detailed specifications of Cation / Anion Exchange Membranes’. Available at: http://www.astom-corp.jp/en/product/images/astom_hyo.pdf. (Accessed: 7 July 2016).
- Długołęcki, P., Dąbrowska, J., Nijmeijer, K. and Wessling, M. (2010) ‘Ion conductive spacers for increased power generation in reverse electro dialysis’, *Journal of Membrane Science*, 347, pp. 101–107.
- van Egmond, W.J., Saakes, M., Porada, S., Meuwissen, T., Buisman, C. and Hamelers, H (2016) ‘The concentration gradient flow battery as electricity storage system: Technology potential and energy dissipation’, *Journal of Power Sources*, 325, pp. 129–139.
- Güler, E., Elizen, R., Vermaas, D.A., Saakes, M. and Nijmeijer, K. (2013) ‘Performance-determining membrane properties in reverse electro dialysis’, *Journal of Membrane Science*, 446, pp. 266–276.
- Nagarale, R.K., Gohil, G.S. and Shahi, V.K. (2006) ‘Recent developments on ion-exchange membranes and electro-membrane processes.’ *Advances in colloid and interface science*, 119, pp. 97–130.
- Pitzer, K.S. and Mayorga, G. (1973) ‘Thermodynamics of electrolytes. II. Activity and osmotic coefficients for strong electrolytes with one or both ions univalent’, *Journal of Physical Chemistry*, 77, pp. 2300–2308.

Veerman, J., de Jong, R.M., Saakes, M., Metz, S.J. and Harmsen, G.J. (2009) 'Reverse electro dialysis: Comparison of six commercial membrane pairs on the thermodynamic efficiency and power density', *Journal of Membrane Science*, 343(1), pp. 7–15.

6 OVERALL DISCUSSION

The chapters of this thesis represent the development of a series of separation processes which combine with combustion to form an integrated processing system (i.e. the Nano Membrane Toilet, NMT) to deliver an enhanced treatment sanitation service at a single household scale. Importantly, the combined solution could provide a competitive alternative to current sanitation avenues in terms of cost, reliability, desirability, sustainability and energy neutrality, the feasibility for which will be critically addressed through the following questions:

6.1 How would we realise a household scale integrated separation system?

The NMT will accept a daily loading of 15 L urine and 2.5 kg faeces representing ten people (Rose et al., 2015). The proposed integrated system based on the findings within this thesis, is portrayed in Figure 6.1. Initial solid/liquid separation can be facilitated by gravity sedimentation, allowing passive separation of a large fraction of the liquid and concentration of the faecal sludge fraction before screw separation (Cruddas et al., 2015). The screw's role is to enable solids recovery for the combustor. Full faecal solids recovery can be achieved within 1000 revolutions, when mixing faeces with an equal mass of urine, and operation at 400 rpm, however with an output of 15 wt.% solids (Chapter 2). Mixing is initiated by screw contact and therefore choke length is an important consideration. In order to reach autothermal combustion conditions, 70 wt.% solids would need to be reached (Onabanjo et al., 2016). Further increase of the solids concentration can be achieved by reducing the urine ratio and rotational speed below 400 rpm to prevent water uptake (Chapter 2). In addition, identification of an optimum extrusion aperture size which is sufficient to prevent blockages and restrictive to initiate sludge consolidation when combined with a compression style screw should facilitate dewatering to up to 25 wt.% solids. However, the criticality for transport is the sticky phase which is identified between 25-40 wt.% solids for wastewater sludge (Peeters et al., 2010). Heating the screw chamber to induce evaporation or blending a drying agent (toilet paper) could assist in carrying the faecal sludge past the sticky phase where it can be efficiently transported and ignited at 40 wt.% solids (Onabanjo et al., 2016).

Separation can also be enhanced for the liquid fraction. The extent of faecal contamination can be controlled by implementing a bowl size of ≤ 5 L capacity to facilitate immediate liquid dispersion through the weir (also controlling the mixing ratio) and batch mode screw operation will minimise agitation events (Cruddas et al., 2015). However, even at a urine to faeces ratio representing full faecal contamination (10:1), which will be limited in practice, thermally driven membranes evidenced high quality water production within a

single step. In fact, thermally driven processes demonstrated better suitability for water reuse from the concentrated wastewater matrix of faecally contaminated urine (FCU) than conventional pressure driven filtration, concluded by key reuse aspects such as water quality, relative flux and odour management (Chapter 4). Membrane distillation (MD) proved to be the most readily implementable process due to producing the highest quality permeate, high productivity unaffected by faecal contamination and manipulation of odour profiling which can be adopted to change perception (Chapter 4). In order to process 15 L d^{-1} FCU by MD, a minimum membrane area of 0.2 m^2 is required (Chapter 4). This calculation is based on the flux reported by Kamranvand et al. (2018) using a single fibre at $3.05 \text{ L m}^{-2} \text{ h}^{-1}$, as condensation occurred as a result of over productivity within the tightly packed MD module, resulting in fluxes lower than the reported literature (Kamranvand et al., 2018; Urtiaga et al., 2001).

Daily, 9330 J of salinity gradient energy from urine will enter the NMT (15 L urine and generated permeate, equivalent to 2.59 Wh d^{-1}). A hybrid MD-RED (membrane distillation-reverse electrodialysis) configuration was demonstrated (Chapter 5), where MD provided RED with a urine feed and a high quality permeate characterised by a conductivity and chemical oxygen demand (COD) of 0.2 mS cm^{-1} and 253 mg L^{-1} respectively. When drawing a current of 2.5 A m^{-2} , 47 % of the theoretical energy in urine could be recovered, which translates to the operation of a low power hydraulic devices (0.25 W) for fluid transport for 4.9 hours. However, the cell design was based on conventional lab scale designs in literature (Tufa et al., 2018) and therefore appropriate scaling for the NMT is required to maximise energy recovery or peak power outputs, where a trade-off exists. In order to maximise energy utilisation, an option is to reverse engineer the system for low voltage devices, to minimise peak power demand and practice system scheduling. If moving towards maximising power outputs to match unit demand, upscaling through series and parallel configurations can be implemented, which have been reported to increase voltage and current respectively (Moreno et al., 2018b). Furthermore, determining the optimum operating temperature ($\leq 50 \text{ }^\circ\text{C}$), urine concentration factor (≤ 18) and current draw which balances electro and water osmosis can provide peak power to sustain higher power output appliances. Importantly, 80 % of the available system energy is extractable when both solution concentrations are halfway towards reaching equilibrium (van Egmond et al., 2017). Operating the system until the retentate and permeate streams are not fully mixed, provides the most efficient extraction window in terms of the compromise between energy recovered

and operational energy usage, in addition to maintaining low permeate conductivities for reuse opportunities.

Abbreviations
 FCU: Faecally contaminated urine
 RPM: Revolutions per minute
 MD: Membrane distillation
 RED: Reverse electrodialysis

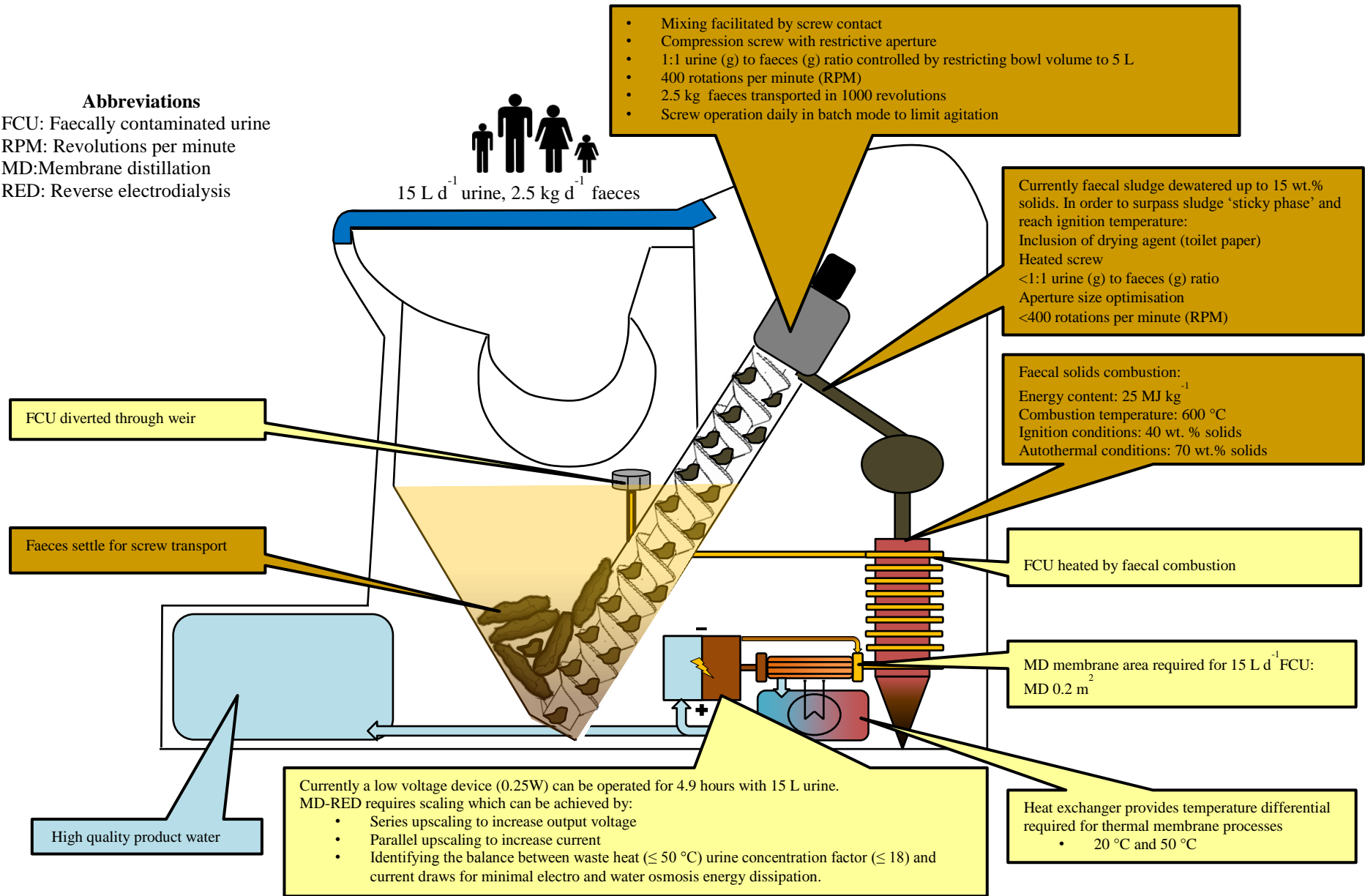


Figure 6.1 Illustrative integration of the separation processes within the Nano Membrane Toilet at household scale.

6.2 How can the NMT process the liquid phase to meet ISO 30500?

For non-sewered sanitation systems to receive ISO 30500 certification, product outputs must demonstrate safety and reliability through referenced standards for reuse or discharge (International Organisation for Standardisation, 2018). Category A advises unrestricted urban use (i.e. landscape irrigation, toilet flushing, handwashing) and Category B suggests surface water discharge or restricted urban use (i.e. where public access is controlled). It was concluded that MD was the most 'implementation ready' thermally driven membrane process for FCU treatment (Chapter 4), as within a single stage, most of the ISO 30500 Category B requirements were met and productivity was not impacted by faecal contamination. However, rigorous testing is required to enable greater profiling and confidence to conform to the standard. The key limiting factor was urea hydrolysis, resulting in increased pH, and subsequent volatile free NH_3 transfer into the permeate, compromising the requirements for total nitrogen (TN) and pH which are 15 mg L^{-1} and 6-9 respectively. Treatment options for TN and pH can be passively integrated into the current system. Urea hydrolysis is facilitated by the enzyme urease, which is produced by microbial activity (*Escherichia coli* and other faecal coliforms) during urine storage (Udert et al., 2003; Zhao et al., 2013; Zhou et al., 2017). Therefore its prevention can be actioned by addressing its microbial source. Zhou et al. (2017) demonstrated microbial inactivation at $70 \text{ }^\circ\text{C}$, which was sufficient to maintain urine below pH 8 and therefore comprise a higher fraction of non-volatile NH_4^+ rather than NH_3 . A feed temperature maintained at $70 \text{ }^\circ\text{C}$ is still achievable from waste heat and proportionally increases flux (Arrhenius relationship) and the selectivity of water over ammonia (Xie et al., 2009). Additionally, the permeate can be passively incorporated within the electrode rinse solution of the RED cell, where ammonia is electrochemically oxidised by the free chlorine produced at the electrodes during redox (Zhou et al., 2018). Zhou et al. (2018) reported an ammonia removal efficiency of 98 %, and in theory the free chlorine could serve as an additional disinfection barrier.

In order to satisfy Category A, the permeate COD should not exceed 50 mg L^{-1} to minimise pathogenic regrowth. The faeces to urine mixing ratio (10:1) utilised within this thesis represented maximum faecal contamination to demonstrate treatment robustness and reliability. Initial solid/liquid separation passively facilitated by solids sedimentation and urine weir diversion, occurs shortly after entering the bowl.

Therefore, average COD loading of the liquid will realistically be closer to that of urine, which is four times lower (Chapter 4). Furthermore, a proportion of organics within the permeate represent VOCs which are selectively transported by MD (Chapter 4), where enrichment factor decreased temporally due to a reduced concentration gradient. If operated in batch mode, the initial concentrated fraction can be discarded to further strip out VOCs from the permeate, and reduce odour intensity. The ISO 30500 documentation recommends that the product water is 'non-odorous' (International Organisation for Standardisation, 2018) based on the fact that a malodorous product will dissuade the user (Cruddas, Parker and Gormley, 2015). Importantly, this thesis has demonstrated that odour can be alternatively managed by changing the negative perception of faecal odour, through the manipulation of odour profiles (Chapter 3, 4). Hydrophobic PV (pervaporation) using PDMS (polydimethylsiloxane), which demonstrated a hedonistically pleasant permeate resembling a cleaning product, was characterised by a similar VOC profiling to MD due to the shared selectivity to compounds possessing higher volatility (Chapter 4). With the appropriate ammonia management, the MD's odour perception would match that of PV(PDMS).

Consideration is also required for the retentate, which will be highly concentrated in COD and nutrients. A zero liquid discharge route could be explored through integration with microbial fuel cells (MFCs) where organics and nutrients are electrochemically degraded by bacteria, while recovering energy from the chemical potential of the organic fraction in FCU. This process has been applied to urine where removals of COD, TN and TP have been demonstrated up to 98 % (Gao et al., 2018), 79 % (Ieropoulos et al., 2016) and 82 % (Gao et al., 2018) respectively with power densities up to 21.3 W m^{-2} (Gao et al., 2018). The combined integration of MD with RED (salinity gradient energy) and MFCs (organics chemical potential) provides a synergistic partnership which has potential for greater power opportunities and comprehensive retentate treatment, however this prospect requires further investigation. In the immediate future, the safe to handle retentate (pathogens inactivated by prolonged thermal treatment) is significantly reduced in volume resulting in lower transport costs and could be discarded into the existing pit latrine infrastructure.

6.3 Can the NMT work off-grid without an external source of power?

The NMT aims to deliver a household scale advanced self-sustaining sanitation solution by recovering energy from urine and faeces. Table 6.1 lists the assumptions required to calculate an energy balance for the NMT. Onabanjo et al. (2016) experimentally determined that the energy density of dry faeces is 25 kJ g^{-1} during combustion, which exceeds the heating value for many types of wood (Lyons, Lunny and Pollock, 1985). A ten person scaled NMT will receive around 625g of dry faecal solids equating to 15625 kJ d^{-1} (Jurado et al., 2018). The small scale combustion of faecal solids has progressed such that continued operation over 24 h is possible (Jurado et al., 2018), and with the development of two stage combustion, near complete combustion can be realised which suggests most of this energy will be available as heat, harvested through losses and the peak heat from the exhausted air-flow. Solids-liquid separation by the screw coupled with basic interception, will remove free water to around 25wt.% solids, which is equivalent to the average faecal solids concentration of human faeces (Rose et al., 2015). Autothermal combustion of faeces occurs at 70wt.% solids (Onabanjo et al., 2016), therefore vaporisation energy is only considered for 45 % of the remaining bound faecal water, equivalent to 1125 g. The specific heat of water to increase 1125 g of faecal water by $80 \text{ }^\circ\text{C}$ (to reach $100 \text{ }^\circ\text{C}$, 376.74 kJ) and the latent heat of water vaporisation (2542.50 kJ) equates to 2919.24 kJ. This parasitic energy could be reduced further by identifying the boundary condition between screw tapering with a restricted extrusion aperture size which promotes dewatering versus aperture blockage from particle compaction (Chapter 2). The unique combination of rotational shear together with compression, offers significant advancement for dewatering. Thermally driven processes (Chapter 4) were operated at $50 \text{ }^\circ\text{C}$ and therefore heating 15 L of FCU by $30 \text{ }^\circ\text{C}$, utilises 1883.7 kJ according to the specific heat of water. The combustion of faeces provides the NMT with daily net heat energy recovery of 10822.06 kJ. Even operation at $70 \text{ }^\circ\text{C}$ for microbial intervention (3139 kJ), would realise the energy budget with a surplus of 9566.26 kJ, demonstrating the potential for high quality water within an energy positive system. Furthermore, this value is particularly conservative as it neglects heat recovery (for example latent heat recovery from the permeate), which will increase the free residual heat for other demands or duties.

Whilst the system is primarily focussed on the utilisation of heat energy, and whilst both mechanical energy (e.g. screw) and gravity will be harnessed for liquid transport, there will inevitably be demand for electrical power, for fluid transport. This means that other harvesting techniques are of importance, and an exemplar of this was demonstrated in this thesis through the integration of RED (Chapter 5), which allows harvesting of chemical energy directly from the salinity gradient rather than indirectly through inefficient thermoelectric generators (5-10 % efficiency). According to the ionic concentration of urine (Putnam, 1971), a further 9.33 kJ is available as salinity gradient energy and released using RED. Using the unscaled RED cell in this study, an energy recovery of 44 % was obtained, releasing daily net electrical energy of 4.12 kJ which can be used for the operation of low power devices to support hydraulic or air movement for the membrane processes. For example, a 0.25 W axial fan could be operated for 4.9 hours from 15 L urine and permeate, emphasising the significance of MD-RED for off-grid sanitation.

Table 6.1 Assumptions for calculating the NMT energy balance for a 10 person household

Assumption	Value
Screw operation (J g^{-1})	0*
Energy density of dry faecal solids (kJ g^{-1} faecal solids)	25 ^a
Dry mass daily faeces loading (g d^{-1})	625 ^b
Average extruded faeces solids concentration (wt.%)	15
Specific heat of water to increase by 1 °C (J g^{-1})	4.186
Latent heat of water vaporisation (J g^{-1})	2260
Daily FCU for membrane processing (g d^{-1})	15,000 ^c
Ambient temperature (°C)	20
Temperature differential for faeces water evaporation (°C)	80
Temperature differential required for membrane feed (°C)	30
Daily available salinity gradient energy from urine (J)	9330
Reverse electrodialysis energy recovery (%)	44

*It is assumed that the screw is operated by mechanically stored kinetic energy; ^aOnabanjo et al. (2016);

^bJurado et al. (2018); ^cRose et al. (2015)

6.4 What is the financial benefit of the NMT compared to conventional sanitation solutions?

Centralised wastewater management (CWWM) presently requires between US\$220-940 person⁻¹ for initial capital investment, and between US\$12-28 person⁻¹ y⁻¹ for operational and maintenance costs (O&M) (Cairns-Smith, Hill and Nazarenko, 2014). In comparison, a simple lined 3 m deep pit latrine costs around US\$800 (or ~\$80 per person), with basic O&M services such as pit emptying and repairs costing up to US\$11.5 person⁻¹ y⁻¹ (Washcost, 2012; Ulrich et al., 2016). The advantage of such a decentralised approach is the reduction in infrastructure due to the removal of the sewer network which can account for up to 84 % of the capital costs associated with CWWM (Jung, Narayanan and Cheng, 2018). However, pit latrines are an intermediate storage solution, with the sludge subsequently demanding transport via tankering to a sludge treatment facility. Due to access constraints and disposal charges, unregulated disposal is commonly practiced and faecal sludge is rereleased into the environment (Ingallinella et al., 2002).

The NMT offers comparable advantages to pit latrines in avoiding the cost of sewer infrastructure (Table 6.2). Providing onsite treatment also increases the safe disposal of faecal sludge, as well as avoiding infrastructure costs for centralised faecal sludge provision. The goal of the Bill & Melinda Gates Foundation is to provide such sanitation services at a cost of less than US\$0.05 user⁻¹ d⁻¹; this is to ensure sanitation can be as affordable for all as present pit emptying costs (Table 6.2) are equivalent to between 12% and 125% of an individual's average salary in India and Kenya respectively (Chowdry and Kone, 2012; World Bank, 2019). The NMT was developed based on serving ten people, and lasting for around seven years which was estimated based on typical materials lifetime expectancies for critical components. Using the Foundation's target, this is equivalent to \$180 available per annum, and \$1260 over a period of seven years. The NMT will comprise of a combustion zone, air pump, liquid pump, heat exchangers and a membrane, each of which are modular components that readily exist in a commercial environment. Close analogy can therefore be sought to domestic boilers, which operate at comparable ignition temperatures, and have a unit cost of around US\$770-1100 (The Heating Hub, 2019), in addition to other domestic appliances (whitegoods) such as fridge-freezers (US\$350-600; Improvenet, 2019) and

washing machines (US\$275-450; Kitchens.com, 2019). Whilst each appliance is of comparable complexity, and possesses analogous componentry, these products have penetrated into the domestic market due to their perceived robustness, and have subsequently achieved economies of scale. The proposition is that the NMT can therefore realise such unitary economies of scale by capitalising on already existing supply chains for much of the systems infrastructure. Therefore, the capital cost of a NMT unit is projected at US\$700 (Helbling Technik, 2019), which falls within the cost for the construction of a lined pit latrine for 10 persons, which does not include faecal sludge treatment (Table 6.2).

Inadequate access to sanitation and clean water equates to global economic losses of US\$260 billion y^{-1} (Hutton, 2013), attributed to the associated mortality, reduced productivity and healthcare costs (Lixil, Oxford Economics and WaterAid, 2016). This presents an opportunity for Government to stimulate growth through infrastructure investment. To illustrate, a US\$1 investment in sanitation and water would result in a fivefold economic return (Hutton, 2013). Based on the cost trajectory, investors could therefore be government led service providers driven by regulation, individuals seeking improved sanitation systems, or entrepreneurs seeking to offer innovative solutions. The NMT will require periodic maintenance, for example, to clean the membrane, and so a leasing service model would be applicable, similar to a mobile phone, which would include unit provision and maintenance, as proposed by the Toilet Board Coalition (Toilet Board Coalition, 2017). This could lower the cost barrier for customers, whilst also improving technology reliability through governance by an external service provider, with the knowledge of a high failure rate on the implementation of technology in LICs that are implemented without technical support (Carter and Ross, 2016). As such, a circular sanitation business model for products such as the NMT has been calculated to have a lower overall cost than sewerage systems by a factor of 2 to 14 times (Toilet Board Coalition, 2017), and highlighting its economic advantage compared to current sanitation solutions (which do not include treatment or resource recovery). Therefore, it is feasible to reach the Bill & Melinda Gates Foundation target to provide a sanitation service of less than US\$0.05 $user^{-1} d^{-1}$ (Table 6.2). It is now recognised that user groups ascribe a value to the produced water, considering its use for a number of domestic duties (Cruddas, Parker and Gormley,

2015). Provided the NMT can achieve reuse standards based on the further research proposed, the produced water could improve the value proposition of the system to end users, offsetting NMT cost through cost avoidance of bulk water purchase (Table 6.2), and diminish reliance on contaminated water resources, for which 29 % of the global population presently rely upon (United Nations, 2018).

Table 6.2 Comparison of current sanitation and water costs in low income countries (LICs) with the Nano Membrane Toilet

Sanitation option costs	Cost		Resource value
	Capital (US\$ person ⁻¹)	Operational and maintenance (US\$ person ⁻¹ y ⁻¹)	Clean water (US\$ L ⁻¹ d ⁻¹)
Centralised wastewater treatment (CWW)	220-940 ^a	12-28 ^a	
Decentralised pit latrine (DPL) (3m deep)	40*-80** ^b	1.5-11.5 ^c	
Clean water purchase price			0.0026-0.0522 ^d
Nano Membrane Toilet	70*** ^e	≤8 ****	15 L water recovered for non-potable reuse*****

*Unlined and **Lined assuming a 10 person household; ***Capital cost over a 7 year lifetime for a unit serving a 10 person household; **** Contract service cost targeting ≤US\$0.05 person⁻¹ d⁻¹ (service calculation takes into account the inclusion of the initial capital cost of one NMT unit at \$US10 person⁻¹ y⁻¹); ***** once the system is optimised and rigorously tested against the ISO30500 standard ^aCairns-Smith, Hill and Nazarenko, (2014); ^bUlrich et al. (2016); ^cWashcost, (2012); ^dWaterAid, (2016); ^eHelbling Technik, (2019)

6.5 References

Cairns-Smith, S., Hill, H. and Nazarenko, E. (2014) ‘*Urban sanitation: Why a portfolio of solutions is needed*’, Boston, USA: The Boston Consulting Group. Available at: <https://www.bcg.com/documents/file178928.pdf>. (Accessed: January 7 2019).

Carter, R.C. and Ross, I. (2016) ‘Beyond “functionality” of handpump-supplied rural water services in developing countries’, *Waterlines*, 35, pp. 94–110.

Cruddas, P.H., McAdam, E.J., Kolios, A., Parker, A., Williams, L., Martin, B., Buckley, C.A. and Tyrrel, S. (2015) ‘Biosolids Management Within the Nano Membrane Toilet –

Separation’, Thickening and Dewatering. *WEF/IWA Residuals and Biosolids Conference*. Washington, USA, June 7-10, 2015.

Cruddas, P.H., Parker, A. and Gormley, A. (2015) ‘User perspectives to direct water reuse from the Nano Membrane Toilet.’, *38th WEDC International Conference*. Loughborough, UK, 27-31 July, 2015.

van Egmond, W.J., Starke, U.K., Saakes, M., Buisman, C.J.N. and Hamelers, H.V.M. (2017) ‘Energy efficiency of a concentration gradient flow battery at elevated temperatures’, *Journal of Power Sources*, 340, pp. 71–79.

Gao, Y., Sun, D., Wang, H., Lu, L., Ma, H., Wang, L., Ren, Z.J., Liang, P., Zhang, X., Chen, X. and Huang, X. (2018) ‘Urine-powered synergy of nutrient recovery and urine purification in a microbial electrochemical system’, *Environmental Science: Water Research & Technology*, 4, pp. 1427–1438.

Helbling Technik (2019) *RTTC Cost Analysis – Nano Membrane Toilet Status Report*. Bill & Melinda Gates Foundation Internal Report. Unpublished.

Hutton, G. (2013) ‘*Global costs and benefits of drinking water supply and sanitation interventions to reach MDG target and universal coverage*’, World Health Organisation.

https://www.who.int/water_sanitation_health/publications/2012/globalcosts.pdf.

(Accessed: 8 August 2018).

Ieropoulos, I.A., Stinchcombe, A., Gajda, I., Forbes, S., Merino-Jimenez, I., Pasternak, G., Sanchez-Herranz, D. and Greenman, J. (2016) ‘Pee power urinal – microbial fuel cell technology field trials in the context of sanitation’, *Environmental Science: Water Research & Technology*, 2, pp. 336–343.

Improvenet (2019) *Average cost of kitchen appliances*. Available at: <https://www.improvenet.com/r/costs-and-prices/kitchen-appliance-cost-estimator>

(Accessed: 5 February 2019).

International Organisation for Standardisation (2018) *ISO 30500. Non-sewered sanitation systems -- Prefabricated integrated treatment units - General safety and*

performance requirements for design and testing (Final draft). Available at: <https://www.iso.org/standard/72523.html>. (Accessed: 8 August 2018).

Jung, Y.T., Narayanan, N.C. and Cheng, Y.-L. (2018) 'Cost comparison of centralized and decentralized wastewater management systems using optimization model', *Journal of Environmental Management*, 213, pp. 90–97.

Jurado, N., Somorin, T., Kolios, A.J., Wagland, S., Patchigolla, K., Fidalgo, B., Parker, A., McAdam, E., Williams, L. and Tyrrel, S. (2018) 'Design and commissioning of a multi-mode prototype for thermochemical conversion of human faeces', *Energy Conversion and Management*, 163, pp. 507–524.

Kamranvand, F., Davey, C.J., Sakar, H., Autin, O., Mercer, E., Collins, M., Williams, L., Kolios, A., Parker, A., Tyrrel, S., Cartmell, E. and McAdam, E.J. (2018) 'Impact of fouling, cleaning and faecal contamination on the separation of water from urine using thermally driven membrane separation', *Separation Science and Technology*, 53, pp. 1372–1382.

Kitchens.com (2019) *The cost of washers and dryers*. Available at: <http://www.kitchens.com/product-guide/washers-dryers/washer-dryer-prices/washer-dryer-prices> (Accessed: 5 February 2019).

Lixil, Oxford Economics and WaterAid (2016) *The true cost of sanitation*. Available at: https://www.lixil.com/en/sustainability/pdf/the_true_cost_of_poor_sanitation_e.pdf.

Lyons, G.J., Lunny, F. and Pollock, H.P. (1985) 'A procedure for estimating the value of forest fuels', *Biomass*, 8, pp. 283–300.

Moreno, J., Grasman, S., van Engelen, R. and Nijmeijer, K. (2018) 'Upscaling Reverse Electrodialysis', *Environmental Science & Technology*, 52, pp. 10856–10863.

Onabanjo, T., Kolios, A.J., Patchigolla, K., Wagland, S.T., Fidalgo, B., Jurado, N., Hanak, D.P., Manovic, V., Parker, A., McAdam, E., Williams, L., Tyrrel, S. and Cartmell, E. (2016) 'An experimental investigation of the combustion performance of human faeces', *Fuel*, 184, pp. 780–791.

Peeters, B., Dewil, R., Van Impe, J.F., Vernimmen, L. and Smets, I.Y. (2010) ‘Using a Shear Test-Based Lab Protocol to Map the Sticky Phase of Activated Sludge’, *Environmental Engineering Science*, 28, pp. 81–85.

Putnam, D.F. (1971) *Composition and concentrative properties of human urine*.

Washington, USA. Available at:

<https://ntrs.nasa.gov/archive/nasa/casi.ntrs.nasa.gov/19710023044.pdf>

Rose, C., Parker, A., Jefferson, B. and Cartmell, E. (2015) ‘The Characterization of Feces and Urine: A Review of the Literature to Inform Advanced Treatment Technology’, *Critical Reviews in Environmental Science and Technology*, 45, pp. 1827–1879.

The Heating Hub (2019) *Guide to New Boiler Installation Costs*. Available at:

<https://www.theheatinghub.co.uk/guide-to-boiler-installation-costs> (Accessed: 5 February 2019).

Toilet Board Coalition (2017) *The Circular Sanitation Economy: New Pathways to Commercial and Social Benefits Faster At Scale*. Available at:

http://www.toiletboard.org/media/34-The_Circular_Sanitation_Economy.pdf.

(Accessed: 5 February 2019).

Tufa, R.A., Pawlowski, S., Veerman, J., Bouzek, K., Fontananova, E., di Profio, G., Velizarov, S., Goulão Crespo, J., Nijmeijer, K. and Curcio, E. (2018) ‘Progress and prospects in reverse electrodialysis for salinity gradient energy conversion and storage’, *Applied Energy*, 225, pp. 290–331.

Udert, K.M., Larsen, T.A., Biebow, M. and Gujer, W. (2003) ‘Urea hydrolysis and precipitation dynamics in a urine-collecting system’, *Water Research*, 37, pp. 2571–2582.

Ulrich, L., Salián, P., Saul, C., Jüstrich, S. and Lüthi, C. (2016) *Assessing the Costs of on-Site Sanitation Facilities*. Available at:

https://www.eawag.ch/fileadmin/Domain1/Abteilungen/sandec/publikationen/SESP/Sanitation_Technology/Costing_Report__2016.pdf. (Accessed: 5 February 2019).

United Nations (2018) *Sustainable Development Goal 6*. Available at: <https://sustainabledevelopment.un.org/sdg6> (Accessed: 9 October 2018).

Urtiaga, A.M., Gorri, E.D., Ruiz, G. and Ortiz, I. (2001) 'Parallelism and differences of pervaporation and vacuum membrane distillation in the removal of VOCs from aqueous streams', *Separation and Purification Technology*, 22–23, pp. 327–337.

Washcost (2012) *The cost of sustaining sanitation services for 20 years can be 5-20 times the cost of building a latrine*. Available at:

<https://www.ircwash.org/sites/default/files/IRC-2012-Cost.pdf>. (Accessed: 5 February 2019).

WaterAid (2016) *Water: at what cost? The state of the world's water 2016*. Available at:

https://www.womenforwater.org/uploads/7/7/5/1/77516286/water_at_what_cost_wateraid_2016.pdf. (Accessed: 5 February 2019).

Xie, Z., Duong, T., Hoang, M., Nguyen, C. and Bolto, B. (2009) 'Ammonia removal by sweep gas membrane distillation', *Water Research*, 43, pp. 1693–1699.

Zhao, Z.P., Xu, L., Shang, X. and Chen, K. (2013) 'Water regeneration from human urine by vacuum membrane distillation and analysis of membrane fouling characteristics', *Separation and Purification Technology*, 188, pp. 369–376.

Zhou, X., Li, Y., Li, Z., Xi, Y., Nazim Uddin, S.M. and Zhang, Y. (2017) 'Investigation on microbial inactivation and urea decomposition in human urine during thermal storage', *Journal of Water, Sanitation and Hygiene for Development*, 7, pp. 378–386.

Zhou, Y., Zhao, K., Hu, C., Liu, H., Wang, Y. and Qu, J. (2018) 'Electrochemical oxidation of ammonia accompanied with electricity generation based on reverse electrodialysis', *Electrochimica Acta*, 269, pp. 128–135.

7 CONCLUSIONS AND FURTHER WORK

7.1 Conclusions

This thesis explored the integration of advanced separation processes to recover high quality water and energy for the Nano Membrane Toilet (NMT), utilising waste heat provided by faecal combustion. Although this research focused on implementation within the NMT, the contributions to knowledge are applicable to practitioners, engineers and the wider scientific community addressing non-sewered sanitation through the development and demonstration of sustainable processes, in which the following conclusions can be drawn:

1. Greater faecal solids extrusion occurs when combining a compression screw (tapered shaft and progressive pitch reduction) with a restrictive extrusion aperture, operating below 400 rpm to prevent water transport, reducing particle size to increase sludge mobility towards the feeding zone and increasing sludge viscosity by limiting the urine mixing ratio (Objective 1).
2. Solid phase extraction (SPE) with gas chromatography mass spectrometry (GC-MS) enables liquid phase faecal odourant concentration within and below taste and odour (T&O) thresholds. Such analytical resolution, method accuracy, precision and reproducibility allows for the evaluation of odour treatment at source by membrane technologies with highly selective separations of faecal volatile organic compound (VOCs) (Objective 2).
3. Hydrophilic pervaporative membranes offers the greatest rejection of liquid phase VOCs, however hydrophobic pervaporation, which selectively concentrates floral aromatic VOCs and provides a hedonistically pleasant permeate, implies that odour can be alternatively managed by altering negative perception through profile manipulation (Objective 2).
4. Thermally driven processes can process the daily liquid fraction of a household (15 L d^{-1}), within an energy positive system (+ 9566.26 kJ), using heat energy derived from the combustion of the faecal solids fraction (625 g d^{-1} dry faecal solids) (Objective 3).
5. Thermally driven membranes have potential to be employed within non-sewered sanitation to recover high quality water for reuse within a single stage. Particularly membrane distillation (MD), which may conform to the parameters of ISO 30500,

present robustness to faecal contamination and challenge odour by manipulating VOC profiles, is ready for implementation (Objective 3).

6. The retentate and permeate produced by MD urine treatment provides a salinity gradient for reverse electrodialysis (RED), which converts salinity gradient energy to electrical energy. The RED cell is currently able to extract 44 % of the available energy in urine, allowing for the operation of a low voltage (0.25 W) hydraulic device to support fluid movement for the membrane processes for 4.9 hours. Importantly, the novel and complex urine salt matrix explored, behaves similarly to simple salt matrices (NaCl) conventionally used for RED, through the demonstration of comparable power densities. Therefore urine MD-RED can be considered as a promising avenue for sustainable sanitation solutions through the provision of high quality water and electrical energy using waste heat (Objective 4).

7.2 Further work

The processes investigated within this thesis represent the initial demonstration of advanced separation processes for sustainable non-sewered sanitation, a relatively new research area which requires exploration to achieve Sustainable Development Goal 6 (SDG 6). Several key research areas for further work have been identified from this thesis:

1. Identification of the boundary conditions to facilitate screw dewatering for efficient thermal faecal processing. A trade-off exists in aperture size to prevent blockages by unmasticated food particles, and particle compression for effective dewatering. Screw initiated mixing and coarse particle shredding could also be explored to limit blockages and encourage screw feeding. The inclusion of drying agents such as toilet paper and screw heating also warrants investigation to dewater past the 'sticky stage' of faecal sludge, for enhanced transport. Furthermore, long term trials are required to understand the impact of steady stage screw operation.
2. Quantitative characterisation of pervaporation membrane polymers using a combination of VOC and non-VOC odourants would be beneficial to provide a holistic odour management approach. In combination with hedonic characterisation, it could be possible identify or develop a polymer which can deliver a positive user response, as well as provide high quality water in a single stage.

3. Ceramic pervaporation alternatives such as zeolite structures are known to be robust to fouling, highly selective to water, not prone to swelling and highly productive, however expensive. The investigation and successful application of zeolite membranes for sanitation wastewater could be sufficient to reduce costs due to economies of scale.
4. Investigation into the impact of increased feed temperatures for integrated microbial inactivation, in order to prevent liquid phase VOC (source) production, ammonia release and pH change. Further long term field trials assessing MD is also required to evaluate fouling and provide an understanding to develop mitigation methods.
5. The aim of urine MD-RED for decentralised sanitation is to maximise energy opportunity. However, a trade-off exists between energy recovery (which can sustain low voltage devices for longer periods) and peak power outputs (allowing for the shorter operation of high power appliances with a degree of energy dissipation). This aspect requires further investigation alongside appropriate scaling to realise the full potential of MD-RED. Once optimised, long term field trials are necessary.
6. A zero discharge opportunity exists for the management of MD retentate which is concentrated in inorganic and organic pollutants. Combining MD with RED already addresses the inorganic fraction, while recovering salinity gradient energy as demonstrated in this thesis. The further integration of MD with microbial fuel cells (MFCs), which are known to recover energy from the urine while degrading the organics, could also provide organic fraction management and greater energy opportunities.

APPENDICES

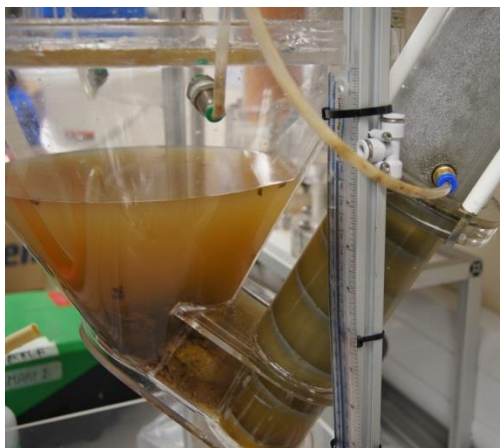


Figure A 1 Screw rig



Figure A 2 Thermally driven membrane processes rig



Figure A 3 Reverse electrodialysis rig

